ESA PSS-03-204 Issue 1
March 1996

Structural Acoustics Design Manual

Prepared by:
Structures and Mechanisms Division
European space Research and Technology Centre
Noordwijk The Netherlands

european space agency / agence spatiale européenne

Published by:
ESA Publications Division,
ESTEC, Noordwijk, The Netherlands

Printed in:
The Netherlands

Price Code:
70 Dutch Guilders

International Standard Serial Number:
ISSN 0379 – 4059

Structural Acoustics Design Manual

PREFACE

ABSTRACT

During the course of research activity on noise-related structural vibration problems, a large quantity of experimental information has been obtained, and methods of predicting the relevant vibration response have been developed. This includes the computer program GENSTEP3 (*GENeral STatistical Energy Program*), based on SEA (Statistical Energy Analysis) concepts, which can be used to predict the response of structural configurations, including the effects of acoustic cavities.

The objective of this manual is to provide the means of predicting the response of equipment and structures to high-frequency vibration environments. The intention is that it should be used from the preliminary design stage onwards. Many of the methods presented here rely on empirical and physical observations as well as mathematical models of the environment and the structural response. The prediction techniques must therefore be used with care and with an understanding of their purpose and limitations.

SOURCES OF INFORMATION

This manual replaces ESA PSS-03-1201 which was first published 1987. Additional studies have been undertaken by ISVR Consultancy Services, University of Southampton (UK). This new version has been revised and extended to include new information in various Chapters, [See also: Chapter 1 - Introduction]. The accompanying computer-program has also been updated to GENSTEP3.

As part of the current editorial process, the whole manual has been reformatted by RJ Technical Consultants (France) to the standard style created for large, YME-controlled technical handbooks.

DOCUMENT STRUCTURE

HANDBOOK LAYOUT

The Structural Acoustics Design Manual is a single-volume document, consisting of the following sections:

- This Preface,
- A full Contents listing for the whole handbook,
- Issue status and control information,
- A section showing the nomenclature used within the handbook,
- A series of Chapters,
- An Appendix,
- Lists of Tables and Figures for the whole handbook, and
- A subject Index.

Chapter

Chapters contain specific information on a named subject. Each Chapter (and Appendix) has the following structure:

- A title block showing:
  - Chapter number,
  - Chapter title.
- A detailed Contents Listing for the Chapter, down to the lowest Topic sub-heading.
- A series of numbered technical Topics.
- A final numbered Topic; 'Referenced Documents' (if appropriate), listing the external References cited in the chapter.

Chapter numbers and titles are shown in each page header, e.g.:

8 - Input Power

Topic

The subject matter of each Chapter is broken down into a series of numbered and titled Topics. Each is a logical block of information and is numbered using the Chapter number plus two sequential digits, with a leading zero if required. This provides the basic internal numbering system for the document. The numbers are always shown in the format: CHAPTER .TOPIC, e.g.

8.03 = Chapter 8, Topic 3

A full contents listing, including Topic numbers and titles, appears in the Handbook Contents at the start of the handbook.

Topic text is further subdivided by two levels of unnumbered, bold-text, sub-headings. These are included in the Contents listing for each Chapter and in the main Contents listing at the start of the handbook.

Figures, Tables and Other Embedded Information

Within each Topic, Figures and Tables are sequentially numbered in the format: CHAPTER.TOPIC.SEQUENTIAL NUMBER, e.g.:

Figure 8.03.1 = Chapter 8. Topic 3. Figure 1

Page Numbering

Pages are numbered sequentially within a Chapter. These numbers appear at the top, outer corner of each page header. They are also included in the Contents listings.

Within the handbook contents, table and figure lists, page numbers are given in CHAPTER-PAGE form, e.g.:

8-3 = Page 3 in Chapter 8.

In Appendix A, page numbers are preceded by a letter in place of the Chapter number, e.g.:

A-4 = fourth page in Appendix A.

REFERENCES

External References

The final Topic in each Chapter is a listing of all of the external documents referred to within it. The numbering is not global, i.e. for each Chapter the Reference numbering starts at [1]. The References are given in the text as, for example, Ref. [1, 2].

Internal References

Where information within one Topic has direct relevance to other Topics, an Internal Reference is used. These appear in the text as, for example, [See: 8.03], [See: A.11] or [See also: Table 13.04.1]. Internal references to other page numbers are not used within the text.

Internal references within a Topic give only the unnumbered heading. e.g. [See: Internal References].

VERSION CONTROL

The handbook includes an Issue Status and Issue Control Record for the whole document. Each Issue or Revision will include a new listing giving the latest Issue Status for all Chapters. The header on each page shows the full ESA PSS document number with the Issue and the Revision numbers.

Chapters showing an earlier Issue or Revision number than that stated on the Issue Status and Control sheets have been superseded, and must be replaced.

The page footer also shows the dated, RJ Technical Consultants file code used for central Version Control purposes only.

USER COMMENTS

It is intended that this manual will be updated to include additions and extensions to the available information. If you have any comments or suggestions concerning the content or format of this publication, or any queries regarding the clarification or interpretation of the information contained herein, please contact:

Mr. D.C.G. Eaton
Structures and Mechanisms Division
ESTEC
Keperlaan 1
NL-2201 AZ Noordwijk (ZH)
The Netherlands

Structural Acoustics Design Manual

Handbook Status & Control Sheet

Chapter	Title	Status	Issue Date	Control Code
	PREFACE			
-	Preface	Issue 1	March 96	saprefa
-	Issue Status & Control Record	Issue 1	March 96	sareva
-	Handbook Contents	Issue 1	March 96	sacnta
-	Nomenclature	Issue 1	March 96	sadefsa
	CHAPTERS			
1	Introduction	Issue 1	March 96	sa01a
2	Prediction Procedure	Issue 1	March 96	sa02a
3	Prediction of Structural Response: Zone 1 - Cylinders	Issue 1	March 96	sa03a
4	Prediction of Structural Response: Zone 2 - Platforms (Direct Acoustic Excitation)	Issue 1	March 96	sa04a
5	Prediction of Structural Response: Zone 3 - Platforms (Contained in Shell Structures)	Issue 1	March 96	sa05a
6	Prediction of Structural Response: Zones 4 to 7	Issue 1	March 96	sa06a
7	Prediction of Sound Transmission & Pressure Levels	Issue 1	March 96	sa07a
8	Input Power	Issue 1	March 96	sa08a
9	Compendium of Loss Factors	Issue 1	March 96	sa09a
10	Recommended Test Procedures for Evaluation of SEA Parameters	Issue 1	March 96	sa10a
11	Response Prediction by Deterministic Methods	Issue 1	March 96	sa11a
12	Test Specifications	Issue 1	March 96	sa12a
13	Damping of Structures	Issue 1	March 96	sa13a
	APPENDICES & LISTS			
A	GENSTEP3: General Theory	Issue 1	March 96	saa1a
-	List of Figures & Tables	Issue 1	March 96	safta
-	Index	Issue 1	March 96	sandxa

The preceding version control table give dates and control codes indicating the latest available version for each Chapter, or other section, making up the Structural Acoustic Design Manual, ESA PSS-03-204. This information is presented on each page of the handbook, at the inner margin, in the page footer. The control data should always match that shown within the relevant Chapter. If this is found not to be true, please contact ESTEC for update information. To assist with consistency of version, replacements for update purposes always consist of complete handbook Chapters, together with complete updates for the associated handbook lists. CHAPTERS AND LISTS MUST ALWAYS BE REPLACED COMPLETE. If inconsistencies are found in the page-footer dates and control codes of a Chapter, contact ESTEC for update information.

Structural Acoustic Design Manual - REVISION HISTORY

Date	Code Suffix	Revision Details
October 1987	-	Original Publication of ESA PSS-03-1201: Issue 1 Revision 0
March 1996	'a'	New format Issue 1 of SADM, renumbered to ESA PSS-03-204. Chapters 1 to 13 and Appendix A. Incorporating revisions made during 1994, 1995 and 1996 by ISVR Consultancy Services, University of Southampton, UK.

[Intentionally Left Blank]

Structural Acoustics Design Manual

HANDBOOK CONTENTS

CONTENTS

Chapter 4 - Prediction of Structural Response (Zone 2)

Chapter 5 - Prediction of Structural Response (Zone 3)

Chapter 6 - Prediction of Structural Response (Zones 4 to 7)

Chapter 7 - Prediction of Sound Transmission & Sound Pressure levels in Contained Spaces

Chapter 8 - Input Power

Chapter 9 - Compendium of Loss Factors

Chapter 10 - Recommended Test Procedures for Evaluation of SEA Paramters

Chapter 11 - Response Prediction by Deterministic Methods

Chapter 12 - Test Specifications

Chapter 13 - Damping of Structures

Appendix A - GENSTEP3: General Theory

List of Figures

List of Tables

Subject Index

Structural Acoustics Design Manual

NOMENCLATURE

VARIABLES

a	Cross-sectional area (of beam, etc.), length.
A	Surface area of structure or cavity (total, transmitting or radiating area).
$A(if)$	Fourier transform of $a(t)$.
$a(t)$, acc, a_g	Acceleration.
b	Length, width.
C	Speed of sound.
C_0	Speed of sound in air.
C_L	Longitudinal wave speed, $=\left(\frac{E}{\rho}\right)^{1/2}$ for beam, and $=\left(\frac{E}{\rho\left(1-\mu^2\right)}\right)^{1/2}$ for plate.
CLF	Coupling loss factor.
C_S	Shear wave speed $=\left(\frac{G}{\rho}\right)^{1/2}$
d	Length, width, diameter, fibre diameter.
D	Bending stiffness of composite panel (neglecting core), $=\frac{E t_f t_c^2\left(1+\frac{t_f}{t_c}\right)^2}{2\left(1-\mu^2\right)}$
dB	Decibel.
DLF	Dissipation loss factor.
D_q	Transverse shear stiffness of honeycomb panel $= G_c\, t_c\, [1 + (t_f/\, t_c)]^2$
E	Modulus of elasticity (Young's modulus).
E_n	Energy of nth subsystem.
f	Centre frequency of band Frequency bandwidth.
F	Bandwidth factor $=\left(\frac{\text{lower limit band}\,(K+1)}{\text{lower limit band}\,(K)}\right)^{1/2}$
f_c	Critical coincidence frequency $=\frac{C_0^2(3)^{1/2}}{\pi t C_L}$
$F(if)$	Fourier transform of force.
f_R, f_r	Ring frequency (of cylinder) $=\frac{C_L}{2\pi R}$
$F(t)$	Force.
g	Acceleration due to gravity.
G	Shear modulus.
G_c	Shear modulus for honeycomb core.
h, H	Thickness, height.
i	$[-1]^{1/2}$
I	Moment of inertia.
I_{NA}	Second moment of area of section, about neutral axis.
I_p	Polar second moment of area about centre of gravity.
J	Torsional stiffness constant.
K	Radius of gyration.
l	Length (of beam, cylinder, etc.).
$\mathbf{l}$	Fibre length.
L	Length.
l_c	Greatest cross-section dimension.
l_e	Total edge length.
ln	Natural logarithm.
l_s	Total length of stiffening.
m	Mass.
M	Mass per unit area of structure.
M_0	Added mass.
n	Number of frames stiffening cylinder, excluding end frames; number of subsystems.
N	Number of modes (or mode count).
$n(f)$	Modal density.
NR	Noise reduction.
p	Acoustic field pressure.
p	Panel perimeter.
$< P^2 >$	Spatial mean square average pressure.
P_{eff}	Effective panel perimeter.
$P(if)$	Fourier transform of power input.
r, R	Radius.

R_{RAD}	Radiation resistance.
SEA	Statistical energy analysis.
Sp, SPL	Sound-pressure level.
t	Thickness (of panel, etc.), time.
t_c	Thickness of honeycomb core.
t_f	Thickness of face sheet (of honeycomb structure).
TL	Transmission loss.
TR	Reverberation time $e^{-T_R \eta \omega} = 10^{-6}$
V	Volume.
V_f	Fibre volume fraction.
$v(t)$	Velocity.
Y	Mobility = $\frac{v(t)}{F(t)}$
Z	Impedance = $\frac{1}{Y}$
α	Average absorption coefficient.
α_1	Truncation ratio.
β_{LT}	Shear loss factor of composite.
β_{mF}	Shear loss factor of matrix.
χ	Rotary inertia term.
$\eta_{0°}$	Flexural loss factor of 0° to outer layer fibre direction.
η_1	Dissipation Loss Factor (DLF, single subscript).
η_{12}	Coupling-loss factor (CLF, double subscript).
η_L	Longitudinal flexural loss factor of composite.
η_{mF}	Flexural loss factor of matrix.
η_T	Transverse flexural loss factor of composite.
κ	Radius of gyration of section about neutral axis, $= \left(\frac{I_{NA}}{a}\right)^{1/2}$ or radius of gyration about centre of gravity of section, $= \left(\frac{I_p}{a}\right)^{1/2}$
λ_0, λ_a	Acoustic wavelength.
λ_c	Wavelength, corresponding to critical frequency $= \frac{C_0}{f_c}$
μ	Poisson's ratio.
ρ	Material density.
ρ_0	Air density.
Π_{12}	Power flow.
ω	Frequency (angular).
Ψ	Semi cone angle.
Υ	Power-absorption coefficient.
$\overline{}$	Bar over symbol denotes time average.
$\langle\ \rangle$	Denotes spatial average.

SUBSCRIPTS

b	Box.
c	Core.
cp	Corrugated plate.
m	Mass corrected.
L	Large.
n	New.
p	Platform.
p	Pressure level.
pp	Plain plate.
r	Reference.
s	Small.
u	Uniform.

ABBREVIATIONS

CFRP	Carbon-fibre-reinforced plastics.
CM	Communication Module.
CNMD	Cone Modal Density Program.
CORRG	Corrugated.
EXPD	Expanded (corrugation).
GENSTEP3	GENeral STatistical Energy Program (Revised Version).
GFRP	Glass-fibre-reinforced plastics.
h.c.	Honeycomb.
HCMD	Honeycomb Modal Density Program.
IABG	Industrieanlagen-Betriebsgesellschaft, Ottobrunn, Munich.
ISVR	Institute of Sound Vibration Research, Southampton.
OASPL	Overall sound-pressure level.
SEA	Statistical energy analysis.
SM	Service Module.

NOTES

Response results refer to 'space- and time-averaged values' $\langle\overline{}\rangle$ unless otherwise stated.

Most results are averaged in 1/3 rd. octave bandwidth with the exception of some 100 Hz constant bandwidth.

Excitation refers to 'reverberant acoustic excitation' unless otherwise stated.

Structural Acoustics Design Manual

Chapter 1
INTRODUCTION

CONTENTS

1.01 GENERAL BACKGROUND

During the execution of various satellite projects in the past, space-vehicle equipment encountered a number of noise-related structural vibration problems. In order to gain a better understanding of these problems, research activity initiated by the European Space Agency has been undertaken. During the course of these research activities, a range of experimental information has been obtained and prediction methods for the relevant vibration response have been developed. This includes the computer program GENSTEP3 (*GENeral STatistical Energy Program*), based on SEA (Statistical Energy Analysis) concepts, which can be used to predict the response of structural configurations including acoustic cavities.

The objective of this manual is to provide the means of predicting the response of equipment and structures to high-frequency vibration environments. The intention is that it should be used from the project design stage onwards, but in certain circumstances some specialist guidance may be required. Prominence is given to the selection of the correct data for use with the GENSTEP3 program. A description of the theory and methods used by GENSTEP3 may be found in Appendix A. It is possible to make use of this information for SEA assessments without using the GENSTEP3 program. Information on scaling methods is given in Chapter 11.

Conventional non-probabilistic response prediction methods are summarised in Topic 1.03 but in general are not considered in detail in this manual in view of the wide frequency spectrum range to be covered. However, the classical normal-mode approach can be useful for predicting the response of low-frequency modes and further information regarding one such method is included in Chapter 11.

1.02 SCOPE

The manual makes use of the concept of zoning. The zoning of typical satellite configurations has been looked at specifically, although the results may be applied with caution to other aerospace vehicles. The structures are divided into zones in which the vibration levels are sensibly constant. Each zone represents a well-defined part, or subsystem area, of the spacecraft and has its own characteristic type of vibration response.

At the present stage of development, the main advantage of the GENSTEP3 program is that it enables one to predict how the response of the different zones might be affected by changing appropriate properties of the structure. Use of the manual is intended to eliminate errors arising from incorrect or unjustified assumptions and eliminate incorrect deductions from the results.

Although the prediction methods are designed primarily for the case of acoustic excitation of structures by a reverberant sound field, the intention is that they should eventually be extended to include high-frequency mechanical vibration transmission (such as may arise via a satellite launcher interface). This information will eventually appear in Topic 8.03.

There is also an intention to provide the means for deriving loading spectra for test specifications and methods of producing high-frequency vibration control through artificial damping treatment. Work is proceeding on these topics and information will be included at a later date in Chapters 12 and 13, respectively.

Development work by ESA has been mostly directed towards empirical aspects rather than to development of SEA modelling.

During the development of the prediction technique, experimental results have been studied. Some of the main observations made on satellite specimens are listed below:

- the response of fabricated and honeycomb platforms,
- the influence of equipment items on the overall system response (this covers uniform mass distribution and also the effects of marked nonuniformity),
- the response behaviour of central support structures, such as cylinders and cones,
- response modifications due to the presence of struts and similar attachments,
- the effect on response behaviour of massive local items such as an apogee boost motor (ABM),
- the effect of appendages and the prediction of their own high-frequency response,
- the effect of structural enclosures.

Where appropriate, these observations and others are incorporated into the guide.

1.03 INTRODUCTION TO ANALYSIS METHODS

This topic provides an overview of methods for use in the prediction of structural response to acoustic excitation and of transmitted sound and vibration.

CLASSIFICATION OF METHODS

A number of different approaches have been developed to allow estimation of response of structures to acoustic excitation and the estimation of transmitted sound or vibration.

This section of the Manual describes the basic features of the approaches and then summarises these in tabular form to assist the engineer to make the most appropriate selections. The distinctions between the approaches as described are restricted for brevity and may be simplistic in some areas. There will be cases which are best covered by an approach other than that apparently most suitable owing to aspects which require specialist knowledge.

The most technical fundamental factors on which the selection of an analysis method should be based are the type of response information required, and the levels of precision and accuracy which are acceptable. The selection will often also be influenced by the time and resources available. Little is known of how to estimate quantitatively the precision and accuracy of a prediction made by the different methods, and the relative accuracy of the methods for different situations is largely based on experience as well as on the methods' inherent characteristics.

All the methods discussed apply only to linear systems.

The methods of analysis fall into two basic categories, namely conventional (analytical and numerical) and probabilistic. Conventional analyses have traditionally been modal in character, but total response methods, in frequency and time domains, have also been developed. The energy-based analyses are usually implemented by means of numerical computation procedures unless very simple structural models are adequate.

The most widespread approach using analytical and numerical methods is to predict free vibrational modes and then obtain the synthesised forced solution by modal superposition. Within these methods, the finite-element approach also allows direct solutions to be calculated, which can therefore cover models with non-ideal spatial distribution of damping.

The probabilistic approach is applied in cases where a system's dynamic behaviour is not known with sufficient certainty, or the size of the analysis is too large, to allow a deterministic approach. (The approach could also be applied to analytical and numerical solutions to cover a possible range of known system parameter values). Statistical Energy Analysis (SEA) is one such method, which only assumes statistical knowledge of the system and so is not in a position to give discrete location and frequency response, only global response. Use of SEA means that the user acknowledges that discrete response prediction is impossible for complex structures owing to uncertainties in their specification and assumes that it is better to obtain an estimate of global response, specifically the energy of a structural subsystem. The SEA method accepts vibrational power as system forcing inputs.

The methods reviewed are outlined very briefly in Table 1.03.1.

CONVENTIONAL RESPONSE PREDICTION METHODS

Methods which produce analytical predictions of response are based on the solution of a set of deterministic equations of motion. When the excitation field is also deterministic, such as for a sinusoidal travelling wave, the whole problem can be formulated deterministically. However, random excitation requires the forcing and response terms in these equations to be statistically reformulated and a family of modal techniques has arisen from the various forms of the equations used in describing the response in a probabilistic manner.

Methods which model the structure in a spatially discrete manner require acoustic forcing also to be represented in a similar manner. However, adequate representation of the cross-correlation of a random acoustic field by discrete forces becomes increasingly more difficult as frequency increases. In that case, acoustic field modelling is better performed by use of boundary-element modelling (BEM) when structural finite-element modelling (FEM) is being applied.

Alternatively, with the advantage of simpler acoustic modelling, the acoustic field and the structure can be modelled by a continuous, rather than lumped, parameter representation. However, although a continuous representation suits the acoustic field modelling, representations of realistic structures can be very limited. Nevertheless, this approach can yield good estimates within its limitations and is relatively simple to apply. It may also be used to obtain first-order estimates of response in cases of greater degrees of structural approximation. Analytical representations of the structural mode shapes are limited and although numerical representations can be used, these greatly increase the complexity of the computation.

Although it is possible to obtain spatial information of the response field from continuous modelling methods, it is simplest to obtain the spatially integrated response. However, the improved representation of the excitation field compared with the lumped parameter methods means that for a simple structure the value of the response parameter which is predicted is likely to be more accurate.

Modal interaction analysis (MIA) estimates the energy transfer between individually identified pairs of modes (one acoustic and one structural mode), and so, although data for discrete modes is required as input to the analysis, this method is included in Topic 1.01 which concerns energy-based modal ensemble methods.

Admittance modelling is an experimentally based method which is reviewed in Topic 1.07, although the analytical aspects are limited to scaling methods.

Method	Structure	Excitation	Predicted Response	Main Restriction	Comments
1. Classical:					
1.1 **Modal:**					
Joint Acceptance	As MIA	All acoustic fields; random or travelling	Modal, usually spatially integrated	As MIA	Applied to response to acoustic excitation. Practically limited to structures with analytical excitation
Finite-Element (modal)	Any	Correlation must be known	Modal, spatial distribution given	Low u.f.l. for large structures	Often very high modelling and computer resources required
Boundary- Elements (modal)	Structure/ fluid interaction	As FE	As FE	As FE	Alternative to acoustic FE for modal or direct structural FEM
1.2 **Non-Modal:**					
Admittance	Any	Any	Point, narrowband, based on realistic damping	Based on experimental data to define input and transmissibility	Applied to scale response from similar situation or to model input as equivalent excitation (motion and impedance required, not forces)
Boundary-Element (time domain)	Fluid/structural interaction	Vibrating structural boundary (by FEM)	Spatial distribution, time history (FFT for spectra)	As F.E.	Recent development
Finite-Element (direct)	Any	Correlation must be known	Total response, not modal, spatial distribution given	More computing resources than modal FE required	System, not modal, parameter values applicable, damping distribution representation possible
2. Energy Methods:					
2.1 SEA	Assembly of sub-systems identifiable by SEA parameters	Broadband, stationary random forces.	Energy level of sub-system	Wider confidence limits at low frequencies and for point excitation. No spatial resolution in subsystems	Excitation spectrum flat over band-width. Bandwidth selected must include all significant coupling modes and resulting coupled modes; suits high modal density systems and distributed forcing
2.2 MIA	Analytical mode-shapes normally required	Narrowband stationary modal	Modal, usually spatially integrated energy level over a mode-set (wide-band)	Analytical structural mode shapes desirable	Accepts modal density < SEA. Lack of energy balance reduces accuracy of response to strongly coupled modes. Practical u.f.l., l.f.l. < SEA

Table 1.03.1 - Vibration Response Analysis Methods

1.04 STRUCTURAL RESPONSE ESTIMATION USING JOINT ACCEPTANCE ANALYSIS

SCOPE OF APPLICATION

An analytical method using continuous parameter formulation is joint acceptance analysis, described in Ref. [1, 2]. This is applied in the case of estimating the response of a structure to acoustic excitation. The excitation fields can be of any type: progressive, diffuse or turbulent. In non-deterministic (i.e. stochastic) cases, the pressure field is expressed in probabilistic terms which can be more satisfactorily achieved for a continuous-parameter model than for lumped element modelling. This method predicts the response of individual modes. It can be applied to the estimation of the response of structures such as launchers under the external sound field due to launch engines or due to turbulence during atmospheric flight.

The approach can be linked to a modal interaction analysis, [See: Topic 1.10], which applies the modal response of the structure predicted by joint acceptance techniques to estimate the coupled energy in a container such as the launcher shroud. This has been developed in Chapter 11.

BASIS OF ANALYSIS

For analytical structural mode shapes, the coupling can be analytically expressed as the joint acceptance function (JAF). With the JAF for a given mode and the excitation field's spectral density known, the spectral density of the generalised force can be calculated and then the structure's response in that mode can be estimated.

The joint acceptance is the ratio of the force coupling to a structural mode to the total excitation force applied. The force coupling to the mode is termed the generalised force.

The JAFs for a number of simple structural elements such as beams, plates and shells have been derived and evaluated [See: Chapter 11]. In addition, the evaluations of functions necessary to derive JAFs for other situations is also addressed. The acoustic mobility (fundamentally the response per unit sound pressure) can be evaluated from an expression containing the JAF so that an estimate (often conservative) of response to a given excitation can be made by simple manual calculation for basic structural elements using, e.g. design data given in Ref. [3].

Joint acceptance takes account of the degree of wave-matching between the acoustic and the structural fields. However, in some cases it can be adequate to base a response estimate on the assumption that the pressure field is in phase spatially over the excited structure. This is representative when the structural dimensions are small with respect to the effective forcing wavelength.

LIMITATIONS OF VALIDITY

The attraction of the method lies in its simplicity of application to response dominated by one or two modes which can be adequately represented by simple analytical functions. The readily available JAFs are limited to simple mode shapes, but in principle, JAFs can be derived for more complex mode shapes.

IMPLEMENTATION

This approach has particularly been used in assessing damage risk, since it has been shown that this is often dominated by response in the fundamental mode. Hence a simple conservative estimate of that response allows a good estimate of the overall damage risk to be made from the r.m.s. stress level which can be derived from the vibration estimate. The dynamic stress is related to the static stress per unit uniformly distributed static pressure by a factor which is a function of the resonant frequency, the spectrum level of the acoustic pressure at the resonant frequency and the damping in the responding mode.

This method of damage risk assessment is described in Ref. [4]. Acoustic fatigue data has been derived on this basis, Ref. [5], but there is little data on the correlation with failures at low numbers of stress cycles as would be appropriate to a single launch exposure. In this case functional damage to attached components could occur before material damage.

In summary, joint acceptance analysis:

- permits all types of acoustic field excitation;
- permits simple modelling of structural response when the structure can be adequately modelled analytically as a simple element.

1.05 FINITE-ELEMENT ANALYSIS (FEA)

SCOPE OF APPLICATION

Finite-element analysis provides information about spatial distribution of response explicitly for both structural and acoustic sections of the model. However, this 'benefit' over other methods is often more illusory than real when modal FEA is used to estimate the total response level from the summation of modal contributions. This is because the phase of a mode is very sensitive to damping, which is often poorly known. The consequences of phase uncertainty thus restrict FEA to the low frequency acoustic regime, where acoustic wavelengths are of the order of the structural dimensions. Also any spatial distribution of damping cannot be represented in modal FEA. If relative phase between modes is inaccurately estimated, then the accuracy of resultant response motion due to components from several modes can also be severely reduced when a system is not lightly damped and modes are not well separated. Stress and strain levels reach maxima at boundaries, however, where the phase has little influence.

Thus, with regard to spatial distribution of response, it is often as valuable to have an estimate based on the probability of response at a given location, referred to an estimated mean value, as it is to have a specific estimate based on uncertain phase estimates. The response probability value for spatial distribution is known for a given number of modes and can be applied to the mean response level estimated by SEA, Ref. [6].

BASIS OF ANALYSIS

For vibration and acoustic applications, the finite-element method is based on the use of Hamilton's principle.

Two approaches by FEA are possible, the direct and the modal approach. In the direct approach, the response at a given frequency is calculated without establishing the individual system modes. This has the major basic advantage of allowing system values rather than modal values to be applied of parameters such as damping levels, non-proportional damping and spatial distribution of damping. The main disadvantage is the very high (often impractical) level of resources required to perform modelling with the consequent full numbers of degrees of freedom since no reduction of degrees of freedom is possible. Each change of excitation or of frequency requires recalculation at full number of degrees of freedom because complex modes (which are frequency dependent) exist for non-ideal damping. Modal FEA reduces the analysis by determining the shapes and natural frequencies of individual modes and assuming that the modes exist independently, so that their individual contributions can be summed to give a total response at a given frequency. Modal FEA employs the variational approach but this gives only approximate properties of the selected elements. Exact properties of complicated elements such as stiffened monocoque fuselages can be determined by using the 'dynamic stiffness' technique instead of the variational modal approach, Ref. [7]. However this analytical modelling is limited, for example to simple boundary conditions.

LIMITATIONS OF VALIDITY

However, fundamental difficulties arise from the requirement to discretise the acoustic field. In the simplest case, which can be well modelled, the field can be represented by point forces applied to the nodal points of the structural elements if the fluid region's dimensions are much less than an acoustic wavelength. If this is not so, the difficulty in well-representing correlation between the discrete points causes significant errors for random excitation fields.

The method is therefore better suited to the estimation of response of fluid fields contained within vibrating structures, although propagating waves in ducts can also be modelled. An introduction to these applications is given by Petyt, Ref. [8]. The contained sound field can be modelled using three-dimensional acoustic-field elements, and radiation of sound into semi-infinite fluid fields by a vibrating field can be modelled by using semi-infinite elements. Non-rigid cavity walls can be modelled.

The major advantage of FEA is that complex structural configurations, whole-body structural modes and coupled fluid-structural modes can be modelled but the upper frequency range is limited to the highest order mode which can be well represented and economically computed. A typical practical upper limit would be of the order of about the twentieth mode for a multi-component structure. For a low mass stiff sub-structure, this may cover a frequency range of several hundred Hz, but less than one hundred Hz for a complete satellite.

For low-density fluids, the in-vacuo structural modes are often adequate representations of structural behaviour, except for the first one or two modes coupled to a sealed contained fluid. Also, stacked area-structures such as solar arrays and antennas can show large effects due to air-coupling, which FEA is well-suited to modelling.

To retain the computation within practical limits, some simplifying assumptions have become adopted such as assuming normal modes, linear behaviour and that all the structural internal damping is viscous.

Thus in summary, FEA:

- permits good modelling of complex structures and of contained acoustic fields,
- requires discretisation of acoustic field, which introduces difficulty in modelling correlation of random exciting acoustic fields,
- often requires a high level of resources,
- needs to be carefully monitored to avoid extending beyond the valid range for good confidence levels.

1.06 BOUNDARY-ELEMENT MODELLING (BEM)

SCOPE OF APPLICATION

This method is used as an adjunct to FEA, as a method of prescribing the conditions of the acoustic field at the structural boundary. The upper frequency is limited normally by the restrictions on the structural modelling already mentioned for FEA.

An application of boundary-element techniques to sound transmission into a fuselage is described in Ref. [9]. A time-domain based approach has been developed Ref. [10], with its application to acoustic scattering assessment described in Ref. [11].

The technique can be used in the prediction of the sound field radiated by a mechanically excited vibrating structure. This is not a topic of concern for this manual, but it can be mentioned that the need for complicated analytical modelling in that class of study can sometimes be avoided by the application of reciprocity in which the blocked acoustic field is experimentally measured at the surface of a rigid scale model of the body, Ref. [12].

BASIS OF ANALYSIS

As an alternative to the use of acoustic finite-elements, the sound pressure in an acoustic field can be calculated analytically at a given point if the motion of the surface of the vibrating sound source is known Ref. [9]. Compared with a high-mesh-density FE model of the acoustic field, this method allows simpler modelling but the solution must be recovered for each receiver point. In FEA, the behaviour of a particular element is affected only by the contiguous neighbouring elements, resulting in a banded matrix which is simple to manipulate, whereas BE analysis produces non-banded matrices which require full processing. Thus, whereas acoustic finite-element modelling requires more model preparation effort but gives the solution at many locations, the boundary- element method offers lower preparation effort but a solution only at an individual response location. It could be applied to prediction of local acoustic levels in an launcher fairing in the neighbourhood of a sensitive spacecraft component. Boundary-elements can also be used to estimate the acoustic field at locations in a semi-infinite radiated sound field where the number of acoustic finite-elements would be impractically high, although the recent advent of 'wave elements' may allow FEA to be applied to semi-infinite space.

1.07 CLASSICAL NON-MODAL; ADMITTANCE MODELLING (TRANSMISSIBILITY METHOD)

SCOPE OF APPLICATION

In order to predict a response of narrow band character with more accuracy than is given by modally averaged input data, it is usually necessary to use frequency response (transmissibility) functions which are either measured or scaled from measurements of structures similar to that of concern. The function usually required is the ratio (complex) of forcing and response functions.

SEA cannot be used to estimate response to a spectrum shape which is not approximately flat over the selected bandwidth. Such non-flat characteristics are shown by some stepper motor drives and could be generated by gearboxes. Narrowband acoustic excitation could occur if a structure is situated in an enclosed field which is driven selectively in a few modes by the container. The effect of a large payload on the field inside a launcher fairing may cause this tendency but has yet to be thoroughly investigated.

BASIS OF ANALYSIS

Admittance modelling is not a modal analysis method; equations of motion are written in physical terms in the frequency domain. It is claimed to be able to address classes of problems additional to those within the scope of modal analyses. Admittance modelling can be applied to derive the excitation acting on a body via a structural transmission path without the need to model the original excitation and transmission path individually, Ref. [13].

LIMITATION OF VALIDITY

The method relies on large amounts of high quality measured data to produce the required system matrices, similar to modal testing data gathering. One form of the method limits the modelling to single degree of freedom representation.

Measurement and assessment of transmissibility on spacecraft is reported in Ref. [14], where it is concluded that although reciprocal measurement may be convenient it may not be valid below frequencies which may range up to several hundred Hz. Reciprocity should therefore be checked on the structure before it is assumed to be valid.

IMPLEMENTATION

An area of application is taking account of the influence of coupled interface mobility of mounted equipment when estimating response of the mounted equipment, excited either internally or via the foundation.

The foundation structure can be represented by its mobility at the equipment mounting locations when the equipment is uncoupled. The measured foundation mobilities can be coupled to the measured mounting mobilities of an existing equipment or coupled to an analytical (e.g. finite-element) model of the supported equipment.

If the velocity at the mounting points of the modelled responding structure is known in the absence of the responding structure (i.e. the 'free' velocity of the mounting points) the response at the mounting locations when the structures are coupled together can be calculated. This avoids the direct measurement or estimation of the forcing levels which can be very difficult or impractical. The response of the driven structure can then be estimated, given the motion at the attachment points.

Once the motion of the mounting points has been estimated for the case of the structure mounted on the foundation, this input can be used to predict remote response on the mounted structure using either measured or predicted frequency response functions.

SEA modelling can be used to predict spatially averaged wideband responses by using the driving point motion and admittance to estimate vibrational power input to the mounted structure. However, use of admittance modelling for the mounted structure allows modal characteristics of the behaviour to be observed in the response functions, although the method does not explicitly consider individual modes.

In summary, compared with classical modal methods, admittance modelling:

- is essentially based on experimental data,
- permits excitation estimates based on response and impedance measurements at the structure's input locations, avoiding estimation or measurement of forces,
- produces total response directly,
- applies narrowband, realistically damped FRF (structural 'filter' functions) to the excitation.

1.08 ENERGY-BASED METHODS

The methods described are:

- Statistical Energy Analysis (SEA), [See: Topic 1.09], and
- Modal Interaction Analysis (MIA), [See: Topic 1.10].

1.09 STATISTICAL ENERGY ANALYSIS(SEA)

SCOPE OF APPLICATION

Even with adequate computing power, the accuracy of discrete modelling required to provide adequate prediction of the structural behaviour in individual high-order modes cannot be achieved, because of the uncertainties in practical factors (including fabrication and fitting tolerances), variations in joints and uncertainty concerning damping distributions. And even if such accuracy could be achieved, the use of modal methods would be inefficient compared with the statistical approach, requiring levels of resources not justified by the confidence levels. The occurrence of high modal overlap also invalidates assessments which assume modal independence.

Statistical Energy Analysis (SEA) is an approach particularly suited to multi-mode structural-acoustic systems excited at frequencies well above their fundamental natural frequencies. Acousticians were forced to adopt a statistical approach to analyses of enclosed acoustic fields from early days of the subject because of the high number of modal natural frequencies in the field at frequencies of greatest auditory concern. Vibration engineers, on the other hand, often find it sufficient to simplify a structural system to a small number of degrees of freedom of low modal order, because structural response is often greatest in low-order modes. However, when structure-borne noise transmission and response to high-intensity sound fields are of concern, the vibration analyst is forced to consider high modal orders because the excitation fields or the radiated fields of concern (e.g. subjective or structurally damaging noise) are usually at frequencies of hundreds or thousands of Hz. A critical overview of SEA is given in Ref. [15].

A limitation of SEA lies in the restriction of dynamic response being described only in terms of energy levels. Thus, in any of the subsystems that make up the total model, the spatial distribution (or local response) is not predicted by SEA (but may sometimes be developed from the SEA value). However, as already mentioned with respect to FEA, spatial variability of levels has been determined for some structures (e.g. platforms) so that confidence limits can be estimated for spatial variation.

The frequency resolution is restricted by the need for a minimum modal density, which usually requires several modes in a bandwidth. However, the frequency resolution is normally adequate for high-modal-order situations.

Even when deterministic analyses are practical, it may be more efficient to apply SEA, if valid, to investigate the effect of changes on a subsystem response when the whole subsystem will be excited by well-distributed forcing. It is in the area of exploring trends and sensitivities by parametric studies that SEA is particularly suited.

BASIS OF ANALYSIS

The method is **statistical** in that it assumes that the systems under analysis are drawn from populations with random parameters Ref. [16], and **energy** is the independent variable employed because there is then no inherent need to distinguish between acoustical and mechanical systems. The former feature derives from the fact that no two nominally identical systems behave identically at high frequencies and system parameters are not known with high precision due to the factors identified above. The use of subsystem energy as the response parameter reduces sensitivity to small-scale detail and allows the principle of conservation of energy to be used as the basis for formulating the governing equations and placing upper bounds on response.

The modelling is based on power-flow/energy relationships, derived for randomly excited systems, which are not normally applicable to narrow band excitation, except in an ensemble-average sense. The systems are represented by modes of vibration over a frequency bandwidth high enough to contain a statistically usable modal population. The bandwidth must not be high enough to obscure important spectral characteristics (practical forcing spectra are often not very flat, for example), and so SEA is most suited to the analysis of high-modal-density systems, Ref. [17].

LIMITATIONS OF VALIDITY

SEA offers a valid approach when a physically coupled structure can be considered with acceptable accuracy as a set of coupled subsystems whose modes are not influenced by the subsystems' inter-coupling and this becomes increasingly valid as modal density (modes/Hz) increases. Thus SEA is not well suited to cases in which the modes of structural subsystems are influenced significantly by the coupling whereas classical modal analysis methods can be used to model systems either as coupled or uncoupled, within the practical modelling limitations already mentioned. SEA is therefore more appropriate for the analysis of weakly coupled subsystems, such as for example, the analysis of acoustic/structural coupling involving gaseous acoustic media.

A further requirement for valid application of SEA is that response of a subsystem can be attributed predominantly to modes having natural frequencies in the frequency band of analysis. Non-modal contributions, such as the inertia contribution to the transmission loss of a panel, can sometimes be modelled as a direct path, [See: Chapter 7].

Where the modal density in a receiving subsystem is very low, the physical response within a frequency band may be dominated by the responses of modes having natural frequencies outside the frequency band. Since SEA estimates the energy transfer only between modes in the same frequency band for all subsystems, large errors are then likely. As a structure becomes more extensive and the number of subsystems grows, the modal density of a subsystem necessary for good estimates of response has been reported to reduce, probably because there are enough modes over the whole system within the bandwidth to excite the receiver. However, this influence on the modal-density criterion remains to be confirmed by ESA studies. It is likely to be more appropriate for strongly coupled subsystems.

The SEA theory, Ref. [16], is based on energy analysis of two coupled oscillators each with one resonance, so the analysis is inherently valid for very low modal densities, but the uncertainties then become very high if the subsystem parameters are only described statistically. The analysis assumes that systems are uncorrelated, which will not be true for a very small number of modes. However, it should be remembered that often in the case of conventional analyses accurate modal parameter values are not known.

As long as the receiving subsystem itself has adequate modal density to be dominated by response to those of its modes which lie in the bandwidth, the predicted level will be well estimated.

There is at present no method with which to estimate the confidence levels of the mean response estimated by SEA, but since these will be least wide when modal densities are sufficient for the subsystem parameter values to be a good average of individual modal values in the bandwidth, the minimum modal density is usually proposed to be at about five modes per bandwidth.

A further requirement for best confidence levels is that the excitation is well distributed over the subsystem so that modes are equally excited. Point mechanical excitation will therefore widen confidence limits. An even bigger influence on uncertainty may result from point excitation at a location of different nature from that described by the subsystem's parameters, for example if it is applied to a local 'hard' point.

Conventional SEA modelling assumes diffuse fields in all subsystems. Wave Intensity Analysis, Ref. [18], can be applied to modify SEA to take account of non-diffuse fields in a subsystem by introducing non-direct coupling factors. These account for the frequency filtering effects which can occur at subsystem junctions.

SEA is usually applied to linear systems under continuous excitation. Some development has also been undertaken for application to transient excitation, e.g. Ref. [19], but little is known yet of the confidence levels given by such modelling.

IMPLEMENTATION

The subsystems of an SEA model are defined by a set of special parameters (some of which are not used in deterministic analyses), namely modal density, dissipation loss factor and coupling loss factor. A review of SEA describing applications is given in Ref. [20]. Much of the remainder of this Manual concerns application guidelines for SEA.

The response is calculated as a vibration energy level which is then converted to a motion level by the relevant kinetic energy relationship. The probability values for spatial distribution of response due to uniformly distributed excitation for a given number of modes is given in Ref. [6], and an empirical investigation is described in Ref. [21].

When a structural model is available for experimental work, a parametric or sensitivity study can be undertaken with most confidence if the coupling and loss parameters for the model are evaluated through measurements on the built-up structure using the Energy Flow Analysis technique, in which each subsystem is excited in turn and the response of each subsystem is measured for each excitation, Ref. [22].

Thus, in conclusion, SEA is the first choice when, in a given frequency band:

- the excitation is broadband and random,
- modal density is high enough to allow the subsystems to be described by average modal properties,
- the response of a subsystem is predominantly in modes with natural frequency in the frequency band of analysis, i.e. predominantly resonant response,
- energy level is an adequate measure of subsystem response,
- the response fields consist of standing, rather than travelling, waves (i.e. damping is not too high),
- the modal overlap factor M in the coupled system is greater than unity, where:

$$M = \frac{\text{average modal half power bandwidth}}{\text{average modal frequency separation}}$$

1.10 MODAL INTERACTION ANALYSIS (MIA)

SCOPE OF APPLICATION

Although not probabilistic in its structure, modal interaction analysis (MIA) is a method which in its practical application produces estimates which have some characteristics in common with those given by SEA. However, the method, (described in Chapter 11) permits analysis to extend beyond some of the limits imposed by SEA. The method is particularly suited to the estimation of energy transferred from a structural vibration field to a contained acoustic field when both fields are modal in character, but neither need be diffuse as is normally required for SEA modelling. In MIA, the response of an individual mode of a subsystem is calculated as if it were due to excitation from a mode of the linked subsystem. However, the analysis is incomplete in that no power balance is considered. A check for an upper boundary of response level therefore needs to be made, by ensuring that the physical limitation of equipartition of modal energy between coupled systems is not breached. Like SEA, MIA does not deal with coupled modes of combined systems.

An advantage over SEA is that MIA permits prediction of non-resonant modal response in a system which can be dominant at low modal densities, allowing the frequency range to be extended to lower frequencies.

BASIS OF ANALYSIS

This method is based on the fact that the energy of vibration of a system is equal to the sum of the energies of orthogonal interacting modes of components of a system. In the case of a uniform cylinder for example, interacting modes of the structure and internal acoustic field of each circumferential order are orthogonal so the energy transfer of each circumferential order can be considered independently and summed to give the overall value. For low-density acoustic media in the enclosed volume, the coupled natural frequencies differ only slightly from the uncoupled values except for a structure's fundamental volume displacement mode which can couple strongly with the fluid field's bulk-compression mode. The analysis will indicate the maximum responses to be at the natural frequencies of the uncoupled mode, and although the coupled mode frequencies could be calculated, other uncertainties in the values of modal parameter values, particularly damping, result in estimated responses usually being expressed as 'modal ensemble' values rather than values for individual modes.

IMPLEMENTATION

A disadvantage introduced by the fact that the analysis is based on assessment of individual mode pairs is that as modal density rises, so does computational effort. However, the practical frequency range may be adequate, for example when the response of sandwich wall cylinders is analysed up to about twice their ring frequency. This application is described in Chapter 7.

Thus in summary, compared with SEA, MIA:

- permits prediction at lower modal density values,
- permits inclusion of non-resonant response,
- permits continuous-parameter acoustic field representation,
- requires data for individual structural modes as input, which may require FEA, deterministic or numerical analysis for structural or acoustic fields,
- imposes an upper frequency limit due to practical limitations of modal data,
- permits prediction of response to non-diffuse sound fields.

Compared with joint acceptance analysis, MIA:

- is based on discrete incidence angle analysis, from which other (e.g. diffuse) field types must be synthesised, rather than being directly applicable to all field types (if JAF is known).

1.11 REFERENCES

[1] R.G. White & J.G. Walker (Editors)
Noise and Vibration, Chapter 3 (B.L. Clarkson)
Ellis Horwood Ltd, 1982, ISBN 0-85312-502-3

[2] D.C.G. Eaton
'Some Considerations of Current and Future Launcher Acoustic Environments: Implications in Terms of Design and Test Requirements'
Proc. of Int. Symposium on Environmental Testing for Space Programmes, Test Facilities and Methods,
ESTEC Noordwijk, Netherlands, 26-29 June 1990
(ESA SP-304, Sept. 1990), pp. 279-286

[3] R.W. White
'Acoustic and Blast Loads on Buildings'
Report WR 66-2

[4] B.L. Clarkson
'Stress in Skin Panels Subjected to Random Acoustic Loading'
J. Royal Aero Soc., Vol. 72(5), Nov. 1968

[5] ESDU: Acoustic Fatigue Sub-series.
Vol. 1, Data Sheet 72015 (5 Vols overall).
Engineering Sciences Data Unit

[6] S.M. Stearn
'Spatial Variation of Stress, Strain and Acceleration in Structures Subject to Broad Frequency Band Excitation'
J. Sound Vib. 12(1), 85, 1970

[7] R.S Langley
'A Dynamic Stiffness Technique for the Vibrational Analysis of Stiffened Shell Structures'
J. Sound Vib., 1992, 156(3), 521-540

[8] R.G. White & J.G. Walker (Editors)
Noise and Vibration, Chapter 16 (M. Petyt)
Ellis Horwood Ltd, 1982, ISBN 0-85312-502-3

[9] R.S. Langley
'An Efficient Method for the Prediction of Aircraft Interior Noise Levels'
Proc. Acoustics '93, I.O.A., Southampton, April 1993, 187-194

[10] J.M. Parot, D. Vaucher Delacroix et al.
'Dimensional acoustics of rigid or moving surfaces: integral formulation, explicit time scheme and subsequent frequency analysis'
University College of Swansea NUMETA-87
Proceedings of the international Conference on: "Numerical methods in engineering: theory and applications"
Swansea (UK) 6-10 July 1987

[11] C. Clerc & J-N Giraudbit
'Acoustic Prediction on Satellite Structure'
Proc. Int. Conf. 'Spacecraft Structures and Mechanical Testing'
Noordwijk, NL, 24-26 April 1991 (ESA SP-321), 210-222

[12] F.J. Fahy
Sound and Structural Vibration, Ch. 6.
Academic Press, London, 1985. ISBN 0-12-247670-0

[13] D.A. Kienholz et al
'Admittance Modelling: Frequency Domain, Physical Coordinate Methods for Multicomponent Systems'
Proc. Internat. Modal Analysis Conference (1988)

[14] N.S. Ferguson & D.C.G. Eaton
'Vibration Characterisation of Low Level Disturbances Induced in Telecommunication Spacecraft'
Proc. Int. Conf: Spacecraft Structures and Mechanical Testing
Noordwijk, Netherlands, 24-26 April 1991
(ESA SP-321 Oct. 1991), pp. 603-608

[15] F.J. Fahy
'Statistical Energy Analysis: a critical review'
Phil.Trans.R.Soc. Lond., A. (1994). To be published

[16] R.H. Lyon
'Statistical Energy Analysis of Dynamical Systems, Theory and Applications'
MIT Press, Mass., USA, 1975

[17] F.J. Fahy & A.D. Mohammed
'A Study of Uncertainty in Application of SEA to Coupled Beam and Plate Systems. Part 1. Computational Experiments'
J.Sound Vib. 158 (1) 45-67,1992

[18] R.S. Langley & A.N. Bercin
'Wave Intensity Analysis of High Frequency Vibrations'
Phil. Trans. R. Soc. Lond., A (1994), 346, 489-499

[19] D. Lednik & R.J. Pinnington
'Prediction of Shock Propagation in Coupled-beam Systems'
Proc. Conf. InterNoise 93, Leuven, 24-26 Aug., 1993, 1851-1854

[20] J.E. Manning
'Statistical Energy Analysis: An Overview of Its Develqpment and Engineering Applications'
59th Shock & Vibration Symposium, Albuquerque,
Oct. 18-20 1988, pp. 25-38

[21] R.E. Powell
'Response Variability Observed in a Reverberant Acoustic Test of a Model Aerospace Structure'
Proc. of 2nd Int. Congress on Recent Developments in Air and Structure-borne Sound and Vibration, March 4-6, 1992, Auburn University, USA, pp. 89-96

[22] N. Lalor
'The Experimental Determination of Vibrational Energy Balance in Complex Structures'
Conference on Stress & Analysis, SIRA; Recent Developments in Industrial Measurement and Analysis, Paper No. 1084, 29

(Intentionally Left Blank)

Structural Acoustics Design Manual

Chapter 2
PREDICTION PROCEDURE

CONTENTS

2.01 GENERAL

Statistical Energy Analysis (SEA) techniques are being developed to produce a design aid for the prediction of structural response to random excitation environments. The current state of development has produced techniques for the prediction of response due to a reverberant excitation sound field. The aim of this Design Guide is to provide set procedures for the prediction of structural response levels for space vehicle structures using SEA and to increase confidence in the use of the GENSTEP3 program suite. Guidelines have been drawn up to produce consistent zoning and modelling of structures and hence consistent response predictions.

During development, the response predictions have been compared with measured structural levels and the technique guidelines developed accordingly. However, test data were not available for all the advanced structural configurations being employed in spacecraft components, so predictions for certain structural configurations (or zones) may not be as accurate, at this stage of development, as they could be within the general tolerances of the SEA techniques. In predicting the response of a new structure, the best way to use GENSTEP3 is, where possible, to run the program with data from a previous structure having a similar form of construction and to compare the results with information from tests performed on that original structure. This will make possible an optimum choice of SEA parameters relevant to the new construction configuration and will permit variation of dimensional and material properties for prediction of the modified configuration. This is effectively a calibrating process for GENSTEP3. For design purposes, the response of structures can still be predicted without a 'calibration' run, but confidence of the results will be somewhat lower.

It should be noted that some of the analytical formulae included in GENSTEP3 (See: Appendix A) for the evaluation of modal density and radiation resistance have discontinuities at certain frequencies.

For plates and cylinders having a frequency-dependent formulation, these discontinuities occur at the critical coincident frequency, f_c, and for cylindrical shell structures at the ring frequency, f_r. Definitions of f_c and f_r are given in the relevant sections. The effect of these theoretical discontinuities is to produce peaks in the response of the affected subsystem at f_c and/or f_r. Whether or not these peaks are 'passed on' to other modelled subsystems will depend on the degree of coupling between the subsystems. It was not thought prudent to attempt to inhibit or reduce the output of these peaks in GENSTEP3, so in practice they have to be ignored. When a large peak is present in the predicted response, it should be checked against the calculated values of f_c and f_r for the appropriate subsystem. If difficulty should occur in isolating the subsystem(s) responsible, the model should be re-run with all CLF values put to zero (i.e. no subsystem coupling present).

An outline of the SEA theory, relevant assumptions, and the definition of zones is given in Topics 2.02 to 2.04 inclusive. The remainder of this chapter presents the basic procedure and guidelines for applying SEA and GENSTEP3. For the actual running of GENSTEP3, Ref. [1] should be consulted.

2.02 OUTLINE OF SEA THEORY

The basic theory of statistical energy analysis is discussed by Lyon, Ref. [2], and typical applications are reviewed by Fahy, Ref. [3], and Pocha, Ref. [4].

The fundamental relation used is that of the conservation of energy for each subsystem, i.e. the balance between power entering and power leaving the subsystem.

The power dissipated by the ith subsystem is:

$$\Pi_{i,DISS} = 2\pi f \cdot \eta_i \cdot E_{i,TOT}$$

and the power transferred from subsystem i to subsystem j is:

$$\Pi_{ij} = 2\pi f \cdot \eta_{ij} \cdot E_{i,TOT} - 2\pi f \cdot \eta_{ij} \cdot E_{j,TOT}$$

The power balance for each subsystem is then:

$$\Pi_{i,IN} = \Pi_{i,DISS} + \Sigma \Pi_{ij}$$

The balance for the whole system results in a set of equations which may be represented in matrix form as:

$$[N]\{E\} = \{\Pi_{IN}\}/2\pi f$$

where $[N]$ contains the coupling loss factors and the dissipation loss factors.

The GENSTEP3 program solves the equation for the subsystem energies, which are in turn converted to the requested form of response.

Appendix A provides the theoretical expressions used to evaluate the relevant SEA parameters in the GENSTEP3 subroutines, and was produced from a previous British Aerospace report, Ref. [1].

2.03 ASSUMPTIONS MADE IN SEA ANALYSIS

The following is a list of basic assumptions and limitations associated with the statistical energy theory and the GENSTEP3 program:

- The effect of nonlinearity on response is ignored. Coupling between structural elements and acoustic fields is assumed to be linear.
- Only a relatively small number of resonant modes significantly contribute to the energy exchange process in any frequency band. The modes that resonate outside the frequency band are not included in the modal count. Though these nonresonant modes may play a role in transmitting energy from one subsystem to another, the energy of vibration they acquire in so doing is assumed to be substantially less than that of the resonant modes.
- The 'energy of vibration' is assumed to mean the long-time-averaged sum of the kinetic and potential energies under stationary random excitation.
- No information is given about spatial concentrations of energy in particular parts of each subsystem. Thus, energy is assumed to be evenly distributed throughout each subsystem.
- The widths of the analysis bands are normally chosen, on the basis of subsystem modal densities, to encompass a reasonably large number of uncoupled subsystem natural frequencies. (1/1 octave and 1/3 octave bands are often used because they are available in standard noise-measurement equipment. However, it would often be preferable to choose constant bandwidths which can provide better low-frequency statistics). It is recommended that for use with the GENSTEP3 program at least five natural frequencies should be present in the analysis band.
- It is recommended that for SEA modelling in general at least five modes with natural frequencies within the frequency bandwidth chosen should be excited by the forcing system. For multipath systems, this requirement can sometimes be relaxed without high loss of confidence, experience showing that useful predictions can be made for only one or two modes per bandwidth if coupling is quite strong. Although the analysis is valid for lower numbers of excited modes, the confidence range of the result becomes very wide. Quantifying confidence limits for SEA modelling is not yet well developed.
- The modal density of a fabricated structure (e.g. a stiffened panel) is assumed to be the sum of the modal densities of the structure's constituent parts.
- For a system of high modal density, the choice of boundary conditions is not critical for the evaluation of modal density.
- The acoustic excitation spectrum must be reasonably smooth.

- The pressure spectrum inside a cylinder with a transversely mounted floor is the same for the two air cavities, irrespective of the position of the floor, and is equal to the pressure spectrum for an internal cavity without a floor (provided the floor does not give a pressure seal between the two compartments).
- The analysis should be restricted to frequencies at which the acoustic wavelength inside a cavity is shorter than the relevant structural dimensions.
- The interior sound field for all acoustic cavities is reverberant.
- For a cylinder, it is necessary for the ring frequency, f_r, to be less than the lower coincidence frequency, f_c. This is unlikely to be appropriate for a cylinder with honeycomb-sandwich wall construction, but is a limitation of the available GENSTEP3 subroutine.
- For stiffened panels, it is necessary (in GENSTEP3) to assume that all the stiffeners are identical and, for the case of a stiffened cylinder, that all frames are also identical.
- GENSTEP3 program has no limitation on the maximum model size.

2.04 DEFINITION OF ZONES

When one has to predict the response of a satellite, it is reasonable to split the configuration into zones, past experience having shown the vibration throughout a zone to be sensibly constant. Each zone represents a well-defined part, or subsystem area, of the spacecraft and has its own characteristic type of response. In defining the zones, no allowance for subsystem characteristics (mass, impedance, etc.) has been taken into consideration. Reference was made to Keegan, Ref. [5], and Westin, Ref. [9], for definition of zones. The structural spacecraft zones are defined as follows:

- **Zone 1 - Primary Spacecraft Structure.** This zone represents the central core of the satellite configuration.
- **Zone 2 - Secondary Spacecraft Structure External to Spacecraft Outer Shell.** This zone represents external platforms used for mounting satellite subsystems. No distinction is made between upper and lower platforms.
- **Zone 3 - Secondary Spacecraft Structure Internal to Spacecraft Outer Shell.** This zone represents internal platforms used for mounting satellite subsystems. No distinction is made between different mounting positions of the internal structure.
- **Zone 4 - Panels, Solar Arrays, Antenna Reflectors.**
- **Zone 5 - Booms and Struts.**
- **Zone 6 -Equipment and attachment.** Originally defined for all kinds of brackets, this zone is modified to include the addition and attachment of equipment.
- **Zone 7 - Massive Equipment Items** (such as Apogee Boost Motor).

Note: Acoustic Spaces - These are grouped together to form a separate class of subsystem, see Chapter 7 - Sound Transmission.

2.05 SEA PROCEDURE STEPS

See Figure 2.05.1.

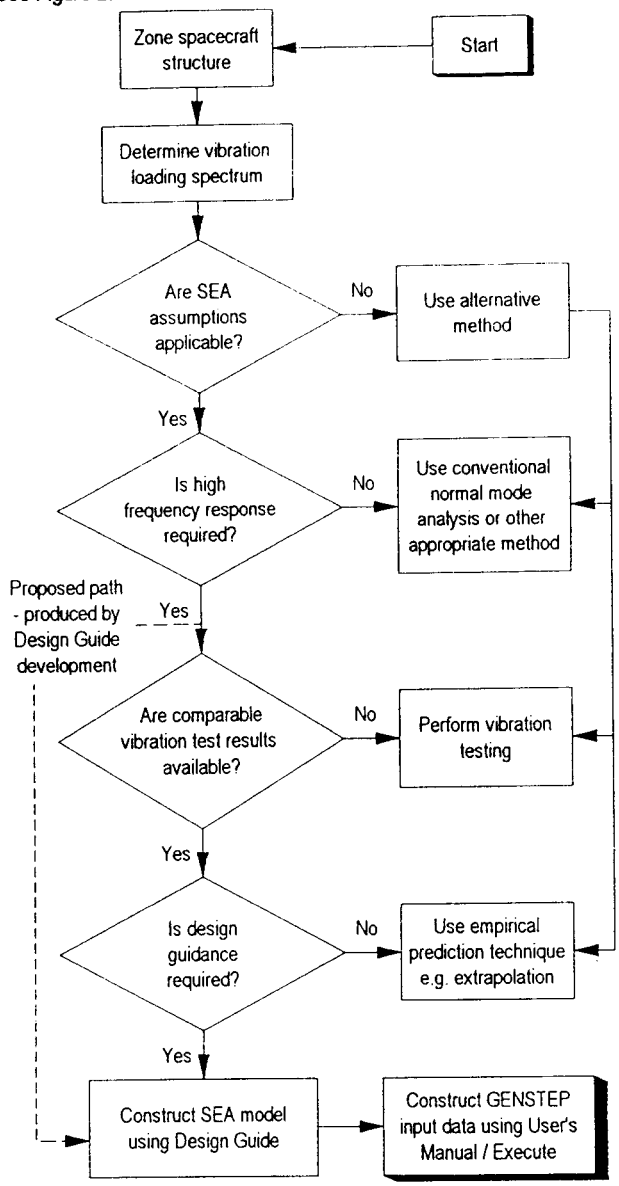

Figure 2.05.1 - SEA Modelling Procedure

STEP 1

Divide the structure configuration under investigation into zones (as defined in Topic 2.04).

STEP 2

Determine the required loading spectrum on the structure. This must be done before any prediction technique can be applied. The excitation spectrum can probably be obtained from loading specifications.

STEP 3

Construct the SEA model. Undertaking this step is determined by the following four questions:

(a) Are the assumptions of SEA [See: Topic 2.04] applicable?

(b) Is high-frequency vibration response (typically frequencies above at least 100 Hz) required?

(c) Are vibration level test results available for similarly constructed satellite configurations?

(d) Is design guidance a requirement for the method?

The answers to all four of the above questions should be positive before Step 3 is undertaken. Note, however, that the requirement of question (c) may be relaxed with the development of the GENSTEP3 prediction technique in this manual (intended to be continually updated). If the answer to a question is negative, then there are three alternatives. These are:

(a) Obtain predicted response using existing methods; for example, a conventional 'normal-mode' analysis for low-frequency response. (Information on conventional methods to be included in Chapter 11).

(b) Subject the configuration to some form of vibration testing. (This may also be necessary in order to ascertain SEA parameters for an unconventional structure.)

(c) Use a scaling method where possible. However it is noted that the scaling methods rely on extensive previous knowledge of vibration measurements on related structural configurations.

If the answer to questions (a) to (d) are positive, then the SEA model may be constructed. Reference must be made to the relevant sections of this manual for information on the modelling techniques and for guidance on the choice of the basic SEA parameters, viz., modal density, dissipation loss factor and coupling loss factor. The zones mentioned in Step 1 are used in constructing the SEA model. Chapter 8 provides guidance for the evaluation of input power and the decision of analysis bandwidth.

STEP 4

The necessary input data, used in the running of the GENSTEP3 program, must be formulated. Reference should be made to the GENSTEP3 User's Guide, Ref. [6].

STEP 5

The calculation of the equilibrium energy distribution is obtained with the aid of the GENSTEP3 program and the required form of response subsequently evaluated. It is suggested that the predicted response be compared with existing vibration specifications to ensure that the results are of the expected order. The results should always be used with a certain amount of caution, it being borne in mind that certain assumptions must be made in any prediction method.

2.06 EXPERIMENTAL OBSERVATIONS

1979 STUDY PROGRAMME

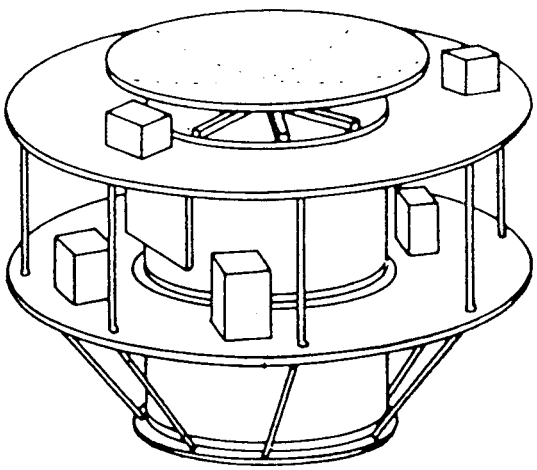

Figure 2.06.1 - Basic EX1

An experimental programme performed at the IABG acoustic facility (October 1979) provided comprehensive data on the response of various dummy satellite configurations 'EX1', [See: Figure 2.06.1], to broad-band reverberant acoustic excitation. The programme was intended as an aid to the assessment of prediction methods, in particular of satellite and equipment responses. The work is reported in Ref. [1, 7]. The main findings of the experimental, investigations are summarised as follows:

- Central core end caps reduce the high-frequency responses of the core.
- Base fixing instead of free suspension of specimen causes only negligible changes to the system response levels and interior noise levels.
- Cable harness attachment significantly reduces the local response, but has little effect on the spatially averaged response.
- Conventional platform coupled to stiffened cylindrical core increases the low-frequency response of the stiffened cylinder.
- Addition of struts to the system affects mainly those frequency bands containing the struts' natural frequencies.
- Addition of component masses to a honeycomb platform decreases the local platform response in proportion to the attached masses. However, the spatial averaged response level remains virtually unchanged to a first order of magnitude (this is subject to refinement investigation).
- Addition of component masses to a built-up platform is highly influenced by the location of the boxes relative to the monitoring accelerometers and stiffeners.
- Addition of component masses to platforms has little effect on the response of the central core structure.
- Carbon-fibre dish antennae are easily excited.
- Addition of an antenna does not significantly alter the response of the other subsystems. (Antennae are usually attached by struts).
- A small solar array attached to the central cylinder increases its response in the mid-frequency range, but the rest of the system is unaffected.
- A typical apogee boost motor (full or empty) has little effect on other components.
- Interior noise levels of shrouds are reduced by about 2 dB/bandwidth when it contains EX1.
- Shroud-enclosed EX1 configuration shows marked differences in response characteristics when compared with a configuration directly exposed to a reverberant sound field:

  In practice, satellite structures are usually tested without a shroud, presumably because a shroud is not usually available or because test-facility conditions do not favour the use of one. It is known, however, that an acoustic test with the shroud removed (but with simulated internal acoustic excitation) can produce satellite responses very different from those obtained in tests carried out with an enclosing shroud. A comparative evaluation of test methods enabling the acoustic response of shroud-enclosed spacecraft structures to be simulated has been made by F.J. On, Ref. [8], in which guidelines are developed that can be helpful in planning and performing environmental tests designed to simulate the effects of launch acoustic noise.

  F.J. On concludes that for acoustic tests carried out without a shroud, but with the spacecraft subjected to the interior acoustic levels, undertesting in the order of 10 dB in acceleration response levels can be expected.

  Tests carried out on the dummy EX1 satellite configuration similarly showed that a shroud-enclosed configuration exhibits response characteristics markedly different from those of the equivalent configuration without the shroud. The adjustment of input 'frequency-band' levels to account for the absence of the shroud offers an effective approach to the simulation of zonal response only. The successful simulation of one zone cannot guarantee successful simulation at all zones. There are currently no methods for assessing the quantitative effects of different sizes and shapes of structural configurations on shroud interior sound field. One effect of the extra boundary conditions created by the presence of 'payloads' is to raise the response frequency of the interior acoustic modes of the nett air space.

1980 STUDY PROGRAMME

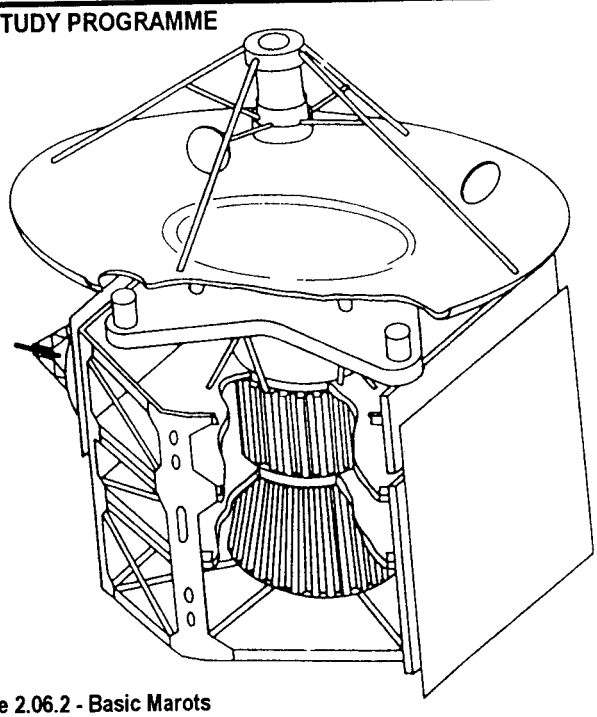

Figure 2.06.2 - Basic Marots

A later experimental programme performed at the IABG acoustic facility (November 1980) provided comprehensive data on the response of various configurations of a Marots satellite test specimen, [See: Figure 2.06.2] subjected to reverberant acoustic excitation. Many observations from these tests confirmed the above findings. Further important observations are listed below:

- The repeatability of the experimental results may give errors up to 20 - 30%.
- The measured difference in the response of subsystems coupled by struts (e.g. antenna or antenna platform) and that of the uncoupled subsystems is generally less than 20 - 30%.
- The measured difference in the response of some rigidly coupled subsystems and that of the uncoupled subsystem is again less than 20 - 30%. However, further investigation is required before this observation may be generalised.
- The measured difference in response between the loaded and the unloaded configuration is generally less than 20 - 30%.
- Corrugated cylinder and cone responses are characterised by several high response peaks. The first peak occurs around 1/4 to 1/2 of the equivalent expanded plain cylinder/cone ring frequency. The other peaks occur just below this 'equivalent ring frequency'.
- Antenna response is relatively high, particularly when feedhorn strut arrangements present a significant portion of the total antenna reflector response.
- Centre fixing of unstiffened panel components enhances low-order modes. The response of a centre-fixed plain panel has been found to be twice the order of the freely suspended panel response at low frequencies.

2.07 SEA MODELLING TECHNIQUE

SEA is able to provide estimates of complex system response because of its ability to deal with groups of modes on a statistical basis. The differing modes of a general satellite configuration are grouped according to the satellite zones defined in Topic 2.04. For any one zone, there may be a number of subsystems (for instance, in Zone 3 there may be an upper and a lower platform), and for any subsystem there may be differing classes of modes that one may wish to identify (for example flexural and torsional). If these differing sets of modes are well coupled, they may be grouped together or, if not, they may be treated as separate subsystems. Acoustic cavities within the system must be similarly identified and treated as a separate class of mode.

Each class of mode for the identified zones and acoustic cavities is represented by a 'box' in the SEA model [See Topic 2.08].

Lyon, page 239 of Ref. [2], states that one of the criteria for modal similarity in defining a subsystem 'box' is that the modes have nearly the same damping. Thus the dissipation of energy by the subsystem 'box' can be represented by a single loss factor. If there is a wide variation in damping within the analysis bandwidth, say a mode or group of modes differing by a factor of 10 from the mean, then that group should be separated to form another subsystem.

In practice, it would be difficult to measure separately the loss factor for two groups of modes in the same bandwidth on a single structural component. If the subsystem were composed of two or more components of differing structural configuration, however, such a measurement might well be possible.

The modal density of a 'box' at frequency f is an indication of the energy storage capacity of the bandwidth Δf. (Modes that resonate outside the bandwidth are not considered). The larger Δf is made, the greater the number of resonant modes for each subsystem, and accordingly the better the response estimate. A fairly exhaustive library of modal densities for shell structures exists, and the more common expressions are included in the coding of the GENSTEP3 program. Table 2.07.1 indicates the subsystem types incorporated into GENSTEP3. The user must decide whether these modal densities are adaptable to the case in question.

The energy flow coupling paths are normally identifiable from inspection of the particular structural configuration by noting a direct interface between any of the chosen zone subsystems.

Subsystem Type	Type Description	Response Type					
		Accel.	Vel.	Disp.	Strain	Stress	Press.
1	Non-catalogued type (See: Note)	✓	✓	✓			
2	Flat unstiffened panel	✓	✓	✓	✓	✓	
3	Constant section beam (transverse vibrations)	✓	✓	✓	✓	✓	
4	Constant section beam (torsional vibrations)	✓	✓	✓	✓	✓	
5	Constant section hoop (transverse vibrations)	✓	✓	✓	✓	✓	
6	Unstiffened cylinder	✓	✓	✓	✓	✓	
7	Cylinder stiffened with frames and/or stringers	✓	✓	✓	✓	✓	
8	Flat panel stiffened with stringers	✓	✓	✓	✓	✓	
9	Flat honeycomb panel	✓	✓	✓			
10	One-dimensional acoustic cavity						
11	Two-dimensional acoustic cavity						
12	Three-dimensional acoustic cavity						✓
13	Cylindrical honeycomb	✓	✓	✓			
14	Double-curved honeycomb	✓	✓	✓			

Key: ✓ - denotes response type available in program.
Note: Subsystem type 1 requires the user to input the required values of modal density and dissipation loss factors since no values are included in the program library.

Table 2.07.1 - Subsystem Type Data and Available Response Type

↓ Type of 1st Subsystem in Coupling Path		Idents of the 19 Permissible Coupling Types Available in GENSTEP3													
Type 1:	Non-catalogued type	*1	*1	*1	*1	*1	*1	*1	*1	*1	*1	*1	*1	*1	*1
Type 2:	Flat unstiffened Panel	*1		2			3	6					14		
Type 3:	Transversely vibrating Beam	*1	2				4	7	8	11				11	11
Type 4:	Torsionally vibrating Beam	*1													
Type 5:	Transversely vibrating Hoop	*1					5								
Type 6:	Unstiffened Cylinder	*1	3	4		5			9	12			15	12	12
Type 7:	Stiffened Cylinder	*1	6	7					10	13			16	13	13
Type 8:	Flat stiffened Panel	*1		8			9	10					17		
Type 9:	Flat honeycomb Panel	*1		11			12	13					18		
Type 10:	1-D Acoustic Cavity	*1													
Type 11:	2-D Acoustic Cavity	*1													
Type 12:	3-D Acoustic Cavity	*1	14				15	16	17	18			19	18	18
Type 13:	Cylindrical Honeycomb	*1		11			12	13					18		
Type 14:	Double-curved Honeycomb	*1		11			12	13					18		
Type of 2nd Subsystem in Coupling Path →		1	2	3	4	5	6	7	8	9	10	11	12	13	14

Key: * Coupling Loss Factor for Coupling Path Type 1 must be supplied by the user, as no program defined types are available

Table 2.07.2 - GENSTEP3 Subsystem Coupling Type Data

The coupling paths are represented by an arrowed line on the SEA model. The GENSTEP3 program contains the necessary subroutines to enable the 'structure-acoustic cavity' coupling to be estimated for the more commonly used structural configurations. Table 2.07.2 is a listing of the catalogued coupling paths recognised by GENSTEP3. It is noted that for the particular case of a panel with both sides subjected to a reverberant noise field, the program coding is such that one must include two coupling paths between the panel and the acoustic space. Chapter 8 gives more information on power input.

The nonresonant coupling path between two acoustic cavities is recognised by GENSTEP3 and must be included in the model. There is no theory readily adaptable to the case of structure/structure coupling. If experimental information relating to the relevant structure/structure coupling is available and is used in the model, it is important that the direction of the coupling should be taken into account. Reverse coupling loss factors are computed by GENSTEP3, making use of the reciprocal coupling relation.

In the SEA model, all coupling paths with the excitation field are included as power inputs. The same comments that apply for coupling loss factors in general apply to power inputs in the particular case of a reverberant excitation field. It is noted, however, that the reverse coupling (component excitation field) is ignored in any subsequent analysis. Different types of power input may be included in the analysis (for example random mechanical power input, turbulent boundary layer). Table 2.07.3 gives a list of power input types incorporated in GENSTEP3.

Input Power Type	Description
1	Non-catalogued type [See: **Note**]
2	Direct power input to a structural subsystem form an acoustic field
3	Direct power input to an acoustic cavity subsystem from an acoustic field due to mass law sound transmission through an adjacent structural subsystem
4	Mechanical input to a structural subsystem
5	Mechanical input to an acoustic cavity subsystem

Note: Power type 1 requires the user to input the required values of power input since no values are included in the program library

Table 2.07.3 - Input Power Type

No theory is available in the GENSTEP3 coding for these alternate sources of power input, but they can be modelled as an uncatalogued type. As noted for two cavities, the direct power input to an acoustic cavity due to mass law sound transmission through an adjacent structural subsystem must be included in the model.

There is no hard and fast rule as to how complex, or simplified, the SEA model should be made. One should be careful, however, of making the SEA model too refined; it must be possible to evaluate the necessary parameters to a similar degree of accuracy. Modelling with many subsystems requires the evaluation of many parameters and can introduce uncertainties which result in a response estimate having no greater accuracy than a simpler system.

The guidelines for SEA modelling presented below are based on experimental observations and experience gained in the use of SEA and GENSTEP3:

(a) Do not overcomplicate the SEA model. Keep the model as simple as possible. Increasing the complexity certainly increases the work, but does not necessarily increase the accuracy.

(b) When the response of the shroud is not required, it is best omitted from the overall model. The excitation field acting on the contained structure has to be ascertained. As a first approximation, it can be taken as the internal field in the shroud cavity. This is found by modelling the shroud alone for a sound transmission estimation, [See: Chapter 7], with the effect of the satellite structure in the enclosure simply allowed for as described in Topic 7.03.
Note: For most practical applications, the sound pressure levels inside the enclosure are stated in the loading specification, e.g. Thor-Delta, Ariane or Space Shuttle cargo bay.

(c) When modelling **stiffened** central shell structures, always include any stiffening members (e.g. stringers or frames) in the model.

(d) As regards the modelling of corrugated structures, the simplest method is to consider an equivalent plain skin structure and use the expanded area (and in the case of cylinders or cones, the equivalent expanded radius). If extra stiffeners or frames are used these should also be included in the model.
Note: There are known deficiencies in this method. The modelling method will be revised when more information becomes available.

(e) When modelling honeycomb platforms/panels, include any inserts in the model (assuming smeared mass), but do not include any stiffening members or equipment boxes. Damping effects of stiffening members or boxes may be included in the DLF parameter.

(f) When modelling conventionally stiffened platforms/panels, include the stiffening members in the model, but do not include any equipment boxes. Damping effects of stiffening members or boxes may be included in the DLF parameter.

(g) Deduce equipment box response from the response of the subsystem to which they are attached and the subsystem-box impedance values.

(h) For a structure assumed only to be subjected to acoustic excitation, do not include relatively 'massive items' such as apogee boost motor (ABM) in the SEA model. The response of a massive item to acoustic excitation is generally negligible.

(i) It is not necessary to include struts in the SEA model, but bear in mind the effect they may have on the damping/stiffness properties of the structure and their effect on adjoining system response at the struts' fundamental frequencies or the frequency band in which these frequencies lie.

(j) It is not usually necessary to model end caps of central support structure or shroud structure. Include effects of changes to damping on the adjoined subsystem (DLF's).

(k) It is not usually necessary to model sound transmission through the ends of a cylinder whether closed or open (model cavity with only direct and mass-law inputs from cylinder).

(l) Nonresonant mass-controlled sound transmission has to be considered whenever a cavity is included in the SEA model. This means allowing for an additional input path.

(m) If a secondary subsystem has a much lower modal energy than a neighbouring subsystem and is not 'in-line' with another subsystem, the subsystem may be ignored or, at most, the coupling loss factor may be included as part of the damping of the dominant subsystem.

(n) Only include coupling paths that would appear to be dominant.

(o) If two linked structural subsystems of similar modal density are equally exposed to a reverberant sound field, then their modal energies will be similar. Consequently, the nett energy flow between the subsystems will be small in comparison with the energies received from the acoustic field.

(p) Assume coupling through struts to be negligible.

Note: Details of subsystem structures and their SEA parameters will be found in the relevant zones' chapter.

2.08 SEA MODELLING EXAMPLES

SEA models are presented for various satellite and space-vehicle configurations, see Figures 2.08.1 to 2.08.15, inc. These examples have been taken from different references and serve to demonstrate the different styles of writing and degrees of complexity of SEA models. Tables 2.08.1 and 2.08.2 present examples of recommended SEA models for different EX1 and Marots satellite configurations previously studied (sketches of the satellites are shown previously in Figures 2.06.1 and 2.06.2). A GENSTEP3 run for model 1, Table 2.08.1, is given with full input and output in the GENSTEP3 User's Manual.

SEA modelling options are shown in Figures 2.08.2, 2.08.3 and 2.08.4. In these cases, the acoustic power input would be defined by use of the ACARD [See: Chapter 8] since no separate acoustic subsystem is shown.

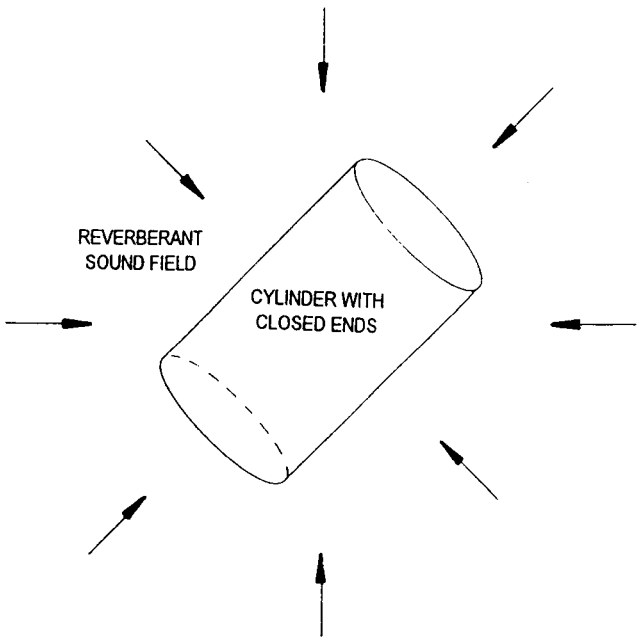

Example 1: Cylinder with Closed Ends

Figure 2.08.1 - Example 1 Structure

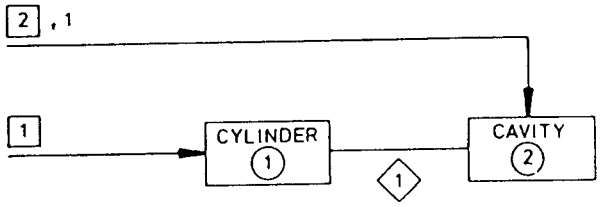

Notation:

- ○ Subsystem identity
- □ Power input identity
- □,1 Mass law power input identity through subsystem1, etc.
- ◇ Coupling path identity

Figure 2.08.2 - SEA Model: End Caps assumed to be nontransmitting

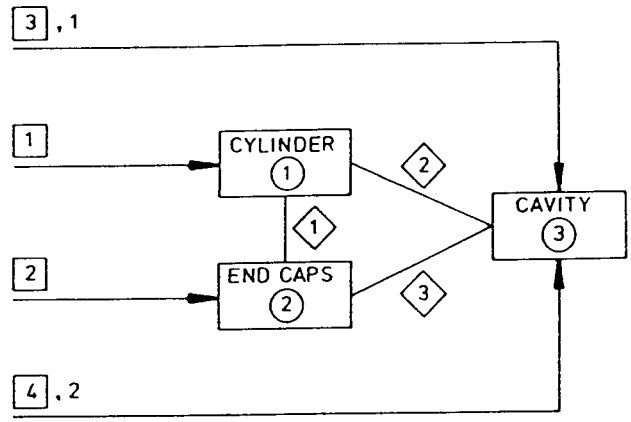

Notation:

- ○ Subsystem identity
- □ Power input identity
- □,1 Mass law power input identity through subsystem1, etc.
- ◇ Coupling path identity

Figure 2.08.3 - SEA Model: End Caps assumed to transmit identically

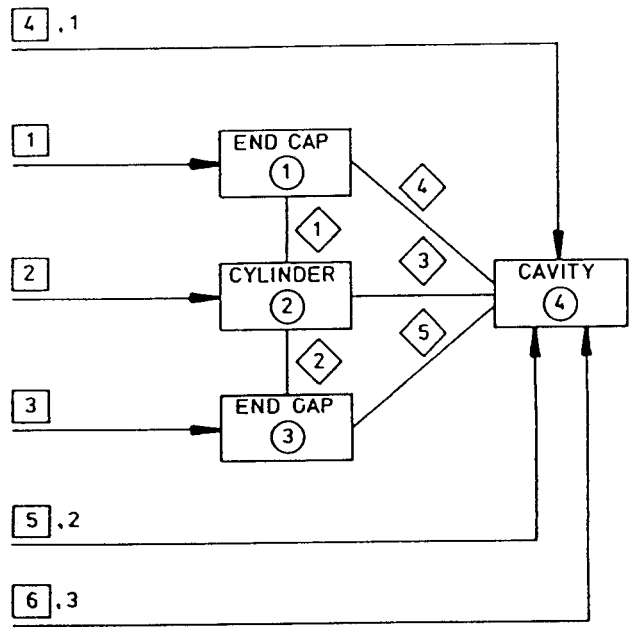

Notation:

- ○ Subsystem identity
- □ Power input identity
- □,1 Mass law power input identity through subsystem1, etc.
- ◇ Coupling path identity

Figure 2.08.4 - SEA Model: All Components being Considered

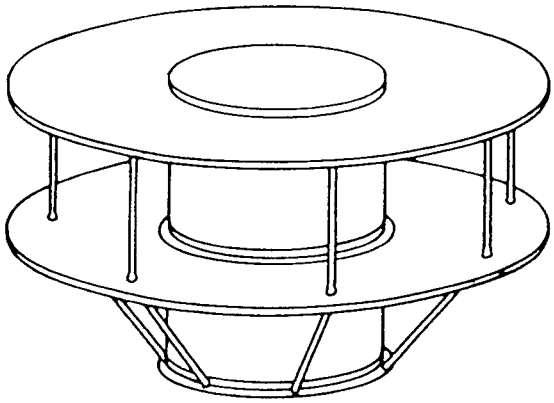

Figure 2.08.5 - Example 2: Structure

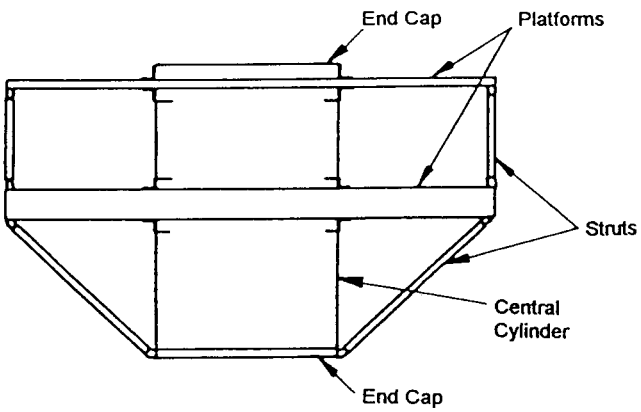

Figure 2.08.6 - Example 2 :Structural Model

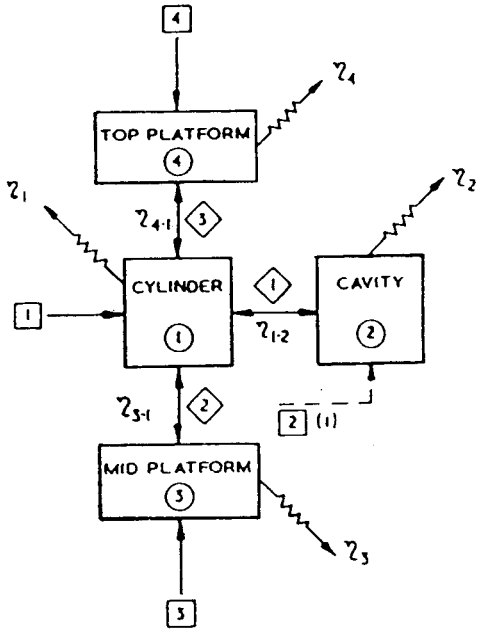

Figure 2.08.7 - Example 2 :SEA Model (1)

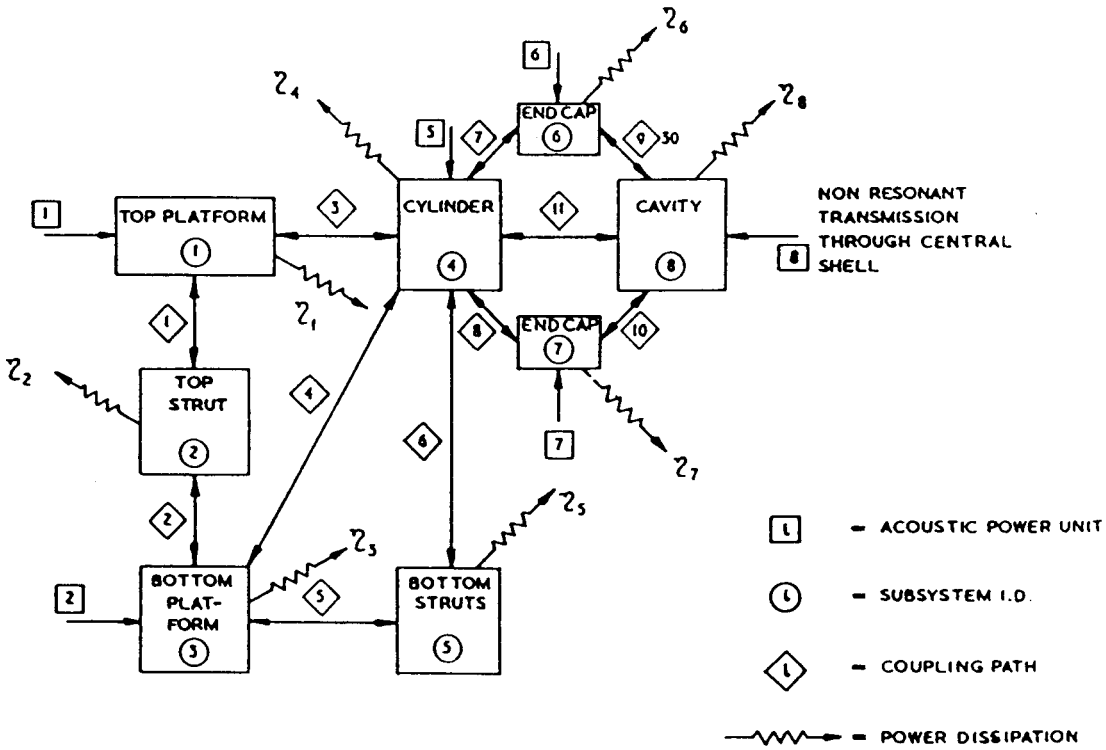

Figure 2.08.8 - Example 2 :SEA Model (2)

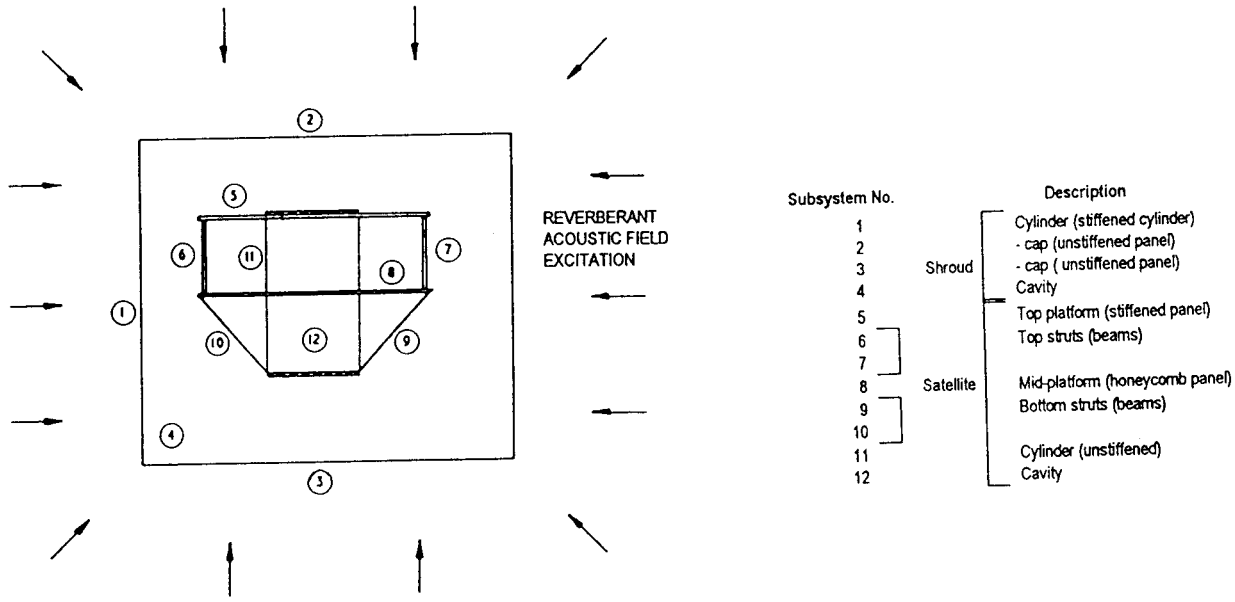

Example 3: Simple EX1 Configuration Enclosed in a Shroud

Figure 2.08.9 - Example 3 : Structural Model

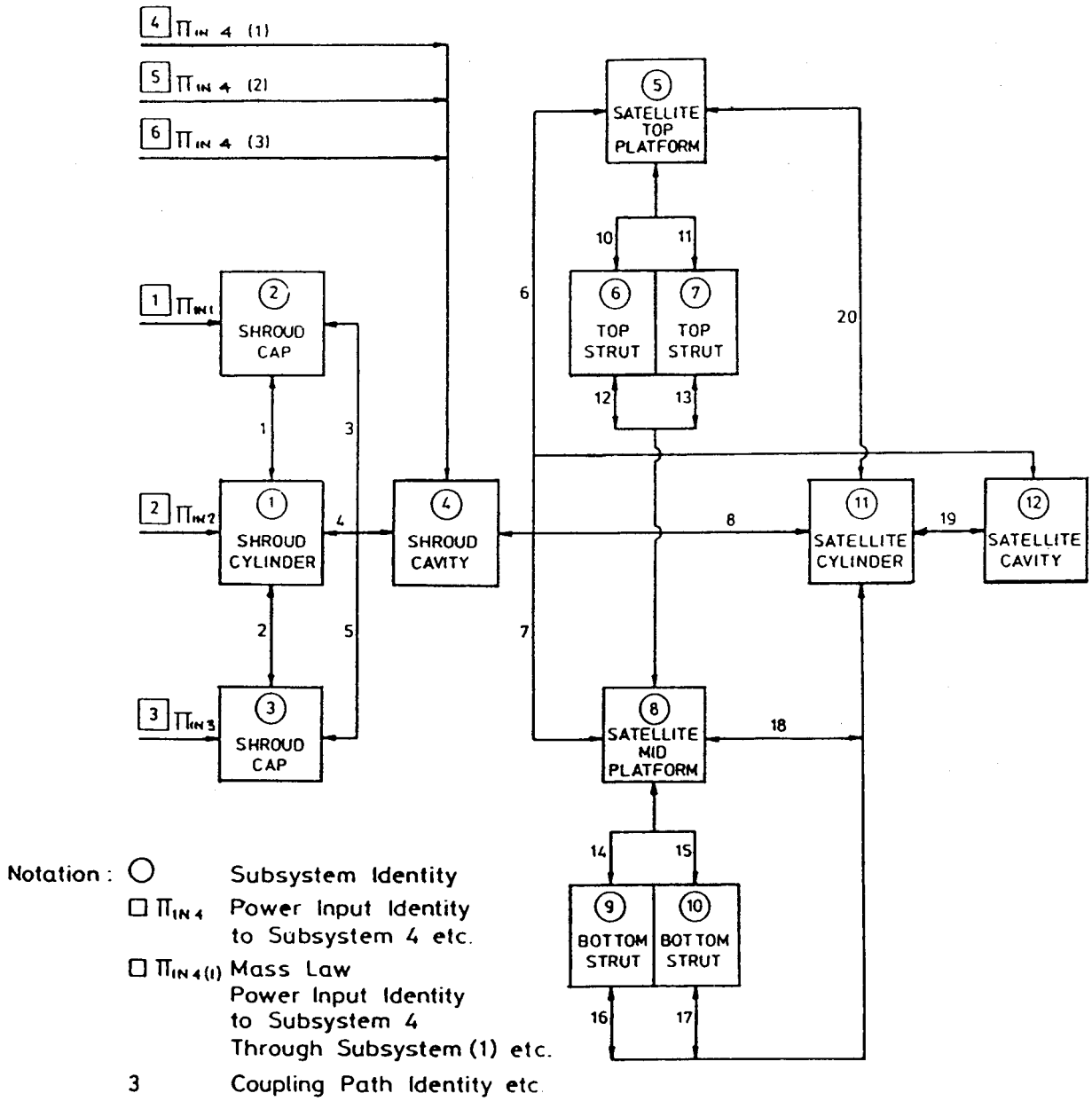

Figure 2.08.10 - Example 3: SEA Model

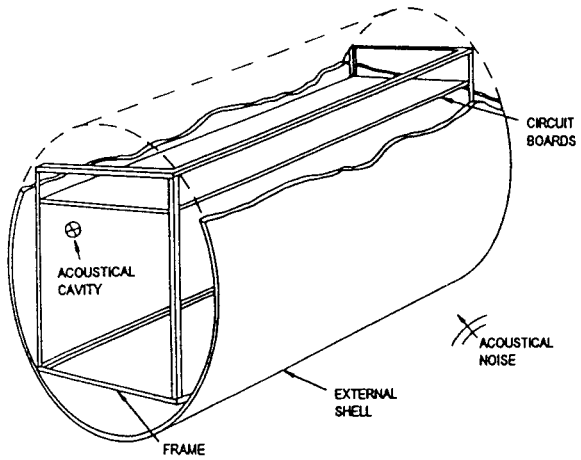

Example 4: Airborne Computer Assembly (from Ref. [2])

Figure 2.08.11 - Example 4: Structure

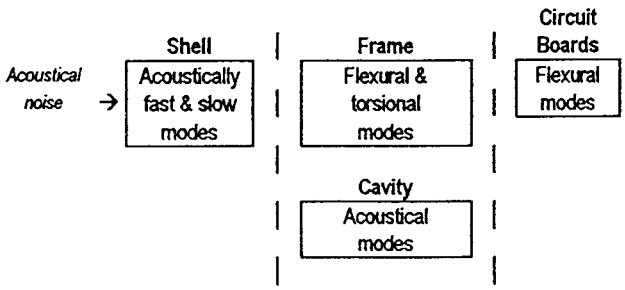

Note: See also Figure 2.08.11

Figure 2.08.12 - Major Sections of the Subsystem

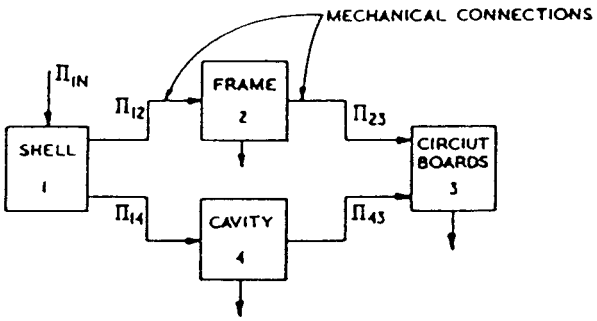

Notation:

2	Subsystem identity, etc.
Π_{1IN}	Input power identity to subsystem 1, etc.
Π_{23}	Coupling path identy between subsystems 2 & 3, etc.

Figure 2.08.13 - Example 4: SEA Model (1)

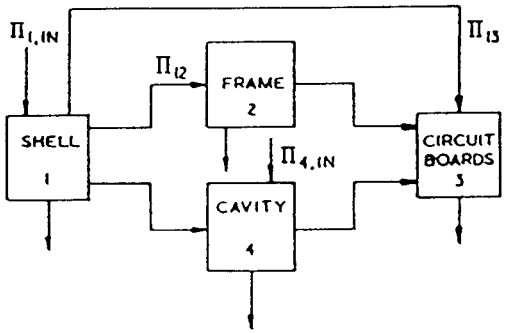

Notation:

2	Subsystem identity, etc.
Π_{1IN}	Input power identity to subsystem 1, etc.
Π_{23}	Coupling path identy between subsystems 2 & 3, etc.

Figure 2.08.14 - Example 4: SEA Model (2)

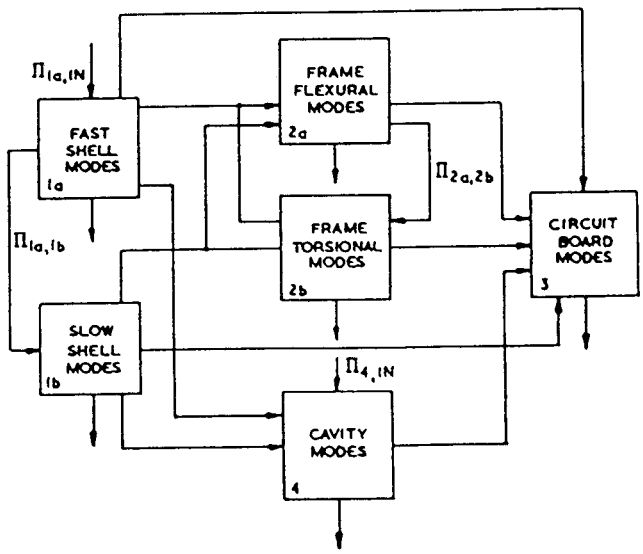

Notation:

2	Subsystem identity, etc.
Π_{1IN}	Input power identity to subsystem 1, etc.
Π_{23}	Coupling path identy between subsystems 2 & 3, etc.

Figure 2.08.15 - Example 4: SEA Model (3)

STRUCTURAL MODEL	SEA MODEL "COUPLED COMPONENTS"	"UNCOUPLED COMPONENTS"	NOTES
1 	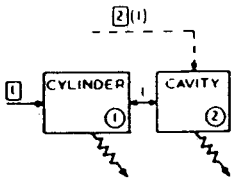		Open cylinder cavity no direct input
2 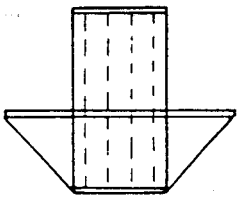	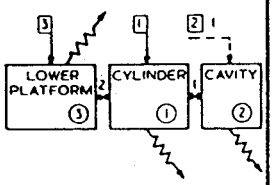		Two inputs to platforms - one either side.
3 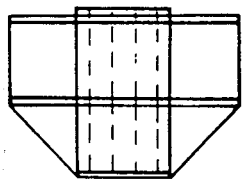	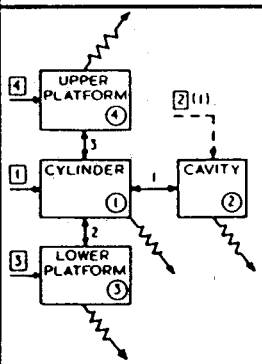		Struts not modelled
4 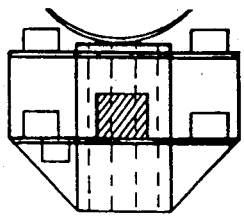	AS FOR 3	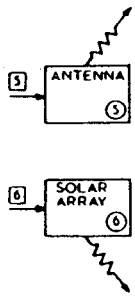	Omit ABM Boxes Cables - obtain box response from unloaded panel response prediction and impedance values

Table 2.08.1 - EX1: Recommended System Configuration Models

STRUCTURAL MODEL	SEA MODEL "COUPLED COMPONENTS"	UNCOUPLED COMPONENTS"	NOTES
5 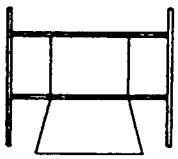	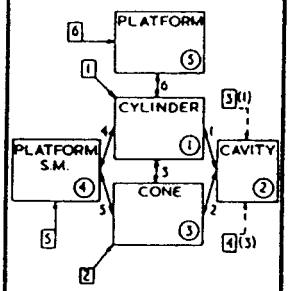	PANEL S.M. 6 PANEL S.M. 7 PANEL C.M. 8 PANEL C.M. 9	Dissipation arrow ~~~→ may be omitted from diagram to avoid confusing overwriting - the presence of subsystem dissipation is assumed.
6 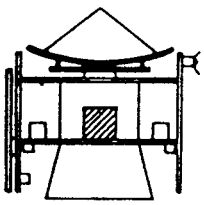	AS FOR 5	AS FOR 5 + ANTENNA PLATFORM 10 L/B ANTENNA 11 S.B. ANTENNA 12	As for 4. Also note, subsystem attached by struts is modelled uncoupled.
7 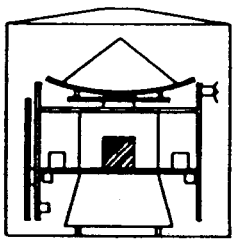	AS FOR 5	AS FOR 6	Shroud not modelled. Excitation field taken as internal field of shroud.

Note: See also Figure 2.06.2

Table 2.08.2 - Marots: Recommended System Configuration Models

2.09 REFERENCES

[1] R.J. Cummins & W. Cooper
'Spacecraft structural acoustic studies'
Final report - ESA CR(P)-1264

[2] R. H. Lyon
'Statistical energy analysis of dynamical systems: theory and applications'
MIT Press (1975)

[3] F.J. Fahy
'Statistical energy analysis - a critical review'
Paper presented at a Colloquium of the Commission Acoustique S51 du Conseil International du Bâtiment, Liverpool (1973)

[4] J.J. Pocha
'Study of the acoustic excitation of structure, theory'
Final Report Vol. 1, (ESA Contract Study)

[5] B.L. Clarkson, R.J. Pope & M.F. Ranky
'Experimental work to evaluate parameters required in the SEA prediction method'
ESA Contract No. 4100/79/NL/PP Rider 1 (1981)

[6] P.J. Williams
GENSTEP2 Users Manual, Version 1.0
BAe Document No. GEN/B45/42592 (1986)
Revised 1994 to GENSTEP3 Users' Manual
ISVR Consultancy Services, Document Ref. R05 4274

[7] R.J. Cummins & I.G. Gray
'Spacecraft structural acoustic studies - investigation, interpretation and simulation of the effects of configuration features on noise-induced structural vibration and sound-transmission characteristics'
Final report. ESA CR(P)- 1366 (1980)

[8] F.J. On (Goddard Space Flight Center)
'A comparative evaluation of test methods to simulate acoustic response of shroud enclosed spacecraft structures'
Paper presented at the 86th Meeting of the Acoustical Society of America, L.A., Calif. (1973)

[9] L. Westin
'Evaluation of Random Vibration and Acoustic Test Results of a Number of ESA Satellites'
ESA Report TTS/78/0036/HR

(Intentionally Left Blank)

Structural Acoustics Design Manual

Chapter 3
PREDICTION OF STRUCTURAL RESPONSE OF ZONE 1 CYLINDERS SUCH AS CENTRAL CORE CYLINDER
(Satellite Core Structure & Cylindrical Shells)

CONTENTS

3.01 GENERAL

The theory presented in the BAe Final Report, Ref. [1], for the SEA prediction of response levels on a cylindrical shell is relevant to most satellite and other aerospace structures. It assumes that the ring frequency, f_r, is less than the lowest coincidence frequency, f_c, which means that the cylinder radius is much greater than the shell thickness. It is assumed that the cylindrical structures referred to in this chapter are of that configuration.

The following types of central support structure (or cylindrical shells) are used:

(a) Unstiffened cylinder;

(b) Conventionally stiffened cylinder;

(c) Integrally stiffened (machined) cylinder,

(d) Corrugated cylinder,

(e) Honeycomb cylinder;

(f) Polygonal shell.

In addition, the core could be a conical configuration comprised of any of the structural types (a) to (f).

The three extreme-end configurations possible for a thin-walled cylindrical shell are shear diaphragm (SD), clamped (C) and free (F). The combinations of these boundary conditions most commonly encountered in satellite structures are:

- F-F open-ended and suspended,
- C-F open-ended and base-fixed,
- SD-SD closed and suspended,
- C-SD closed and base-fixed.

An example of an SEA model for a closed cylinder is shown in Figure 3.01.1

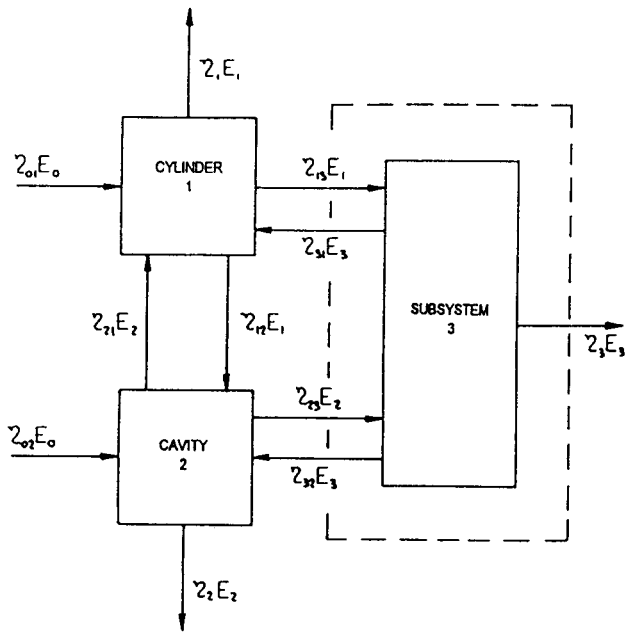

For subsystem 1:

$$\eta_1 E_1 + \eta_{13} E_1 + \eta_{12} E_1 = \eta_{01} E_0 + \eta_{31} E_3 + \eta_{21} E_2$$

Figure 3.01.1 - SEA Model of Closed Cylinder

The model includes a 3-D cavity coupled to the cylindrical shell, but would not necessarily include a coupled subsystem. The following section includes the modelling details for a 3-D cavity, although further information is to be found in Chapter 7 - Sound Transmission.

The required SEA parameters are:

- modal density,
- coupling loss factor, and
- dissipation loss factor.

Where experimental results are available for typical cylindrical shell structures, they are included in this section. Further information is given for loss factors in Chapter 9 and on the recommended test methods in Chapter 10.

The response of the end caps in the case of SD-SD and C-SD boundary conditions is not included in the general discussion since the structure/structure coupling is considered to be of secondary importance. There is a note on the response of end caps in Topic 3.09.

3.02 SEA PARAMETERS FOR TYPICAL ZONE 1 STRUCTURES

The types of typical Zone1 structures described are:

- Unstiffened Cylindrical shell, [See: Topic 3.03].
- Conventionally stiffened shell, [See: Topic 3.04].
- Integrally machined cylinders, [See: Topic 3.05].
- Corrugated cylinder, [See: Topic 3.06].
- Honeycomb cylindrical shell structure, [See: Topic 3.07].

3.03 UNSTIFFENED CYLINDRICAL SHELL

MODAL DENSITY

The modal density of an unstiffened cylinder is included as a subroutine in the GENSTEP3 program. The expressions used are given in the Appendix A, from Ref. [1]. The modal density expression used assumes independence of boundary conditions, i.e.:

$$n(f)_{F-F} = n(f)_{C-F} = n(f)_{SD-SD} = n(f)_{C-SD}$$

The modal density of a 3-D cavity is included as a subroutine in the GENSTEP3 program. Care must be taken when this formulation is used at low frequencies in the case where the acoustic wavelengths are of the same order as the geometric dimensions of the cavity, [See: Chapter 7].

DISSIPATION LOSS FACTOR

Chapter 9 presents measured values obtained for a typical unstiffened cylinder. The values suggest that the DLF is almost constant with respect to frequency.

Note: Data for the DLF of a 3-D cavity are presented in Chapter 7.

COUPLING LOSS FACTOR

There are three kinds of coupling to be considered in the SEA model [shown in Figure 3.01.1]:

- structure/structure coupling,
- structure/acoustic-cavity coupling,
- acoustic-cavity/acoustic-cavity coupling.

The coupling loss in a specific direction being given, the complementary CLF may be found from the reciprocal relationship in each bandwidth:

$$\eta_{pq} = \eta_{qp} \cdot \frac{n(f)_q}{n(f)_p}$$

The structure/acoustic-cavity coupling and the acoustic-cavity/acoustic-cavity coupling may be evaluated theoretically with the aid of standard sound-transmission and coupling formulae, available in BAe Final Report, Ref. [1]. The theory is included in respective subroutines in the GENSTEP3 program based on the expression given in Appendix A.

Currently, not much theoretical information is available for structure/structure coupling. Some experimental results are available, [See: Topic 9.06].

3.04 CONVENTIONALLY STIFFENED CYLINDER

The general comments made concerning the unstiffened core are similarly applicable to the conventionally stiffened cylinder. Conventional stiffening is most likely to be in the form of longitudinal stringers and frames. Since this stiffening affects the mass and modal density of the structure, the difference in the SEA parameters must be considered. The comments presented below give guidance in obtaining the influence of the stiffening on the spatially averaged response of the shell. They do not, unless otherwise stated, give guidance for the prediction of the response of the stiffeners themselves,

MODAL DENSITY

The modal density of a stiffened cylinder is assumed to be the sum of the modal densities of the constituent parts in each bandwidth. For a cylinder stiffened by stringers and frames, the modal density is:

$$n(f)_{\text{stiffened cylinder}} = n(f)_{\text{unstiffened cylinder}} + n(f)_{\text{stringer}} + n(f)_{\text{frame}}$$

GENSTEP3 incorporates the necessary subroutines, but care should be taken when inputting the required SUBSYS data, in particular:

t Thickness of cylindrical shell (do not use 'smeared' thickness),

m Mass per unit area (use 'smeared' mass of the stiffeners and frames over the cylinder surface area).

DISSIPATION LOSS FACTOR

Chapter 9 presents the DLF for a typical stiffened cylinder. The measurements were obtained by the energy method and highlighted the differences in low-frequency damping between an open and a closed cylinder. The DLF of the cavity is assumed to be similar to that in the case of an unstiffened cylinder. In practice, it may be slightly different, since the absorption characteristics of the cylinder may change.

COUPLING LOSS FACTOR

The comments made in the case of the unstiffened cylinders also apply in that of the stiffened cylinder. In the region $f_r < f < f_c$ however, the cylinder, when coupled to an acoustic cavity, acts much like a flat plate. Care must be taken to input the effective perimeter correctly if the GENSTEP3 subroutine is to be used.

RESPONSE OF STIFFENERS

To obtain the response of a stiffener, the following procedure can be used. Assume the cylinder/stiffener coupling is considerably greater than the stiffener damping. The modal energies of the cylinder and the stiffener are therefore:

$$E_{\text{stiffener}} = \frac{n(f)_{\text{stiffener}}}{n(f)_{\text{cylinder}}} \cdot E_{\text{cylinder}}$$

3.05 INTEGRALLY MACHINED CYLINDER

The modelling of the shell depends upon the extent of the machining. If the spacing of the machined stiffeners is small, it is suggested that the core be modelled as an unstiffened cylinder, where 't' is an equivalent smeared thickness. It is then advisable to check whether for the smeared thickness the ring frequency is still less than the critical frequency. If the spacing of the machined stiffeners is large, it is suggested that the shell be modelled as for a stiffened cylinder, where 't' is the skin thickness (stiffener thickness not smeared) and M is a smeared mass per unit area of structure.

MODAL DENSITY

The modal density is assumed to be that of an unstiffened or a stiffened cylinder, [See: previous paragraph].

DISSIPATION LOSS FACTOR

It is recommended that the structural DLF of the shell be treated like that of an unstiffened cylinder. The DLF of the stiffened cylinder is expected to be slightly higher than that of the unstiffened one. The 3-D cavity is treated as in the unstiffened case.

3.06 CORRUGATED CYLINDER

The behaviour of the corrugated cylinder is not fully understood. When compared with an unstiffened plain cylindrical shell, it shows not only a high response in the region associated with cylinder ring frequency, but also similar magnitude response peaks at 1/4 to 1/2 of the ring frequency. This property is associated with the modal density prediction, and several methods for estimating this are given.

MODAL DENSITY

No accurate formulation is available for inclusion in GENSTEP3. So, unless experimental values of modal density are available or can be measured for the relevant structure, the following procedures are presented:

(a) As a first approximation, one can use the flat panel value as calculated from the expression in Topic 6.03. The cylinder is considered 'unwound' as a flat corrugated plate, the resulting modal density being constant with frequency.

(b) An approximation based on the modal density of an unstiffened plain cylinder and an empirical scaling factor. GENSTEP3 is run to predict the modal density for an equivalent (expanded) plain cylinder using:

A = total expanded surface area of corrugated core (a x b) [See: Topic 6.03]

R = equivalent expanded radius = $\dfrac{a}{2\pi} = \dfrac{A}{2\pi \cdot b}$

The ring frequency used in this calculation is based on this equivalent expanded radius, whether the ring frequency exists in the same manner or the frequency for the corrugated cylinder is not yet resolved. It is known that the modal density of the plain cylinder becomes asymptotic to that of the flat panel (same A) at frequencies above the ring frequency. The scaling factor is based on the difference between the values for a plain and a corrugated panel having the same area ($A = a.b$):

$$C = \frac{n(f)_{\text{corrugated}}}{n(f)_{\text{plain}}} = \left[\frac{t}{3.464} \left(\frac{Ay}{Iy} \right)^{\frac{1}{2}} \right]^{\frac{1}{2}}$$

This factor will generally have a value in the range 0.14 - 0.20. An evaluation based on this method will give a better estimate in the low-frequency and 'ring-frequency' regions, but will underestimate the observed peak which exists between these regions. It is recommended that the effects of circumferential stiffening frames be ignored.

(c) Modal densities have been predicted with the aid of a modified version of the VIPASA computer program called VISCAN, Ref.[2, 3, 4]. The VIPASA program can find all required natural frequencies of any prismatic assembly of flat plates which are simply supported at their ends and are rigidly connected along their longitudinal edges. The modifications used by VISCAN are described in Ref. [2]. A compact version of the program, MINIVIPA, together with its documentation, has been published, Ref. [5], and has been similarly modified to produce MINISCAN. This latter program was used to check the results of Ref. [2].

Note: It was considered worth drawing attention to this method of evaluating modal density as it has demonstrated a close resemblance with the analytical solution (as included in GENSTEP3) for the modal density of a plain cylinder and also has been found to compare well with measurements for corrugated panels and cylinders. Although VIPASA and associated programs are available commercially to various users, they are not directly associated with BAe or ESA contracts.

DISSIPATION LOSS FACTOR

Only limited information is available; it is suggested that a DLF of 0.006 is used, [See: Chapter 9].

COUPLING LOSS FACTOR

Again, information is limited; a value of 0.0012 has been measured for honeycomb platform to corrugated cylinder, [See: Chapter 9].

3.07 HONEYCOMB CYLINDRICAL SHELL STRUCTURE

There is little theoretical or experimental information available on the SEA parameters for a honeycomb sandwich construction used as a cylindrical shell. It is recommended that the core be modelled as an uncatalogued subsystem type and that the user input appropriate experimental information as regards modal density, DLF and CLF. If no other information is available, however, the following guide should be used - with caution.

Treat as an unstiffened cylinder with the following amendments to the input subsystem data:

R = mean radius of core,

A = surface area of core,

$$t = \text{equivalent thickness} = \frac{\left(\rho_{f1}h_{f1}+\rho_{f2}h_{f2}+\rho_c h_c\right)}{\rho_m}$$

where: ρ_{f1}= density of facesheet 1, ρ_m = density of equivalent homogeneous plate and h_{f1} = thickness of facesheet 1.

MODAL DENSITY

The user must input the modal density in the form of a table.

Appendix A [Topic A.11] gives an expression for cylinders with identical faceplates.

DISSIPATION LOSS FACTOR

As a guide, a typical DLF for a honeycomb panel is 0.01, [See: Chapter 9].

COUPLING LOSS FACTOR

The recommendations made for the unstiffened cylinder also apply here.

3.08 CONICAL SHELL STRUCTURE

Note: This section will be revised.

There is no adequately proven prediction method, but the following procedure is recommended in the absence of other information. The main problem is that of evaluating the modal density. The comments here refer to a conical configuration constructed from plain skin. There is also a short note on corrugated and stiffened conical configurations at the end of the chapter. For other types of construction, the user is referred to the relevant subsection on cylindrical structures, [See: Topic 3.04, 3.05,etc.], for the differences to be expected between the various forms of construction. The method of modelling suggested is described.

FOR SMALL TO MODERATE CONE ANGLES

The input to GENSTEP3 is to be taken as that for an equivalent cylinder. The equivalent cylinder input data are as follows:

$$R = \frac{R_L + R_S}{2}$$

and:

$$A = 2\pi RH$$

these dimensions being as shown in Figure 3.08.1.

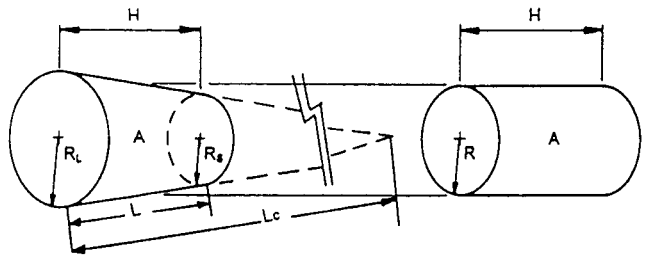

CONE EQUIVALENT CYLINDER

Figure 3.08.1 - Cone and Equivalent Cylinder

The response of this equivalent cylinder gives an approximate estimate for the response of a conical shell with a small to moderate cone angle, as shown in Figure 3.08.2.

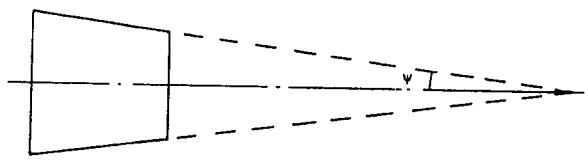

Note: A limit of Ψ <20° is suggested

Figure 3.08.2 - Limiting Cone Angle

Modal density

The modal density of the conical shell of small to medium cone angle is assumed to be the same as that of an equivalent cylinder. The equivalent cylinder modal density may be calculated by means of GENSTEP3.

For large cone angles; based on Ref. [6] (with corrections):

Low frequencies; $\Omega_1, \Omega_2 < 1$; $n(f) = \dfrac{0.83 A \Omega_1^{1/2}}{hc(\cos\theta)^{1/2}(L/L_c)^{1/4}}$

High frequencies; $\Omega_1, \Omega_2 > 1$; $n(f) = \dfrac{1.27}{(L/L_c)^{1/5}} \cdot \dfrac{A}{ch}$

where:

$\Omega_1 = \omega R_L/c$, $\Omega_2 = \omega R_L/c$,

$c = (E/\rho)^{1/2}$, R_L = radius of base, R_S = radius of top,

ω = frequency (rads.),

A = surface area of truncated conical surface,

h = wall thickness, L & L_c = slant heights (see Figure 3.08.1).

Note: For **corrugated conical** structures:

(a) As a first approximation, for corrugated conical structures with a small cone angle, the flat corrugated panel value can be used as calculated from the expression in Topic 6.03. The cone is considered 'unwound' and the resulting modal density is constant with frequency.

(b) If the modal density is to be calculated by the equivalent cylinder method, then values for an equivalent expanded plain cylinder should be input to GENSTEP3, [See: Figure 3.08.3], where:

A_{EXPD} = expanded surface area of corrugated area

R_{EXPD} = equivalent expanded radius $= \dfrac{A_{EXPD}}{2\pi H}$

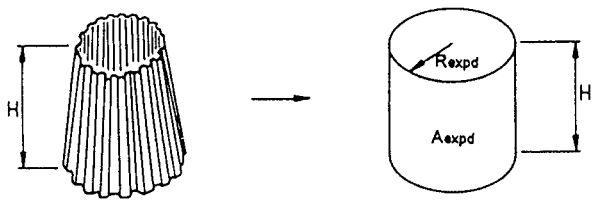

Figure 3.08.3 - Corrugated Cone and Equivalent Expanded Cylinder

This relationship is subject to future revision.

Dissipation loss factor

Some information is given in Chapter 9. DLF for a corrugated cone should be similar to that for a corrugated cylinder.

Coupling loss factor

Some information is available in Chapter 9.

3.09 MISCELLANEOUS

Coupling of satellite end caps (diaphragms) to other structural subsystems is generally found to be of second order and therefore may be neglected. If the response of the end caps is required, then the easiest method is to model them alone.

3.10 REFERENCES

[1] R.J. Cummins & W. Cooper
'Spacecraft structural acoustic studies'
Final report - ESA CR(P)-1264

[2] F.W. Williams & J.R. Banerjee
'Accurately computed modal densities for panels and cylinders including corrugations and stiffeners'
UWIST Tech. Report. (To be published in the Journal of Sound and Vibration)

[3] W. Wittrick & F.W. Williams
'Buckling and vibration of anisotropic or isotropic plate assemblies under combined loading'
International Journal of Mechanical Sciences, 16, 209 (1974)

[4] W.J. Stroud & M.S. Anderson
'PASCO: Structural Panel Analysis and Sizing Code, Capability and Analytical Foundations'
NASA TM-80181 (1981)

[5] F.W. Williams & C.J. Wright
'A compact computer program for calculating buckling stresses and natural frequencies of vibration of prismatic plate assemblies'
Int. Journal for Numerical Methods in Engineering, 12, 1429 (1978)

[6] F.D. Hart & K.C. Shah
'Compendium of Modal Densities for Structures'
NASA CR-1773, July 1971

(Intentionally Left Blank)

Structural Acoustics Design Manual

Chapter 4
PREDICTION OF STRUCTURAL RESPONSE OF ZONE 2
(Platforms Subjected to Direct Acoustic Excitation)

CONTENTS

4.01 GENERAL

The theory underlying the prediction of the response of an external platform with the aid of SEA techniques is outlined in Appendix A; taken from Ref. [1]. The following types of platform construction are available:

- plain (unstiffened plate),
- conventionally stiffened,
- integrally machined,
- corrugated,
- honeycomb.

Probably the most common construction for satellite design is the honeycomb platform, where the prediction of response may be further complicated by the use of metallic or non-metallic face sheets on a metallic or non-metallic core.

In general, the boundary conditions of a platform external to a central support structure are such that it may be considered clamped on the inner edge and free on the outer edge. The basis for the SEA model is shown in Figure 4.01.1.

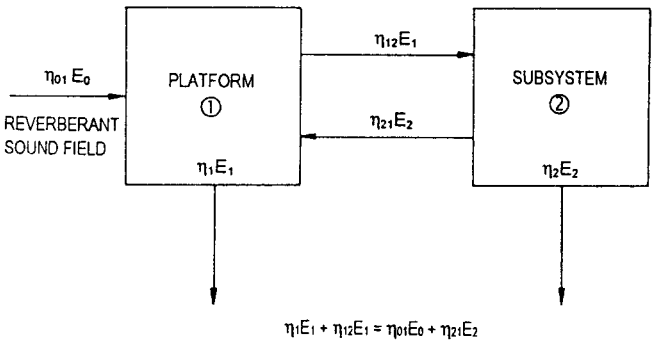

Figure 4.01.1 - SEA Model Basis

Notes on the evaluation of SEA parameters are given below. Some general information is also included in Chapter 3 on cylindrical structures. Guidance on the number of power inputs one should include when modelling platforms is given in Topic 8.02 - Modelling of acoustic excitation. See Chapter 9 for further information on loss factors.

4.02 SEA PARAMETERS FOR TYPICAL ZONE 2 STRUCTURES

The typical structures described are:

- Unstiffened platform, [See: Topic 4.03].
- Conventionally stiffened panel, [See: Topic 4.04].
- Integrally machined platform, [See: Topic 4.05]
- Corrugated platform, [See: Topic 4.06].
- Honeycomb platforms, [See: Topic 4.07].

4.03 UNSTIFFENED PLATFORM

MODAL DENSITY

The modal density of a flat unstiffened panel is included as a subroutine in the GENSTEP3 program, [See: Appendix A]. The following assumptions are made when one determines the required input data:

- modal density is independent of boundary conditions;
- the modal density of an irregularly shaped plate is taken to be the same as that of a rectangular plate having the same area and the same material properties. The only exception is that of a circular plate, where GENSTEP3 incorporates the required correction factor.

DISSIPATION LOSS FACTOR

The DLF for a plain panel or platform must be input into GENSTEP3 in the form of a table of values or as a single average value. The recommended value for DLF is 0.004. Further information is given in Chapter 9.

COUPLING LOSS FACTOR

A note on the types of CLF is given in Topic 3.03 and in Appendix A. GENSTEP3 does not evaluate structure-to-structure coupling and it is necessary to provide values of CLF from the information available in Chapter 9.

4.04 CONVENTIONALLY STIFFENED PLATFORM

In general, the comments made for the case of the unstiffened platform also apply in the case of the conventionally stiffened platform. The additional comments made below are intended to give guidance in determining the influence of the stiffeners on the spatially averaged response of the platform. Unless there is a statement to the contrary, they are not intended to give guidance in predicting the stiffener response.

MODAL DENSITY

The modal density of a stiffened panel is assumed to be the sum of the modal densities of the panel's constituent components:

$$n(f)_{stiffened} = n(f)_{unstiffened} + n(f)_{stiffener}$$

At high frequencies, the contribution of the stiffener's modal density becomes negligible. GENSTEP3 incorporates the necessary subroutines, but care should be taken when inputting the required SUBSYS data; in particular:

t = skin thickness of platform
do not smear stiffeners

m = mass/unit area of structure
do smear mass of stiffeners

s = total length of stiffeners
(all stiffeners assumed to be identical in section)

The modal density of an irregularly shaped panel is idealised as that of a rectangular panel of the same surface area.

DISSIPATION LOSS FACTOR

Chapter 9 presents DLF values for stiffened panels and platforms. The recommended value for a typical construction is 0.0076.

COUPLING LOSS FACTOR

The comments made with respect to the unstiffened platform also apply to the case of the stiffened platform. The presence of the stiffeners affects the radiation characteristics, and hence the structure/acoustic-cavity coupling, at frequencies less than the critical frequency. This is incorporated in the relevant GENSTEP3 subroutine.

RESPONSE OF STIFFENERS

Modelling the stiffeners as separate subsystems is generally considered over elaborate. If the response of the stiffeners is required, then the following method is suggested:

- Assume the panel/stiffener coupling to be considerably greater than the stiffener damping.
- The modal energies of the panel and the stiffener are therefore equal and:

$$E_{stiffener} = \frac{n(f)_{stiffener}}{n(f)_{panel}} \cdot E_{panel}$$

4.05 INTEGRALLY MACHINED PLATFORM

The general comments made with respect to the plain unstiffened platform also apply here. The modelling of the integrally machined panel depends upon the extent of the machining. The recommendations apply to the spatially averaged response.

MODAL DENSITY

If the height of the machined stiffeners is less than twice the skin thickness, the modal density is taken to be that of an unstiffened panel with an equivalent smeared thickness. If the height of the machined stiffeners is greater than twice the skin thickness, the modal density is that of an equivalent conventionally stiffened panel. Care must be taken when inputting the following parameters:

t = skin thickness
do not smear stiffeners

m = mass/unit area
do smear mass of stiffeners over panel surface.

DISSIPATION LOSS FACTOR

There is little available information for integrally machined panels. It is recommended that a value of 0.005 be used for panels and platforms.

COUPLING LOSS FACTOR

No specific information is available for machined panels. The recommendations made in Topic 9.05 should be followed.

4.06 CORRUGATED PLATFORM

While this form of construction is common for the central core structure, it is unlikely to be employed for equipment-mounting platforms. Nominally, however, flat panels could he used; these will be considered as Zone 4 type structures, [See: Chapter 6].

4.07 HONEYCOMB PLATFORMS

Note: This topic will be revised.

Many permutations of metallic and non-metallic honeycomb cores and faceplates are available. GENSTEP3 has a subroutine that makes it possible to evaluate the modal density of a honeycomb panel with orthotropic core and faceplates of different thickness.

MODAL DENSITY

- **Metallic cores and faceplates**: Experimentally measured values are usually of the order of 0.005 modes/Hz.
- **Metallic cores with CFRP faceplates**: A value for Young's modulus (E) is required for the faceplate material. This will need to be obtained experimentally or estimated from available data. As a guide for a typical platform having a light-alloy core and carbon/epoxy composite faceplates (laminated from three carbon-fibre prepreg layers at plying angles of [0°/60°/120°] to obtain near isotropic properties), Young's modulus has been taken as 48 GPa.

  Note: Reasonable agreement has been found for a limited number of examples, with a tendency to underestimate the experimentally obtained values.

DISSIPATION LOSS FACTOR

The recommended value for the DLF is 0.01. [See: Chapter 9 for more information].

COUPLING LOSS FACTOR

The recommended values for the CLF of honeycomb platforms attached to typical cylinders and cones are given in Topics 9.01 and 9.05.

Antenna Platforms

Platforms used for mounting antennae have been constructed from thick honeycomb (e.g. typically 75 mm thick). These are locally attached by struts to the parent structure (instead of being edge-attached by continuous angles).

The following assumptions for SEA parameters are recommended:

- **Modal density**: Treat as for honeycomb platform.
- **Dissipation loss factor**: Assume a DLF value of 0.007.
- **Coupling loss factor**: Assume zero coupling (CLF = 0).

4.08 ESTIMATION OF LONGITUDINAL & TRANSVERSE HONEYCOMB SHEAR MODULI (G_{cx} & G_{cy})

The accurate estimation of honeycomb shear moduli is of primary importance for the evaluation of modal density. The information in this section is based on uniform hexagonal aluminium honeycomb core, which is the most common form, [See: Figure 4.08.1 and Table 4.08.1]. Any honeycomb mentioned here is of this type, although the information may be used as an approximation for other types if necessary. Information has been correlated and compiled from data published by several manufacturers. Two graphs are presented:

- Figure 4.08.2 - Foil thickness/cell size vs core density,
- Figure 4.08.3 - Longitudinal and transverse shear moduli, G_{cx} and G_{cy}, vs core density.

Knowledge of foil thickness and cell size will give core density (based on hexagonal cell construction). Then from core density, values of G_{cx} and G_{cy} can be found.

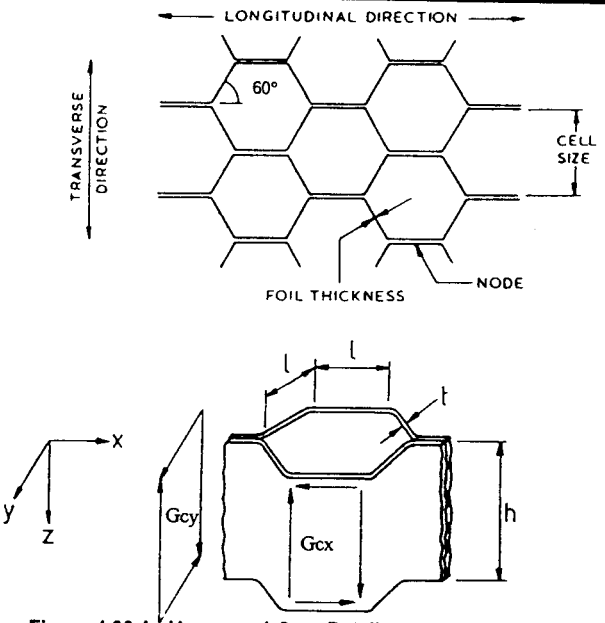

Figure 4.08.1 - Hexagonal Core Details

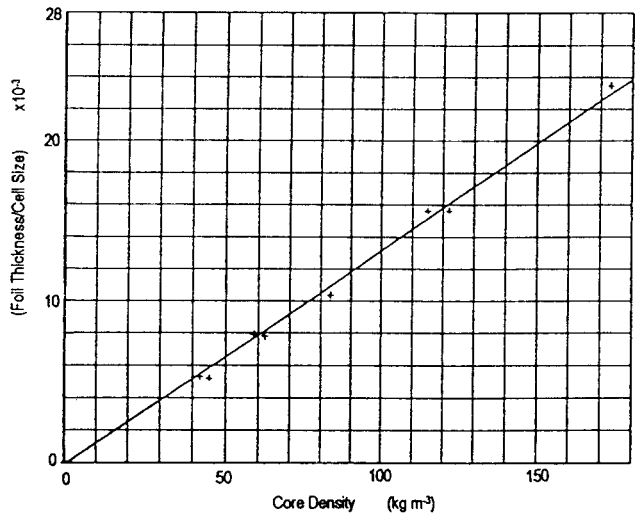

Figure 4.08.2 - Deduction of Core Density from Cell Details

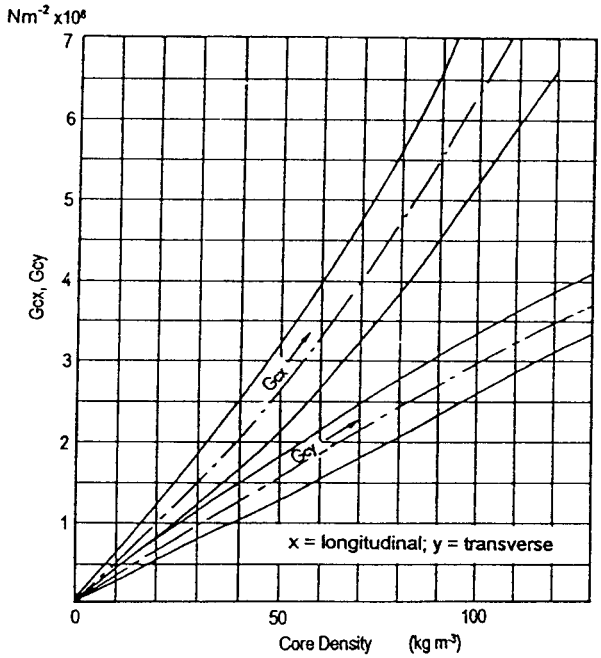

Figure 4.08.3 - Deduction of Longitudinal and Transverse Shear Moduli

4.09 SPATIAL VARIATION OF PLATFORM RESPONSE

SEA predicts only spatially averaged response. However, analysis for a honeycomb panel, Ref. [2], has given an estimate of 95th percentile level at 52 dB above mean square response level.

4.10 REFERENCES

[1] R.J. Cummins & W. Cooper
'Spacecraft structural acoustic studies'
Final report - ESA CR(P)-1264

[2] M.E. McNelis
'A Modified VAPEPS Method for Predicting Vibroacoustic Response of Unreinforced Mass Loaded Honeycomb Panels'
Proc. Inst. Envir. Sciences, 1989, 64-71

Cell Size inch / mm	Foil Thickness inch / mm	Core Density lb/in2 / kg/m2	Compressive Strength lb/in² / kg/m² No Skins	Compressive Strength lb/in² / kg/m² With Skins	Shear Strength lb/in² / kg/m² Transverse	Shear Strength lb/in² / kg/m² Longitudinal	Core Shear Modulus lb/in² / kg/m² Transverse	Core Shear Modulus lb/in² / kg/m² Longitudinal
1/8	0.001	3.9	309	368	124	205	29500	47000
3.2	0.025	62.4	0.217	0.259	0.087	0.144	20.8	33.0
1/8	0.002	7.6	828	1038	352	550	57600	91000
3.2	0.050	121.7	0.581	0.729	0.247	0.387	40.5	64.0
1/8	0.003	10.8	1275	1645	570	850	82000	129200
3.2	0.075	173.2	0.897	1.158	0.400	0.598	57.7	90.8
3/16	0.001	2.8	165	200	75	126	20000	32300
4.8	0.025	44.8	0.116	0.140	0.053	0.088	14.0	22.7
3/16	0.003	7.4	800	998	340	529	55200	89000
4.8	0.075	118.5	0.562	0.702	0.239	0.372	39.5	62.6
1/4	0.001	2.1	94	110	54	89	13100	21200
6.4	0.025	33.6	0.066	0.077	0.038	0.062	9.17	14.9
1/4	0.002	3.8	292	350	120	194	28700	45800
6.4	0.050	60.8	0.305	0.246	0.084	0.136	20.2	32.2
1/4	0.003	5.5	536	647	212	350	41800	66200
6.4	0.075	88.1	0.377	0.455	0.149	0.246	29.4	46.6
1/4	0.004	7.2	770	960	326	510	54900	86700
6.4	0.100	115.3	0.541	0.675	0.229	0.358	38.6	61.0
3/8	0.002	2.6	143	174	69	115	18200	29500
9.5	0.050	41.7	0.100	0.122	0.045	0.081	12.8	20.7
3/8	0.003	3.7	280	338	115	186	28000	44700
9.5	0.075	59.3	0.197	0.237	0.081	0.131	19.7	31.4

Table 4.08.1 - Dimensions and Mechanical Properties for Uniform Hexagonal Aluminium Honeycomb

Structural Acoustics Design Manual

Chapter 5
PREDICTION OF STRUCTURAL RESPONSE OF ZONE 3
(Platforms Contained within a Shell Structure)

CONTENTS

5.01 GENERAL

The theory underlying the prediction of the response of an internal platform with the aid of SEA techniques is similar to that for an external platform. Reference is made to Chapter 4 (Zone 2 structures) where applicable, in order to avoid duplication of information.

As for external platforms, the following construction configurations are available:

a) plain skin,

b) conventional stiffened plain skin,

c) integrally machined,

d) corrugated,

e) honeycomb (including combinations of metallic and non-metallic face-sheets and core).

In practice, configurations (b) and (e) are most prevalent.

In general, an internal platform is not subjected directly to the excitation sound field. The inter-structure coupling and the coupling between the adjoining cavity and platform are very important. An internal platform may be either transversely or axially located in the structure. For a transverse platform, the boundary conditions will usually be fully fixed, whereas an axial (longitudinal) platform may have a mixture of end conditions, see Figure 5.01.1.

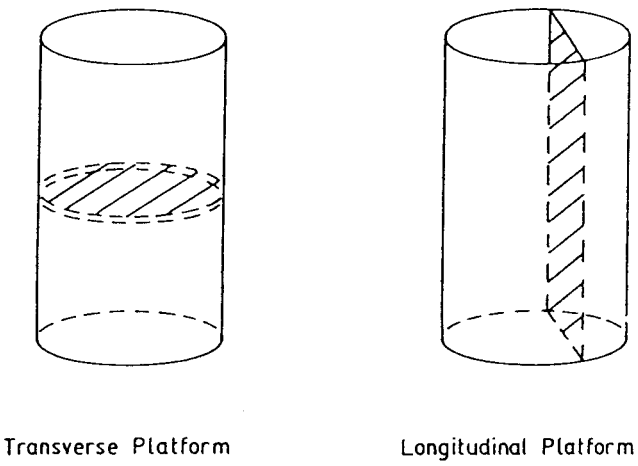

Figure 5.01.1 - Platform Boundary Conditions

It is necessary to make certain assumptions about the sound pressure spectrum inside the main shell structure. It is assumed that the pressure spectrum is the same for the two cavities, irrespective of the floor location, and that it is equal to the pressure spectrum for an internal cavity without a floor. However, problems exist at low frequencies for sound fields in the relatively small enclosures provided by a central structure, or even by a shroud structure, [See: Chapter 7].

The pressure of a platform acting as an acoustic boundary wall will tend to increase the low-frequency effects.

The basis for a SEA model is shown in Figure 5.01.2.

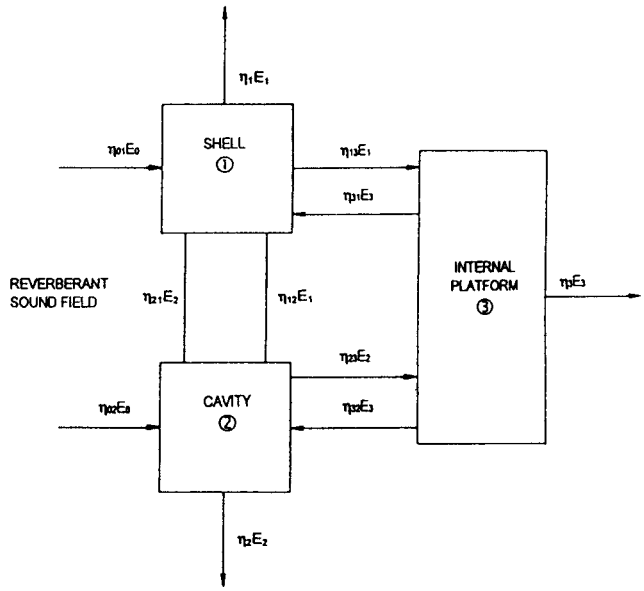

Figure 5.01.2 - SEA Model: Platform

5.02 SEA PARAMETERS FOR TYPICAL ZONE 3 STRUCTURES

Unless any further data become available specifically for internal platforms, it should be assumed that the decisions regarding the choice of SEA parameters will be the same as those for external platforms. Therefore, follow the guidelines given in Topic 4.02 for the different structural configurations, and those in Topic 7.07 for modelling the cavity.

Structural Acoustics Design Manual

Chapter 6
PREDICTION OF STRUCTURAL RESPONSE OF ZONES 4 to 7

CONTENTS

6.01 GENERAL

This chapter covers the prediction of structural response for the configuration Zones 4 to 7, which are defined as follows:

- **Zone 4**: Panels, solar arrays, antenna reflectors, [See: Topics 6.02 to 6.06 inc.],
- **Zone 5**: Booms and struts, [See: Topic 6.07],
- **Zone 6**: Equipment and attachment, [See: Topics 6.08 to 6.12 inc.],
- **Zone 7**: Massive equipment items, [See: Topic 6.13].

In Figure 6.01.1 the Marots structure is used to illustrate these zones.

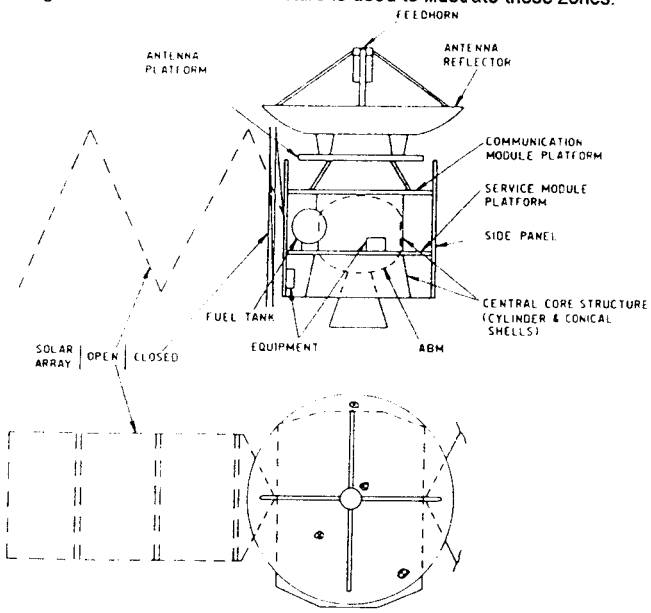

Figure 6.01.1 - Sketch of MAROTS Layout

6.02 ZONE 4: PANELS, SOLAR ARRAYS, ANTENNA REFLECTORS (SEA SIDE-BRANCH SUBSYSTEMS)

Generally structural panels can be dealt with in a manner identical to that described with respect to Zone 2 (platforms). Reference to the relevant structural configurations in Topic 4.02 will provide the SEA parameters. Some configurations which were not included in Zone 2 are now considered here.

CORRUGATED STRUCTURES

Although this form of structure is common on central core configurations it is unlikely to be used for equipment platforms. However, there are possible applications in flat configurations.

SOLAR-ARRAY STRUCTURES

These usually consist of several panels clad with solar cells and folded in the launch configuration. The best model that can be suggested for the folded configuration is that of a single folded panel with one input. Note the method of 'pin mounting' the solar array: the effect of the hinged structure presents further complications.

CURVED STRUCTURES

Single and double curvature of panels is particularly applicable to antenna reflector structures.

6.03 ZONE 4: CORRUGATED PANEL

See Figure 6.03.1.

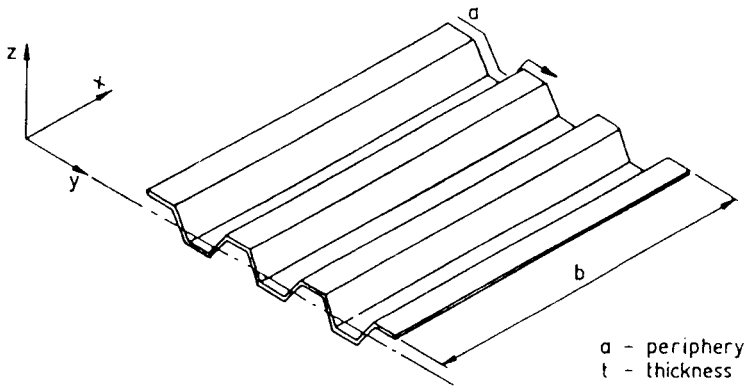

Figure 6.03.1 - Corrugated 'Flat' Panel

MODAL DENSITY

The complete theoretical analysis for the modal density of a corrugated panel is difficult. An approximate relation has been developed in Ref. [1], taking the modal density for a corrugated plate as:

$$n_{cp}(f) = \frac{a.b}{2C_L}\left(\left(\frac{A_x}{I_x}\right)^{1/2} \cdot \left(\frac{A_y}{I_y}\right)^{1/2}\right)^{1/2}$$

where (see Figure 6.03.1):

a is the peripheral length,

b is length along corrugation,

C_L is longitudinal wave speed,

A_x, A_y are the cross-sectional areas,

I_x, I_y are the second moment of areas.

and:

$$n_{cp}(f) = \frac{a.b}{2C_L}\left(\frac{3.464}{t}\left(\frac{A_y}{I_y}\right)^{1/2}\right)^{1/2}$$

where:

t = skin thickness.

The modal density given by this expression is independent of frequency. Experimental evidence shows that this may predict a slightly high modal density.

Notes:

- This expression is available in GENSTEP3.
- Modal densities of shell structures, in particular corrugated panels and cylinders, have been predicted with the aid of VIPASA and related computer programs, [See: Topic 3.06].

DISSIPATION LOSS FACTOR

The recommended value is 0.006.

COUPLING LOSS FACTOR

For coupling to acoustic space, compute as for flat plate using total expanded area. [See: Topic 9.05 for structure-to-structure coupling].

6.04 ZONE 4: SOLAR ARRAY PANELS

Generally a solar array will consist of a honeycomb panel with solar cells and associated equipment distributed over its surface.

MODAL DENSITY

Compute as for a honeycomb panel [See: Topic 4.07] using the total mass (mass of bare panel, mass of solar cells and associated equipment), but excluding mass of edge or closure members.

DISSIPATION LOSS FACTOR

The effect of attaching solar cells and other items to the surface of the basic panel will be to increase the DLF. A value of 0.02 is recommended, unless better information is available.

COUPLING LOSS FACTOR

A CLF of 0.0 is recommended for structure-to-structure coupling.

6.05 ZONE 4: CURVED PANELS (INCLUDING ANTENNA REFLECTORS)

The main effect of curvature on the SEA parameters is to modify the modal density. The case of a cylinder is dealt with in Chapter 3 under Zone 1 structures. The modal density of a doubly curved shallow shell has been formulated on the assumption that two ring frequencies can be defined for the two principal radii of curvature [See: Appendix A, Topic A.12]. The solution is complicated, however, and until the methods are developed further it is recommended that modal density and DLF be determined experimentally, especially for antenna reflectors. Otherwise, the following points need consideration.

MODAL DENSITY

Use the appropriate flat-panel solution for similar construction, taking the total surface area as the equivalent flat panel area. Except at very low frequencies, the flat-plate solution will tend to underestimate the modal density for a double-curvature panel.

DISSIPATION LOSS FACTOR

Use the appropriate flat-panel values from Chapter 9.

COUPLING LOSS FACTOR

Use the appropriate flat-panel values from Chapter 9.

ADDITIONAL NOTE CONCERNING MODAL DENSITY FOR CURVED PANELS

Two approximations have been presented in Ref. [2] for special cases of the double curvature expression. These have not yet been shown to be sufficiently accurate for prediction purposes. However, if experimental data are available, the trends implied may be useful for data interpretation [See: Chapter 10 for methods of measurement].

Modal density of a plate having single curvature

$$n(f)_{curved} = n(f)_{flat}\left(\frac{f}{f_r}\right)^{2/3} \quad \text{for } f<f_r$$

$$n(f)_{curved} = n(f)_{flat} \quad \text{for } f>f_r$$

Modal density of a spherical shell

$$n(f)_{sphere} = 0 \quad \text{for } f<f_r$$

$$n(f)_{sphere} = n(f)_{flat}\frac{f^2-f_r^2}{f^2} \quad \text{for } f>f_r$$

where:

$$f_r = \frac{1}{2\pi R}\left(\frac{E}{\rho}\right)^{1/2}$$

is the ring frequency of a cylinder having the same radius of curvature, R.

This result can also be used for assessing the modal density of a dish reflector, although the cross section of a large reflector may be complicated and this may reduce the accuracy of the estimate.

6.06 ZONE 4: SEA SIDE-BRANCH SUBSYSTEMS

In many cases, the effects due to panels individually treated can be estimated by modelling the system of which they are part as an SEA side-branch subsystem.

Ref. [3] concluded that:

- Side-branch subsystems which are not excited by a vibration input themselves will act as a sink of energy reducing response on the rest of the structure.
- For weakly coupled systems the side-branch can be considered as an added damping term on the subsystem to which it is attached, with the effective total damping equal to the sum of the original damping loss factor and the coupling loss factor.
- The report gives an estimate for the coupling loss factor from a satellite side panel to a solar array. In some frequency ranges this could add 10-20% to the effective damping of side panels.
- The resulting reduction in response will depend on the location of the vibrational power input.
- The effects predicted are fairly small relative to the current overall uncertainty in on-station damping.

6.07 ZONE 5: BOOMS AND STRUTS

These items are used on many satellite configurations. On specimens tested to date, it has been found that struts respond at their natural beam and torsional modes, but have little effect on the response of the components to which they are attached. It is recommended that, unless the response of the struts themselves is required, the struts should be omitted from the system model. If the response of a strut or boom is required, GENSTEP3 includes subroutines that make it possible to evaluate the modal density of beam-type transverse and torsional modes. It is suggested that a DLF of 0.005 be used with zero coupling (CLF = 0.0) for the case of strut or boom response. However, a large boom item would be in its folded, or stored, configuration for a launch situation, which would make modelling as a separate subsystem difficult.

For items connected to the main structure by struts alone, such as an antenna platform or solar array, it is recommended that zero coupling be assumed (CLF = 0.0).

An analytical study has concluded that a side-branch subsystem is adequately represented by additional dissipation loss to be included in the supporting subsystem DLF value, Ref. [3].

6.08 ZONE 6: EQUIPMENT AND ATTACHMENT

This zone covers the effect of the equipment and attachment items on the structural vibration levels and the prediction of the vibration response levels appropriate to the equipment items.

The method recommended for modelling structural features and equipment items is repeated from Topic 2.07:

- If an item may be considered isolated on the structural surface (e.g. equipment box), its mass **should not** be included in the structural subsystem.
- If an item can be considered as part of the structure (e.g. stiffener, frame), then its mass **should** be included in the structural subsystem.

As most pieces of equipment are mounted on platforms or panels of honeycomb construction, most of the development has been concerned with this type of structure.

6.09 ZONE 6: EQUIPMENT MOUNTED ON HONEYCOMB PLATFORMS OR PANELS

For equipment distributed in discrete units (e.g. boxes) on a honeycomb platform, experimental measurements have shown that the local response of the supporting structures is changed, but that there is little effect on the spatial average response at positions remote from the equipment. The test evidence applies to at least a 10-to-1 ratio of equipment mass to platform mass (this latter includes the mass of inserts and adhesive). More heavily loaded panels and concentrated heavy loads have not been investigated.

MODAL DENSITY

Evaluate as for a honeycomb platform, [See: Topic 4.07].

DISSIPATION LOSS FACTOR

The value of DLF recommended is 0.020, but see Topic 9.04 - Frequency Dependence of DLF, for further explanation.

COUPLING LOSS FACTOR

CLF values are as advised for honeycomb platform [See: Topics 9.01 and 9.05].

RESPONSE EVALUATION

It is recommended that the mass of the platform (or panel) plus the mass of the attachment inserts be used for the evaluation of modal density. Investigations have shown, however, that a closer estimate of response can be made if only the platform mass (less inserts) is used to evaluate the spatial average response. The mass of the equipment should not be used in either evaluation.

6.10 ZONE 6: EQUIPMENT MOUNTED ON CONVENTIONALLY STIFFENED STRUCTURE

Experimental measurements have shown that both equipment boxes and wiring harness bundles, attached to flat plate structure stiffened with stringers, have a large effect on the local response adjacent to the item, but little effect on the spatial average response of the remaining subsystem structure. The local effect is also usually limited by the proximity of the attachment mountings to the stiffener(s).

6.11 ZONE 6: ASSESSMENT OF EQUIPMENT RESPONSE LEVELS

Initial investigations have been performed for predicting the acceleration at an equipment box mounting point. These investigations were based on the platform acceleration level (spatial average) and the mounting point impedances. The acceleration level at a box mounting point can be found from:

$$a_b^2(t) = a_p^2 \left| \frac{\langle Z_p \rangle}{\langle Z_p \rangle + Z_b} \right|^2$$

where:

$a_p^2(t)$ = platform acceleration level without the equipment item mounted at the equipment location,

$\langle Z_p \rangle$ = average point impedance for the platform at the box mounting positions,

Z_b = point impedance for the mounting position on the box.

on the basis of the frequency band average values.

If the equipment is sparsely distributed in the locality of the item of concern, $a_p^2(t)$ = spatially averaged unloaded platform acceleration level. If the equipment location is close to other equipment, the unloaded platform level can overestimate $a_p^2(t)$ by up to an order of magnitude.

Investigations with a panel representative of a satellite side-wall panel (+ X Olympus) showed that mass loading, even without any damping effects significantly reduced the panel's response levels above about 400 Hz at an equipment item's mounting locations, in the absence of the item.

Most effect occurs due to the initial loading of about five times panel mass. Mass loading also affects local panel impedance values, causing increase in modulus at high frequencies, but when applying the formula for $a_b^2(t)$ given above, the net result of these two counteracting influences is typically to cause an overestimate of equipment response.

Thus, panel mass loading needs to be accounted for in SEA model predictions. This is not yet fully researched. The simplest approach ('smeared' mass) calculates the vibrational energy using only the platform (wave-bearing) mass and then converts this to response assuming the total mass is appropriate for the kinetic energy. This has been found to overcorrect and greatly underpredict the mounting locating value of $a_p^2(t)$ except for low levels of loading.

However, the spatially averaged level is not representative of the equipment mounting bare panel-patch position, and so it would be appropriate to apply an augmentation factor, for example the 95th percentile value of +5.2 dB on mean squared response, as described in Ref. [4].

Further, the panel response when loaded with real equipment is likely to be reduced by more than given by a pure mass-loading effect, owing to the added damping and energy absorption provided by real equipment. The preceding observations related to tests made with dummy equipment, Ref. [8].

Notes:

(a) When measurements of the loaded panel are available, the unloaded platform acceleration level, $a_p(t)$, may be substituted by $k.a_p^*(t)$, where $a_p^*(t)$ is the spatially averaged level with equipment fitted, measured not less than 75mm from the nearest equipment and k has the values given in Table 6.11.1. If measurements are closer than 75mm, the values of k need to be increased (e.g. doubled at 40mm). A minimum value of k = 1 would apply to measurements remote from sparsely distributed equipment, i.e. for equipment to be located in a large unpopulated area of panel.

Frequency (kHz)	k
≤ 1	3
> 1	1.5

Table 6.11.1 - Loaded Panel: k values

(b) The combined impedance, $\langle Z_p \rangle + Z_b$, should preferably be measured directly with the box in place on the platform, in complex form. Alternatively the box mounting point impedance may be measured separately or, for initial design purposes, it may be calculated from:

$$Z_b = \frac{2\pi f.M}{N} \quad \text{(imaginary)}$$

where:

M = total box mass

N = number of box mounting points

In the special cases where component impedances are estimated as wholly real or imaginary, the impedance expression can be rewritten using moduli:

$$\left| \frac{\langle Z_p \rangle}{\langle Z_p \rangle + Z_b} \right| = \frac{|\langle Z_p \rangle|}{|\langle Z_p \rangle| + |Z_b|}$$

(c) Some experimental measurements for the point impedance of platforms and equipment boxes have been made during the initial investigations using a 'study' specimen, Ref. [5], and during testing the Olympus satellite STM, Ref. [6]. Values for a service module floor and side panel are shown in Figure 6.11.1. It has been found that the impedance for a typical platform can be taken as 1000 N.s.m^{-1} (real) as an initial design value.

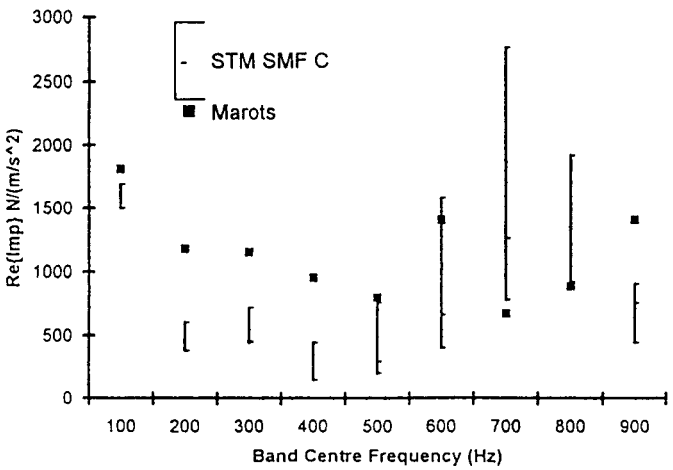

Figure 6.11.1 - Real Part of Impedance of Honeycomb Panels

Alternatively, based on Ref. [7], the following expression for the predominant real part of point impedance of a rectangular, simply supported honeycomb-core sandwich platform (remotely excited) can be derived, to an upper frequency limit f_u:

$$\frac{1}{Z_p} = \frac{1}{8(B\mu)^{1/2}} + \frac{2\pi f}{4S}$$

where:

$$f_u = \frac{1}{4A}\left(\frac{S}{\mu}\right)^{1/2} \text{ Hz.}$$

μ = mass per unit area of panel,

h_c = thickness of core,

b = width of panel,

c = length of panel,

A = area of force application (per mounting foot),

$S = G_c h_c (1 + h_f/h_c)^2$,

G_c = core shear stiffness,

h_f = faceplate thickness,

$B = E_f \cdot h_f \cdot h_c^2 (1 + h_f/h_c)^2 / [2(1 - \upsilon^2)]$,

E_f = tensile modulus of faceplate,

ν = Poisson's ratio for faceplate.

Note: The imaginary part can also be significant in determining the response close to a point-driving location.

The influence of the boundary conditions will mainly occur below f_1:

$$f_1 = \frac{1}{2\pi}\left(\frac{S\pi}{\mu}\right)^{1/2}\left(\frac{1}{b^2} + \frac{1}{c^2}\right)^{1/2} \text{ Hz.}$$

The influence of the spacecraft beyond the panel's attachment is not usually significant. Tests have shown that a simple frame for the panel attachment results in very similar platform response to attachment to the spacecraft structure.

(d) When adequate spectral data are available, narrow band admittance modelling can be applied, [See: Topic 1.07].

6.12 ZONE 6: INTERNAL RESPONSE OF EQUIPMENT

Investigations undertaken with electronic equipment boxes mounted on honeycomb panels, Ref. [8], showed that typical internal equipment response is very frequency selective due to mechanical filtering effects of the platform and equipment structure. Typical mode orders at maximum response frequencies were less than about twenty for the panel and less than about five for a circuit board.

Due to these low modal orders, vibration levels frequency-averaged over 50 Hz bands were found to be well predicted by simple finite-element modelling of a pcb stack in equipment. The acoustic forcing excitation level was modelled as a mechanical input to the platform which caused a spatially averaged platform response equal to the averaged measured level on a sparsely loaded platform, Ref. [9].

FEA modelling for estimating internal response permits phasing of the equipment attachment points to be taken into account which is desirable because the input to an equipment is not well represented by a single monitoring location. Transmissibility between acoustic field and equipment component is sensitive to phase difference between mounting locations. Changes in panel loading cause phase changes between mounting locations, possibly even causing reductions in magnitude at one mounting point when the internal response has actually increased. The change in average magnitude over four locations around and close to the equipment can give a good indication of the change in internal response.

Equipment location, orientation and panel loading all influence equipment internal response. Ranges of acceleration and strain levels (not PSD) measured at the location of maximum circuit board response and at the peak response frequency were found, Ref. [8], to vary over the following ranges, with strain range in brackets [ ].

(a) location influence (single box on panel);

1 : 1.4 [1 : 1.4]

(b) orientation influence (single box on panel);

1 : 2.3 [1 : 1.1]

(c) loading (monitored box at one fixed location);

1 : 2 : 1.6 [1 : 0.6 : 1.3]

(1 : 3 : 6 no. of boxes). Hence increasing loading can increase or reduce internal response. These values were measured in one particular box. Repeating the tests twice more with different boxes, for the cases of a single box and of six boxes loading the panel, showed a range of acceleration results from 1: (1.2 to 1.6).

It has been found that the internal response of an equipment box is sensitive to its assembly in the peak frequency response regions, influencing transmissibility by a factor of three in one case of circuit board response.

Values of resonant amplification factor up to about 3 have been found between small components and their circuit boards. The components monitored were ICs (dual-in-line through-soldered and top-hat) and flat two-wire mounted upright components.

6.13 ZONE 7: MASSIVE EQUIPMENT ITEMS

This description would apply to an item such as an apogee boost motor (ABM). It has been found from experimental work that the presence of a simulated ABM mass has little effect on the response of a spacecraft structure subjected to reverberant acoustic excitation.

There appears to be no need to model a massive equipment item with the structure when the latter is subjected to acoustic excitation only.

Note: The situation may be different for mechanical excitation input; this has not yet been investigated.

6.14 REFERENCES

[1] B.L. Clarkson, R.J. Pope & M.F. Ranky
'Experimental work to evaluate parameters required in the SEA prediction method'
ESA Contract No. 4100/79/NL/PP Rider 1 (1981)

[2] R. H. Lyon
'Statistical energy analysis of dynamical systems: theory and applications'
MIT Press (1975)

[3] N.S. Ferguson & M.G. Smith
'The Effect of a Side-Branch Subsystem in SEA Modelling'
Report R04 4274, ESA Contract 7501/87/NL/PP(CCN4), 1994

[4] M.E. McNelis
'A Modified VAPEPS Method for Predicting Vibroacoustic Response of Unreinforced Mass Loaded Honeycomb Panels'
Proc. Inst. Envir. Sciences, 1989, 64-71

[5] B.L. Clarkson & R.J. Pope
'Experimental determination of modal densities and loss factors of spacecraft components'
ESA Contract No. 4100/79/NL/PP (1980)

[6] J.N. Pinder, et al.
'Satellite In-Orbit Health Monitoring: Synthesis and On-board Data Handling'
Final Report, Vol. 2
ISVR Consultancy Services, University of Southampton
ESA Contract No. 10235/92/NL/PP(SC), June 1994

[7] B.L. Clarkson & M.F. Ranky
'On the measurement of the coupling loss factor of structural connections'
Journal of Sound & Vibration, 94 (2), 249 (1984)

[8] J.N. Pinder & D.C.G. Eaton
'Acoustically Induced Vibration of Platform Mounted Equipment Containing Printed Circuit Boards'
Proc. Int. Conf., 'Spacecraft Structures and Mechanical Tests'
Noordwijk, 24-26 April 1991 (ESA SP-321, Oct. 1991)

[9] J.N. Pinder
'FEA Modelling of Platform and Equipment Box Response'
ESA Contract No. 7501/87/NL/PP(CCN3), Report R01 4119
June 1992

Structural Acoustics Design Manual

Chapter 7
PREDICTION OF SOUND TRANSMISSION AND SOUND PRESSURE LEVELS IN CONTAINED SPACES

CONTENTS

7.01 SEA MODELLING: GENERAL

The SEA technique enables an acoustic space to be modelled as a subsystem in conjunction with structural subsystems. The GENSTEP3 program can predict the response of an acoustic space contained in a structural component. This response can be expressed as an average sound-pressure spectrum and, if required, as a noise reduction (NR) level. In addition, the transmission loss (TL) can be found for the containing structure, provided that it can be considered as the only component transmitting into the enclosed cavity.

The SEA technique directly models resonant response of subsystems which may include an acoustic space. In addition, energy is transferred by a non-resonant excitation which is often significant below the critical frequency but which can be effectively incorporated in the SEA model.

The nonresonant sound transmission is based on the direct power input to the acoustic cavity by the surrounding noise field, the coupling between this excitation and the cavity depending on the limp-wall, mass-law sound transmission, see: Ref. [1] (Section 2.3.7). This power input has to be included when an acoustic space is modelled as a separate subsystem. It is assumed that the absorption of the cavity is sufficiently low to allow the enclosed sound field to be considered reverberant.

An example of a SEA model for an enclosed cavity is shown in Figure 7.01.1.

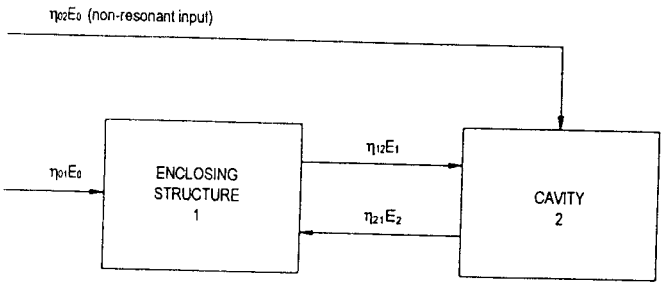

Figure 7.01.1 - SEA Model for an Enclosed Cavity

However, the mass law model is only valid for flat panels, below their critical frequency. For a uniform homogenous-wall cylinder, below its ring frequency, an additional term must be added to the equivalent flat plate TL value, from Ref. [2]:

$$TL_{cyl}(non-res) = TL_{flat-plate} + A$$

where: $A = 20\log_{10}\left\{\pi \Big/ \left[2\sin^{-1}\left(\upsilon_0\left[1-\left(\upsilon_0 f_r/f_c\right)^2\right]^{1/2}\right)^{1/2}\right]\right\}$ dB

where: $\upsilon_0 = f/f_R$

- For steel and aluminium:
  - ring frequency $f_r \approx 7.92\times10^2/R$ Hz
  - critical frequency f_c; $f_c/f_R \approx R/67h$,

  where R = radius (m).

  The expression for A is valid only for:

  $1/B < 1$

  $(1-B^2)^2 >> \eta^2 B^4$

  $(\rho_m c/2\eta\rho)(12^{1/2}/C_L) >> 2B/(1-B^2)^2$

  where: $B = \upsilon_0 f_R/f_c$

  $C_L = \left[\dfrac{E}{\rho_m(1-\mu^2)}\right]^{1/2}$ longitudinal speed of sound in cylinder material

- Cylinder properties:

  η = structural loss factor,

  ρ_m = volume density,

  μ = Poisson's ratio.

- For acoustic medium:

  ρ, c are density, speed of sound respectively.

Above the flat-plate critical frequency, the non-resonant energy transfer is much less than the resonant energy transfer.

7.02 SEA PARAMETERS FOR CONTAINED SPACES

MODAL DENSITY

The modal density for a contained space is evaluated by GENSTEP3 with the aid of a standard formula for a 3-D cavity (this covers the usual case for a cavity having similar dimensions in all three axes). This is the formula used for room acoustics (e.g. concert halls), but it is also assumed to be applicable to smaller volumes and to irregularly shaped spaces. This evaluation is restricted to frequencies at which the acoustic wavelength in the cavity is less than the enclosing structural dimensions.

GENSTEP3 also includes options for two other special cases for enclosed spaces. First for a 1-D space which is defined as any cylindrical space in which one-dimension is significantly greater than the other two and the wavelength of sound is greater than the greatest cross dimension. Secondly, for a 2-D space, which is defined as a thin, flat space, the formula is valid provided that the wavelength of the sound is greater than twice the depth of the space. These two options are probably of limited use for spacecraft structures.

DISSIPATION LOSS FACTOR

A theoretical expression for DLF is given by:

$$\eta = \frac{C\cdot A\cdot\alpha}{8\pi\cdot V\cdot f}$$

where:

A = total surface area of cavity,

V = volume of cavity,

C = speed of sound in enclosed medium (340 m.s^{-1} in air, standard temperature and pressure),

f = centre frequency of bandwidth,

α = absorption coefficient.

The DLF has to be input to GENSTEP3 as a table with a value for each analysis bandwidth. However, the absorption coefficient, α, has first to be evaluated for the cavity. α can vary with frequency, although in most cases a constant value found from the following information will suffice.

For the case of low absorption (fairly reverberant space), the Sabine (approximate) Formula can be used to evaluate α from a measurement of reverberation time:

$$T_R = \frac{0.161V}{A\cdot\alpha} \text{ seconds (For SI units)}$$

For the case of higher absorption, the Norris-Eyring Formula may be more appropriate:

$$T_R = \frac{0.161V}{A\left[-2.3\log_{10}(1-\alpha)\right]} \text{ seconds (For SI units)}$$

The reverberation time; T_R, of an enclosure is defined as the time required for the SPL to decrease 60 dB. T_R may be measured in suitable bandwidths by means of a standard decay technique.

Some experimental data for α and η are available from Ref. [3, 4] for hard-surfaced cylindrical enclosures. These are presented in Table 7.02.1 together with the enclosure dimensions. Ref. [5] gives some further data used for the Space Shuttle payload bay and payloads; a summary of these data is given in Table 7.02.2.

Cylinder Dimensions	Ref. [3]	Ref. [4]
Radius (m)	0.381	0.322
Internal length (m)	2.31	0.75
Volume (m³)	1.053	0.2443
Total internal surface area (m²)	6.445	2.169
Internal surface condition	Plain metal cylinder, stiff end faced with laminated plastic.	Plain metal cylinder, plain metal ends.
Typical	0.038	0.035

Measured values of α versus frequency, in 1/3 octave bands for cylinder in Ref. [3]

Centre Frequency (Hz)	α	Centre Frequency (Hz)	α
50	0.058	800	0.018
63	0.053	1000	0.033
80	0.044	1250	0.038
100	0.053	1600	0.035
125	0.044	2000	0.053
160	0.058	2500	0.048
200	0.026	3150	0.041
250	0.024	4000	0.035
315	0.010	5000	0.033
400	0.035	6300	0.044
500	0.016	8000	0.048
630	0.026	10000	0.041

Table 7.02.1 - Measured Absorption Coefficients for Cylinder

Recommended values of α for different surfaces are given in Table 7.02.3 and the effect of different surfaces, equipment and structures in the enclosure is discussed in Topic 7.03.

Metal surface	0.035 to 0.04
Metal surface + stiffeners	0.05
Typical payload e.g. satellite having many surfaces, cables, insulation, etc.	0.18
Metal surface + absorptive material	0.40

Typical Values for Absorption Coefficient α
(Assuming no variation with frequency)

	Octave Band Centre Frequency (Hz)						
	31.5	63	125	250	500	1K	2K
One layer No gap	0	0.05	0.07	0.11	0.6	0.4	>0.2
One Layer Gap	0.05	0.065	0.1	0.125	0.4	0.4	>0.25
Two layers No gap	0.03	0.06	0.1	0.2	0.5	0.5	>0.2
Two layers Gap	0.08	0.075	0.125	0.22	0.5	0.52	>0.3

Note: The actual dimensions used for these tests are not known. The thinnest layer used on the Shuttle is 1.9 cm thick

Table 7.02.3 - Absorption Coefficients for TCS Thermal Insulation Materials, Ref. [5]

COUPLING LOSS FACTOR

The CLF for the structure/acoustic-cavity coupling is computed by GENSTEP3 after the radiation resistance of the structure (in this case, the transmitting structure surrounding the cavity) has been evaluated. The complementary CLF (cavity/structure) will be computed by means of the reciprocal relation.

The nonresonant power input is governed by the coupling of the excitation field with the cavity. In addition, it would also be possible to have the case of nonresonant transmission between two contained cavities through the dividing structure. The CLF for acoustic-space/acoustic-space coupling is evaluated by GENSTEP3 with the aid of standard sound transmission formulae, [See Appendix A].

Frequency (Hz)	Door	Bulkhead	Sidewall & Bottom (Base)	Sidewall With TCS			Bottom With TCS			TCS Beneath Payload	Payload
				STA582-919	STA919-1307	Average	STA582-919	STA919-1307	Average		
31.5	0.100	0.040	0.040	0.050	0.140	0.095	0.050	0.140	0.095	0.140	0.175
40		0.040	0.040	0.055	0.140	0.098	0.060	0.140	0.100	0.140	
50		0.040	0.040	0.060	0.145	0.103	0.065	0.145	0.105	0.145	
63		0.040	0.040	0.065	0.150	0.108	0.075	0.155	0.115	0.155	
80		0.050	0.050	0.075	0.165	0.120	0.095	0.170	0.133	0.170	
100				0.085	0.180	0.133	0.110	0.195	0.153	0.205	
125				0.100	0.200	0.150	0.125	0.230	0.178	0.260	
160				0.105	0.240	0.173	0.140	0.280	0.210	0.360	
200				0.115	0.280	0.198	0.165	0.375	0.270	0.500	
250				0.125	0.370	0.248	0.220	0.480	0.350	0.570	
315				0.210	0.460	0.335	0.310	0.540	0.425	0.605	
400				0.305	0.505	0.405	0.415	0.565	0.490	0.615	
500				0.400	0.525	0.463	0.480	0.570	0.525	0.615	
630				0.400	0.530	0.465	0.505	0.570	0.538	0.595	
800				0.400	0.530	0.465	0.520	0.570	0.545	0.570	
1000				0.400	0.520	0.460	0.530	0.565	0.548	0.550	
1250				0.400	0.510	0.455	0.535	0.560	0.458	0.530	
1600				0.400	0.505	0.453	0.535	0.550	0.543	0.510	
2000				0.400	0.490	0.445	0.535	0.540	0.538	0.500	
2500				0.395	0.470	0.433	0.525	0.530	0.525	0.490	
3150				0.390	0.455	0.423	0.520	0.520	0.520	0.480	
4000				0.390	0.430	0.410	0.510	0.510	0.510	0.470	
				1.9 cm thick	2.5 - 4.4 cm thick + air gap		3.8 cm thick	2.5 - 4.4 cm thick + air gap			

Table 7.02.2 - Estimated Absorption Coefficients for Payload Bay

7.03 EFFECT ON SEA PARAMETERS OF EQUIPMENT AND/OR STRUCTURES IN A CONTAINED SPACE

Measured data are not available for most of these effects, but assumptions are suggested based on the referenced information.

Measured total absorption values of satellites and of an empty Ariane 4 fairing are given in Figure 7.03.1. The effect of the presence of a satellite is to reduce the noise level inside the fairing by about 8 dB at about 500 Hz and 1 kHz, but by only 1 or 2 dB at low frequencies. However, counteracting this reduction is an increase in noise due to the effect of the satellite occupying volume, with the biggest influence at low frequencies so that the overall result is likely to be an increase in noise at low frequencies and a small reduction at mid-frequencies compared with noise levels in an empty fairing, Ref. [6].

The prediction of the sound field inside the fairing of a loaded launcher is discussed in Ref. [7].

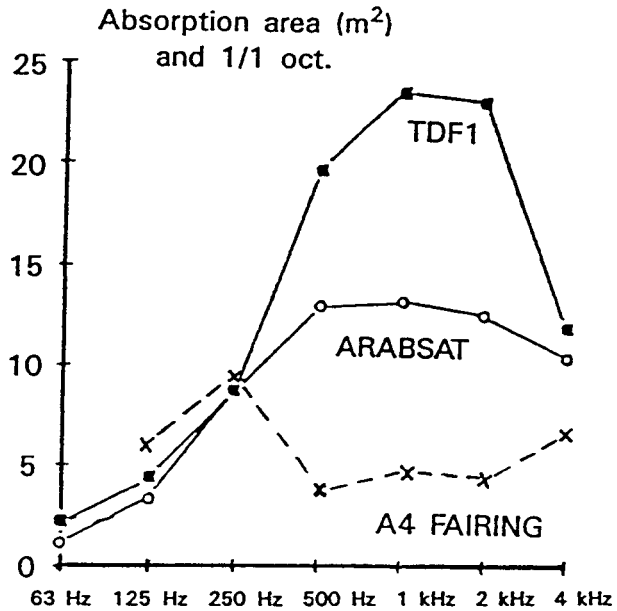

Figure 7.03.1 - Measured Absorption Areas for Two Satellites, Ref.[6] & Ariane 4 Fairing (Empty)

DISSIPATION LOSS FACTOR

The volume of the structural or equipment item should not be included with the value used for the volume of the enclosed space (3-D option).

Where surfaces having different absorption characteristics exist in the enclosure, either a measured value for the average absorption coefficient, α_{AV}, is required or α_{AV} can be estimated from individual surface values (these are values of α obtained with the aid of the formulae presented in Topic 7.02). Thus:

$$\alpha_{AV} = \frac{1}{A} \sum_{i=1}^{N} A_i \cdot \alpha_i$$

where:

$A = \sum_{i=1}^{N} A_i$ is the total area of all the surfaces.

Then:

$$\eta = \frac{C \cdot A \cdot \alpha_{AV}}{8\pi \cdot V \cdot f} \quad \text{as before.}$$

Recommended values of α for various surfaces are given previously in Table 7.02.3.

A special case could occur, where the item occupies a large percentage of the total volume available in the 'empty' enclosed space, thus producing a remaining space best modelled by the 2-D option, see: Figure 7.03.2.

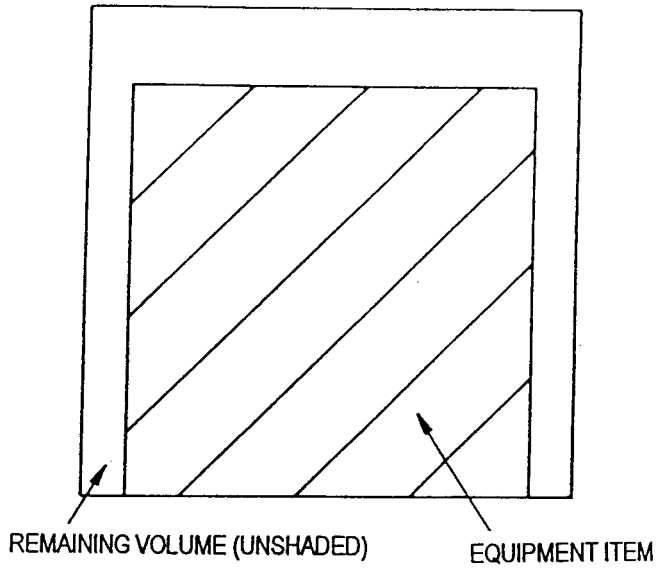

Figure 7.03.2 - Equipment in a Contained Space

The DLF will usually be increased by additional items intruding into the basic cavity space. Allowance can be made for the reduction in volume, the increase in surface area and the estimated change in absorption coefficient. Generally metallic components should not change α, but the addition of absorptive material will increase its value.

COUPLING LOSS FACTOR

It is possible that certain structural items attached to the cavity walls could increase the CLF by increasing the radiation. However, it is probably best to ignore this effect in most models, unless sufficient details are available for the item to be modelled as a separate subsystem.

7.04 PREDICTION OF SOUND-PRESSURE LEVELS AT LOW FREQUENCY

The sound transmission for a structural shell, as predicted by the GENSTEP3 program, is incorrect in the low-frequency region. This results in predicted sound-pressure levels for a cavity which are too high for the low-frequency region, this being also the region of low modal density. Experimental measurements which have been made inside various cylinders show a large fluctuation in SPL dependent on measurement location, e.g. see Ref. [1, 3]. This is mainly because the internal noise field produced in the cavity is not diffuse at wavelengths which are large with respect to the dimensions of the cavity. The assumption is, of course, that the excitation field is diffuse.

7.05 NOISE REDUCTION

The most readily assessed practical measure of sound transmission is the noise reduction, NR, which is defined as the difference in sound pressure levels, in dB, between the source space and the receiving space. GENSTEP3 has the option to output the NR from source space (whether external excitation field or a contained space) to receiving space. If the source space is not coupled to the receiving space in the system model, the NR can still be found from the matrix REDNOS. It may be necessary to allow for a low-frequency (low-modal-density) error as mentioned in Topic 7.04, and the large fluctuation of sound-pressure levels which occur at low frequencies inside small enclosures should be remembered.

A method for predicting the NR for a launcher payload fairing is described in Topic 7.07.

7.06 TRANSMISSION LOSS

GENSTEP3 also has the option to output the value of transmission loss, TL, for the intervening structure, although it can only allow for transmission through one structural configuration. The TL is calculated from the NR by correcting for the acoustical properties of the source and receiving spaces. This correction tends to be controlled by the average sound absorption coefficient, α_{AV}, for the surfaces of the receiving space. GENSTEP3 computes α_{AV} from the DLF for the receiving space. **It should be noted that the value of α is measured or estimated by the user for the evaluation of the DLF of the contained space [See: 7.07] which is program input data.**

If the TL option is requested, GENSTEP3 uses the Norris-Eyring formula [See: 7.07] for computing α from the DLF. The TL is calculated as follows:

$\alpha < 0.2$:

$$TL = NR + 10\log_{10}\left(\frac{A_3}{A_2 \cdot \alpha}\right)$$

$0.2 < \alpha < 0.8$:

$$TL = NR + 10\log_{10}\left(\frac{1}{4} + \frac{A_3 \cdot (1-\alpha)}{A_2 \cdot \alpha}\right)$$

$\alpha > 0.8$ (Transmission from enclosure to outdoors):

$$TL = NR - 6$$

where:

A_2 is the area of the transmitting structure,

A_3 is the total surface area of the receiving enclosure,

the values for NR and TL are expressed in dB.

Note: The range of values of α allowed for in GENSTEP3 is wider than that likely to be encountered in spacecraft structural work. The expressions are those used in room acoustics from Ref. [8].

7.07 ESTIMATING NOISE REDUCTION PROVIDED BY CYLINDERS

INTRODUCTION

The sound field strength inside a cylinder due to an external sound field can be estimated with the aid of Statistical Energy Analysis (SEA), but only if the external incident sound field is diffuse, because only then can the structural radiation efficiency be used to estimate the structural response, subject to a lower limiting frequency for acceptable confidence levels. However, in the case of a fuselage or fairing exposed to launcher engine noise, for example, the sound field may not be well represented as diffuse, and to assess sound transmission from specific incidence angles and lower frequencies other types of analytical model are required. Finite-element techniques can be applied, but their practical and economic upper frequency limit is restrictive. A simpler method using modal interaction analysis (MIA) has therefore been developed to allow the influence of the main structural and acoustic parameters to be investigated, Ref. [9, 10]. A general description of MIA is given in Chapter 11.

This method has been applied to some cylindrical structures which fall within a range of expected interest, and comparison with measured values is given below to indicate the expected accuracy of the predictions.

It is expected that the absolute performance of a construction indicated as favourable on the basis of MIA results will be assessed for its absolute performance by means of a more complete analysis, which will model the structure, its excitation and radiation (e.g. by finite or boundary element analysis, as in Ref. [11, 12]) as far as is practical. Those models can also indicate spatial distribution of sound pressure level, in contrast to the spatially averaged values to which the simpler technique is limited.

MIA can be implemented in this application by means of the computer code PROXMODE, which is available to ESA, Ref. [13].

Note: This code has **not** been subject to ESA software quality assurance.

Although MIA can be used to predict transmission due to diffuse incident fields, by synthesising the field from a set of discrete angles, the diffuse field case can be evaluated from the treatment by Szechenyi, Ref. [2]. However, the data in Ref. [2] are applicable only to monocoque cylinders.

LIMITATIONS OF ACCURACY

- Assumptions of ideal sinusoidal analytical structural boundary conditions and in-vacuo eigenvalues will give significant inaccuracy in the frequency range containing very low order modes. Modal decomposition of higher (e.g. hyperbolic) analytical functions or use of numerically defined mode shapes are options for development.
- In the higher frequency ranges normally of most concern for large cylinders, prediction accuracy is sometimes controlled by the application of equipartition of modal energy between the structure and the internal acoustic field. Optimisation of the structural modal energy estimate and the establishment of values for confidence levels when this criterion needs to be applied (to make allowance for significant re-radiation of energy back to the incident field) require further development.
- The structural analysis which provides the eigenvalue input data for the acoustic analysis must use a good model of the structure although very high accuracy of eigenvalues for higher order modes is not required because of the high modal densities.
- The method gives the spatially averaged internal noise level. The method is limited to simple internal space geometries (cylindrical or annular).

7.08 MIA APPROACH TO NOISE REDUCTION (PROVIDED BY CYLINDERS)

INTRODUCTION

The analysis is based upon the assumption of cylindrical geometry and has two basic steps:

- first the structural response of a cylindrical mode due to the external acoustic forcing field is calculated,
- then the coupling between that mode and the acoustic modes of the gas in the enclosed cavity is calculated with the aid of MIA (in general there is no need for fully coupled dynamic analysis).

This is repeated for all the structural modes having their natural frequency in the frequency band of concern. The resulting acoustic modal energies are summed and then converted into the corresponding spatially averaged sound pressure level. The numbers of resonant mode pair couplings in a frequency band could range from none at low frequencies, up to several thousand at high frequencies. Even if there are no mode pairs with natural frequencies in a particular frequency band, the significant off-resonance contributions from selected mode pairs are included in the sound transmission estimate. It is unusual for the contribution of a single mode pair to dominate the resulting frequency band value.

EXTERNAL COUPLING

Plane wave scattering

Each cylindrical structural mode has an axial and a circumferential order (m, n), see: Figure 7.08.1. The analysis developed in Ref. [13] assumes that the sound field consists of one or more incident progressive plane waves and that the ends of the cylinder are simply supported. The blocked pressure field at the surface of the cylinder is calculated, the diffraction of the incident waves by the 'rigid' cylinder being taken into account. Any one plane wave can be decomposed into a set of cylindrical waves, the sum of which satisfies the boundary condition on the rigid cylinder. Each cylindrical component has a single circumferential order (n). Similarly, each structural mode of uniform cylindrical structure has a unique circumferential order; only acoustic components and structural modes of the same order can couple. The fraction of the plane incident wave which is matched to the circumferential mode of order n is termed the 'scattering coefficient' for mode n, giving a family of circumferential mode order curves of scattering coefficient versus frequency. These reach a maximum value which decreases with increasing mode order but occurs at a frequency which increases with mode order.

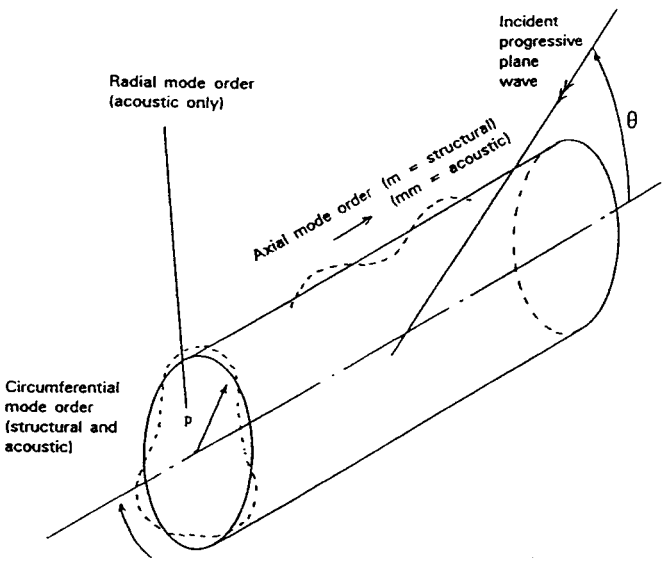

Figure 7.08.1 - Cylinder and Mode Order Notation

Generalised force

When the overall force driving a particular cylindrical mode (termed the 'generalised' force) is calculated, the mode shapes of the flexible cylinder are taken into account, in the circumferential direction by virtue of the modal scattering coefficient, and in the axial direction by the joint acceptance function (JAF) [See: Chapter 11].

The resulting expression for the spectral density of the generalised force, $S_{F,(mn)}(\omega)$, for random excitation is given by:

$$S_{F,(mn)}(\omega) = S_{p,(n)(\omega)} \cdot K \cdot j_m^2(k_z)$$

where:

$S_{p,(n)(\omega)}$ = spectral density of block pressure,

m = axial mode order,

n = circumferential mode order,

K = function of (R/L),

R = radius of cylinder,

L = length of cylinder,

$j_m^2(k_z)$ = Joint Acceptance Function.

Structural response

With the coupling, or 'joint acceptance', taken into account in the generalised force expression, the response is calculated as if for a single-degree-of-freedom system. Structural response W_{mn} in the mn mode at frequency ω is expressed by the following relationship:

Generalised displacement response =

[Gen.force/Gen.mass] x [Dynamic magnification factor]

$$\text{as} \quad W_{mn} = (F_{mn}/M_{mn})\left[(\omega_{mn}^2 - \omega^2) + i(\eta_{mn}\omega\omega_{mn})\right]^{-1}$$

In spectral density terms:

$$S_{w,(mn)}(\omega) = \left(S_{F,(mn)}(\omega)/M_{mn}^2\right)\left[(\omega_{mn}^2 - \omega^2)^2 + (\eta_{mn}\omega\omega_{mn})^2\right]^{-1}$$

where: η_{mn} is the sum of the dissipation and external radiation loss factor and ω_{mn} is the natural frequency of mode m, n.

The resonance proximity term expresses the frequency matching whilst the degree of spatial coupling for mode m, n can be appreciated from the behaviour of the joint acceptance function.

For the simply supported case, the characteristics of the joint acceptance function are illustrated in Chapter 11 for the beam function used to approximate a cylinder's axial behaviour. The 'coincidence' condition, occuring when the response and excitation wavelengths are equal at the excitation frequency, is here termed 'external coincidence'.

The general effect on external coincidence of the parameters of the cylinder and of the incident acoustic field may be appreciated from Figure 7.08.2. External coincidence occurs when the linear curve of the excitation field's axial wavenumber intersects the structural dispersion curves. The structural dispersion 'curves' for resonant axial modes only exist at the axial modal frequencies, so that resonant-coincidence occurs only when the external wavenumber curve passes through a mode resonance point. However, the principle is clarified by reference to a complete dispersion curve.

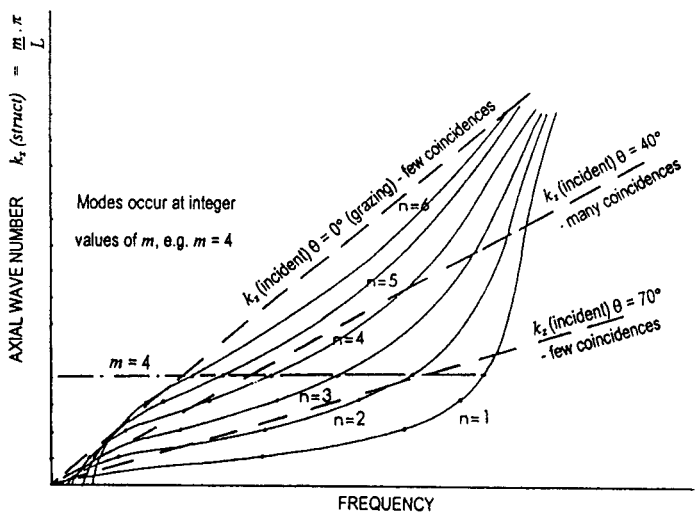

Figure 7.08.2 - Structural Mode Dispersion Curves for Cylinder

In Figure 7.08.2, the effect of the grouping of curves in the vicinity of the ring frequency, ω_{ring}, can be seen, leading to high densities of coincidence in the frequency domain. The ring frequency is the natural frequency of the diametric breathing mode of zero circumferential order of the equivalent infinitely long uniform cylinder. For a homogeneous cylinder wall:

$$\omega_{ring} = c'_\ell / a$$

where:

a = mean radius, and

c'_ℓ = longitudinal speed of sound in a plate of cylinder wall material.

For a sandwich-wall cylinder:

$$\omega_{ring} = \frac{1}{a}\left[\frac{E_\theta h_f}{\rho_f h_f + \frac{\rho_c + h_c}{2}}\right]^{1/2}$$

where:

E_θ = tensile module in circumferential direction,

ρ_f, h_f = faceplate density, thickness (similar faceplates assumed),

ρ_c, h_c = core density, thickness.

For a given cylinder, external coincidence varies only with the angle of incidence, as this determines the gradient of the external wavenumber line. The gradient decreases as incidence angle changes from grazing to normal. Changes to the cylinder's dispersion curve will be produced by anything which changes the natural frequencies of the modes. Below the ring frequency, reducing the natural frequencies raises the dispersion curve, and would cause coincidence to occur closer to grazing incidence, and at lower frequencies. Figure 7.08.3 shows this effect for a single circumferential mode. Each circumferential mode can be considered separately since there can be no coupling between modes of different circumferential order. Near ring frequency, the S-bend nature of the dispersion curve causes less predictable changes. From Figure 7.08.2 it can be seen that the density of coincidences can suddenly increase for small changes in angle of incidence.

Criteria are applied to the selection of mode pairs to avoid the inclusion of weakly coupled pairs and hence to economise on CPU time.

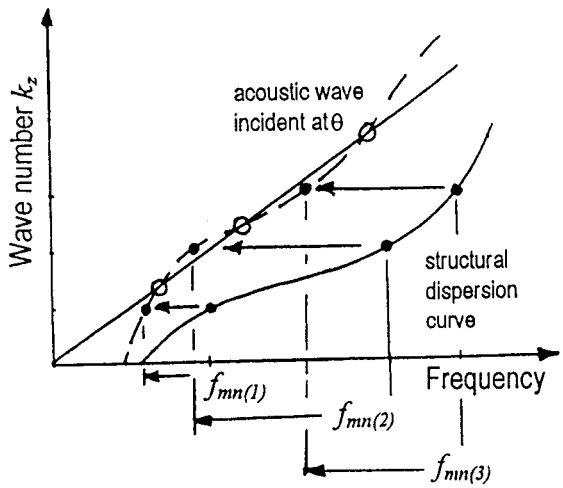

Note: Reducing structural natural frequencies shifts dispersion curves towards a given incidence wavenumber line.

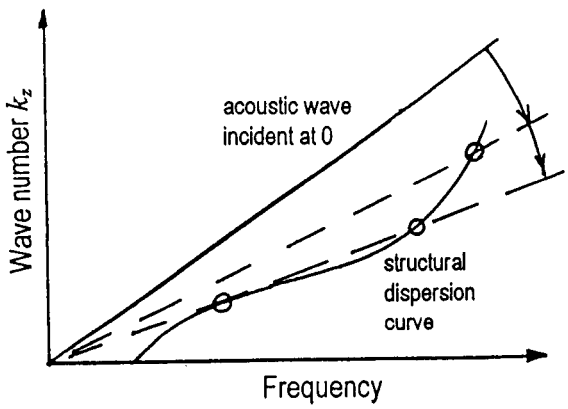

Note: Increasing incidence angle of excitation field shifts external wavenumber curve towards a given structural curve, leading to single the multiple coincidences.

Figure 7.08.3 - Effect of Structural and Incident Field Changes on Occurrence of External Coincidence

INTERNAL COUPLING ESTIMATION BY MIA

To estimate noise levels inside the cylinder, the response of the acoustic modes to structural mode vibration is calculated, frequency by frequency, by means of a modal interaction analysis.

The coupling once again peaks when coincidence occurs, in this case as shown by the intersection of internal dispersion curves and structural dispersion curves, again for a common circumferential mode order as indicated by Figure 7.08.4. Both sets of dispersion curves now only exist in reality at resonance frequencies. Their intersections at these points are 'internal' coincidences. It will be understood that circumstances of maximum transfer of energy to the internal sound field are encountered when an external coincidence and an internal coincidence occur at or near the same frequency.

All cavity modes are coupled to each structural mode to some extent, but the analysis is restricted to cavity modes which exhibit good coupling. Since the analysis proceeds in two separate uncoupled stages, there is no mechanism for feedback of acoustic energy to poorly excited structural modes which acts as a form of damping for the acoustic modes. Hence the acoustic energy can build up to a level which contravenes the limiting condition of equipartition of modal energy under broadband excitation. Equipartition is imposed as an upper limit on the acoustic modal energy, using all available structural and acoustic modes in a band. The modelling has been coded so that the coupling is evaluated at a set of discrete frequencies and then summed over one-third octave bands. The contributions from the selected mode pairs are then summed to give the overall noise reduction in each band.

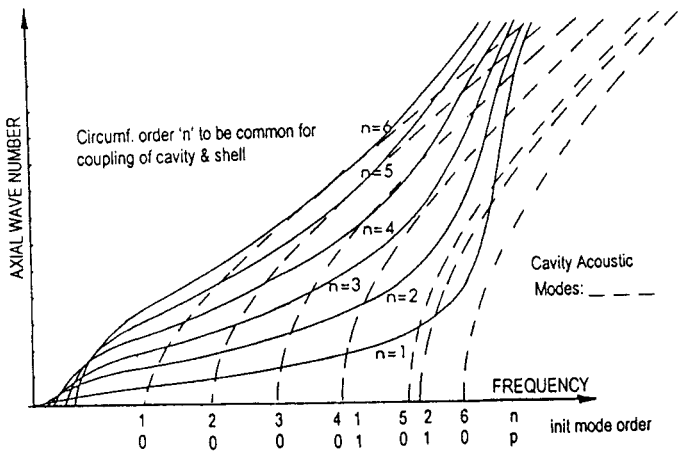

Figure 7.08.4 - Structural and Internal Acoustic Mode Dispersion Curves

MULTI-COMPONENT INCIDENT FIELDS

The external sound field at launch is usually of primary concern and this can be modelled as several progressive plane waves of the required relative level. The noise reduction is assessed for individual component plane waves and then the overall noise reduction computed. A reverberant sound field can also be modelled, by an option within the analysis.

7.09 CYLINDERS: COMPARISON OF PREDICTIONS WITH MEASURED NR VALUES

To test the model, a series of experiments was performed using sandwich wall construction cylinders scaled to represent structures similar to the full-size European Ariane 4 launcher fairing, Ref. [9]. The wall construction of the models used orthotropic carbon fibre reinforced plastic (CFRP) faceplates of lay-up and properties close to the full-scale construction, but the aluminium honeycomb core thickness and overall dimensions were at one quarter scale. The test frequency range, scaled on the overall dimensions, covered the structural behavioural regimes of the full-size fairing when reduced to the equivalent cylinder. Properties of the model cylinders and the assumed fairing properties are shown in Table 7.09.1.

Parameter	Scaled	A4 (Assumed)
Face Plates (CFRP, common)		
Thickness mm	1.0	0.9
Elastic mod. N/m² E9		
Tensile circumf.	26.2	20.4
Tensile axial	69.5	66.3
Shear in plane	19.3	12.4
Density kg/m³ E3	1.6	1.7
Core (aluminium honeycomb)		
Thickness mm	5	24
Shear mod. N/m² E6		
Circumf.	150	80
Axial	240	140
Density kg/m³	48	48.7
Wall		
Length m	0.94	8.7
Diameter m	0.9	4
Mass/area kg/m³	4.0	4.1
Structural damping (loss factor)	0.01	0.01
f_{ring} (Hz)	1349	234
f_{crit} axial/circumf. (Hz)	1038/1692	186/483

Table 7.09.1 - Properties & Dimensions of Empty Unlined Cylinders

Predictions have been made using the code of Ref. [13]. The structural eigenvalues were estimated separately from the MIA model for in-vacuo modes by an analysis based on Baker and Hermann's theory, Ref. [14]. The internal acoustic modes are assumed to be independent of the structural field. The predicted and measured cylinder performance is shown as noise reduction values (NR, dB) where:

NR = (Incident sound pressure level at the structure's location in the absence of the structure) – (spatially averaged internal sound pressure level).

Some predicted spectra of noise reduction values are shown in Figures 7.09.1 and 7.09.2, with measured results superimposed. Also superimposed are corresponding measured and calculated changes, since it is the sensitivities rather than absolute values which the method is designed to predict. The predicted effects of changing the wall construction of the cylinder are shown in Figure 7.09.3.

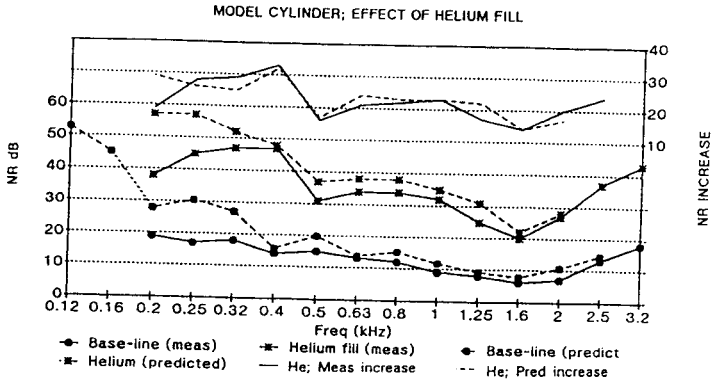

Figure 7.09.1 - Measured Effect of Helium Fill (Model Cylinder)

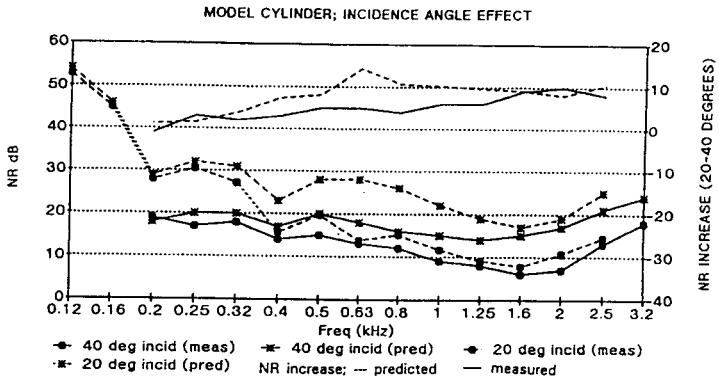

Figure 7.09.2 - Measured Effect of Incidence Angle (Model Cylinder)

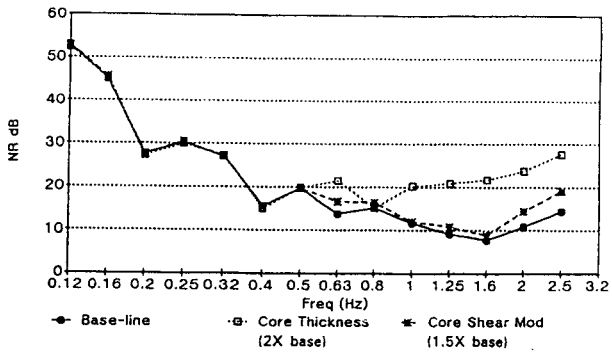

Figure 7.09.3 - Predicted Effect of Change in Core Properties (Model Cylinder)

7.10 CYLINDERS: APPLICATION TO LARGE SHELLS

Few data are available for full-size sandwich construction cylinders, but a comparison is shown in Figure 7.10.1 between some predicted and some preliminary measured values for an Ariane 4 fairing. The fairing incorporates a nose cone and is made of two halves, on a diametrical split-line, but this was modelled as a simple cylindrical shape.

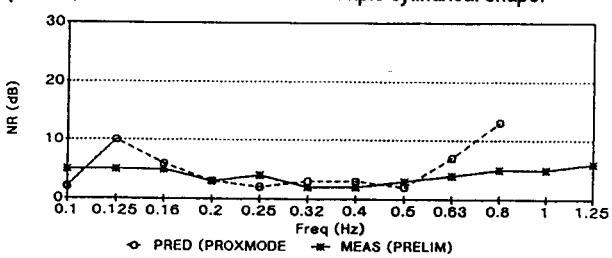

Figure 7.10.1 - Noise Reduction of Ariane 4 Fairing (Reverberant Incidence)

The prediction of very low values of noise reduction is due to the high modal density over the frequency range of interest, even for the relatively stiff real wall construction. For example, there are four flexural mode eigenvalues in the 32 Hz centre frequency octave band for the 4m diameter cylinder, but only 3 values in the 250 Hz band for the experimental scaled model cylinder. This difference triggers the invocation of the equipartition limit for the model but not for the full-scale structure. Even with this limitation, negative values of noise reduction are possible. There is a difficulty in applying this criterion to a limited bandwidth, since a judgement has to be made as to which structural modes contribute significantly enough to the acoustic field response to warrant being included in the structural modal energy estimate. When the energy limiting criterion is invoked, the value of the internal absorption has no influence on the internal noise level. The physical reason is that the modal–average coupling loss factor exceeds the acoustic dissipation loss factor.

7.11 REFERENCES

[1] R.J. Cummins & W. Cooper
'Spacecraft structural acoustic studies'
Final report - ESA CR(P)-1264

[2] E. Szechenyi
'Sound Transmission Through Cylinder Walls Using Statistical Considerations'
J. Sound Vib., 19(1), 83-94 (1971)

[3] R.J. Cummins
'Sound transmission into closed cylinder'
MSc Dissertation, University of Southampton (1970)

[4] B.L. Clarkson & R.J. Pope
'Experimental determination of modal densities and loss factors of spacecraft components'
ESA Contract No. 4100/79/NL/PP (1980)

[5] L.D. Pope & J.F. Wilby
'Space-Shuttle payload bay acoustics prediction study: Final report, Vol. 2: Analytical model'
Bolt, Beranek and Newman Report No. 3286 (1976)

[6] G. Borello
'Effect of the Payload on the Surrounding Internal Acoustic Environment at Lift-Off'
Proc. Int. Conf. 'Spacecraft Structures and Mechanical Testing'
Noordwijk, NL, 24-26 April 1991
ESA SP-321, Oct 1991, pp. 945-948

[7] B. Ritchie & M. Beldi
'Ariane 4 Internal Acoustic Environment: Interpretation of Flight Data with a Vibro-acoustic Model of the Upper Part of the Launcher'
Proc. Int. Conf. 'Spacecraft Structures and Mechanical Testing'
Noordwijk, NL, 24-26 April 1991
ESA SP-321, Oct. 1991, pp. 211-217

[8] L.L. Beranek
'Noise Reduction'
McGraw-Hill (1960)

[9] J.N. Pinder, M.E. House & F.J. Fahy
'Preliminary Study of the Noise Reduction in the Ariane 5 Payload Bay Given By the Fairing and SPELTRA'
Final Report. ESA Contract No. 6675/86/F/F1, 1987

[10] J.N. Pinder & F.J. Fahy
'A Method for Assessing Noise Reduction Provided by Cylinders'
Proc. Inst. of Acoustics, 15(3), 1993, pp. 195-205

[11] M.A. Hamdi
'Méthodes de discrétization par éléments fines et éléments finis de frontière'
In: Rayonnement acoustique des structures, C. Lesueur (Editor)
Editions Eyrolles, 1988

[12] M. Faust, G. Schweickert & F. Strobel
'Structure-Acoustic Finite Element Analyses for Noise Reduction Investigations of Launcher Payload Compartment Structures Made of CFRP Sandwich Material'
Proc. Int. Conf. 'Spacecraft Structures and Mechanical Testing'
Noordwijk, 24-26 April 1991 (ESA SP-321)

[13] PROXMODE. Personal-Computer code
ISVR Consultancy Services, 1993
University of Southampton, England
Note: NOT subjected to ESA software quality assurance procedures

[14] E.H. Baker & G. Hermann
'Vibration of Orthotropic Cylindrical Sandwich Shells Under Initial Stress'
AIAA Journal, 4, No. 6, pp. 1063-1070, June 1966

(Intentionally Left Blank)

Structural Acoustics Design Manual

Chapter 8
INPUT POWER

CONTENTS

8.01 GENERAL

GENSTEP3 has been developed mainly for the prediction of response due to a reverberant sound field. This chapter gives guidance on the method for inputting power from a reverberant sound field.

The prediction of response levels due to a mechanical vibration source is also given but the response uncertainty range for this localised form of excitation is greater than for distributed loading by typical exposure to a sound field, because the fundamental SEA assumption that global properties are appropriate for each subsystem is not being satisfied.

8.02 ACOUSTIC EXCITATION (REVERBERANT SOUND FIELD)

Although the theory applies to a diffuse reverberant sound field, the use of sound-pressure levels from rocket, jet and probably aerodynamic boundary-layer noise will be acceptable for most purposes. The acoustic excitation band levels for the payload compartment of a typical launch vehicle are given for reference purposes in Table 8.02.1.

1/3 Octave Band Center Frequency (Hz)	Sound Pressure Level (dB) Ref. 2 x 10^{-5} N m^{-2}	
	Lift-Off 5 seconds/mission	Aeronoise 5 seconds/mission
31.5	122.0	112.0
40.0	124.0	114.0
50.0	126.0	116.0
63.0	127.5	118.0
80.0	129.5	120.0
100.0	130.5	122.0
125.0	132.0	124.0
160.0	133.0	125.0
200.0	133.5	126.5
250.0	134.0	127.0
320.0	134.5	127.0
400.0	134.5	127.0
500.0	134.0	127.0
630.0	133.5	125.0
800.0	133.0	123.0
1000.0	132.0	119.0
1250.0	131.5	118.0
1600.0	130.0	117.0
2000.0	129.0	115.0
2500.0	128.0	113.0
3200.0	126.5	111.0
4000.0	125.0	109.0
5000.0	124.0	107.0
6300.0	122.5	105.0
8000.0	121.0	102.0
10000.0	120.0	101.0
OAL	145.0	137.0

Table 8.02.1 - Typical Payload Compartment Noise Levels

CHOICE OF ANALYSIS BANDWIDTH

A general rule for the selection of the analysis bandwidth is that it should include at least five modes for a structural subsystem and ten modes for an acoustic space subsystem. However it is probable that reasonable estimates of response can be obtained when structural subsystems with less than five modes per bandwidth are included in SEA models.

The choice of a constant bandwidth is preferred for analysis purposes, but a constant percentage bandwidth is also commonly used. Table 8.02.2 gives the internationally preferred octave and one-third octave band levels, including the lower and upper cut-off frequencies. The latter is particularly useful, as GENSTEP3 requires input of the lower and upper frequencies of the total analysis range together with the number of bandwidths. It should be noted that the excitation sound-pressure levels may only be available in constant percentage bandwidth form; these will require conversion to constant bandwidth if that is the chosen standard for analysis prediction.

An information message is available in GENSTEP3 to indicate when a pre-set modal density (modes/Hz) is not obtained by any subsystem.

Octave Bands			1/3 Octave Bands		
Approx. lower cut-off frequency (Hz)	Center frequency (Hz)	Approx. upper cut-off frequency (Hz)	Approx. lower cut-off frequency (Hz)	Center frequency (Hz)	Approx. upper cut-off frequency (Hz)
11	16	22	14.1	16.0	17.8
			17.8	20.0	22.4
			22.4	25.0	28.2
22	31.5	44	28.2	31.5	35.5
			35.5	40.0	44.7
			44.7	50.0	56.2
44	63	88	56.2	63.0	70.8
			70.8	80.0	89.1
			89.1	100.0	112.0
88	125	177	112.0	125.0	141.0
			141.0	160.0	178.0
			178.0	200.0	224.0
177	250	355	224.0	250.0	282.0
			282.0	315.0	355.0
			355.0	400.0	447.0
355	500	710	447.0	500.0	562.0
			562.0	630.0	708.0
			708.0	800.0	891.0
710	1000	1420	891.0	1000.0	1122.0
			1122.0	1250.0	1413.0
			1413.0	1600.0	1778.0
1420	2000	2840	1778.0	2000.0	2239.0
			2239.0	2500.0	2818.0
			2818.0	3150.0	3548.0
2840	4000	5680	3548.0	4000.0	4467.0
			4467.0	5000.0	5623.0
			5623.0	6300.0	7079.0
5680	8000	11360	7079.0	8000.0	8913.0
			8913.0	10000.0	11220.0
			11220.0	12500.0	14130.0
11360	16000	22720	14130.0	16000.0	17780.0
			17780.0	20000.0	22390.0

Table 8.02.2 - Internationally Accepted Octave & One-Third Octave Bands

EVALUATION OF INPUT LEVEL

The input to GENSTEP3 is in terms of sound-pressure level (SPL) in N.m^{-2}. Usually SPL excitation levels are quoted in decibels (dB) and can be converted to pressure levels with the aid of the reference level:

$$\text{SPL dB} = 10\log_{10}\frac{p^2}{p_0^2} = 20\log_{10}\frac{p}{p_0}$$

where the usual reference level is:

$$p_0 = 20 \times 10^{-6}\ \text{N.m}^{-2}\ (\text{or } 20\ \mu\text{Pa})$$

(One should check whether this is indeed the reference level that has been used, although it is the usual standard for the aerospace industry).

Note: It is band level that is required and if SPL spectrum levels are quoted they should be converted to band level by multiplying by the bandwidth. In decibel form this is:

$$dB = 10\log_{10}\frac{\Delta f}{1}$$

where:

Δf is the bandwidth required in Hz, and

1 Hz is the reference bandwidth for spectrum level.

ASSOCIATED VOLUME

GENSTEP3 requires values to be input for the volume, surface area and edge length of the space enclosing the sound field. It is recommended that the following values be used:

V = 800 m³,
S = 593 m²,
L = 140 m.

These values are applicable to the reverberant chamber where much of the development testing was performed, but are also acceptable for use with external noise sources. The volume V is used for the evaluation of the energy of the excitation field and the evaluation of its modal density; in the resulting computation for input power, V is almost exactly cancelled.

MODELLING OF ACOUSTIC EXCITATION

Two options are available within GENSTEP3 to represent acoustic excitation. The AFIELD card allows power input to be applied directly to structural subsystems, or alternatively a separate acoustic subsystem can be modelled; see: Figure 8.02.1. There is an important distinction in the loss factors required for the excited structural subsystem for these alternative approaches.

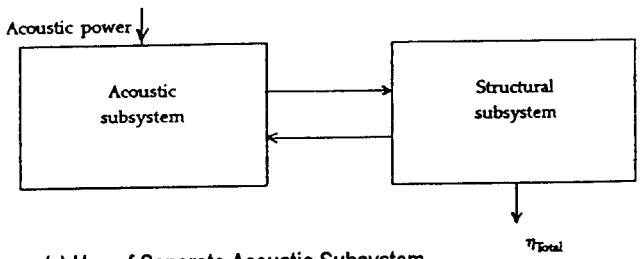

(a) Use of Separate Acoustic Subsystem

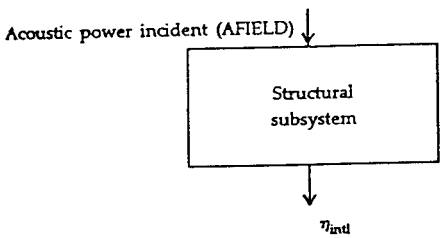

(b) Use of Direct Acoustic Incident Power (AFIELD)

Figure 8.02.1 - Representations of Acoustic Vibration

The direct power input (AFIELD) option requires **total** dissipation loss factors to be specified for the excited subsystem, i.e. radiation plus internal loss factor components, as can be estimated from the overall damping measured from in-air testing.

With this option, the radiation effect (radiation resistance) is calculated by GENSTEP3 only for estimating the sound power input to the excited subsystem. The complementary radiation effect on response (radiation damping) is assumed to be included within the total loss factor value specified by the GENSTEP3 user, within the data specifying the excited structural subsystem. It is necessary for the total loss factor to include the same radiation characteristics as calculated by GENSTEP3 (i.e. to be frequency dependant, showing peaks at coincident frequencies) otherwise, for example, the receiver subsystem will show a large peak in response where a high radiation efficiency is calculated which is not balanced by a high radiation damping contribution in the total loss factor as would occur in practice.

The alternative use of a separate acoustic subsystem avoids this possibility, because GENSTEP3 uses the same basis to calculate both energy input and the receivers radiated energy and the user only defines the internal dissipation loss factor. However, a small additional calculation is required outside GENSTEP3 to calculate the sound power input to the acoustic subsystem if only the sound pressure level of the acoustic field and the absorption characteristics are known.

When using the direct power input (AFIELD) option, a power input should be provided in the SEA model for all structural subsystems on which the acoustic excitation field impinges directly. Allowance should also be made for **nonresonant transmission** through a structural subsystem to enclosed acoustic subsystems, [See: Topic 7.01].

A general rule for modelling current satellite structures is:

- **Single power input:** Zone-1, Zone-2, Zone-3, Zone-4, Zone-5 and Zone-7 structures.
- **Nonresonant input:** enclosed cavities and sound-transmission situations.

8.03 MECHANICAL VIBRATION

Allowance has been made in GENSTEP3 for the input of mechanical power to both structural and acoustic subsystems. As yet, however, the correct calculation and application procedures have not been developed. The following method has been proposed as a means of estimating the power transmitted at a typical satellite connecting ring, Ref. [1].

POWER TRANSMISSION: SATELLITE/LAUNCH VEHICLE INTERFACE OR TEST ADAPTOR RING

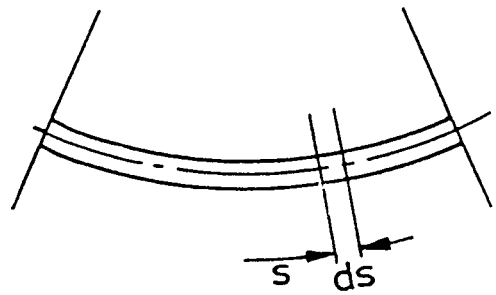

Figure 8.03.1 - An Element from the Launch Vehicle or Test Adaptor Ring

In Figure 8.03.1, consider an element, of length ds, of the connecting ring at position s on the periphery. Let the force on the ring element be $f(s,t)ds$.

If the velocity of the ring is $v(s,t)$ then the power transmitted across the element is $\overline{f(s,t)v(s,t)}ds$ This can be written as:

$$\overline{v^2(s,t)}\,\mathrm{Re}\left(\frac{f(s,t)}{v(s,t)}\right)ds$$

or:

$$\overline{v^2(s,t)}\cdot\mathrm{Re}\{Z(s)\}ds$$

where the velocity and impedance values are for the coupled state.

In the higher-frequency region it may be reasonable to assume that the frequency, average velocity and impedance do not vary significantly around the periphery of the ring. If this is the case, then the total power transferred can be obtained simply by integrating the element of power around the ring. Thus the average total power transferred in a frequency band is:

$$P(f)=\frac{2\pi R}{(f_2-f_1)}\int_{f_1}^{f_2}\overline{v^2(t)}\,R\{Z\}\cdot df$$

It is usual to measure acceleration and make use of Fourier transforms to get the frequency band levels. The power input can then be written as:

$$P(f)=\frac{2\pi R}{(f_2-f_1)}\int_{f_1}^{f_2}\frac{|A(if)|^2}{f^2}\cdot\mathrm{Re}\{Z\}\cdot df$$

This will be a relatively simple relation to evaluate and should give a good estimate of the power transmitted by mechanical vibration if the basic assumption is reasonably accurate.

The attachment ring is relatively stiff compared with the local structure of the launch vehicle and the satellite at the junction point. Thus the frequency averaged acceleration is not likely to vary considerably around the periphery of the ring. The possible variation in impedance of the satellite at its adapter ring will have to be investigated further.

Impedance values measured at the mounting ring of the Marots satellite were measured in the free uncoupled condition, Ref. [2], in the radial and axial directions, see Figure 8.03.2 and Table 8.03.1. Values were also measured for the free platform at the ring used for attachment to the central cylinder; see Figure 8.03.3 and Table 8.03.2.

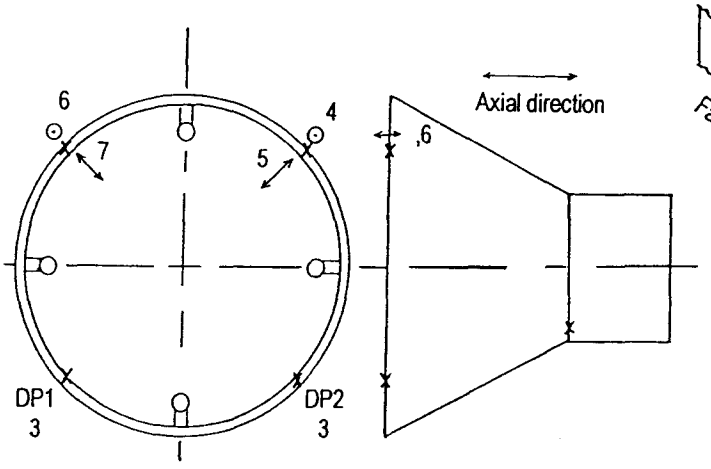

Figure 8.03.2 - Impedance Measurement Locations at a Base Fixing Ring Attachment

Centre Frequency (Hz)	Real (Impedance) N/(m/s)	
	Axial	Radial
100	693	74.9
200	5300	1870
300	1300	1790
400	1190	1860
500	3130	1090
600	2610	1660
700	2070	566
800	1390	758
900	2520	123
1000	1000	233
1100	1190	1750
1200	528	308
1300	396	630
1400	604	351
1500	899	1020
1600	459	2050
1700	745	1360
1800	1030	649
1900	902	329
2000	934	550
2100	794	427
2200	463	298
2300	505	235
2400	859	232
2500	553	350
2600	272	245
2700	709	447
2800	883	222
2900	496	197

Table 8.03.1 - OTS Cone and Cylinder Assembly: Real Part of Impedance Averaged Over 100 Hz Bandwidth

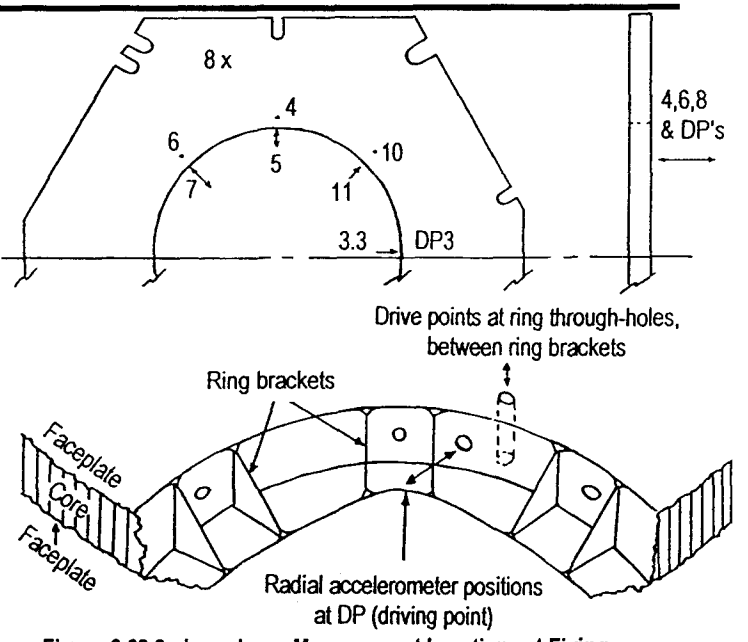

Figure 8.03.3 - Impedance Measurement Locations at Fixing Points of OTS Platform to Central Cylinder

Centre Frequency (Hz)	Real (Impedance)
100	378
200	758
300	904
400	837
500	942
600	1050
700	943
800	1880
900	1270
1000	1190
1100	1770
1200	932
1300	1460
1400	1650
1500	1740
1600	1830
1700	1430
1800	1310
1900	1810
2000	1980
2100	1850
2200	1450
2300	2070
2400	1810
2500	1850
2600	1260
2700	1850
2800	1470
2900	1150

Table 8.03.2 - OTS Platform: Real Part of Impedance Averaged Over 100 Hz Bandwidth

The coupled impedance required to estimate power input from motion rather than from force levels is given by the expression in Topic 6.11, where the real part of impedance adequately represents the complex impedance.

ONBOARD EXCITATION

GENSTEP3 includes the scope to enter values of point force and impedance data so the power input from vibration sources on board a spacecraft during its service can be included; [See: GENSTEP3 Manual, Section 7, Power Card]. When the force is known, only the receiving structure's impedance is required, without taking account of the forcing structure's impedance.

A test method for characterising the excitation of a spacecraft by on-board mechanisms is proposed in Ref. [3].

8.04 REFERENCES

[1] R.J. Cummins
'Development of structural acoustic design guides'
Final report. ESA CR(P)-1916, (1981)

[2] J.N. Pinder
'Experimental Work Associated with Acoustic Design Manual for Statistical Energy Analysts'
Final Report (Technical Report No. 16)
ESA Contract Number 6546/85/NL/PH(SC). October 1986

[3] J.N. Pinder
'Satellite In-Orbit Health Monitoring: Synthesis and On-Board Data Handling'
Final Report, Vol. 2
ESA Contract Number 10235/92/NL/PP(SC), June 1994

(Intentionally Left Blank)

Structural Acoustics Design Manual

Chapter 9
COMPENDIUM OF LOSS FACTORS

CONTENTS

9.01 SUMMARY OF VALUES

DISSIPATION LOSS FACTORS

Table 9.01.1 gives a summary of the typical DLF values recommended for use with SEA models.

These values were measured in air and so include radiation loss.

Structural Configuration	Suggested DLF
Unstiffened cylinder	0.001
Stiffened cylinder	0.002
Plain platform or panel	0.004
Conventionally fabricated platform or panel	0.008
Integrally machined platform or panel	0.005
Honeycomb panels/platforms, metallic	0.020
Honeycomb panels/platforms, CFRP face sheets	0.020
Corrugated cylinder (+ stiffening rings)	0.006
Corrugated cone (+ stiffening rings)	0.006
Large antenna (L Band)	0.040

Table 9.01.1 - SEA Models: Typical Dissipation Loss Factors (DLF)

Notes:

- For further information on the spread of values: See: Figure 9.03.1 and Topic 9.03.
- For the effect of equipment on panels and platforms: See: Topic 9.04.
- For the DLFs of other aerospace structures: See: Topic 9.04.
- For the effect of thermal tiles on the DLF of structure: See: Topic 9.04.
- For the DLF of fibre-reinforced plates: See: Topic 9.04.
- For the DLF of acoustic cavities: See Topic 7.07.
- For the measurement of DLF: See Topic 10.03.

COUPLING LOSS FACTOR

Acoustic-space/structure and acoustic-space/acoustic-space CLF values are evaluated by the GENSTEP3 program. The theoretical expressions are given in Appendix A.

There is little information available on the CLF values for structure-to-structure coupling, but Table 9.01.2 gives the recommended CLF for three important junctions (from Topic 9.06).

CLF For Honeycomb Platform Coupled To:	
Plain cylinder	0.0020
Corrugated cylinder	0.0012
Corrugated cone	0.0058

Table 9.01.2 - SEA Models: Typical Coupling Loss Factor (CLF)

General advice on the selection of CLF values for structure-to-structure coupling is given in Topic 9.07.

9.02 GENERAL

It is intended that this section should provide a compilation of available information on dissipation and coupling loss factors (DLF and CLF) for use in SEA analysis.

The CLF parameter is only used in SEA analysis, but the DLF parameter is directly related to the viscous damping ratio (DLF, $\eta = 2\delta$) and information may be available from other structural dynamics sources. However, other forms of dynamic structural analysis consider the response of individual modes, so the damping information is usually that for a single mode. SEA considers groups of modes contained in bandwidths, and it is the DLF for a group of modes, that is required, so an individual modal damping may not give sufficient information.

The test methods used to measure DLF and CLF are very important, a large spread of data has been found when values obtained by differing techniques have been compared. Research has been performed on developing methods, and the current recommended techniques are presented in Chapter 10. Much of the data presented in this section will have been obtained by procedures other than those recommended in Chapter 10. Work has been performed at ISVR, Southampton University, on improving test techniques and comparing methods. Ref. [1, 2, 3] cover a comparison of DLF measurement techniques and Ref. [4, 5] cover the recent investigations on CLF measurement. The available data are mainly for aluminium structures, although there is some information for non-metallic configurations.

Information on DLF values for contained spaces (acoustic subsystems) is given in Chapter 7 and the method of computing CLF values for contained spaces is given in Appendix A.

9.03 DISSIPATION LOSS FACTORS (DLF)

The values of DLF which were measured during the course of the ESA/BAe/ISVR investigations Ref. [6, 7, 8, 9, 10] are shown in Figure 9.03.1, as a spread of values for the frequency range 63 to 2 kHz, together with the mean value. There appears to be no predictable variation with frequency over this range, so a constant DLF value has been used for the SEA prediction work (usually the mean value). The data, presented in Figure 9.03.1, were obtained mainly from components of the two structures used during development work of EX1 and Marots, [See: Figures 2.06.1 and 2.06.2]. Full dimensions and structural properties of these components are given in Ref. [9].

It is expected that variations in DLF will exist for changes in configuration on similar components, and it is generally recommended that the mean value be used from the component that is closest to the required configuration. A table of recommended values is given in Topic 9.01.

There may also be a variation due to the test technique employed. The majority of values in Figure 9.03.1 have been obtained by the decay technique, [See: Topic 10.3], but with acoustic excitation rather than mechanical point excitation from a vibrator. The difference between these two types of excitation has not been fully investigated, but the differences between the decay and energy methods in the case of mechanical excitation are reported in Ref. [3]. It was shown that when the modes in the band have similar loss factors (as is usually the case), the energy method gives a result very close to that obtained from the decay method. These values are very close to the arithmetic average of the loss factors of the individual modes in the band. It was also shown that only when the band contains one or two very lightly damped modes amongst several more heavily damped modes is there a difference between the two methods. In this case it is better to use the energy result in the SEA calculations; as recommended in Topic 10.03.

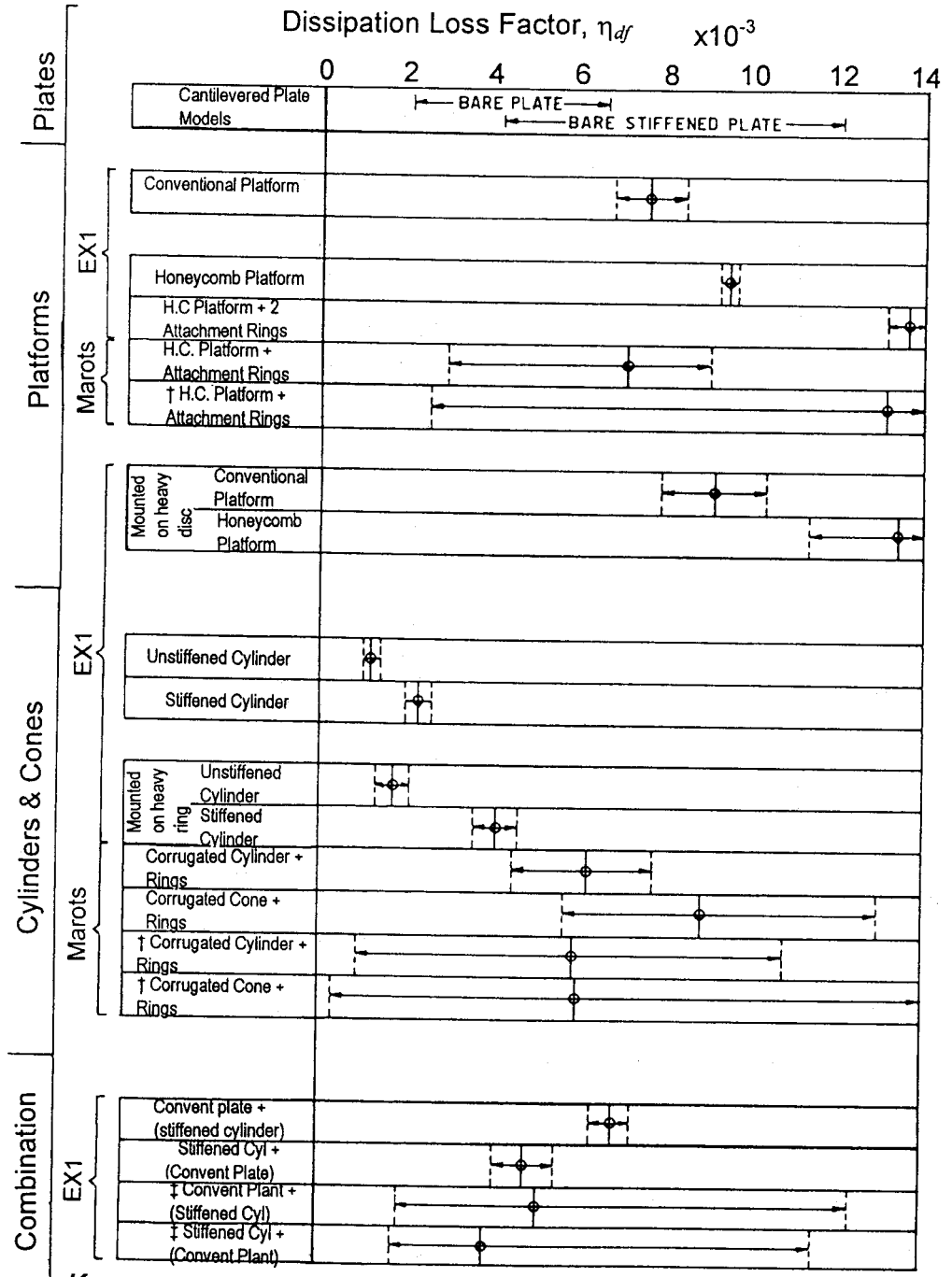

Key:

† Values obtained from decay tests - one subsystem damped.

‡ Values obtained from energy method.

ϕ Mean Value.

|←→| Scatter.

Note: The components considered above are coupled by bolting to continuous aluminium angle.

Figure 9.03.1 - EX1 & Marots Development: Structural Component DLF values

9.04 ADDITIONAL DATA ON DLFs

RECENT MEASUREMENTS

Uniform Open-Ended Cylinder

Ref. [1, 3] give details of tests performed on an open-ended single skin metal cylinder, and the results shown in Figure 9.04.1 confirm the recommended value of η_{AV} = 0.0012.

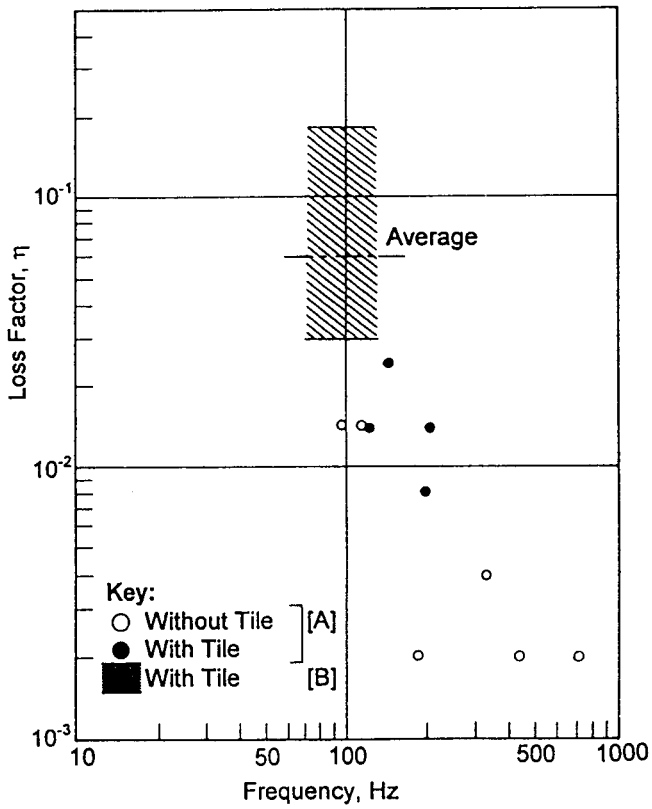

Figure 9.04.1 - Damping of Shuttle Fuselage Structure with and without TPS Tiles

Closed Cylinders

Ref. [12] gives measured values for a sandwich-wall construction with CFRP faceplates. Values over 100 Hz to 4 kHz range from 0.01 to 0.07, most probably greatly influenced by being attached to steel end plates in that instance.

Flat Plate (Metal)

Ref. [1, 3] describe measurements on a flat metal plate, basically used to investigate differences between the decay and energy test techniques. In the undamped test condition, the average DLF was between 0.004 and 0.005, values similar to those previously recommended for use in Topic 9.01.

Honeycomb Panel (Metal Core and Faceplates)

DLF measurements were made on a flat honeycomb panel (as used on the Space Shuttle Pallet) by means of both decay and energy techniques, Ref. [3]. An average DLF of 0.02 was found.

- Approximate panel size: 0.67 m x 0.855 m,
- Core thickness: 18.5 x 10^{-3} m.

Honeycomb Platform (Metal Core and Faceplates)

Measurements of loss factor have been made on honeycomb platforms from representative satellite structures. Ref. [1, 3] present an assessment of DLF on a honeycomb platform from the Marots structure (having light-alloy core and faceplates). For frequencies above ca. 250 Hz, an average value of DLF, η_{AV} = 0.020, was shown, see: Figure 9.04.1.

Honeycomb Platform (Metal Core and CFRP Faceplates)

Further DLF measurements were evaluated for the SMOP (Structural Mass Optimisation Programme) structure produced for a research programme. Platforms of different thickness were examined, Ref. [13]. However, the masses which are estimated for the honeycomb platforms and used in the energy relationship have subsequently been found to be too low when compared with the SMOP mass breakdown data (which were not available at the time of the experiment). Reassessment of DLF values gives for the:

- Upper platform, η_{AV} = 0.023,
- Lower platform, η_{AV} = 0.017.

The values show that CFRP faceplates do not appear to change the DLF significantly; the recommended value, η_{AV} = 0.020, is the same as that for metallic honeycomb panels and platforms.

Corrugated core structures

Measurements were also made on the central core structure of the SMOP specimen, see above, reported in Ref. [13]. The corrugated cylinder was manufactured from a very thin sheet and presented measurement difficulties, particularly local flexing at the excitation input location. This may account for the higher than expected DLF of η_{AV} = 0.025 to 0.030. It is recommended that the value of η_{AV} = 0.006 be used until further information becomes available.

The SMOP lower core structure, which was conical with a half-angle of 11°, was not solely a corrugated shell, but consisted of a plain conical inner skin bonded to a corrugated outer shell. Allowing for a mass correction, see: Honeycomb Platform, we find for the measured average damping the value η_{AV} = 0.006 to 0.007, which agrees with the previously recommended value for corrugated structure of η_{AV} = 0.006.

Large antenna

Measurements on an OTS L-band antenna are reported in Ref. [13], both with and without the feed horn struts. Some of the DLF values, measured by different techniques, are shown in Figure 9.04.1. The average DLF was η_{AV} = 0.040 and this value is recommended for use.

FREQUENCY DEPENDENCE OF DLF

It has been suggested that the DLF for a plain panel or platform may be taken to be frequency dependent as follows:

$$f < 80\text{ Hz} \qquad \text{DLF} = 0.040$$

$$80 \le f < 2500\text{ Hz} \qquad \text{DLF} = \frac{1.8}{f^{0.87}}$$

$$f \ge 2500\text{ Hz} \qquad \text{DLF} = 0.002$$

The basic data for this suggestion are not available. It is thought that it may be based on data exhibiting wide scatter such as that given in Ref. [14], see also: Topic 9.04 - Other Aerospace Structures.

EFFECT OF EQUIPMENT BOXES ON PLATFORMS & PANELS

Little practical information is available, except that adding equipment items will tend to increase the damping of the platform or panel. The degree of DLF increase will depend on the amount of equipment involved, its base surface area, method of attachment, etc. At present, the advice is to use values at the high end of the quoted range for the panel/platform construction unless better information is available.

Measurements on a honeycomb platform with and without boxes, indicated a 20% to 25% increase in damping, Ref. [11], which can be used if an unloaded value is known. Otherwise, suggested values are given in Table 9.04.1.

Component	DLF range	Suggested DLF for loaded component
Plain, conventionally stiffened corrugated panels.	0.005 - 0.015	0.015
Honeycomb panels and platforms.	0.005 - 0.030	0.030
Solar arrays.	0.014 - 0.040	0.040

Table 9.04.1 - DLF: Effects of Equipment (Suggested Values)

OTHER AEROSPACE STRUCTURES

Information is available for metallic aircraft structures and the Engineering Science Data Unit (ESDU) has collated much data, Ref. [14]. A large scatter in values is shown in Ref. [14]. Various discrete frequency test methods have been employed on a large selection of structures to evaluate the viscous damping ratio for individual response frequencies (in practice it would have been the more prominent or highly excited modes which were measured). It is usually taken that, for viscous damping, the damping ratio is inversely proportional to frequency and the graphs presented in Ref. [14] show a line with this slope drawn through the points. However, the scatter is such that a constant value of damping could also be taken, certainly over the main frequency range of 100 - 1000 Hz. Table 9.04.2 summarises the values from Ref. [14]. On the basis of the quoted range of values and an estimated constant value, the values are expressed as DLF values (i.e. as $\eta = 2\delta$).

Form of construction	Quoted range of DLF	Estimated DLF
Skin stringer(conventional)	0.01 - 0.06	0.020 (flat) 0.030 (curved)
Integrally stiffened machined skin	0.006 - 0.024	0.010
Flat honeycomb panels and wedges	0.020 - 0.060	0.040 (flat) 0.015 (wedges)

Table 9.04.2 - DLF: Form of Construction

Note: The DLF values quoted in Table 9.04.2 were, in general, obtained from specimens assembled to aircraft standards and mounted in specimen surround frames. The skin-stringer frame panels are often assembled with interfacial compounds which are used for sealing purposes, but which have the additional effect of increasing the damping. The honeycomb structures are probably sections of aircraft control surfaces and would be attached for test purposes along one edge only, whereas the test honeycomb panels were probably attached on all edges to a test support structure. All these features would have tended to **increase** the measured damping ratio.

It is advised that these values provide suitable estimates for vehicles such as the Space Shuttle or constructions like the Space Lab. However, they are higher than the DLF values used for satellite constructions. The DLF values obtained for the satellite component tests do **not** include losses which occur at component-to-component attachments.

EFFECT OF ATTACHING THERMAL TILES TO STRUCTURE

Ref. [15] gives some details of tests to measure the increased damping effect from adding thermal protection tiles to typical Space Shuttle structure. Thick silica tiles (58 mm) were bonded to a 4 mm thick Nomex felt strain-isolator pad which in turn was bonded to the structural skin of 0.81 mm thick aluminium with riveted stiffeners. The values of DLF, shown in Figure 9.04.1 are based on two separate test assessments, A and B, the average test values being quoted in Table 9.04.3.

Test	Average DLF without Tiles	Average DLF with Tiles
A	0.006	0.015
B	Not assessed	0.06

Table 9.04.3 - DLF: Effect of Thermal Protection Tiles

FIBRE-REINFORCED PLATES

The loss factor of fibre-reinforced plastics (FRP) is dependent on many parameters. Furthermore, there are an infinite number of variations of fibre type, matrix, volume fraction, lay-up etc. Consequently, a complete characterisation of the damping of every composite material is self-prohibitive. However, the loss factors of a number of typical laminae, laminates and sandwich structures have been complied to illustrate the effect of some of these parameters and, it is hoped, to enable the designer to estimate a fair approximation of the loss factor for any conventional composite. All results given are measured data, interpolation and extrapolation having been avoided. No statistical confidence levels are available for the quoted data.

The magnitude of the loss factor of an FRP depends primarily on the energy dissipation characteristics of the resin. However, these characteristics are similar for conventional resins used in FRP's, e.g. epoxies, polyesters, etc. Consequently, in the absence of data for the relevant resin, data provided below for epoxy or polyester will suffice.

Furthermore, the effects of frequency on FRP loss factor depend upon the frequency effect on the matrix and the relative contribution to the modal behaviour of the matrix. Resins utilised generally exhibit little variation in properties with frequency and therefore these effects may also be ignored in the first instance, in accordance with the advice given in Topic 9.03. However, the mode shape (dependent on frequency), being a fundamental parameter in determining FRP loss factor, must be taken into consideration at all times, see: Figures 9.04.2 to 9.04.6. All values assume all edges free (unclamped).

Approximate Mode Shape	Loss Factor: Carbon/epoxy $V_f = 0.05$	Loss Factor: Glass/epoxy $V_f = 0.05$
	0.01	0.01
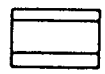	0.008	0.008
	0.009	0.01
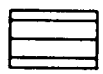	0.008	0.002
	0.008	0.005
	0.008	0.007

0° ——

Figure 9.04.2 - Modal Loss Factors of Continuous Fibre-reinforced Plates: Layup $[0]_8$

Approximate Mode Shape	Loss Factor: Glass/epoxy V = 0.6	Loss Factor: Carbon/epoxy (reliable data not found)
	0.005	
	0.009	
	0.005	
	0.005	
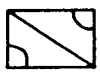	0.005	
	0.005	

0° →

Figure 9.04.3 - Modal Loss Factors of Continuous Fibre-reinforced Plates: Layup [45/-45/45/-45]s

Approximate Mode Shape	Loss Factor: Carbon/epoxy V = 0.34	Loss Factor: Glass/epoxy V = 0.45
	0.01	0.01
	0.002	0.005
	0.004	0.008
	0.002	0.003
	0.003	0.005
	0.005	0.009

0° →

Figure 9.04.4 - Modal Loss Factors of Continuous Fibre-reinforced Plates: Layup [0/90]2s

Approximate Mode Shape	Carbon/epoxy V_f = 0.5	Glass/epoxy V_f = 0.6
	0.07	0.09
	0.002	0.005
	0.003	0.007
	0.001	0.004
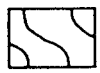	0.002	0.006
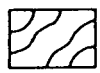	0.003	0.006

0° →

Figure 9.04.5 - Modal Loss Factors of Continuous Fibre-reinforced Plates: Layup [0/90/45/-45]s

Approximate Mode Shape	Loss Factor: Carbon/epoxy V_f = 0.6	Loss Factor: Glass/epoxy V_f = 0.6
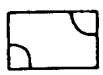	0.002	0.007
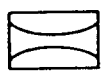	0.001	0.006
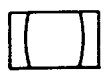	0.001	0.004
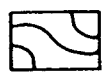	0.002	0.005
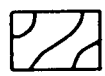	0.002	0.005
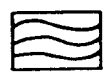	0.002	0.004

0° →

Figure 9.04.6- Modal Loss Factors of Continuous Fibre-reinforced Plates: Layup [0/-60/60]2s

The effect of fibre type and volume fraction of fibres (V_f) upon a loss factor is given in Tables 9.04.4 to 9.04.6 and Figures 9.04.7 to 9.04.9. Furthermore, the loss factor is greatly affected by the fibre orientation. The variation of loss factors with respect to fibre orientation for a number of fibre-reinforced composites is shown in Figures 9.04.10 to 9.04.20. The lay-up terminology used is given in Figure 9.04.21.

DLFs for honeycomb panels with fibre reinforcement were measured in two other investigations and the results are plotted in Figure 9.04.22. The mean DLF for all the data plotted is 0.031. However, this value is heavily weighted by the high DLFs at the low frequency measured in investigation E. Since these tests were conducted in a propagating wave tube, it is possible that the results were influenced by acoustic radiation damping,

Note: Dissipation loss factor evaluation for enclosed acoustic cavities may be found in Chapter 7 - Sound Transmission.

Fibre Type/Resin	Longit. Flex. Loss Factor η_L	Trans. Flex Loss Factor η_T	Shear Loss Factor β_{LT}
Boron/Epoxy:			
Continuous	0.002	0.2	0.2
Carbon/Epoxy:			
Continuous	0.001	0.01	0.01
Short Aligned †	0.001	0.01	0.008
Short Random	0.007	0.007	0.008
Glass/Epoxy:			
Continuous	0.001	0.008	0.01
Short Aligned ‡	0.002	0.008	0.01
Short Random	0.01	0.01	0.01
Glass/Polyester:			
Short Random *f*	0.01	0.01	0.01
Aramid/Epoxy:			
Continuous	0.01	0.02	-

Key: † l = 2.25 mm
‡ l/d = 100
f V_f = 0.3

Note: See Figures 9.04.7 to 9.04.9 for variations of $\eta_L, \eta_T, \beta_{LT}$ respectively with volume fraction (V_f).
See Figures 9.04.10 to 9.04.12 for variations of $\eta_L, \eta_T, \beta_{LT}$ respectively with fibre orientation for carbon & glass reinforced epoxy.

Table 9.04.4 - Typical Values of Material Loss Factors for Unidirectional Fibre-reinforced Laminae at Volume Fraction 0.5

LAY-UP: CROSS PLIES (See also: FABRICS)		
Carbon/Epoxy	[See: Figure 9.04.13]	
Glass/Epoxy	[See: Figure 9.04.14]	
Boron/Epoxy [±45]	$\eta_{0,90}$ = 0.015	
LAY-UP: [0/-60/60/60/-60/0]		
Carbon/Epoxy	[See: Figure 9.04.15]	
Glass/Epoxy	[See: Figure 9.04.16]	
LAY-UP: [0/90/45/-45/-45/45/90/0]		
Carbon/Epoxy	[See: Figure 9.04.17]	
Glass/Epoxy	[See: Figure 9.04.18]	
LAY-UP: [±0]		
Carbon/Epoxy	[See: Figures 9.04.19 and 9.04.20]	
LAY-UP: [90/+30/-30/-30/+30/90]		
Carbon/Epoxy	η_0 = 0.0004	
LAY-UP: FABRICS		
	η_{warp}	$\eta_{\pm 45°}$
Carbon/Epoxy	0.005	-
Carbon/Phenolic †	0.01	-
Glass/Epoxy	0.007	-
Aramid/Epoxy	0.02	0.02
Aramid/Polyester	0.02	0.02
Aramid/Vinylester	0.02	0.02

† Phenolic resins can cause significant frequency dependency.

Table 9.04.5 - Typical Values of Material Loss Factors for Multidirectional Continuous Fibre-reinforced Laminae at Volume Fraction 0.5

(a) Carbon/Epoxy Faceplates (Vf = 0.5) - Aluminium Honeycomb case

Lay-up	Flexural Loss Factor for 0, 90
[0/60/-60/-60/60/0]	0.004
[90/30/-30/-30/30/90]	0.005
[0/90/0/0/90/0]	0.004
[-45/45/-45/-45/45/-45]	0.012
Al alloy	0.003

(b) Carbon/Epoxy Faceplates (Vf = 0.5) - Nomex Honeycomb case

Lay-up	Plate Modal Loss Factor
[0/90]	Varies with mode shape. Average 0.004., i.e. very similar to carbon/epoxy aluminium honeycomb case.
[-45/+45]	
[-60/60]	
[-75/+75]	
[-30/30]	

(c) Aramid/Epoxy Faceplates (Vf = 0.5) - Nomex Honeycomb case

Lay-up	Plate Modal Loss Factor
[-45/-45]	0.012

Table 9.04.6 - Typical Loss Factors of Sandwich Structures incorporating Fibre-reinforced Plastics

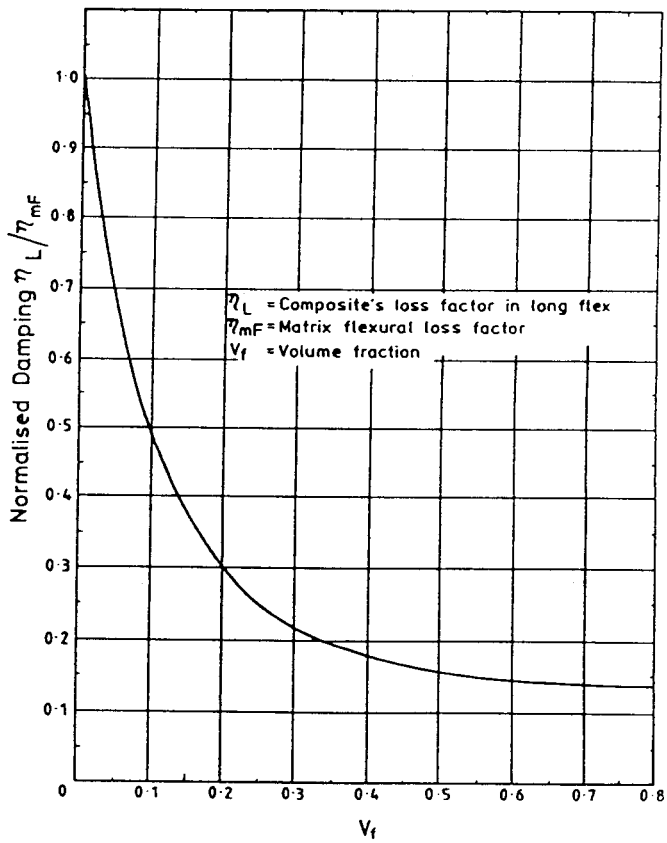

Figure 9.04.7 - Normalised Loss Factor in Longitudinal Flexure, based on Ref. [16]

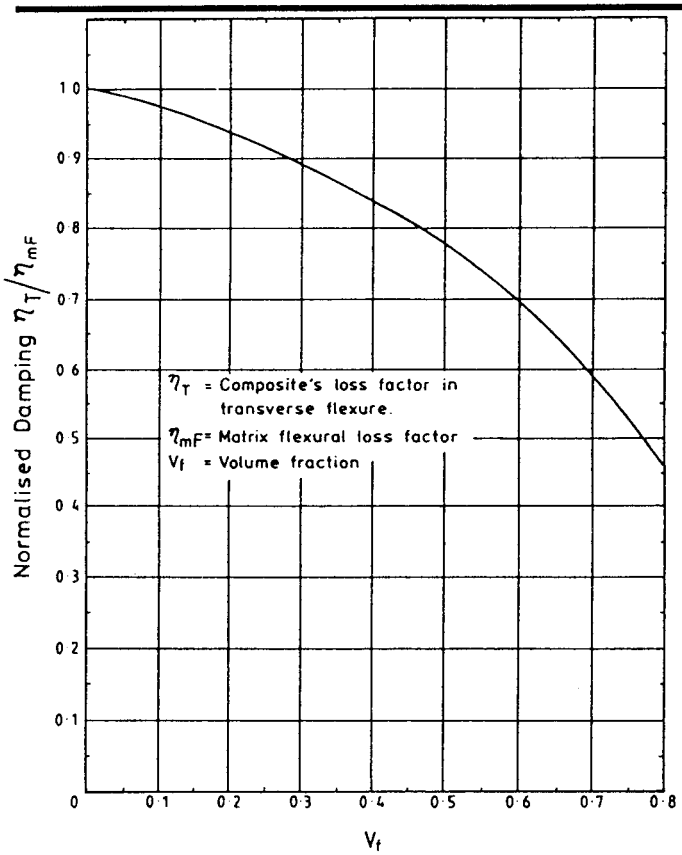

Figure 9.04.8 - Normalised Loss Factor in Transverse Flexure, based on On Ref. [16]

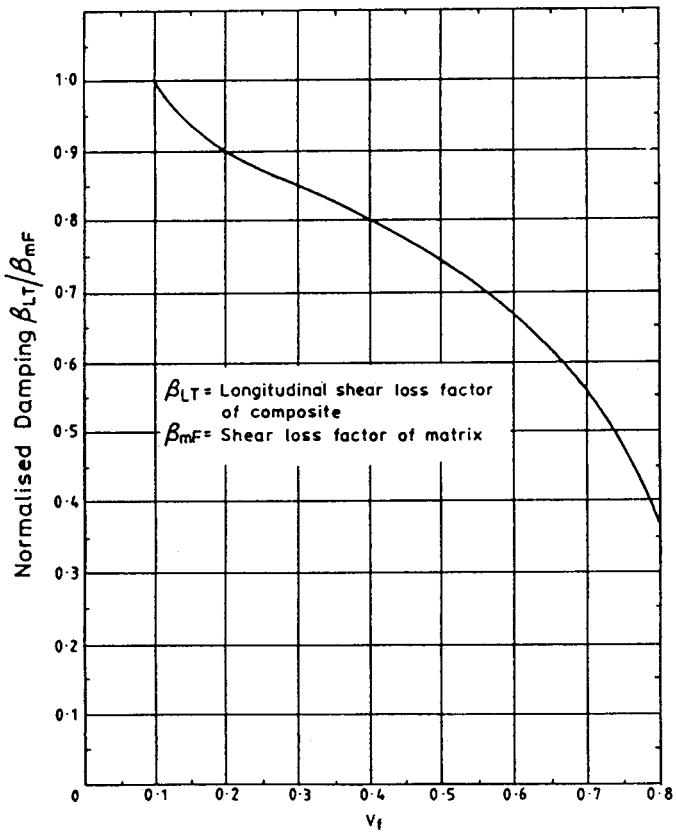

Figure 9.04.9 - Normalised Loss Factor in Longitudinal Shear, based on Ref. [16]

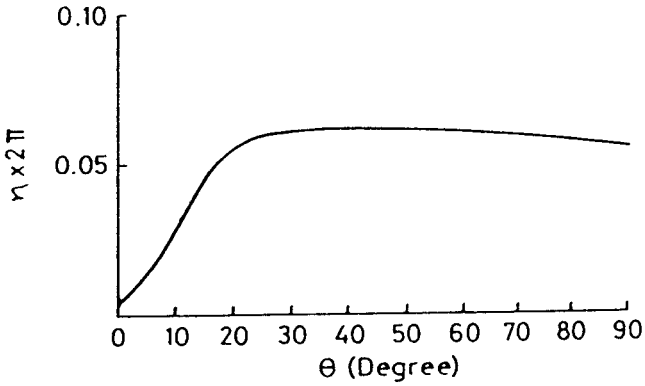

Figure 9.04.10 - Variation in Flexural Damping with Fibre Orientation for CFRP (Volume Fraction 0.5)

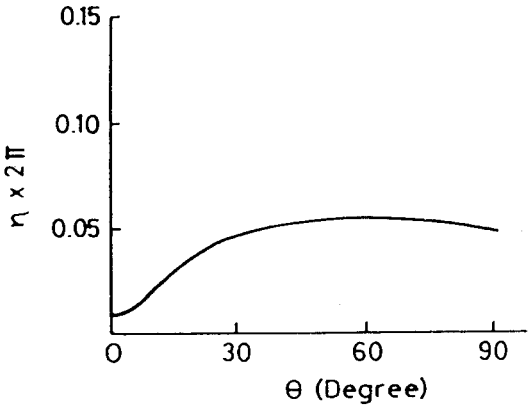

Figure 9.04.11 - Variation in Flexural Damping with Fibre Orientation for GFRP (Volume Fraction 0.5)

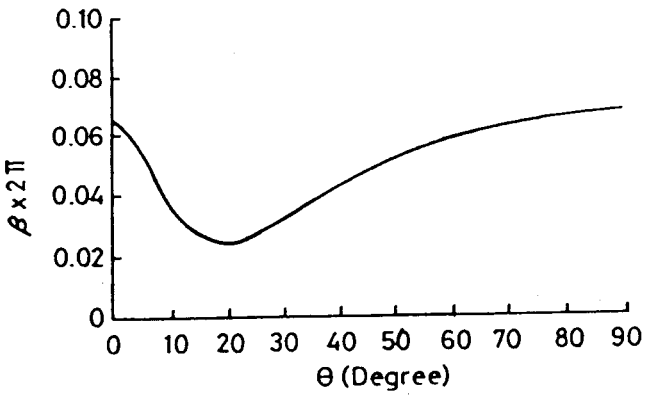

Figure 9.04.12 - Variation in Torsional Damping with Fibre Orientation for CFRP (Volume Fraction 0.5)

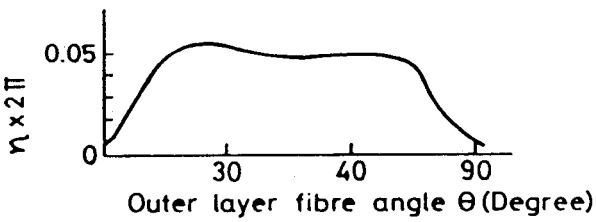

Figure 9.04.13 - Variation in Flexural Damping with Outer Layer Fibre Orientation for Cross-ply CFRP

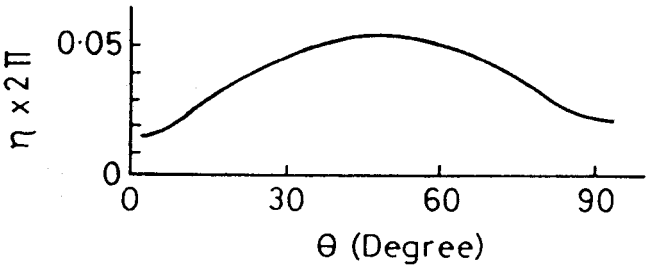

Figure 9.04.14 - Variation in Flexural Damping with Outer Layer Fibre Orientation for Cross-ply GFRP

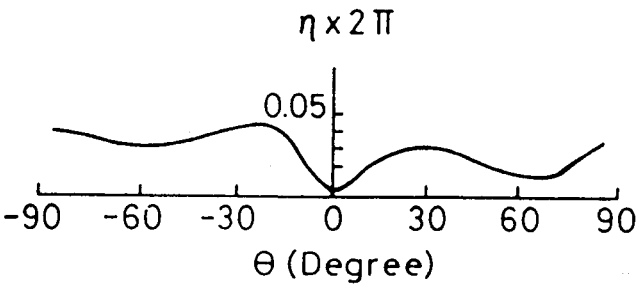

Figure 9.04.15 - Variation in Flexural Damping with Outer Layer Fibre Orientation for $[0/60/-60]_s$ CFRP

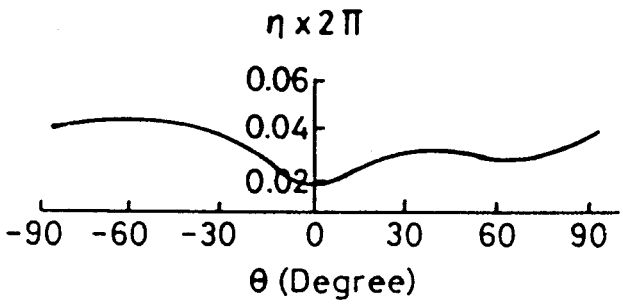

Figure 9.04.16 - Variation in Flexural Damping with Outer Layer Fibre Orientation for $[0/60/-60]_s$ GFRP

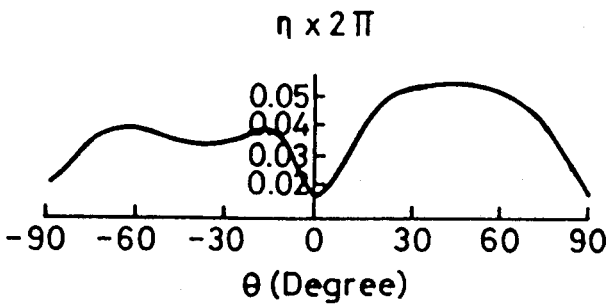

Figure 9.04.17 - Variation in Flexural Damping with Outer Layer Fibre Orientation for $[0/90/45/-45]_s$ CFRP

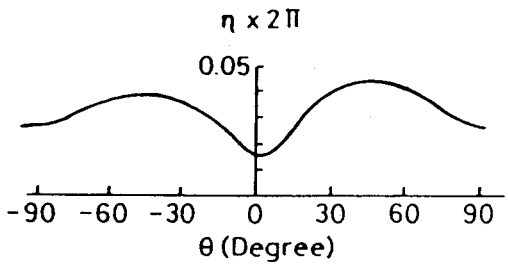

Figure 9.04.18 - Variation in Flexural Damping with Outer Layer Fibre Orientation for $[0/90/45/-45]_s$ GFRP

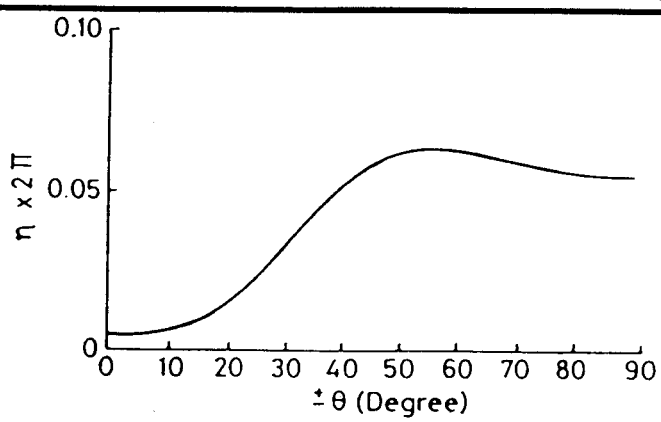

Figure 9.04.19 - Effect of Ply Angle on Flexural Damping of CFRP (Volume Fraction 0.5)

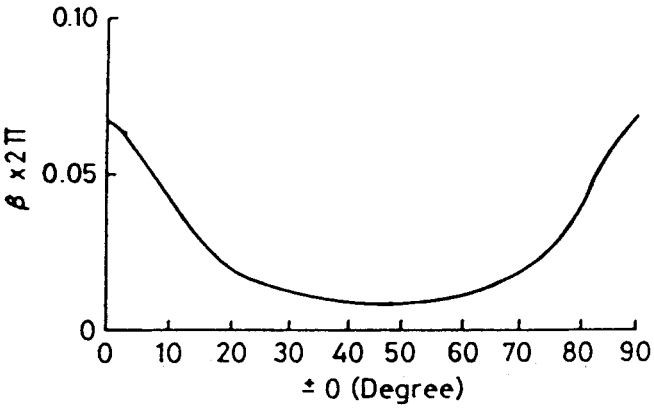

Figure 9.04.20 - Effect of Ply Angle on Shear Damping of CFRP (Volume Fraction 0.5)

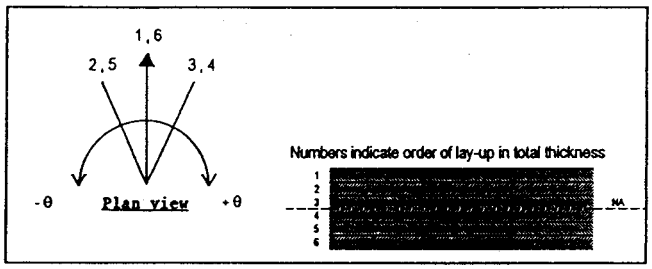

(a) Symmetrical Lay-up; Six layer example, orientation relative to outer fibre orientation

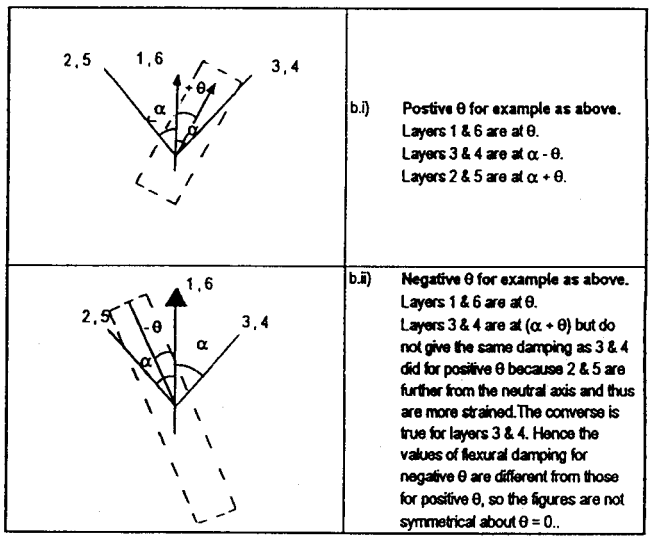

(b) Relation to outer layer fibre orientation Θ
[See: Figures 9.04.12 to 9.04.16]

Figure 9.04.21 - Lay-up Terminology for Fibre-reinforced Composites

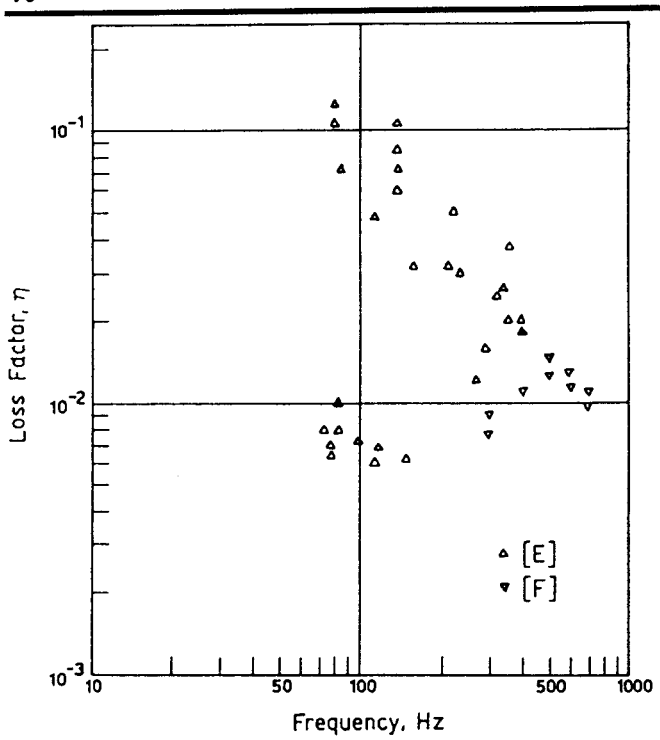

Figure 9.04.22 - Damping of Honeycomb Structures with Fibre-reinforced Faceplates

DAMPING OF SPACECRAFT ASSEMBLIES IN SPACE

Investigations are reported in Ref. [17] for estimates of DLF derived from measurements from Olympus satellite.

9.05 COUPLING LOSS FACTORS (CLF)

This section deals with CLF evaluation for structure-to-structure coupling. The other two types of coupling - acoustic-space/structure, which is important for input power, and acoustic-space/acoustic-space, which relates to the nonresonant transmission through structure - are dealt with theoretically (See: Topic 2.03, Chapter 7 and Appendix A).

Structural wave transmission analysis yields the coupling loss factor η_{ij} in the form (Lyon, Ref. [18]):

$$\eta_{ij} = c_{gi} L_{ij} \langle \tau_{ij} \rangle / \pi \omega A_i$$

where:

c_{gi} and A_i are the group velocity and surface area of subsystem i,

L_{ij} is the length of the junction between the two subsystems, and

$\langle \tau_{ij} \rangle$ is the diffuse field wave transmission coefficient.

Thus the coupling loss factor is predicted to be dependent on:

- frequency,
- the structural dimensions, and
- the group velocity.

Formulae for values of τ_{ij} for simple perpendicular junctions are given in Ref. [19]. These are developed for more general simple geometries in Ref. [20]. Application requires numerical integration, with τ_{ij} dependent on incident and transmitted wave types and on frequency.

For more complex geometries, the application of finite element modelling is being developed. Since only the subsystems connected at the junction of concern need to be modelled, estimates can be made to frequencies much higher than if the whole structure were to be modelled. The estimate is not very sensitive to dissipation loss values in the coupled subsystems so the CLF value is largely dependent on geometry, which can be well-defined.

Investigations have been performed to develop suitable test techniques for the measurement of CLF. One test method, for two interconnected uniform structures, initially required one structure to be heavily damped while a decay test was performed on the undamped structure. This was then repeated with the other structure heavily damped. However, the value of CLF could not be readily separated from the other loss factors involved and the requirement that each structure should be heavily damped could prove inconvenient. A technique was then developed that did not require any form of additional damping. It was similar in operation to the modal-density and DLF measurement methods and is described in Topic 10.04.

More recent investigations are described in Ref. [4, 5], which make use of this test technique. Moreover, Ref. [5] describes a method of analysing the measurements to produce the best estimate of CLF. A summary of these CLF measurements is also included in Ref. [21].

An alternative experimental technique is Energy Balance Analysis Ref. [22], in which each subsystem of a typical built-up structure is excited in turn, allowing all the terms in the energy balance matrix including DLF and CLF to be determined. Application to the Ariane 5 cryogenic engine (Vulcain) is described in Ref. [23].

9.06 EXPERIMENTAL CLF VALUES

Experimental values of CLF for structural subsystem junctions are available for several plate-to-plate conditions and for honeycomb platform attached to a central core structure, see Table 9.06.1. Although fluctuation of CLF with frequency was found, it is recommended that a constant value be taken for the structural couplings examined. The reciprocal CLF value is computed by GENSTEP3 from the ratio of the modal densities of the two subsystems.

CLF for plate-to-plate junction	
With welded or double-angle attachment	= 0.002
With solid section attachment	= 0.001
(Both plates tested had similar modal densities; configurations shown in Figure 9.06.1)	
CLF for flat plate to corrugated plate	
For double-angle and solid section attachment:	
Corrugated plate to flat plate	= 0.001
Flat plate to corrugated plate	= 0. 0001
(The modal density of the flat plate tested was approximately 10 times that for the corrugated plate, Ref. [4])	
CLF for honeycomb platform coupled to:	
Plain cylinder	= 0.0020
Corrugated cylinder	= 0.0012
Corrugated cone	= 0.0058
See Figure 9.06.2.	

Table 9.06.1 - CLF: Structural Subsystem Junctions

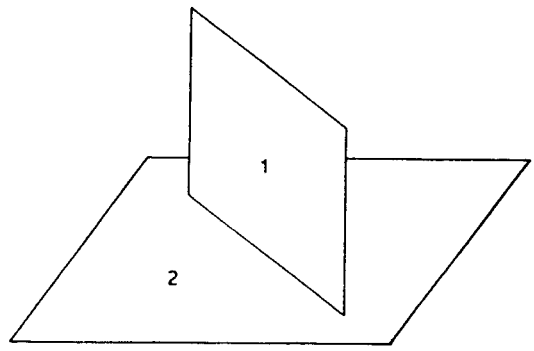

3 different forms of junction

- spot welded.
- back to back steel angles bolted.
- square section solid steel bars (bolted)

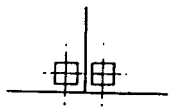

Flat Aluminium plates joined at right-angles; thickness = 1.2 mm.
Plate 1, 0.88m x 0.44m, Modal density = 0.1 modes/Hz.
Plate 2, 0.68m x 0.43m, Modal density = 0.07 modes/Hz.

Figure 9.06.1 - Flat-plate to Flat-plate Junctions

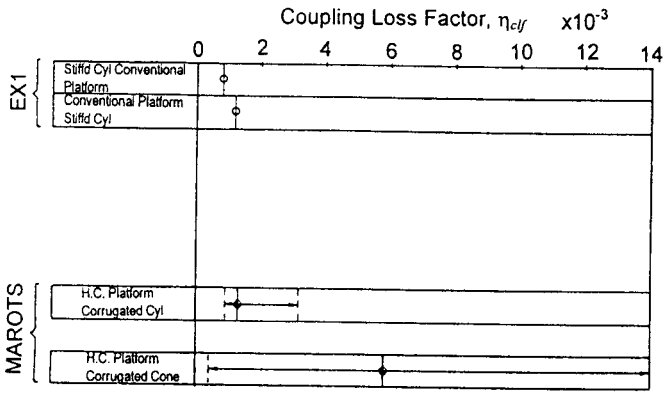

Note: Values obtained from decay tests - one subsystem damped.

Figure 9.06.2 - Coupling Loss Factor, η_{clf}

9.07 SELECTION OF CLF VALUES FOR STRUCTURE-TO-STRUCTURE COUPLING: GENERAL ADVICE

As there is still little information available on values of CLF for structure-to-structure coupling, it will be necessary, in some cases, to estimate values. For the types of satellite structure currently being investigated, which are subjected to a reverberant acoustic excitation, the precise CLF value used does not have too great an influence on the response of the main components. For most satellite structural components the CLF values will be in the range 0. 001 to 0.010. Owing to the method of attachment, discrete or locally attached components, such as antennae and solar arrays, may have very low coupling with the main structure, say in the range 0.0001 to 0.001.

Where available, recommended CLF values are given in the sections dealing with the structural zones.

Note: If there is some concern over the choice of CLF values, their effect on the model can be examined by a repeat run on GENSTEP3 with the CLF values set to zero (no coupling between subsystems).

9.08 REFERENCES

[1] B.L. Clarkson & R.J. Pope
'Experimental determination of modal densities and loss factors of flat plates and cylinders'
Journal of Sound & Vibration, 77 (4), 535 (1981)

[2] B.L. Clarkson & M.F. Ranky
'Frequency average loss factors of plates and shells'
Journal of Sound & Vibration, 89 (3), 309 (1983)

[3] M.F. Ranky & B.L. Clarkson
'Frequency average loss factors of plates and shells'
Technical Report No. 4
ESA Contract No. 4100/79/NL/PP Rider 2

[4] B.L. Clarkson & R.J. Pope
'Experimental determination of coupling loss factor'
Technical Report No. 6
ESA Contract No. 4100/79/NL/PP Rider 2, February (1982)

[5] B.L. Clarkson & M.F. Ranky
'On the measurement of the coupling loss factor of structural connections'
Journal of Sound & Vibration, 94 (2), 249 (1984)

[6] R.J. Cummins
'Sound transmission into closed cylinder'
MSc Dissertation, University of Southampton (1970)

[7] R.J. Cummins & W. Cooper
'Spacecraft structural acoustic studies'
Final report, ESA CR(P)-1264

[8] R.J. Cummins & I.G. Gray
'Spacecraft structural acoustic studies - investigation, interpretation and simulation of the effects of configuration features on noise-induced structural vibration and sound-transmission characteristics'
Final report, ESA CR(P)-1366 (1980)

[9] R.J. Cummins & I.R. Farrow
'Study of the evolution of structural acoustic design guides'
ESA CR(P)-1609 (1981)

[10] B.L. Clarkson, R.J. Pope & M.F. Ranky
'Experimental work to evaluate parameters required in the SEA prediction method'
ESA Contract No. 4100/79/NL/PP Rider 1 (1981)

[11] B.L. Clarkson & R.J. Pope
'Experimental determination of modal densities and loss factors of spacecraft components'
ESA Contract No. 4100/79/NL/PP (1980)

[12] J.N. Pinder, M.E. House & F.J. Fahy
'Preliminary Study of the Noise Reduction in the Ariane 5 Payload Bay Given By the Fairing and SPELTRA'
Final Report
ESA Contract No. 6675/86/F/F1, 1987

[13] B.L. Clarkson, M.F. Ranky & K.T. Brown
'Experiment work associated with high frequency induced vibration'
Final report. Technical Report No. 14
ESA Contract No. 5122/82/NL/PP, June (1983)

[14] ESDU Data Item 73011 with Amendment A. March 1974
Engineering Sciences Data Unit
(27 Corsham St., London N1 6UA)

[15] L.D. Pope & J.F. Wilby
'Space-Shuttle payload bay acoustics prediction study:
Final report, Vol. 2: Analytical model'
Bolt, Beranek and Newman Report No. 3286 (1976)

[16] R.G. Ni & R.D. Adams
'A rational method for obtaining the dynamic mechanical properties of lamina for predicting the stiffness and damping of laminated plates and beams'
Composites, 15(3), 193 (1984)

[17] M.G. Smith
'Damping of Built-up Structures In Air and In Vacuo'
ISVR-CS Ref R06 4643, ESA P/O No. 142357
Task Report, March 1995

[18] R.H. Lyon
'Statistical Energy Analysis of Dynamical Systems, Theory and Applications'
MIT Press, Mass., USA, 1975

[19] L. Cremer, M. Heckl & E.E. Ungar
'Structure-Borne Sound'. 2nd Edition
Springer-Verlag, Berlin, 1988

[20] R.S. Langley & K.H. Heron
'Elastic Wave Transmission Through Plate/Beam Junctions'
Journal of Sound & Vibration, 143 (2), 241-253 (1990)

[21] R.J. Cummins
'Development of structural acoustic design guides'
Final report. ESA CR(P) - 1916, (1981)

[22] R.S. Ming, G. Stimpson & N. Lalor
'On the Measurement of Individual Coupling Loss Factor in a Complex Structure'
Proc. InterNoise 90 Conf., Goteburg, 1990, 961-964

[23] A. Kernilis et al.
'Vibroacoustics Environment of Rocket Engines'
Proc. International Conf. Acoustic and Dynamic Environment of Space Transportation Systems
CNES/ONERA, Jouy-en-Josas, 8-11 Feb. 1994, 259-280

Structural Acoustics Design Manual

Chapter 10
RECOMMENDED TEST PROCEDURES FOR EVALUATION OF SEA PARAMETERS

CONTENTS

10.01 GENERAL

This chapter contains the recommended procedures for evaluating SEA parameters where no theoretical or empirical solution is available. The basic ideas behind these indirect methods for estimating the modal density and loss factors are:

- that the point impedance of a structure is directly related to the modal density, and
- that the power flow into a structure is equal to the power dissipated plus the power transmitted to attached components.

Ideally the procedures require the use of the computer software developed specifically for the analysis of the measured data and presented in Ref. [1]. Further information on the theory and development of these test techniques is given in Ref. [2, 3, 4, 5, 6].

10.02 MODAL DENSITY EVALUATION

THEORY

The method is based on the relationship:

$$n(f) = 4M \cdot A \cdot \mathrm{Re}(Y) \text{ for random structures,}$$

where:

Y is the measurement of the point mobility,

M is the mass/unit area,

for a bandwidth f_1 to f_2 Hz with centre frequency f_0 Hz.

The final equation used in the on-line computation is the following:

$$n(f_0) = \frac{1}{(f_2 - f_1)} \int_{f_1}^{f_2} 4M \cdot A \cdot \mathrm{Re}\left(\frac{-i \cdot A(if)}{2\pi f \cdot F(if)}\right) df$$

SPECIMEN AND TEST CONDITION

For a very lightly damped structure, damping tape may be added (usually at the edges) to avoid measurements that give rise to data-processing errors. The structure should be freely suspended on thin wires. The environment of the test room should be quiet during the test measurement.

FORCE INPUT

The specimen should be driven by means of an electromagnetic coil-and-magnet force generator so designed as not to add appreciable damping to the system. The drive should be through an impedance head to a small stud attached to the specimen. Impedance heads such as the Bruel & Kjaer Type 8000/1 have been used successfully and an attachment stud diameter of 6.5 mm should provide satisfactory measurements up to 4 kHz.

The location of the input stud should be in the central area of the structure, although the exact centre of a symmetrical structure should be avoided, as should locations close to edges and bounding members close to a large mass. Very thin material, such as that used for corrugated structures, can also give problems due to local flexing close to the input stud.

TEST MEASUREMENTS

The preferred excitation is a transient force input in the form of a rapidly swept sine wave. Alternatively, broad-band random excitation may be used, but the transient input has the advantages of greater accuracy. Usually three to four measurement locations are sufficient.

DATA ANALYSIS

For the analysis, a constant frequency bandwidth (rather than constant percentage) should be used and it should be chosen wide enough to include at least five modes.

ALLOWANCES FOR MASSES AND/OR STIFFENERS

The following guidelines were developed for honeycomb structures, but may have application to other structural configurations.

Mass correction for impedance measurements

When the impedance head mounting stud is attached to an insert in a honeycomb panel, then the mass of the insert should be added to the mass of the mounting stud in the impedance measurement correction procedure.

Mass correction for use in experimental evaluation

The corrected mass is required for use in the formula:

$$n(f) = 4M \cdot A \cdot \mathrm{Re}(Y)$$

i.e. MA = (total measured mass) - M_a

where: M_a is the mass of any large individual items, such as heat-sink plates, edge stiffeners/attachment members, edge closure members, mounting members, etc.

The total measured mass will include the mass of core plus adhesive and the mass of items distributed over the panel, such as mounting inserts and cable clips.

10.03 EVALUATION OF DISSIPATION LOSS FACTOR

This energy method evaluates the average loss factor in the frequency bandwidth selected and has the advantage that the test can be combined with the modal density assessment. The decay method, see: Measurement of DLF by Decay Method, gives a comparable value in many cases, but involves a longer test time, see: Comparison of Energy & Decay Method.

THEORY

This indirect method is based on the following relationship:

$$\eta(f) = \frac{2\pi f \cdot P(if)}{MA\left\langle |A(if)|^2 \right\rangle}$$

where: $P(if)$ is the Fourier transform of the power input.

TEST METHOD

The specimen preparation, force input. measurement and analysis methods are similar to those set out in Topic 10.02. However, damping tape that has been applied to the specimen for a modal density measurement should be removed before this loss-factor evaluation starts. Moreover, recent work on honeycomb structure has shown that the choice of analysis bandwidth should not be made too wide, particularly in the low-frequency region, because a low value for DLF from a single mode can affect the overall band average to a marked degree. Several miniature accelerometers (six is probably a minimum) should be used to obtain the spatial average of the surface acceleration. Note that the drive point acceleration should not be included in the averaging.

Recent work has shown that these measurement locations should not be situated too far from the drive point on large specimens such its platforms.

CORRECTIONS FOR NONUNIFORM STRUCTURES

It is not possible to use the method on structures which have a few large masses or a few stiffeners. However, in the case of honeycomb structures which have many mounting inserts, the additional mass can be assumed to be uniformly distributed and the additional mass added to the MA term in the denominator of the equation in Topic 10.03 - Theory.

MEASUREMENT OF DLF BY DECAY METHOD

This involves a test arrangement similar to that described in Topic 10.03 - Test Method; it requires a steady input excitation applied by the vibrator (this may be broad band or of a bandwidth similar to that of the analysis). The input is cut abruptly and the decay of the response accelerometer measured by means of a storage oscilloscope or a level recorder. The DLF can be found from this decay rate:

$$DR = 27.3 \times f \times \eta$$

where:

DR = decay rate in $dB.s^{-1}$

f = band centre frequency

η = DLF

Acoustic excitation can be used, but is not recommended for structures at present. It does have to be used, however, for the measurement of the DLF of acoustic subsystems (contained spaces). The necessary formulae are given in the Topics of Chapter 7 concerning sound transmission.

COMPARISON OF ENERGY AND DECAY METHODS

Recent investigations reported in Ref. [6] have compared measurements made by the energy and decay techniques for evaluating DLF. These test results show that for uniform structures the average loss factor of a group of modes in a frequency band can be obtained either by the energy method or by the decay method. There is no significant difference between the results from the two methods when the modes in the bands have similar loss factors. However, when the group of modes in the analysis band does not have similar loss factors, the decay record is not a straight line, and it may be difficult to deduce an appropriate average value. In these cases, the energy method gives the result required for the SEA calculations. Compensation for the effect of uniformly distributed masses can be made by including the total mass in the energy calculations, as noted in Topic 10.03 - Corrections for Nonuniform Structures.

10.04 EVALUATION OF COUPLING LOSS FACTOR

This method is only applicable to two interconnected uniform structures and evaluates the average CLF in the frequency bandwidth selected.

THEORY

This experimental method is based on the following relation:

$$\eta_{12}(f) = \eta_2(f) \cdot \frac{n_2(f)\left\langle |A_2(if)|^2 \right\rangle}{n_2(f)\left\langle |A_1(if)|^2 \right\rangle - n_1(f)\left\langle |A_2(if)|^2 \right\rangle}$$

where the dissipation loss factor, $\eta_2(f)$, and the modal densities, $n_1(f)$ and $n_2(f)$, can be determined by the experimental methods given in Topics 10.02 and 10.03 for the two separate items.

TEST METHOD

The components should be in the same state as for the individual loss factor tests, The application of damping tape is not necessary. The procedure for specimen mounting, force input, measurement and analysis is the same as that set out in Topic 10.02. As in Topic 10.03 - Test Method, several miniature accelerometers (minimum of six on each component) should be used to obtain the spatial average of the surface acceleration. Empirical assessments have shown that the drive point acceleration should not be included in the averaging. The complementary CLF ($\eta_{21}(f)$) can be found by repeating the test but now driving the second component; the subscripts 1 and 2 in the equation in Topic 10.04 - Theory will not be interchanged. The complementary CLF could be found from the following relation:

$$\eta_{21}(f) = \eta_{12}(f) \cdot \frac{n_1(f)}{n_2(f)}$$

10.05 SIGNAL MEASUREMENT TECHNIQUES

An improved technique for measurements on lightly damped structures is reported in Ref. [7]. This technique is especially useful for reducing errors when the mobility of typical spacecraft structure is measured for the purpose of evaluating modal density with the aid of the relation set out in Topic 10.02 - Theory.

A schematic diagram of the idealised measurement system is shown in Figure 10.05.1.

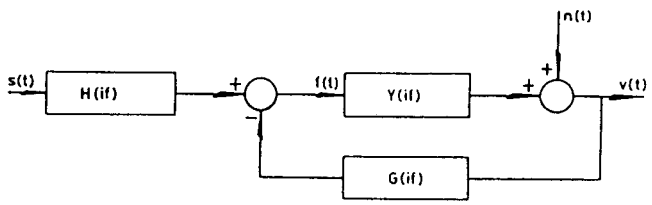

Where:

H(if)	transfer function of the power amplifier and vibration exciter
G(if)	transfer function describing the shaker/structure interaction
Y(if)	Point mobility of structure
f(t)	force signal
S(t)	Original test signal
V(t)	Structure velocity signal

Figure 10.05.1 - Improved Signal Measurement Technique (using three signal channels)

CONVENTIONAL (TWO-CHANNEL) METHOD

In the conventional method, the signals, $f(t)$ and $V(t)$, are measured and the estimated power spectrum, $S_{ff}(if)$, and the cross-spectrum, $S_{fv}(if)$, computed. The mobility is given by:

$$\overline{Y}(if) = \frac{S_{fv}(if)}{S_{ff}(if)}$$

From this the real part of mobility is obtained. It has been found that significant errors can be introduced when this method is used on lightly damped structures and in such cases damping tape has been added to the structure to increase damping.

IMPROVED (THREE-CHANNEL) METHOD

The new method relies on the acquisition of a third signal, $S(t)$, which is the original signal used to drive the power amplifier. The three signals are used to compute the cross spectra, $S_{sf}(if)$ and $S_{sv}(if)$. The mobility of the structure is given by:

$$\overline{Y}(if) = \frac{\overline{S}_{sv}(if)}{\overline{S}_{sf}(if)}$$

This method was found to give significantly improved results.

10.06 REFERENCES

[1] B.L. Clarkson & R.J. Pope
'Experimental determination of modal densities and loss factors of spacecraft components'
ESA Contract No. 4100/79/NL/PP (1980)

[2] B.L. Clarkson, R.J. Pope & M.F. Ranky
'Experimental work to evaluate parameters required in the SEA prediction method'
ESA Contract No. 4100/79/NL/PP Rider 1 (1981)

[3] R.J. Cummins & I.R. Farrow
'Study of the evolution of structural acoustic design guides'
ESA CR(P)-1609 (1981)

[4] B.L. Clarkson & M.F. Ranky
'Modal densities of honeycomb plates'
Journal of Sound and Vibration, 91(1), 103 (1983)

[5] B.L. Clarkson & R.J. Pope
'Experimental determination of modal densities and loss factors of flat plates and cylinders'
Journal of Sound and Vibration, 77(4), 535 (1981)

[6] B.L. Clarkson & M.F. Ranky
'Frequency average loss factors of plates and shells'
Journal of Sound and Vibration, 89(3), 309 (1983)

[7] K.T. Brown
'Measurement of modal density: an improved technique for use on lightly damped structures'
ISVR Memo No. 631. (Not produced on ESA contract.) (1982)

Structural Acoustics Design Manual

Chapter 11
RESPONSE PREDICTION BY DETERMINISTIC METHODS

CONTENTS

11.01 INTRODUCTION

As explained in Topic 1.03, probabilistic methods such as SEA are not always appropriate or necessary. Normal mode and scaling methods offer alternative approaches, some of which will be described in this chapter in sufficient detail to allow application in straightforward situations, with references to permit expansion to more complicated cases.

The approaches covered are:

- Joint acceptance for coupling between acoustic fields and structures,
- Scaling extrapolation,
- Modal Interaction Analysis (MIA).

In addition, some development of the finite-element (and associated boundary-element) method is given to go beyond the introduction in Chapter 1, although it is outside the scope of this manual to give sufficient instructive text for its application without specialist training.

11.02 JOINT ACCEPTANCE ANALYSIS

INTRODUCTION

This method has already been introduced, [See: Chapter 1]. It allows an analytically based estimate to be made of modal structural response to acoustic excitation which can be deterministic or stochastic. It was developed particularly for aerospace application in the 1960s and provides simple modelling of structural response when the structure can be adequately modelled analytically as a simple element.

The response of a structure to acoustic excitation depends on the level and spatial distribution of the applied force, and also, for structures showing highly modal behaviour as is assumed in this section, on the structure's modal characteristics. The relevant characteristics are the mode shapes, the proximity of the resonant frequencies to each forcing frequency and the damping levels. The overall response can be given by the sum of the responses in individual modes, which are regarded as independent of each other for structures that behave linearly.

The value of the forcing level for each mode depends not only on the overall level of the incident field but also on the spatial (wavelength) matching between the trace wavelength incident of the structure's surface and the wavelength of the structural mode. The force which is coupled to a given mode is termed the 'generalised' force for that mode.

The square of the ratio of the amplitude of the generalised force to the total force is termed the 'joint acceptance'.

The application of this method is presented here with regard to damage-risk estimates during the launch phase. Although the noise levels are approaching those for non-linear acoustic field behaviour, (qualification levels 146 dB overall for Ariane 4, for example), this guideline is only intended to show how an initial assessment may be made of a potentially damaging situation. It assumes that linear behaviour occurs.

It is expected that if a severe response is then indicated, a more precise analysis or an experiment will be performed.

GENERALISED FORCE AND JOINT ACCEPTANCE FUNCTION

The generalised force $L_r(t)$ at a given frequency, where r is the structural mode designation, is of the descriptive form:

$L_r(t)$ = (incident pressure term) x (surface area of structure term) x (joint acceptance) x (time dependence)

The resulting expression for the spectral density (double-sided) of the generalised force, $S_{F(r)}(\omega)$, for random excitation is given by:

$$S_{F(r)}(\omega) = S_{p(\omega)}.K.j_r^2(k_y)$$

where:

$S_{p(\omega)}$ = spectral density of blocked pressure (double-sided),
r = structural mode order,
K = constant function of dimensions of exposed structure,
$j_r^2(k_y)$ = joint acceptance function,
y = position along beam.

The joint acceptance value is a measure of how well the wavelength of the incident field spatially matches the structure's wavelength for the given mode order r, and therefore of how well the driving excitation can couple into the structure's resonant response. This will be its maximum response in the case of a flat excitation spectrum. The effective component of wavelength at the structure's surface is the 'trace wavelength' of a plane wave incident on a beam, [See: Figure 11.02.1].

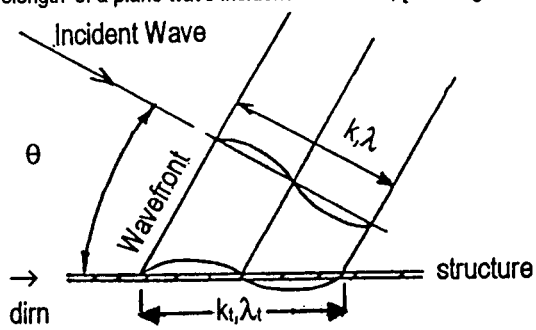

k_m = modal wavenumber in structure
$k_t = k.\cos\theta$ (= $k_{(acoustic)}$) $\lambda_t = \lambda.\cos\theta$

Figure 11.02.1 - Trace Wavelength & Wavenumber of Incident Wave

For the simplest case of a straight beam, the joint acceptance functions for the flexural modes have the characteristic shape shown in Figure 11.02.2. Functions for this and some other common structural elements are considered in 'Joint Acceptance function for Basic Structural Elements'.

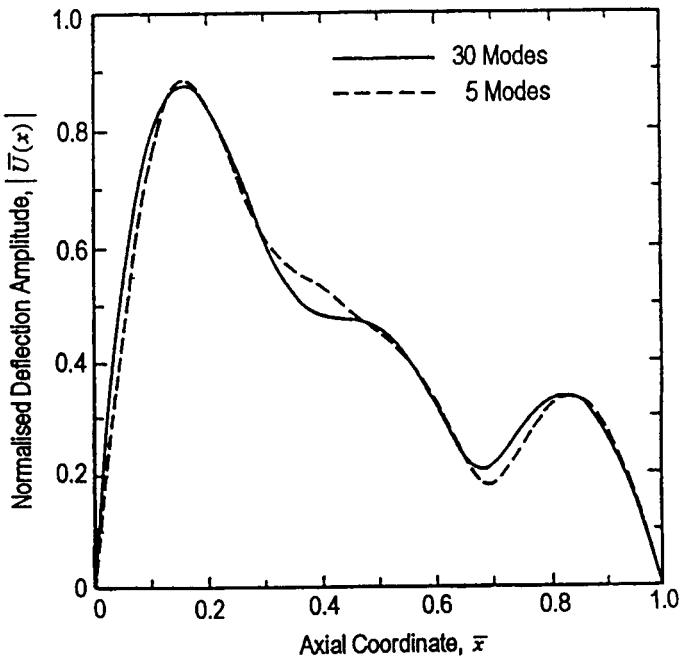

Figure 11.02.2 - Comparison of Normalised Deflection Amplitude determined by Modal Analysis Method for 5 and 30 Modes and for δ=1.0, λ=9.6095

In many cases, it is likely that the highest damage risk will be given by response in one of the first few modes of the structure. Since these modes are usually well separated, a simple calculation can be made as an initial assessment and it is in this context that the method is proposed as applicable. In the case of white noise excitation, it is found that the first mode's response dominates the contribution to the fatigue estimate in the region of linear behaviour, see Ref. [1, 2, 3] but when the sound field has been filtered by a launcher fairing so that the spectrum has some narrowband character, responses above the first order may dominate. A single mode's domination of overall response is less marked for non-linear behaviour, which tends to broaden the modal response in the frequency domain. An approximate method which extends beyond the first mode has been proposed by Blevins, Ref. [4, 5], but application to honeycomb panels is not reported.

The joint acceptance function (JAF) depends on the nature of the incident acoustic field and the structural mode shape, so the JAF includes modal order dependencies. In the payload bay, the sound field will be non-diffuse because of the limited space between the payload and the launcher fairing. However, there will be multiple angles of incidence and in a simple analysis as is to be considered here, the diffuse-field assumption is made for an initial estimate.

The structural mode shapes depend on the form, bending stiffness and boundary conditions of the structure. When complete structures or local structural areas can be modelled in terms of simple elements (beams, simple plates, cylinders) for which JAFs can be readily evaluated or have been published in the literature, the generalised force estimate is reduced to a simple calculation. Experience has shown that the in-vacuo mode may be an inadequate representation. Stacked area-structures such as solar arrays and antennas can show large effects due to air-coupling.

Other boundary conditions can also influence low modal order mode shapes significantly, even though natural frequencies may be little affected. To take practical boundary support conditions into account is often a very major problem even for a sophisticated analysis, so the error introduced by assuming idealised boundary conditions will be no greater in the very simple assessment proposed if the other analyses also make such assumptions.

RESPONSE

The out-of-plane response of a structure in the r th mode to random noise is given in terms of displacement power spectral density ($S_{W_r}(\omega)$) by:

$$S_{W_r}(\omega) = \left(S_{F_r}(\omega)\right)/M_r^2\left[\left(\omega_r^2-\omega^2\right)^2+\left(\eta_r\omega_r\omega\right)^2\right]^{-1}$$

where:

$S_{F_r}(\omega)$ = spectral density of generalized force for mode r,

M_r = modal mass,

ω_r = natural frequency,

η_r = modal loss factor,

$$\left[\left(\omega_r^2-\omega^2\right)^2+\left(\eta_r\omega_r\omega\right)^2\right]^{-1} = |H|^2/\omega_r^4,$$

H = dynamic magnification factor.

When 'coincidence' occurs, that is when the driving and resonant frequencies coincide ($\omega = \omega_r$) as well as the joint acceptance being a maximum, the general modal displacement response is given by:

$$\overline{W_r(t)^2} = \pi\, S_p(\omega_r)\cdot A^2 j_r^2(\max)/\left(M_r^2\eta_r\omega_r^3\right)$$

where $W_r(t)$ is the generalised co-ordinate for the rth mode. The displacement at position y on the structure is given by the product of the generalised co-ordinate and the relative mode shape function for mode r, $\phi_r(y)$.

Thus the mean square modal response is given by:

$$\overline{\left\{W_r(t)\phi_r(y)\right\}^2}$$

Modal damping η_r is composed of structural and radiation components.

Coincidence conditions cause the highest response, so the first step would be to estimate response for coincidence. If this yields an unacceptable result, the likelihood of coincidence should be investigated. Since the bandwidth of the excitation field will generally be sufficient to contain the resonant frequency, frequency matching will occur, so it is the spatial matching which will require examination. This is determined by the behaviour of the JAF, which can vary by an order of magnitude over half a decade of frequency. The JAFs for the most common structural elements are shown below in 'Joint Acceptance for Basic Structural Elements', where the derivation of additional JAFs is also described.

If the initial response at resonance is estimated to be too high so that a better estimate must be made, then for the example of a one-dimensional system the following relationship applies for random excitation, if the modes can be considered to be uncoupled:

$$\overline{W(y)^2} = A^2\sum_n\left(\phi_n^2(y)\int_0^\infty\left\{\frac{G_p(f)\,j_n^2(f)}{\left[\left(k-\omega^2 m\right)^2+\left(\omega c\right)^2\right]}\right\}df\right)$$

where:

$G_p(f)$ = acoustic pressure spectral density (single-sided, = $4\pi\, S_p(\omega)$),

$\phi_n(y)$ = relative mode shape for n^{th} mode of point y,

A = surface area of beam on which noise pressure acts,

$j_n^2(f)$ = square of joint acceptance.

This can be simplified and expanded if the following assumptions are made:

- the structure is lightly damped (total modal loss factor η_n is small),
- $j_n^2(f)$ and $G_p(f)$ are constant close to each natural frequency. For either term taken individually, the values are not necessarily the same at each natural frequency.

Then:

$$\overline{W(y)^2} = \frac{A^2}{4}\sum_n\frac{\phi_n^2(y)\cdot G_p(f_n)\,j_n^2(f_n)}{M_n^2\eta_n\omega_n^3}$$

The above relationships assume excitation over the whole of the responding surface. In the case of local excitation, a significant 'near-field' spatial effect can occur, whereby in general there is an apparent attenuation of response as distance from the excitation site increases. This occurs when the structural modes are not sufficiently uncoupled to avoid cross-mode terms influencing the total response. Ref. [6] illustrates that for a particular beam, at the natural frequency of the third mode, with damping of all modes at 0.5 critical, the maximum r.m.s. response value in the third of the beam length most remote from the excited end is only about half that in the section nearest the source.

In Figure 11.02.2, modal summation over the first ten modes was required to give a result within 2% of an exact solution, but just the first five modes gave a good estimate.

Note: This 'near-field' effect cannot be predicted with the use of SEA. Consequently, when SEA is used, point force (or other non-uniformly distributed) loading conditions give rise to much wider confidence levels in spatial distribution of response than does uniformly distributed loading.

Ref. [7] introduces the concept of acoustic mobility from similar formulations and develops simplified design data, [See: Table 11.02.1]. The application of such classical modal response relationships (as opposed to probabilistic response analyses such as by SEA) to make initial estimate of response of simplified representations of spacecraft and launcher structures has been discussed in Ref. [8].

Acoustic Mobility $Y_{ac} = \left[\dfrac{S_{\ddot{x}}(f)\cdot m^2}{S_p(f)}\right]^{\frac{1}{2}}$ (dimensionless)

m = mass per unit surface area

$S_{\ddot{x}}(f)$ = spectral density of acceleration response out of plane

Spatially averaged $<Y_{ac}>$, and values for a specific location ℓ, $Y_{ac}(\ell)$ can be evaluated, to give respectively $\langle S_{\ddot{x}}(f)\rangle$ and $S_{\ddot{x}}(f)$ max.

Maximum values occur for excitation at panel natural frequency.

Normalised (1) Maximum Value of Acoustic Mobility for Fundamental Mode of a Square Uniform Panel, Subjected to Normal Incident Sound Wave	
$<Y_{ac}>$	$8/\pi^2$
$Y_{ac}(\max)$	$16/\pi^2$

Notes:

1 Values are normalised with respect to resonant amplification factor Q, i.e. Y_{ac}/Q.

2 Values are for single frequency or narrowband of noise at fundamental frequency panel. They also apply to the fundamental mode response for a diffuse field when the quantity $f_{1,1}\ a/c$ is less than 0.5, where: a = edge length, c = acoustic velocity.

3 The incidence direction of excitation is parallel to a plate edge.

4 Values given are for simply-supported edges. Values for other boundary conditions are within approx. ± 40%, increased clamping causing $<Y_{ac}>$ to reduce and $Y_{ac}(\max)$ to increase.

5 Values are reduced as the angle of incidence increases towards grazing.

Table 11.02.1 - Acoustic Mobility Values for a Panel, Ref. [7]

ESTIMATION OF DAMAGE (STRESS) DUE TO VIBRATION INPUTS

Ref. [27] contains the original work on this subject. In some cases, estimation of the vibration level (as acceleration spectral density) is adequate, for example where the structural component has to satisfy a specified limit either for its own safety or by virtue of providing a mounting for other equipment.

In other cases, or if a limit waiver is to be considered, the damage implication of the estimated vibration response is required. When damage is caused by structural strain, the first step is to assess the strain arising from the estimated vibration response.

In fact, the simplest assessment is not based on a vibration response estimate which requires values of joint acceptance, but on much more gross assumptions.

In addition to the assumption that the response is predominantly in a single mode, the simplest methods as adopted in design guides (such as Ref. [2, 3]) also assume the following in order to simplify the estimation of stress, usually at a conservative value (i.e. an upper bound estimate):

- the response is predominantly at the fundamental natural frequency,
- the vibration mode shape is the mode of deflection when subjected to uniform static pressure, with fully fixed edge restraint usually assumed,
- the excitation pressure is in-phase over the whole panel surface area (i.e. trace wavelength of incident pressure field is long compared with the structural wavelength),
- the pressure PSD is a constant value close to the resonant frequency.

Then the mean square stress at a point $\overline{\sigma^2(t)}$ is given by:

$$\overline{\sigma^2(t)} = \frac{\pi}{4\xi} f_r G_p(f_r)\sigma_{sp}^2$$

where:

f_r = natural frequency of fundamental mode (Hz),

$G_p(f_r)$ = spectral density of acoustic pressure,

σ = static stress at the point of interest due to unit static pressure over the whole surface,

ξ = damping ratio of the fundamental mode.

In contrast to this method, multimode estimates using SEA give spatially averaged mean square estimates of stress, but give no estimate of stress at a point (Ref. [28]).

Where power spectra density data are available for vibration response, the latter's relationship to fatigue life can be considered. This is discussed in Ref. [9].

JOINT ACCEPTANCE FUNCTION FOR BASIC STRUCTURAL ELEMENTS

The joint acceptance is the ratio of the generalised force for the mode to the total excitation force. This is a function of the integral, over the structure's surface exposed to the pressure field, of the product of the excitation and response functions, the latter being the mode shape in the case of a finite structural element. The excitation function can be expressed in terms of a spatial correlation coefficient. Thus for a given structural element, the joint acceptance will in general be a function of the excitation and vice versa.

The joint acceptance functions for some common and relatively simply combinations of excitation and structural mode shape have been published (e.g. Ref. [7, 10]) as analytical expressions, together with the upper bounds given by enveloping the functions for sets of structural modes, where the functions have similar forms. This typically occurs above the lowest order modes, for either even or odd order modes.

These 'standard' joint acceptance functions are given below. When others are required, then the necessary algebraic integration of the waveforms and mode shapes to produce the relevant expressions can be performed by algebraic computer software (for example Ref. [11]), or with the assistance of relevant integration formulae such as were derived for Ref. [12]. In Ref. [12], fifty-six integrals are evaluated of the general type:

$$I = \int_{x_1}^{x_2} x\exp(ax)\sin(h)(mx+p)\cos(h)(nx+q)\,dx$$

The structural mode shapes required to give the response function $W_r(x,y)$ can be obtained from the literature, such as Ref. [13]. The joint acceptance values for various combinations of acoustic field and structural elements then become those given in Topics 11.03 to 11.05.

The derivations of the joint acceptances for beam, plates, rings and cylinders are given in Ref. [6, 14], and the cylinder results are summarised and applied to a particular structure in Ref. [10].

11.03 JOINT ACCEPTANCE: BEAM

RANDOM LEVEL PLANE WAVE EXCITATION

Simply supported

If the beam is assumed to be simply supported at its ends:

joint acceptance function $$j_m^2(k_y) = 2(m\pi)^2 \left\{ \frac{1 - (-1)^m \cos kL}{\left[k_y^2 - (m\pi/L)^2\right]^2} \right\}$$

where:

k_y = axial component of incident field wavevector, [See: Figure 11.02.1],

m = axial mode order,

L = length of beam.

The characteristics of this joint acceptance function are illustrated by Figure 11.03.1. Under maximum spatial matching conditions, the acoustic trace wavelength equals the structural wavelength and the value of the JAF is about 0.25 for $m > 2$. Equispaced peaks occur at diminishing levels both at lower and higher wavelength ratios. Thus, for example, as the angle of incidence increases from grazing towards normal, the coupling value represented by the JAF passes through half-cycles of increasing amplitude until the max-max or absolute peak is reached at the equal wavelength conditions, after which the value passes through half-cycles of decreasing amplitude. The 'coincidence' condition which occurs when the response and excitation wavelengths are equal at the excitation frequency is here termed 'external coincidence'.

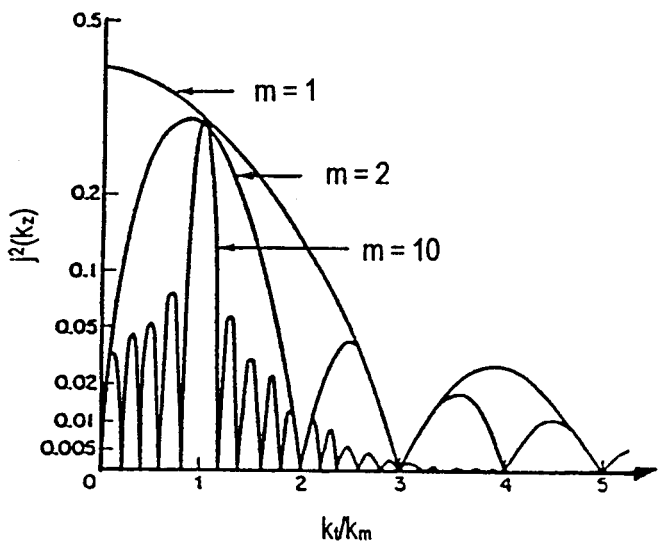

Figure 11.03.1 - Variation of Joint Acceptance $j^2(k_z)$ with Wavenumber Ratio k_t/k_m

Clamped-Clamped

This gives a complicated general expression and so only the approximate envelope for frequencies near or below coincidence is presented (λ_t = trace acoustic wavelength, L = beam length).

Odd-Order Modes	Even Modes
1. When $L/\lambda_t \to 0$; 1st mode; $j_1^2(f)_{max} = 0.275$. Higher modes; $j_n^2(f)_{max} \approx \left[\frac{64 A_n^2}{[(2n+1)\pi]^2}\right]_{n=3,5,7}$ Note: For $n \geq 2$, $A \approx 0.661$.	1. When $L/\lambda_t \to 0$; $j_n^2(f)_{max} \approx \frac{32 A_n^2}{[2n+1]^2}\left(\frac{L}{\lambda_t}\right)^2_{n=2,4,6....}$ Note: For $n \geq 2$, $A \approx 0.661$.
2. When $L/\lambda_t \approx \frac{n}{2} + \frac{1}{4}$; For $n > 1$, $j_n^2(f)_{max} \approx .21$	2. When $L/\lambda_t \approx \frac{n}{2} + \frac{1}{4}$; $j_n^2(f)_{max} \approx .21$

The envelope of values for the first three modes is shown in Figures 11.03.2 to 11.03.4 as the lower curve in each case.

Note: Each of these Figures relates to a beam on simple supports but with rotational end fixing ranging from free at both ends to fully clamped at both ends, Ref. [7].

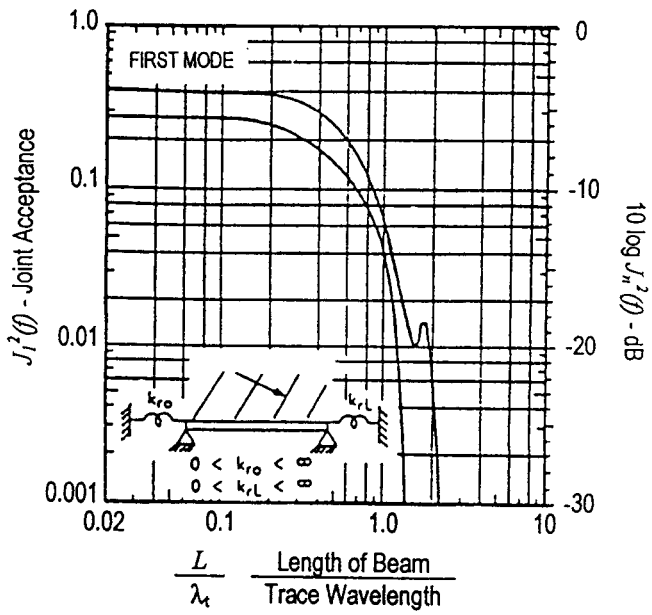

Figure 11.03.2 - Joint Acceptance: Beam, First Mode, Ref. [7]

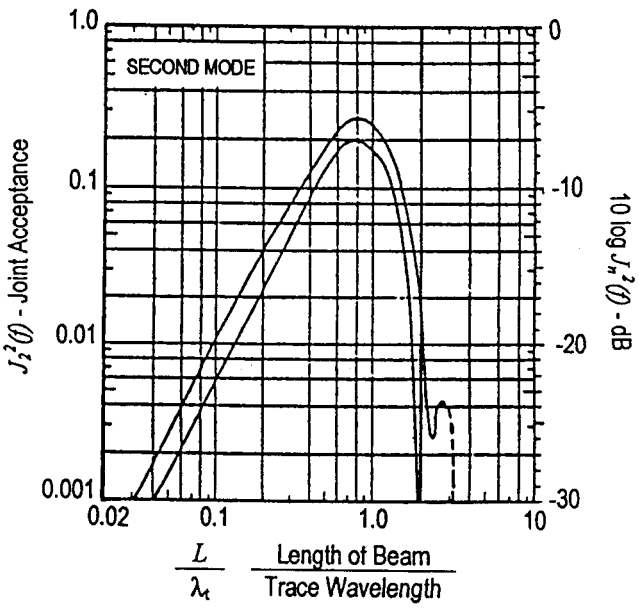

Figure 11.03.3 - Joint Acceptance: Beam, Second Mode, Ref. [7]

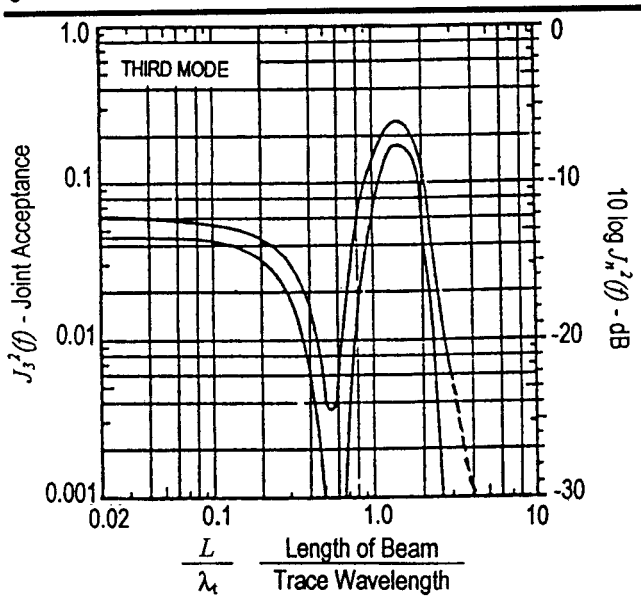

Figure 11.03.4 - Joint Acceptance: Beam, Third Mode, Ref. [7]

Pinned supports with rotational stiffness (i.e. moments applied)

This case requires numerical evaluation, but the range of values between the extremes of simply supported and fully clamped conditions is seen in Figures 11.03.2 to 11.03.4. In most cases below coincidence (abscissa value of unity) the difference is not very large. It is therefore recommended that the upper-bound simply supported values be used.

One end free, one end clamped or guided

Only the fundamental mode joint acceptance has been presented, as given below and shown in Figure 11.03.5.

$\alpha = L/\lambda_t$, (length/trace acoustic wavelength)

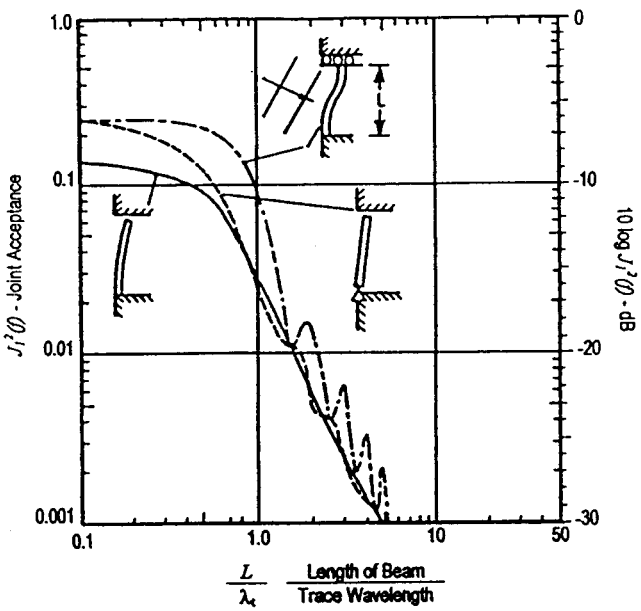

Note: An approximation for the first bending mode of tall buildings subjected to acoustic excitation, Ref. [7]

Figure 11.03.5 - Joint Acceptance for the Fundamental Mode of Beams with One-end Free or Guided, Ref. [7]

- **Clamped-free:**

$$j_1^2(f) = \frac{(2/\pi)^2}{A}\left[\frac{1-8\alpha^2}{B} + \frac{2}{A} - \frac{\cos 2\pi\alpha}{B} - \frac{\sin 2\pi\alpha}{2\alpha A}\right]$$

where: $A = (1 - 16\alpha^2)$, $B = 8\alpha^2$.

Limiting values: 1. When $\alpha \to 0$, $j_1^2(f) \to 0.132$,

2. When $\alpha >> 1$, $j_1^2(f) = \frac{1}{4\pi^2} \Big/ \left(\frac{L}{\lambda_t}\right)^2$

- **Clamped-guided:**

$$j_1^2(f) = \left(\frac{2}{\pi}\right)^2\left[\frac{1-\cos 2\pi\alpha}{32\alpha^2} + \frac{\alpha^2(1+\cos 2\pi\alpha)}{4(1-4\alpha^2)^2}\right]$$

Limiting values: 1. When $\alpha \to 0$, $j_1^2(f) \to 1/4$,

2. When $\alpha \to \infty$, $j_1^2(f) \to \frac{1}{2\pi^2}\alpha^2$

- **Pinned-free:**

$$j_1^2(f) = \left(\frac{2}{\pi}\right)^2\left(\frac{1}{16\pi^2\alpha^4}\right)\left[\frac{1-\cos 2\pi\alpha}{2} + \pi\alpha(\pi\alpha - \sin 2\pi\alpha)\right]$$

Limiting values: 1. When $\alpha \to 0$, $j_1^2(f) \to 1/4$,

2. When $\alpha \to \infty$, $j_1^2(f) \to \frac{1}{4\pi^2}\alpha^2$

Note: For low α, $j_n^2(f)$ is less than for a simply supported beam, and for high α, $j_n^2(f)$ reduces at a lower rate than for the simply supported beam.

REVERBERANT SOUND FIELD

Simply supported

$$j_n^2(f) = \frac{1}{(2\pi m)^2\alpha}\left[C_{in}A - C_{in}B\right] + \frac{1}{4\pi\alpha}\left[S_iA - S_iC\right] + \frac{1}{(m\pi)^2}\left[\frac{1-(-1)^m\cos 2\pi\alpha}{1-(2\alpha/m)^2}\right]$$

where: $\alpha = L/\lambda$ (Note: λ not 'trace-λ' is required).

Cosine integral, $C_{in}(v) = \int_0^v \frac{1-\cos y}{y}\,dy$

Sine integral, $S_i(v) = \int_0^v \frac{\sin y}{y}\,dy$

y = distance along beam.

The joint acceptance values of the first three modes are shown in Figure 11.03.6 with those for the progressive excitation field shown for comparison. Figures 11.03.7 and 11.03.8 show curves for a wider range of modes.

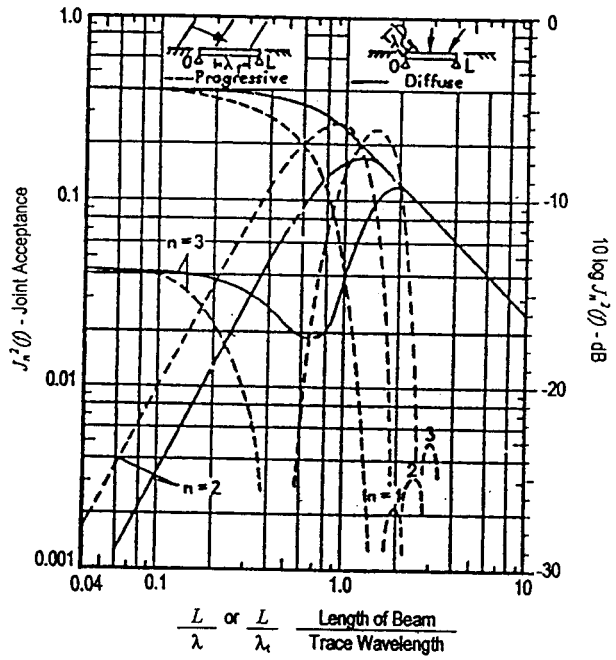

Figure 11.03.6 - Comparison of Joint Acceptance for First Three Modes of Simply-supported Beam (for Progressive Wave & Diffuse Field), Ref. [7]

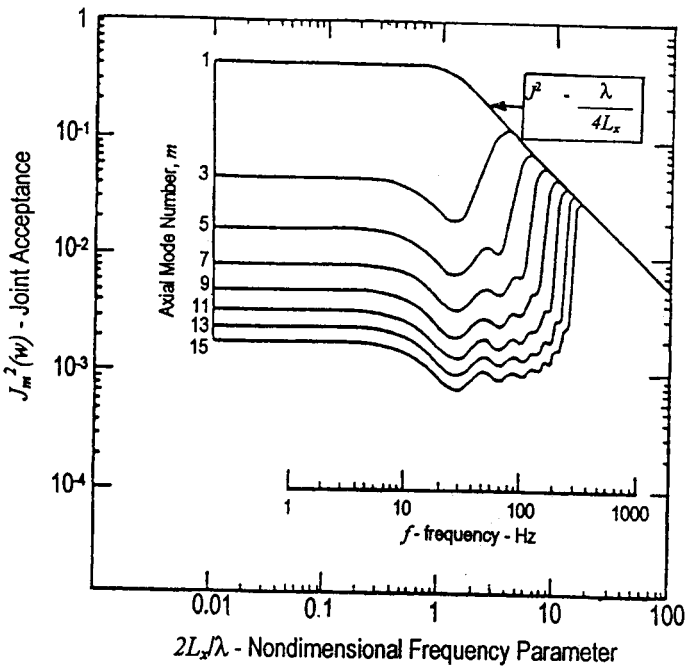

Figure 11.03.7 - Joint Acceptance of Odd-numbered Axial Modes of Cylinder for Reverberant Acoustic Field, Ref. [10]

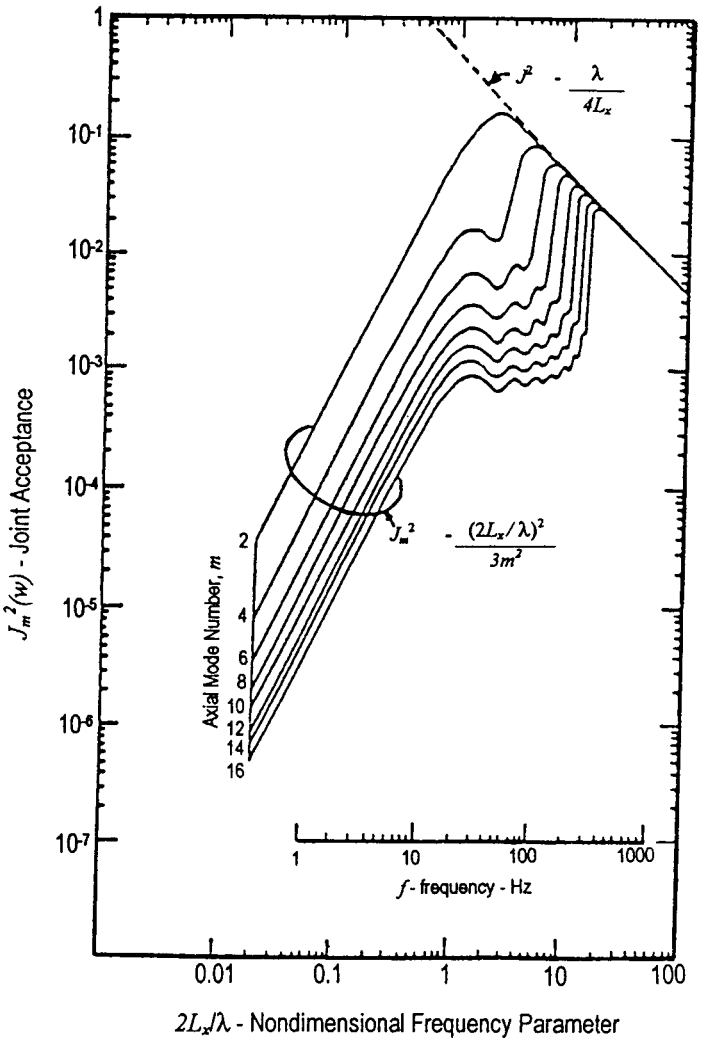

Figure 11.03.8 - Joint Acceptance of Even-numbered Axial Modes of Cylinder for Reverberant Acoustic Field, Ref. [10]

The peak value at coincidence, above the fundamental mode order, occurs for the diffuse field at a value of α which corresponds to a plane wave incident at about 48° to normal.

The trends shown at low frequencies are those for odd order modes; the joint acceptance is similar for both types of excitation, but for even orders, the values can be up to 3 times higher for progressive field excitation. At coincidence, the diffuse field value is $2/(n + 1)$ less than the progressive field value, for mode order $n > 1$.

At high frequencies the joint acceptance for all modes for the diffuse fields decreases at rate $(1/\alpha)$, compared with up to $(1/\alpha^4)$ for progressive fields.

The limiting values are given in Table 11.03.1.

	L/λ (1)	$J_n^2(f)$ Progressive Waves	$J_n^2(f)$ Diffuse Field
Odd Modes:	$L/\lambda \to 0$	$(2/n\pi)^2$	$(2/n\pi)^2$
	$L/\lambda = n/2$	1/4	-
	$L/\lambda = (n+1)/2$	-	$1/2(n+1)$
	$L/\lambda >> n/2$	$(2/n\pi)^2/(L/\lambda_t)^4$	$(1/4)/(L/\lambda)$
Even Modes:	$L/\lambda \to 0$	$(2L/n\lambda_t)^2$	$1/3(2L/n\lambda)^2$
	$L/\lambda = n/2$	1/4	-
	$L/\lambda = (n+1)/2$	-	$1/2(n+1)$
	$L/\lambda >> n/2$	$(n/2\pi)^2/(L/\lambda_t)^4$	$(1/4)/(L/\lambda)$

(1) $\lambda = \lambda_t$ Trace Wavelength for a Progressive Wave

Table 11.03.1 - Comparison of Limiting Values of Joint Acceptance for a Simply-supported Beam (for progressive wave & diffuse sound field), Ref. [10]

BOUNDARY-LAYER TURBULENCE

The space correlation function used in Ref. [10] for boundary-layer turbulence is:

$$\exp\left(-\delta_y|z|\right)\cdot\cos\left(\frac{2\pi\Delta_y z}{\lambda}\right)$$

where:

$z = y\text{-}y'$ when the whole beam length is exposed to turbulence,

y, y^1 = locations between which correlation is required,

δ_y = exponential decay rate of turbulent boundary-layer pressures along the beam.

An expression for $j_m^2(f)$ is given in Ref. [10]; derived in Ref. [6, 14].

$$j_m^2(f) \approx \frac{2}{(m\pi)^2}\left[\frac{P}{\Delta^2}+\frac{m\pi r}{2\Delta}\right]$$

where: $\Delta = \left[1+A^2+B^2\right]^2 - 4A^2$

$P = \left[1-A^2+B^2\right]^2 - 4A^2B^2$

where: $A = \gamma_y/m\pi$, $B = \delta_y/m\pi$,

γ_y = pressure correlation length = $(2\pi f\cdot L/U_c)$,

U_c = convection velocity.

This is a simplified version of joint acceptance, valid when δ_y is high, due to a high ratio of structural length to boundary-layer thickness. This is also valid for a rectangular plate and a cylinder along the y-axis and axis of revolution respectively and is illustrated in Figure 11.03.9.
The form of the above joint acceptance is illustrated for the Apollo SLA (cylindrical representation) in Ref. [10].

Without the restriction on δ_y value, the values of joint acceptance at coincidence ($\gamma_y = m\pi$) are given in Ref. [6] as:

$$j_m^2(f_{coin}) = \frac{1}{2}\left[\frac{C^2-\delta_x^2}{\left[\delta_x^2+C^2\right]^2}+\frac{2}{\delta_x^2+C^2}-\frac{1}{\delta_x^2}\right]\left(1-\exp(-\delta_x)\right)+\frac{\delta_x/2}{\delta_x^2+C^2}+\frac{1}{2\delta_x}$$

where: $C = 2m\pi$.

11.04 JOINT ACCEPTANCE: PLATES

RANDOM LEVEL PLANE PROGRESSIVE WAVE EXCITATION

Simply supported

Using a co-ordinate system with y and z in the plane of the plate, for mode order mn of a rectangular plate of edge lengths a and b:

$$j_{mn}^2(f) = \frac{1}{(ab)^2}\int_0^a\int_0^a\int_0^b\int_0^b \overline{R}_p(y,y',z,z',f)\,\phi_{mn}(y,z)\,\phi_{mn}(y',z')\,dy\,dy'\,dz\,dz'$$

where: $\phi_{mn}(y,z) = \phi_m(y)\cdot\phi_n(z)$

i.e. the mode shape of the plate is the product of the mode shape of two simply supported beams.

$\overline{R_p} = (y,y',z,z')$ = the space correlation coefficient.

For a simple mode such as m = 1, n = 2 (one nodal line), in each orthogonal direction, there is a unique angle of incidence relative to the normal which gives coincidence with the plate mode. If the incidence is at an angle to the orthogonal direction, the joint acceptance is reduced. Figure 11.04.1 shows these values as decibel contours.

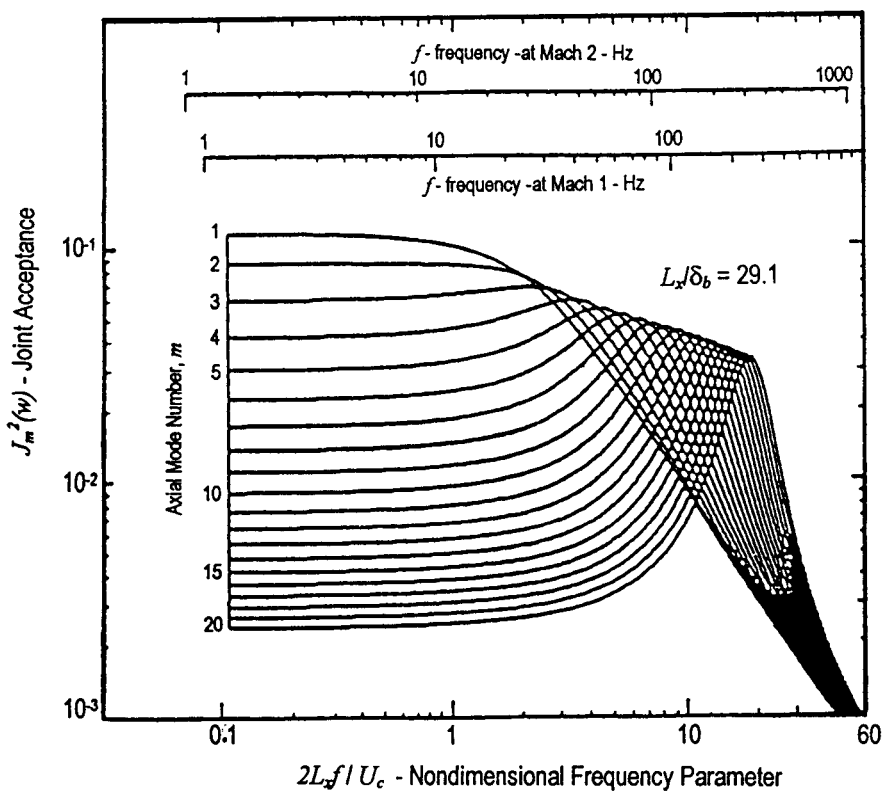

Note: This form also applies to beams and plates.

Figure 11.03.9 - Joint Acceptances of Axial Shell Modes of Cylinder for Boundary Layer Turbulence, Ref. [10]

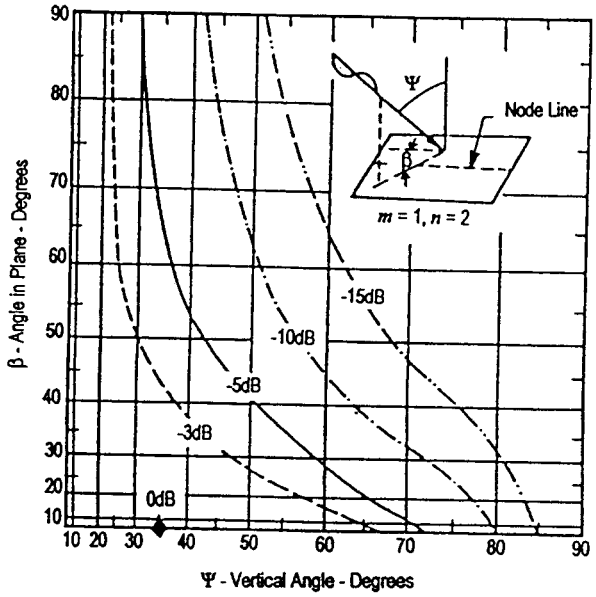

Note: Contours of $10 \log J^2_{mn}(f)$, in dB, relative to maximum value, as a function of angles of incidence ϕ and β for plane wave excitation of a rectangular panel vibrating in its' 1,2 mode.

Figure 11.04.1 - Joint Acceptance Function: Plate, Ref. [7]

When the progressive wave field is travelling parallel to one edge of the rectangular plate, the joint acceptance is the product of the joint acceptances for beams along the two axes, thus:

$$j^2_{mn}(f) = j^2_m(f) \cdot j^2_n(f).$$

Along the axis perpendicular to the wavefront,

$$j^2_m(f) = \frac{2}{(m\pi)^2}\left[\frac{1}{1-\left(\frac{2a/m}{\lambda_t}\right)^2}\right]^2 \left[1-\cos m\pi \cos(2\pi a/\lambda_t)\right]$$

Along the axis perpendicular to the wavefront (where all points are in-phase), equivalent to a normally incident wave,

$$j^2_n(f) = \left(\frac{2}{n\pi}\right)^2$$

Since these are the one-dimensional beam relationships, the plate value can be found by reference to beam curves.

For the first mode $m = n = 1$ of a simply supported plate, for normal incidence,

$$j^2_{1,1}(f)_{max} = 0.164$$

This value is also correct for any angle of incidence for plate with $\alpha_b < 0.2$ where $\alpha_b = b/\lambda_t$, b = longest size.

The maximum values of joint acceptance for several boundary conditions, for the fundamental mode of rectangular plates, is given in Table 11.04.1.

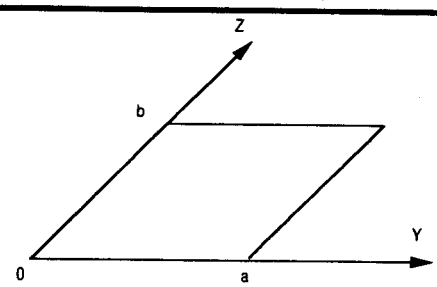

$J_{1,1}^2(f)_{max}$

Boundary Condition at $y = 0, a$	Boundary Condition at $z = 0, b$			
	SS	SC	CC	CF
FF	0.405	0.325	0.2755	0.132
SS	0.164	0.132	0.111	0.0535
SC		0.106	0.0895	0.0429
CC			0.0760	0.0364
CF				0.0174

Key: F: Free.
S: Simple or pinned edge.
C: Clamped or fixed edge.

Note: In all cases, mounting in an infinite baffle is assumed.

Table 11.04.1 - Max. Value of Max. Joint Acceptance squared for Fundamental Mode of Uniform Plates with Various Boundary Conditions under Uniform Acoustic Loads, Ref. [7]

DIFFUSE FIELD EXCITATION

An approximate solution is again available as the product of the joint acceptances of diffusely excited beams showing the one-dimensional mode shapes in the orthogonal directions of a rectangular plate. This slightly over-predicts the joint acceptance at low frequencies. The values for the first three modes for square plates are shown in Figure 11.04.2.

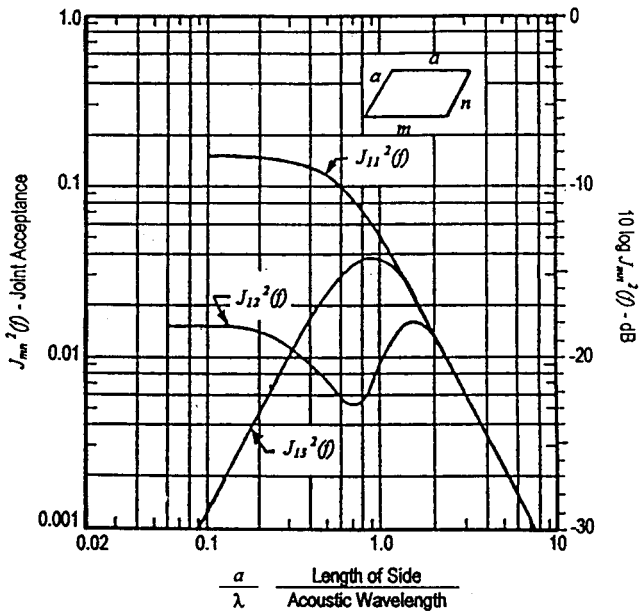

Note: Joint acceptance of 3 vibration modes (1-1, 1-2 and 1-3) of a simply-supported square panel in a diffuse sound field, Ref. [7].

Figure 11.04.2 - Joint Acceptance: Plate in a Diffuse Sound Field

BOUNDARY-LAYER EXCITATION

For convection parallel to one edge of a rectangular plate, the functions given above for a beam are appropriate.

11.05 JOINT ACCEPTANCE: RINGS AND CYLINDERS

PROGRESSIVE WAVE EXCITATION

The structural behaviour of a cylinder differs from that of a plate due to the membrane effect arising from structural continuity around the circumference.

In the circumferential direction, the acoustic excitation is described by the acoustic scattering coefficient and the joint acceptances can be estimated as described in Ref. [10]. In the axial direction, mode shapes are close enough to those for a beam for the beam values to be adequate, [See: Figure 11.03.1].

In the circumferential direction, the space correlation factor assumed in Ref. [6] is relevant for waves in a set of narrow ducts fitting around the cylinder. For the case of free-field incidence, the cylinder coupling was calculated in Ref. [15] in terms of the scattering coefficient,

$$\text{i.e.}\ \frac{\text{scattered field pressure modal amplitudes}}{\text{incident free - field pressure}} = \frac{2}{\pi k_x a}\left|\frac{\varepsilon_n i^{n+1}}{H_n^1(k_x a)}\right|$$

where: k_x = radial wave number, = $k \sin \theta b_i$

i = angle of incidence (relative to axis of revolution)

n = circumferential mode order

ε_n = 1 for $n = 0$, = 2 for $n \neq 0$

H_n^1 = Hankel function of 1st kind = $J_n + i\, Y_n$

J_n, Y_n = Bessel functions.

At low frequencies, the scattering coefficients are very small, increasing towards unity and then reducing slowly as frequency increases.

Obtaining the correct behaviour at high frequencies requires very precise Bessel function evaluation.

REVERBERANT FIELDS

The axial mode joint acceptance can again be assumed to be as for a beam; as given above, [See: Figures 11.03.7 and 11.03.8]. The circumferential modes are given in Ref. [14] and shown in Figure 11.05.1:

$$j_n^2(f) = \frac{1}{2\pi ka}\left[S_i\{2\pi(n+ka)\} - S_i\{2\pi(n-ka)\}\right]$$

$$+\frac{1}{2(n\pi)^2}\left[\frac{1-\cos(2\pi ka)}{1-\left(\frac{ka}{n}\right)^2}\right] \quad \text{at } n \neq 0,$$

$$= \frac{S_i\{2\pi ka\}}{\pi ka} - \frac{1-\cos 2\pi ka}{2\pi^2 (ka)^2} \quad \text{at } n = 0$$

where the sine integral function, $S_i(v) = \int_0^v \frac{\sin x}{x} dx$

If algebraic computation is not available, advice on approximate evaluations of $S_i(v)$ can be sought in Ref. [14].

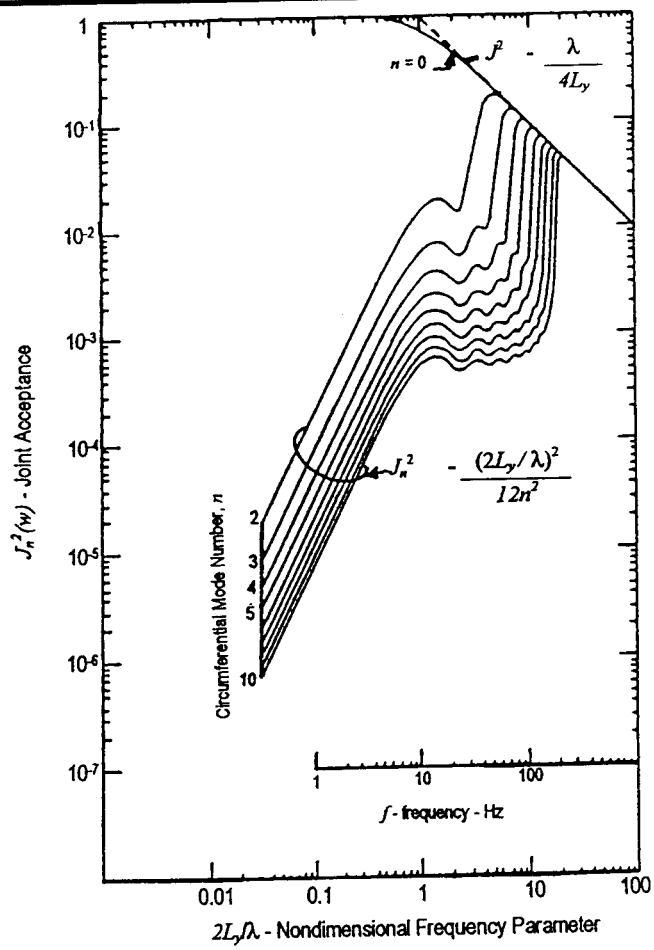

Figure 11.05.1 - Joint Acceptances of Circumferential Ring Modes of Cylinders for Reverberant Acoustic Field

BOUNDARY-LAYER TURBULENCE

The relationships given above for a plate are equally applicable for a cylinder in the axial direction.

In the circumferential direction, Ref. [14] gives:

$$j_n^2(f) = \frac{2\delta_y}{(2\pi n)^2 + \delta_y^2} + 2\frac{(2\pi n) - \delta_y}{\left[(2\pi n)^2 + \delta_y^2\right]^2}\left[1 - e^{-\delta_y}\right]$$

where: δ_y = circumferential exponential decay rate for turbulent boundary-layer pressures,

$$\delta_y = 2\left[\frac{2\pi a\omega}{U_c} + \frac{2\pi a}{\delta_b}\right]$$

a = radius,

U_c = boundary-layer convection velocity,

δ_b = boundary-layer thickness.

When δ_y is large, only the first term of the expression for $j_n^2(w)$ is significant. An example of the joint acceptance is shown in Figure 11.05.2 (i.e. for circumferential modes). In this case, $2\pi a/\delta_b$ = 54.3.

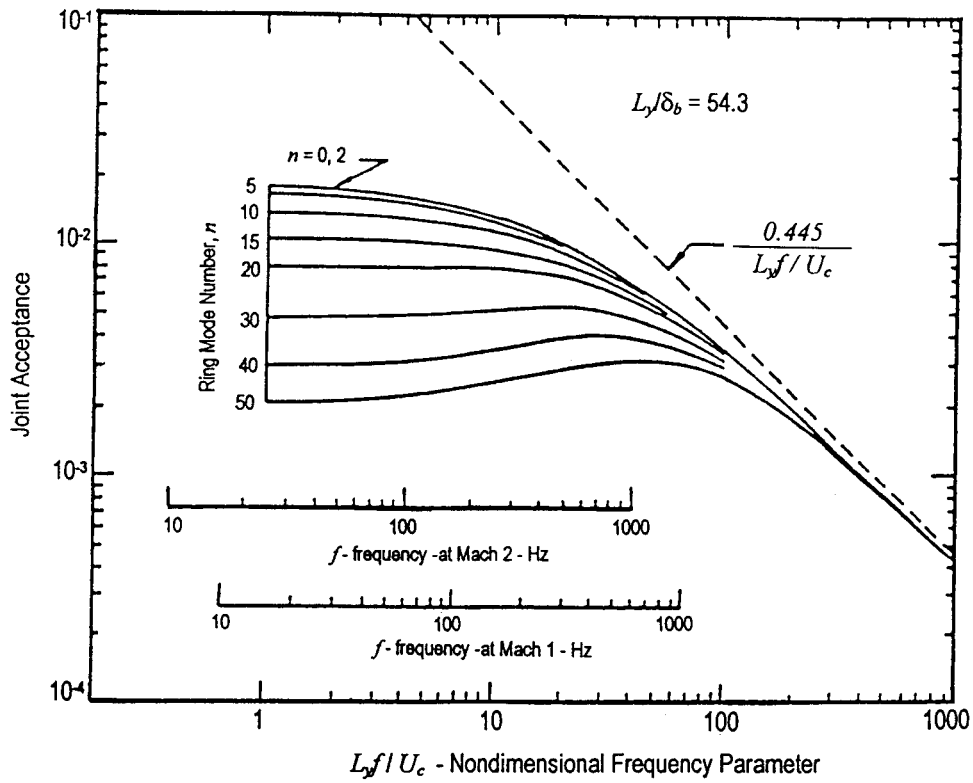

Figure 11.05.2 - Joint Acceptances of Cylinder Ring Modes for Boundary Layer Turbulence, Ref. [10]

11.06 MODAL INTERACTION ANALYSIS (MIA)

This method was introduced in Chapter 1 as a means of predicting coupling between bounded fluid fields and finite structures, and is described in Ref. [16]. The fluid field's behaviour is described by a differential equation for each of its modes, assumed uncoupled, whereas the joint acceptance approach is appropriate for un-enclosed non-modal fluid behaviour. (A further alternative of interaction analysis by Green's function is not considered here, being mathematically complicated, but it can include the fluid's coupled modes; see Ref. [16].

Although the fluid is considered to be contained within rigid boundaries, the MIA approach does in effect operate with coupled modes of the structure. Solutions of the analysis make use of the property that the motions and energies of the coupled components can be expressed in terms of the combinations of the uncoupled modes, although the latter are not physically present. The energy of the system is equal to the sum of the energies of the uncoupled modes.

A coupling coefficient is given by the integral of the product of the structural and acoustic mode shape functions $\phi_p(r_s)$ and $\psi_n(r_s)$ respectively, over the surface of the structure,

$$C_{np} = \frac{1}{S} \int_s \psi_n(r_s)\ \phi_p(r_s) ds$$

where: S = surface area of structure,

n = mode order of fluid,

p = mode order of structure,

r = location on S.

Best coupling can only occur at frequencies above the critical frequency, with the important exception of the fundamental mode which can couple efficiently with the zero-order bulk compression of the fluid. For simplicity, it is assumed that the structural in-vacuo modes are damped sufficiently lightly to avoid cross-coupling. For this coupling by a simply supported panel,

$$C_{np} = \frac{1}{S} \int_0^e \int_0^f \sin\left(\frac{\pi x}{e}\right) \sin\frac{\pi b}{f}\, dS = \frac{4}{\pi^2}$$

where: e, f are panel edge lengths.

The mode shape of the fundamental coupled mode can differ significantly from the in-vacuo fundamental mode shape.

In PSD terms, the displacement response of a panel in mode p at frequency ω due to coupling with excitation fluid mode n is given by:

$$S_{w,p}(\omega) = \frac{S_n(\omega) C_{np}^2}{\Lambda_p^2 \left[\left(\omega_p^2 - \omega^2\right)^2 + \left(\eta_p \omega \omega_p\right)^2 \right]}$$

where:

$S_n(\omega)$ = PSD of nth mode of fluid (surface blocked pressure),

Λ_p = panel modal mass in pth mode,

S = structural surface area excited,

η_p = modal loss factor of fluid,

ω_p = natural frequency of fluid mode.

The predicted maximum coupled response will have maxima near the uncoupled resonance frequencies because only uncoupled modes are considered in the analysis. In reality the maxima will occur near the coupled system resonances, for which the frequencies would have to be calculated as an additional exercise. Unless this is done (and even then, modal damping information is unlikely to be available), MIA should be considered as a modal-ensemble approach, for which good confidence can only be expected when several modal couplings occur within a frequency bandwidth for which the response system energy is predicted. In these respects, the predicted results have similarities with the results of statistical energy analysis.

A limitation when coupling levels are high arises (as mentioned in Chapter 1) when energy transfer has to be limited to equipartition of average modal energy levels between the fluid and structural systems over the frequency band.

11.07 FINITE-ELEMENT ANALYSIS (FEA)

This modelling technique was introduced in Chapter 1. Its fundamental basis will now be described briefly. For further information Ref.[2], on which this summary is based, can be consulted.

The technique is employed as a means of obtaining solutions to the equations of motion of systems for which analytical solutions are not possible. This is necessary for most practical structures which are not adequately modelled as idealised uniform components such as beams, plates and shells. Approximate solutions can be obtained, for example, by applying the Rayleigh-Ritz method, from which the finite-element displacement method is derived.

The equations of motion are formulated with the aid of Hamilton's Principle. Under this, in the time interval between t_1 and t_2, the kinetic energy T of a system, its strain energy U and the work done W by the non-conservative forces, can be said to obey the relationship:

$$\delta \int_{t_1}^{t_2} (T - U + W)\, dt = 0 \qquad \text{(A)}$$

where: δ is the first variation of the integral.

The deformation of a multiple-degree-of-freedom system can be described by n independent displacements q_1 to q_n. The above condition of Hamilton's integral being stationary then reduces to:

$$\frac{d}{dt}\left(\frac{\partial T}{\partial \dot{q}_j}\right) + \frac{\partial D}{\partial \dot{q}_j} + \frac{\partial U}{\partial q_i} = f_j, \quad j = 1 \text{ to } n \qquad \text{(B)}$$

The equations in this set are Lagrange's equations. D is a dissipation function and f_j is the generalised force, which is equal to the work done by the applied forces when the component q_i undergoes a unit displacement.

The Rayleigh-Ritz method expresses the displacement $u(x,t)$ of a one-dimensional structure, in the x direction, as:

$$u(x,t) = \sum_{j=1}^{n} \phi_j(x) q_i(t) \qquad \text{(C)}$$

where: $\phi_j(x)$ are prescribed functions of x but $q_j(t)$ are unknown functions of t.

Using this form of displacement expression in the T, D, U and W energy component expressions reduces the continuous structure to be analysed to a multiple-degree-of-freedom system with displacements q_i as degrees of freedom. The equations of motion then can be expressed as:

$$[M]\{\ddot{q}\} + [C]\{\dot{q}\} + [K]\{q\} = \{f\} \qquad \text{(D)}$$

where: $[M]$, $[C]$ and $[K]$ are mass, damping and stiffness matrices, and $\{f\}$ is a column matrix of generalised forces corresponding to generalised displacements $\{q\}$.

If equation (D) is solved to determine $\{q\}$, the latter can be substituted into equation (C) to allow $u(x,t)$ to be found. The solution is an approximation, with accuracy increasing with n if functions $\phi_j(x)$ satisfy certain criteria, some of which depend on the order p of derivatives within the integral in equation (A).

Constructing a set of prescribed functions $\phi_j(x)$ is very difficult for practical structures. It is however possible to construct such functions automatically by using the 'finite- element displacement method'.

A set of reference (node) points are selected on the structure, each of which is assigned a number of degrees of freedom (displacement, slope, etc.). A set of functions is then constructed so that each gives a unit value for one degree of freedom and zero values for the others.

The structure between boundaries defined by the smallest set of nodes (e.g. 4 for a rectangle) is termed an element. Standardised representations of common elements (plates, rings, shells, etc.) have been developed so that real structures can be modelled as assemblages of such elements.

To solve equation (D) for free vibration, assuming no damping, substituting $q = \{A\}\, e^{i\omega t}$ gives:

$$\left[K - \omega^2 M\right]\{A\} = 0$$

Several methods can be applied to solve this linear eigenvalue problem, the choice being largely determined by the order of the K and M matrices. The number of degrees of freedom is typically very high unless reduction techniques are applied. In symmetrical structures, the symmetric and antisymmetric modes can be considered independently, and for other structures the degrees of freedom giving least strain energy can be subjugated to 'slave' status, others being 'master' degrees of freedom. A further option is based on division of a large structure into substructures.

The nature of the excitation forces determines the method of solution for forced vibration. The solution required is of equation (D). This can be achieved directly but because of the large number of degrees of freedom often arising due to a necessarily large number of nodes, reduction by modal substitution is a common approach. (The modelling restrictions imposed by a modal approach, mainly concerning representation of damping, are discussed in Chapter 1).

The modal substitution method employs:

$$\{q\} = [\phi]\{\xi\} \qquad \text{(E)}$$

where matrix $[\phi]$ represents the modes of vibration of the structure. When the lower-order modes contribute most of the vibration, the number of elements in $\{\xi\}$ is much less than that in $\{q\}$. If equation (E) is substituted into (D), multiplying by $[\phi]^T$ gives:

$$\{\ddot{\xi}\} + \left[\tilde{C}\right]\{\dot{\xi}\} + [\lambda]\{\xi\} = [\phi]^T\{f\}$$

where: $[\lambda]$ is a diagonal matrix of eigenvalues, and $\left[\tilde{C}\right] = [\phi]^T[C][\phi]$.

A further simplification is obtained by assuming that the damping is hysteretic, to give a matrix of a form which causes no coupling between the equations of motion of individual modes. The end result is a set of single-degree-of-freedom equations of motion, which can be solved by standard techniques (although random response requires special techniques).

If $[C] = a_0[M] + a_1[K]$, then $\left[\tilde{C}\right]$ is of the form $a_0[I] + a_1[\lambda]$, where a_0 and a_1 are gained from modal damping data, but this is only appropriate for light damping. Uncoupling modes of heavily damped structures requires application of complex modal analysis.

11.08 BOUNDARY ELEMENT METHODS

This method was introduced in Chapter 1. The principle is briefly described below, on the basis of Ref. [2].

In this method, the solid boundary (the structural surface) immersed in a fluid can be represented by a finite set of boundary elements. This allows an approximate solution to be found for the pressure distribution on the surface of the structure when it vibrates. Then the pressure can be found at any point in the fluid because the solution of the special case (at the structure's surface) of the integral equation for the general location in the fluid provides the required information.

The surface pressure distribution is given by:

$$\tfrac{1}{2}\, p(\underline{\zeta}) = \int_s \left\{ p(\underline{\xi})\, \frac{\partial G}{\partial n(\underline{\xi})}\, (\underline{\zeta},\underline{\xi}) + i\rho a_o\, k\, v_n\, (\underline{\xi})\, G\, (\underline{\zeta},\underline{\xi}) \right\} dS\, (\underline{\xi})$$

where: $\underline{\zeta}$ is a boundary surface location,

$\underline{\xi}$ is a boundary position vector,

$n\underline{\xi}$ denotes the normal at position $\underline{\xi}$,

S is the structural surface (see Figure 11.08.1).

The density, speed of sound and wave number are denoted by ρ, a_o and k respectively.

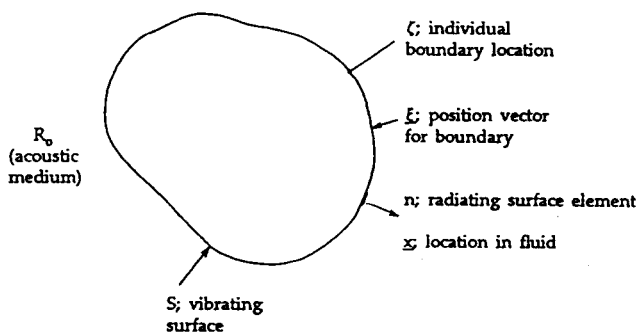

Figure 11.08.1 - Boundary Element Parameter Notation

$G(\underline{x},\underline{\xi})$ is the free-space Green's function (i.e. the solution to the Helmholz equation in free-space) given by:

$$G(\underline{x},\underline{\xi}) = \frac{\exp\left[-ikd(\underline{x},\underline{\xi})\right]}{4\pi d(\underline{x},\underline{\xi})}$$

$$\text{and} \quad d(\underline{x},\underline{\xi}) = \left|\underline{x} - \underline{\xi}\right|$$

where: $\underline{x}$ is a location in the fluid.

The surface pressure distribution is approximated by application of boundary element modelling.

At the structure's surface, over each element, equilibrium of pressure and continuity of velocity are expressed as:

$$v_n = [N_s]_e \{v\}_e, \quad p = [N_a]_e \{p\}_e$$

where: $[N]_e$ is an element displacement function,

subscripts s and a refer to structure and acoustic field respectively,

$\{\ \}_e$ denotes a column matrix for an element.

When v_n is known, p can be determined.

This gives a surface pressure distribution of the form:

$$[A]\{p\} = [B]\{v\}$$

where: $\{p\}$ and $\{v\}$ are column matrices of nodal pressures and velocities. Solution of this equation gives the nodal pressure values.

The pressure at location $\underline{x}$ is given by:

$$p(\underline{x}) = \int_s \left\{ p(\underline{\xi})\, \frac{\partial G}{\partial n(\underline{\xi})}\, (\underline{x},\underline{\xi}) + i\rho a_o\, k\, v_n\, (\underline{\xi})\, G\, (\underline{x},\underline{\xi}) \right\} dS\, (\underline{\xi})$$

where the boundary element analysis provides $p(\underline{\xi})$, and $v_n(\underline{\xi})$ is known.

The pressure, $p(\underline{x})$, can then be evaluated directly, the boundary element method only being used to determine the pressure at the structural surface.

In contrast, finite-element modelling would require the three-dimensional fluid to be modelled as an element mesh, which is a much more extensive analysis than the element modelling of the vibrating surface.

Proprietary software is available, such as Ref. [18].

11.09 RESPONSE PREDICTION BY A GENERAL EXTRAPOLATION PROCEDURE

An extrapolation procedure is a common technique used for predicting vibration levels on aerospace flight vehicles in general. This approach consists of extrapolating vibration data measured on previous structures to the new structure of interest. This may be accomplished by using pooled data from one or more general vehicles (termed general extrapolation) or by specific data from a selected similar vehicle (termed specific extrapolation). In either case the extrapolation rules have been arrived at either analytically or empirically. Ref. [19, 20] contain reviews of the major published procedures.

A summary of these procedures is given in the following sections, followed by a recommendation as to the most convenient procedure and an example that demonstrates both accuracy and limitations in use.

Two further scaling methods which incorporate SEA parameters are also described.

The general extrapolation method or approach includes all those procedures that use empirical relationships developed from regression studies of past data to predict vibration environments in future vehicles. Such procedures are widely used for the prediction of flight vehicle vibration.

11.10 MAHAFFEY-SMITH METHOD

Mahaffey and Smith (M-S), Ref. [21], were the first to apply this method using data obtained on B-52 and B-58 aircraft.

First, acoustic measurements were made at a sufficient number of locations to permit an adequate definition of the distribution of fluctuating pressures over the vehicle surface. These measurements were then analysed in octave bands to determine their frequency content. Figure 11.10.1 shows the resulting distribution of sound-pressure levels for the octave bands from 300 to 600 Hz over the surface of the B-58 during ground run-up of its turbojet engines.

Vibration measurements were then made at various locations throughout the vehicle, including structure adjacent to points of equipment attachment, and were similarly analysed in the octave bands. These data were next used to plot vibration magnitude vs sound-pressure level, as measured on the vehicle surface closest to the vibration measurements. Figure 11.10.2 shows this plot for the 300-to-600 Hz octave band.

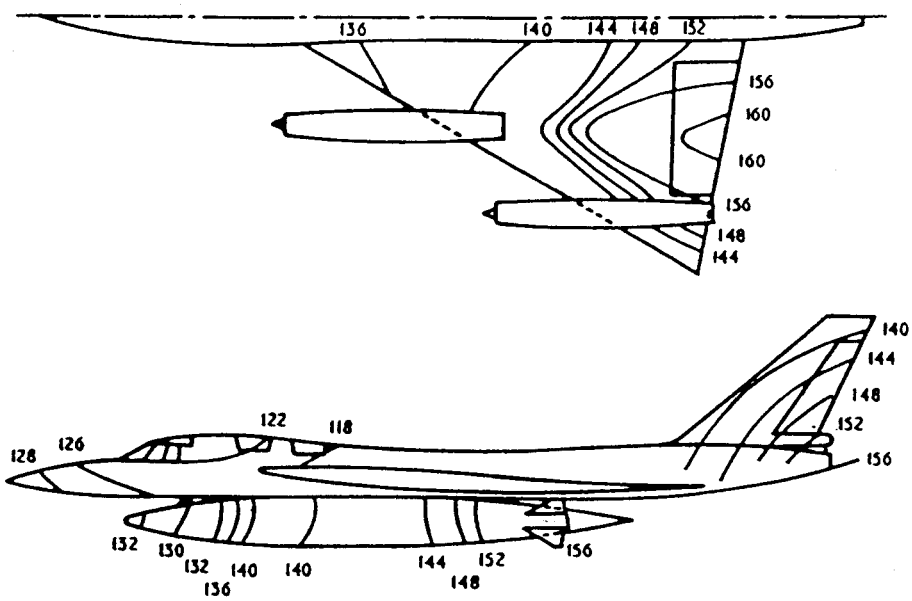

Figure 11.10.1 - Sound Pressure Level Contours for the B-58 in the 300-600 Hz Octave Band

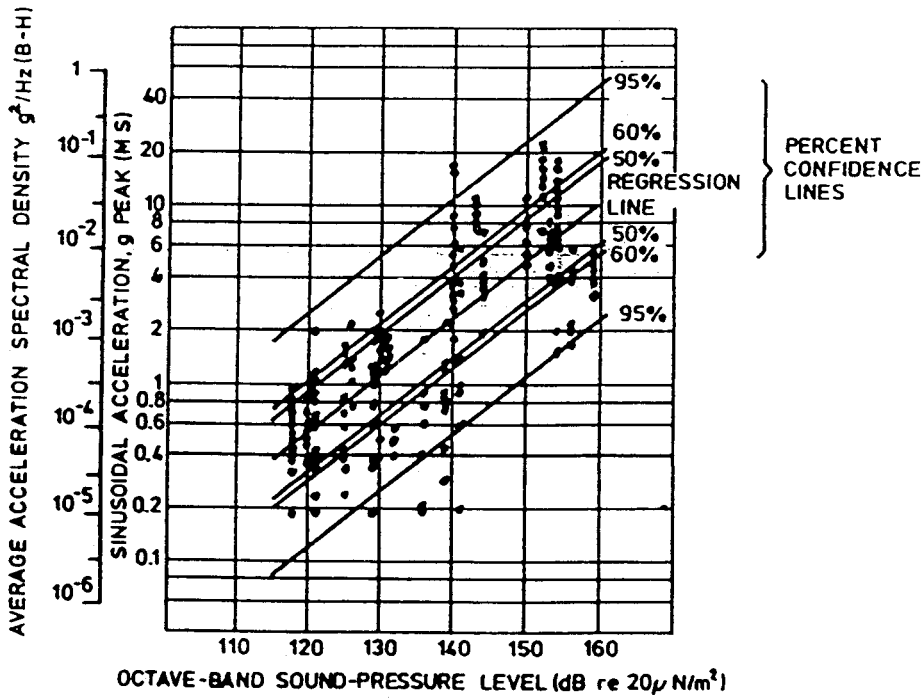

Figure 11.10.2 - Vibration Prediction Curves for Mahaffey-Smith & Brust-Himmelblau Methods (in the 300-600 Hz Octave Band)

ASSUMPTIONS

- All flights to which the procedure will be applied are dynamically similar to that of the B-52 aircraft.
- Vibration is due principally to acoustic noise excitation during take-off.
- Spatial variations in vibration can be considered a random variable.
- Vibration response is the same in all three orthogonal directions.
- Peak response is equal to 3.3 times the r.m.s. response.

INFORMATION REQUIRED

- Measurements or prediction of acoustic noise environment.

ADVANTAGES

- The procedure is simple and easy to use.
- No structural design details are required.

LIMITATIONS

- The procedure is based upon aircraft data only. The applicability of the procedure to spacecraft data is questionable.
- No excitation factors other than acoustic are considered.
- The prediction of vibration in terms of peak g's is inappropriate for the case of random vibration environments.
- No distinction is made between different equipment mountings and different orthogonal directions.

11.11 BRUST-HIMMELBLAU METHOD

Brust and Himmelblau (B-H) reconverted the M-S vibration measurements from peak values to the original r.m.s. values (a factor of 3.3), then squared them and divided by the octave band widths to express the random vibration in more suitable units; the (mean square) acceleration spectral density average over the octave band.

The specific acoustic vibration frequency response function suggested by Brust and Himmelblau is presented for each frequency octave band in Figures 11.11.1 and 11.11.2. They correspond to the upper 60% scatter limit for individual limits. For the use of the B-H method, the assumptions, information needed and limitations are the same as those already mentioned in Topic 11.10.

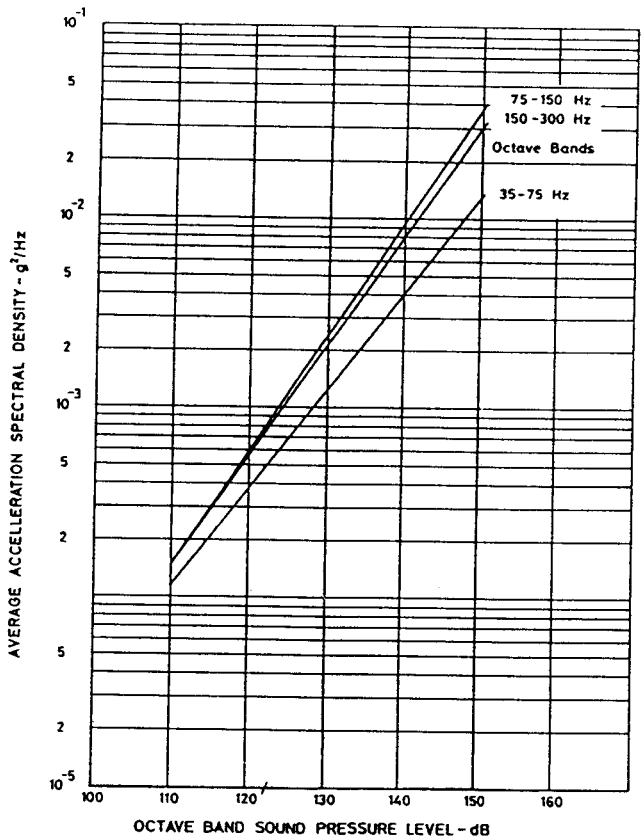

Figure 11.11.1 - Prediction Curve for Brust-Himmelblau Method (35-300Hz)

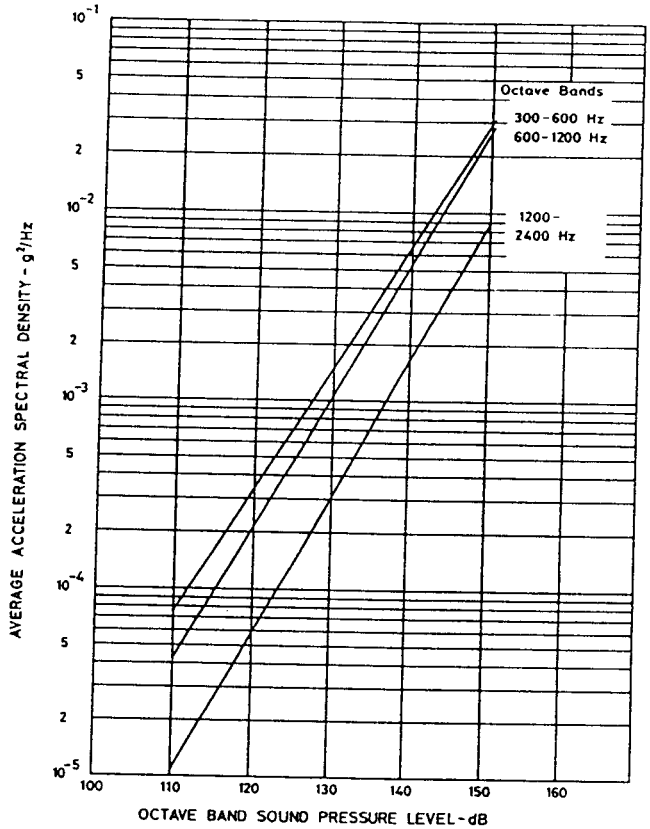

Figure 11.11.2 - Prediction Curve for Brust-Himmelblau Method (300-2400 Hz)

11.12 ELDRED, ROBERTS & WHITE (E-R-W) METHODS

Eldred, Roberts and White (E-R-W) summarised the results of two vibration data studies which could be used for vibration prediction. The first is based upon aircraft missile data, [See: Topic 11.13] and the second is based upon ballistic missile data, [See: Topic 11.14].

11.13 E-R-W METHOD NO.1

Method No. 1 consists of an acoustic vibration frequency response function developed from the Snark Missile data. The data were analysed in octave bands, the vibration being presented in g_{rms} and the acoustic noise presented in dB. The data are plotted with vibration as the ordinate and acoustic noise as the abscissa in Figure 11.13.1 for overall levels and in Figure 11.13.2 for band levels. No statistical analysis was performed, however.

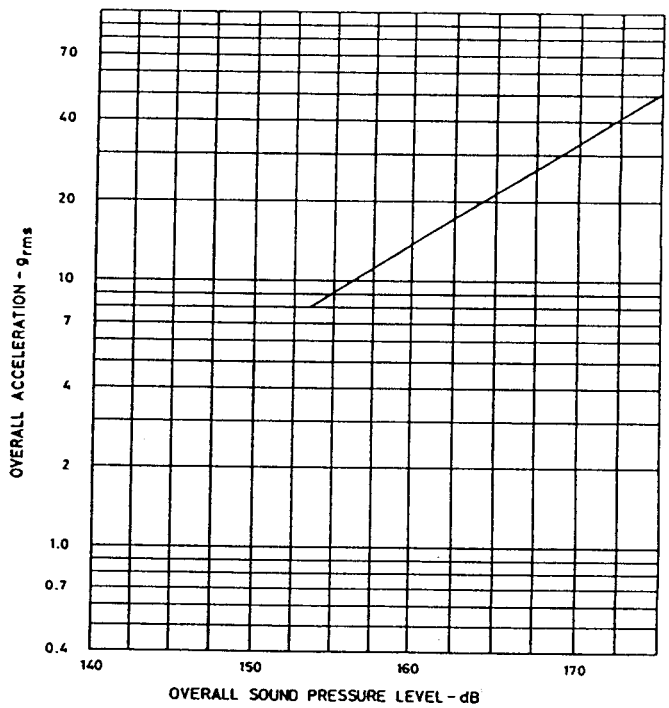

Figure 11.13.1 - Correlation between the Vibration Level & External Acoustic Excitation of Snark Missile OAL Levels

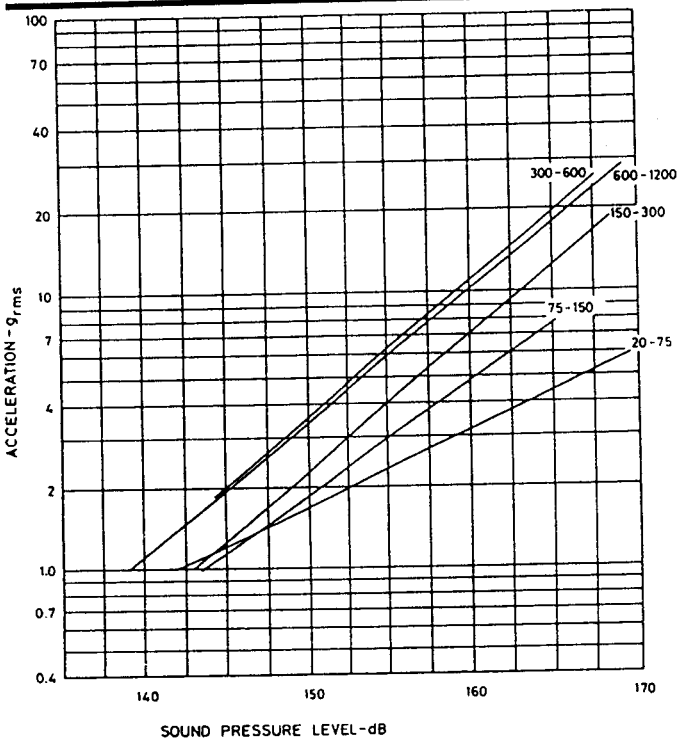

Figure 11.13.2 - Correlation between the Vibration Level & External Acoustic Excitation of Snark Missile (Octave Bandwidth: 20-1200 Hz)

ASSUMPTIONS

- All flight vehicles to which the procedure is to be applied are dynamically similar to the Snark Missile.
- Vibration is due principally to acoustic noise during take off.
- Spatial variations in the vibration can be considered a random variable.
- Vibration is the same in all three orthogonal directions.

INFORMATION REQUIRED

- Measurements or predictions of acoustic noise environments.

ADVANTAGES

- The procedure is simple and easy to use.
- No structural design details are required.

LIMITATIONS

- The procedure is based upon a limited amount of aircraft missile data only. The application of the procedure to other types of flight vehicle is questionable.
- No excitation factor other than acoustic noise is considered.
- No distinction is made between different equipment mountings and different orthogonal directions.
- No statistical considerations are directly incorporated in the prediction curves.

11.14 E-R-W METHOD NO. 2

In addition to the E-R-W method No. 1, the second method is based on the response of a single mechanical oscillator to a random force applied to the mass:

$$\sigma_{\ddot{w}}^2 = \frac{\pi \cdot f_n Q \cdot S_f(f_n)}{2M^2}$$

where $\sigma_{\ddot{w}}$ is the r.m.s. acceleration response; f_n, Q and M are resonant frequency, amplification factor and mass of the structure of interest, respectively, and $S_F(f_n)$ is the force spectral density of the random force at a frequency corresponding to the natural frequency of the oscillator. The equation to obtain $\sigma_{\ddot{w}}$, provides a reasonable approximation when the random force has a band-limited flat spectrum and the oscillator has a Q greater than or equal to 20. In order to apply this equation to a multi-modal structure, which is typical of space vehicles, E-R-W suggested that the right-hand side of the equation be multiplied by a multi-modal response factor, β. To determine the value that should be used for this factor, E-R-W examined vibration and acoustic data obtained from several vehicles.

Figure 11.14.1 shows β as a function of the normalised wave number ($\pi f \cdot D/C$), where D is the vehicle diameter and C the speed of sound in air (C = 340 m.s^{-1}).

ASSUMPTIONS

- All flight vehicles to which the procedure is to be applied have dynamic characteristics similar to conventional ballistic missiles.
- Vibration is due principally to acoustic noise during lift-off.
- Vibration is proportional to the total integrated pressure over the surface of the structure of interest, divided by the structural weight.
- The normal modes of the vehicles are uncoupled.

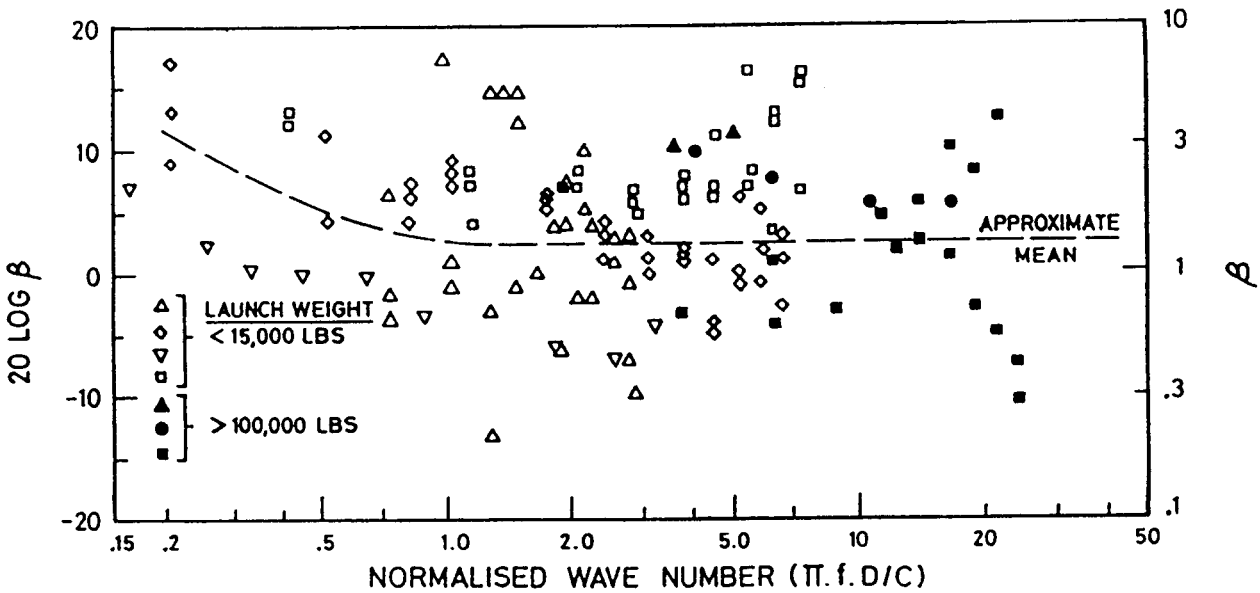

Figure 11.14.1 - Variation of the Parameter β with Wavenumber

INFORMATION REQUIRED

- Measurements or predictions of the acoustic noise environment.
- Estimates for the mass of each structure of interest.
- Estimates for the damping ratio of structural modes of vibration. (The authors suggest using an assumed $Q \cong 15$.)
- Estimates for the natural frequency of the structural modes of vibration.

ADVANTAGES

- The procedure is relatively simple.
- Only rudimentary structural details are required.

LIMITATIONS

- The procedure is based upon ballistic missile data only. The application of the procedure to other types of flight vehicles is questionable.
- No excitation factors other than acoustic noise are considered.
- The procedure provides no suggestions for estimating the required structural natural frequencies.

11.15 CURTIS METHOD

Curtis observed that the vibration (caused by flow-induced aerodynamic noise) measured on aircraft during high-speed flight was related to aerodynamic pressure, q. The method developed was based on the assumption that the random vibration environment for aircraft can be described by a broad-band vibration background plus several superimposed narrowband vibration spikes representing resonant structural response modes.

The data were obtained during flight at dynamic pressures in a range from 90 to 1760 psf (1 psf = 47.88 Nm^{-2}). It was concluded from this data that, for equipment mounted **inside** a typical aircraft, the broad-band and peak vibration background can be described by a power spectral density in g^2/Hz of:

$$\left.\begin{aligned} S_b(f) &= 0.006(q/2130)^2 \\ S_s(f) &= 0.11(q/2130)^2 \end{aligned}\right\} \quad 10 \le f \le 2650\ \text{Hz}$$

$$\left.\begin{aligned} S_b(f) &= 0.011(q/2130)^2 \\ S_s(f) &= 0.13(q/2130)^2 \end{aligned}\right\} \quad 20 \le f \le 150\ \text{Hz}$$

$$\left.\begin{aligned} S_b(f) &= 0.02(q/2130)^2 \\ S_s(f) &= 0.23(q/2130)^2 \end{aligned}\right\} \quad 150 \le f \le 2000\ \text{Hz}$$

where: q = the free stream dynamic pressure in psf,

$S_b(f)$ = the broad-band power spectral density, and

$S_s(f)$ = the peak power spectral density.

ASSUMPTIONS

- All flight vehicles to which the procedure will be applied are dynamically similar to the four aircraft used in developing the procedure (F-84, B-59, F-101 and F-106).
- Vibration is due principally to aerodynamic boundary-layer turbulence during flight at high dynamic pressures.
- The vibration environment can be described by a broad-band vibration background with almost constant spectral density plus one or more superimposed narrow-band vibration spikes.
- For equivalent flight conditions, differences in the vibration environment between different aircraft or different specific locations in the same aircraft can be accounted for by variations in the centre frequencies of the narrow-band vibration spikes.
- The vibration to be predicted is that of internal or external exposed equipment.
- Spatial variations in the vibration can be considered a random variable.
- Vibration is the same in all three orthogonal directions.

INFORMATION REQUIRED

- Estimate of maximum dynamic pressure.
- Estimate of first few natural frequencies of structure in question (desired but not necessary).

ADVANTAGES

- The procedure is simple and easy to apply.
- No structural details are required, although estimates of the first few natural frequencies are desirable.
- The resulting predictions can be implemented as vibration tests on testing equipment with limited capacity.

LIMITATIONS

- The procedure is based upon aircraft data only. The application of the procedure to spacecraft data is questionable.
- No excitation other than boundary layer turbulence is considered.
- No distinction is made between different equipment mountings and different orthogonal directions.
- The procedure is unconservative for unloaded structural vibration predictions.

11.16 FRANKEN METHOD

The Franken method was designed to permit the prediction of acoustically induced skin vibration levels for cylindrical structures on the basis of external sound-pressure levels, vehicle diameter and average surface weight density of the vehicle skin. Vibration measurements were made in radial direction only. For each band, the r.m.s. vibration was multiplied by the average weight per unit of area of the structure, 'W' and then divided by the sound-pressure level in decibels. The generalised frequency response function is presented in Figure 11.16.1.

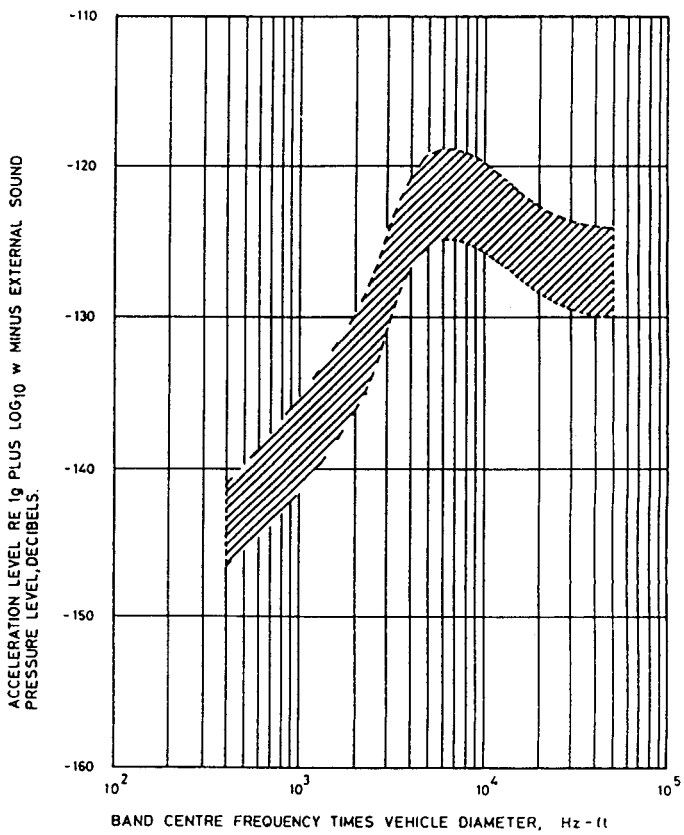

Figure 11.16.1 - Frequency Response Function for Franken Method

The specific procedure for employing Figure 11.16.1 is as follows:

(1) Divide the abscissa by the average vehicle diameter, measured in feet. This converts the abscissa to a frequency scale in Hz.

(2) Add the quantity 'external sound-pressure level (dB) minus $20LogW$' to the ordinate. 'W' is the average surface weight density of the vehicle skin, measured in psf. This converts the ordinate to a vibration level in dB with respect to 1 g r.m.s.

ASSUMPTIONS

- All flight vehicles to which the procedure is to be applied have dynamic characteristics similar to those of the Jupiter and Titan-I vehicles.
- Vibration is due principally to acoustic noise during lift-off or other pressure fields during flight which can be estimated.
- Vibration magnitude is directly proportional to the pressure level of the excitation and inversely proportional to the surface weight density of the structure,
- Predominant vibration frequencies are inversely proportional to the diameter of the vehicle.

INFORMATION REQUIRED

- Predictions of the acoustic noise environment.
- Average surface weight density of the structure.
- Diameter of vehicle.

ADVANTAGES

- The procedure is simple and easy to use.
- Only rudimentary structural details are required.

LIMITATIONS

- The procedure predicts only radial skin vibration levels.
- The procedure is based upon a limited amount of space vehicle data only. Its application to other types of flight vehicles is questionable.
- No excitation forces other than acoustic noise are considered, although the procedure can be applied to flight predictions if appropriate pressure-field estimates are available.

11.17 WINTER METHOD NO. 1

Winter, who assisted in the development of the Franken method, has modified the method after adding Minute Man, Skybolt and Genu data to previously used Jupiter and Titan-I data.

The vibration measurements from these vehicles were individually identified with a 1/3 octave band acoustic pressure spectrum acting on the structure, and an average surface weight density for the structure.

The resulting frequency response function based on 1/3 octave band data and normalised to a vehicle diameter of 10 feet, is shown in Figure 11.17.1. The assumptions, required information, advantages and limitations are the same as those for the Franken method discussed in Topic 11.16.

For Winter method No. 2, see Topic 11.21.

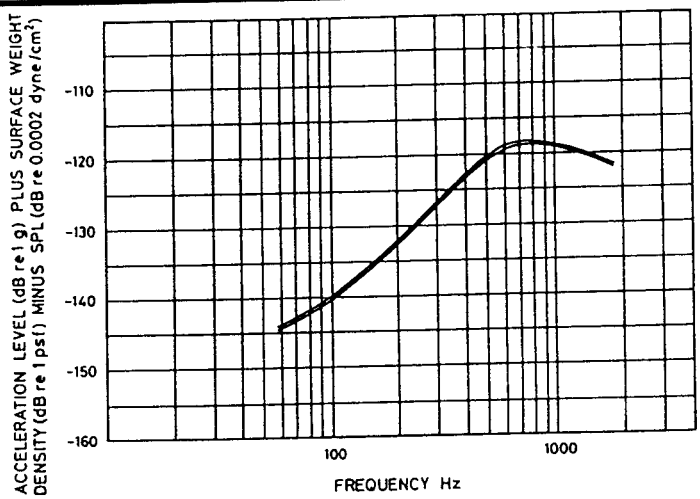

Figure 11.17.1 - Basic Frequency Response for Winter Method

11.18 SPECIFIC EXTRAPOLATION APPROACH

The specific extrapolation approach includes procedures which predict vibration environments in future vehicles by scaling measured data from a similar previous vehicle. The specific extrapolation method is more flexible in that vibration levels may be predicted for any desired type of structure, provided information is available for the 'data vehicle'.

Furthermore, predictions may be obtained for any desired flight condition by extrapolating the measurements from the data vehicle for that flight condition. Those methods described are:

- Condos and Butler, [See: Topic 11.19].
- Barret, [See: Topic 11.20].
- Winter (Method No. 2), [See: Topic 11.21].

11.19 CONDOS AND BUTLER METHOD

Condos and Butler (C-B) were the first to utilise data obtained on the Titan-I missile in conjunction with the following equation in order to predict vibration on Titan-II:

$$\frac{S_{\ddot{w},n}(f)}{S_{\ddot{w},r}(f)} = \frac{S_{p,n}(f)}{S_{p,r}(f)}\left(\frac{\langle \rho h \rangle_r}{\langle \rho h \rangle_n}\right)^2$$

where $S_p(f)$ is the pressure spectral density of the acoustic noise average over the applicable section of the vehicle; $\langle \rho h \rangle$, the average structural mass per unit of exposed area; and n and r are subscripts denoting new and reference vehicles respectively. $S_{\ddot{w}}$ is the power spectral density for the acceleration response.

ASSUMPTIONS

- The data vehicle and the new vehicle of interest have similar missions and structural design.
- Vibration magnitude is directly proportional to the pressure level of the excitation and inversely proportional to the surface weight density of the structure.

INFORMATION REQUIRED

- Vibration measurements for the data vehicle.
- Measurements or predictions for the acoustic noise for the data vehicle.
- Predictions for the corresponding pressure environment of the new vehicle.
- Average surface weight densities for the structure of the new and data vehicles.

ADVANTAGES

- The procedure is relatively easy to use.
- Only rudimentary structural details are required.
- The procedure yields reasonably accurate results if the new and data vehicles are quite similar.
- The procedure is flexible and can be applied to any types of structure in any flight vehicle for any flight condition, as long as appropriate measurements are available from the data vehicle.

LIMITATIONS

- Extensive measurements from experiments on a previous similar vehicle are required.
- The accuracy of the prediction is heavily dependent upon the quantity and quality of the measurements from the data vehicle, and upon the similarity of the data vehicle to the new vehicle.

11.20 BARRET METHOD

The Barret method was originally proposed for applications to rocket-powered space vehicles. It is similar to the C-B method discussed in Topic 11.19, except that this method includes suggestions for predicting the structural vibration induced by direct mechanical transmission from rocket motor vibration.

The method initially assumes that the structure of the vehicle of interest can be divided into two distinct categories as follows:

- Structure susceptible to acoustic and aerodynamic pressure fluctuations.
- Structure not susceptible to acoustic and aerodynamic pressure fluctuations.

The first category would include skin panels, skin stiffeners, and bulkheads. The second category would include structural beams and components mounted on rocket engines. For the first category, the extrapolation rule suggested is:

$$S_n(f) = S_d(f) \cdot \left(\frac{\langle \rho h \rangle_d}{\langle \rho h \rangle_n} \right)^2 \frac{Sp_n(f)}{Sp_d(f)} \cdot F$$

where the subscript n denotes new and d denotes the data vehicle; $S(f)$ is the power spectral density for the acceleration response; $S_p(f)$ is the excitation; ρ is the mass density and h is the average thickness of structure. F is the attenuation factor to account for component loading:

$$F = \frac{W_n}{W_n + W_c}$$

where W_n is the weight of structure in an area where a component is to be mounted and W_c the weight of the component.

For the second category, the extrapolation rule suggested is the following:

$$S_n(f) = S_d(f) \frac{(NVT)_n}{(NVT)_d} \cdot \frac{W_d}{W_n} F$$

where N is number of rocket motors, V the exhaust gas velocity of each rocket motor and T the thrust of each rocket motor.

ASSUMPTIONS

- The data vehicle and the new vehicle of interest have similar missions and structural designs.
- The vehicle structure can be divided into structure that is and structure that is not susceptible to acoustic and aerodynamic pressure fluctuations.
- For structures susceptible to acoustic and aerodynamic pressure fluctuations, vibration is directly proportional to the pressure level, and inversely proportional to the surface weight density of the structure.
- For other structures, vibration is directly proportional to the number of rocket motors and exhaust gas velocity and thrust of each motor, and inversely proportional to overall structural weight.
- Spatial variations in the vibration can be considered a random variable.

INFORMATION REQUIRED

- Vibration measurements for the data vehicle.
- Measurements or predictions for acoustic noise, aerodynamic turbulence, rocket motor exhaust gas velocity and thrust for the data vehicle.
- Predictions for the corresponding pressure environments and rocket motor performance for the new vehicle.
- Average surface weight density or overall weight for the structures of the data and new vehicles.

ADVANTAGES

- The procedure is relatively easy to use.
- Only rudimentary structural information is required.
- The procedure yields reasonably accurate results if the data and new vehicles are quite similar.
- The procedure includes suggestions for predicting beam and truss vibration, and for predicting vibration with and without component loading.
- The procedure is flexible. At least part of the procedure can be applied to any type of structure in any flight vehicle for any flight condition, as long as appropriate measurements are available from the data vehicle.

LIMITATIONS

- Extensive vibration measurements from experiments on a previous similar vehicle are required.
- The accuracy of the predictions is heavily dependent upon the quantity and quality of the measurements from the data vehicle, and upon the similarity of the data vehicle to the new vehicle.

11.21 WINTER METHOD NO. 2

Winter method No. 2 is the same as Winter method No. 1, except for the generalised frequency response function used for predictions developed in each case by evaluating data measured on a particular vehicle which is similar in mission and structural design to the new vehicle of interest. The assumptions, information required, advantages and limitations are the same as those for method No. 1, see Topic 11.17.

11.22 SCALING OF ATTACHED EQUIPMENT RESPONSE (RANDOM VIBRATION)

The relationship between unit testing level and equipment mass given in specification ESA PSS-02-301, Ref. [26] provides a means of scaling response of equipment of different mass when the panel to which it is mounted is subject to a constant level of acoustic excitation. This level is the qualification level for the purposes of Ref. [26], but it could be a different level although there is some uncertainty that the scaling will be as appropriate due to the possibility of non-linearity between the qualification level and lower levels.

As the equipment mass increases, its response (at its mounting feet) reduces, over a maximum range of 20:1. The power spectral density (g^2/Hz) ratio between equipment 1 and 2 is:

$$\frac{PSD_1}{PSD_2} = \left(\frac{M_1 + 20}{M_1 + 1} \right) \Big/ \left(\frac{M_2 + 20}{M_2 + 1} \right)$$

11.23 RECOMMENDED EXTRAPOLATION PROCEDURE

Although any of the extrapolation procedures summarised in Topics 11.09 to 11.22, inc. could be used in principle, the lack of appropriate reference vehicle data tends to limit the choice when a good degree of accuracy is required. The various procedures have been examined and until more suitable reference data is available it is recommended that the approach of Condos and Butler (Topic 11.19) be used.

11.24 NOTES ON THE USE OF THE CONDOS-BUTLER METHOD

- As stated in Topic 11.19 , $S_{\ddot{w}}$ is the power spectral density for the acceleration response. If so required, the relationship may be rewritten so that the new and reference response levels are expressed in linear, as opposed to squared, terms (i.e. in band level g or linear spectral density $g.\text{Hz}^{-1/2}$). The relationship is then:

$$\langle a_g \rangle_n (f) = \langle a_g \rangle_r (f) \cdot \left(\frac{S_{p,n}(f)}{S_{p,r}(f)} \right)^{\frac{1}{2}} \frac{\langle \rho h \rangle_r}{\langle \rho h \rangle_n}$$

- The sound-pressure levels should be for similar sound sources, e.g. rocket noise or aerodynamic boundary layer noise. Predictions from one source type to another will introduce further inaccuracies.
- The $\langle \rho h \rangle$ terms are best expressed as an average mass per unit area for the structure. Allowances can then be made for the mass of stiffeners, frames, inserts, etc., in the structural area of interest. However, problems can arise when heavy structural items are present on one structure only, as the mass/unit area for the 'correct' prediction may lie between the extremes of including/excluding all the mass of that item; [See: Topic 11.25].

11.25 CHECKING THE CONDOS-BUTLER PROCEDURE

The extrapolation procedure was checked against information available from development tests. The comparison presented here is taken from Ref. [22] (which includes dimensions and materials properties for both test vehicles). The configurations used in the extrapolation are shown in Table 11.25.1.

'Reference' Data Vehicle based on a configuration of the EX-1 test model, [See: Figure 11.25.1].	'New' Vehicle based on a configuration of the MAROTS service module, [See: Figure 11.25.2].
Data available: Stiffened cylinder response Mid H/C platform response	**Data required:** Corrugated cylinder response Corrugated cone response Honeycomb mid-platform response Honeycomb side-panel response

Table 11.25.1 - Checking Condos-Butler Procedure: Configurations

'Reference' Data Vehicle - EX-1 (C9 1979)

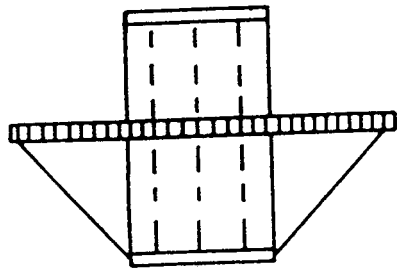

Figure 11.25.1 - EX1 Test Module

'New' Vehicle - MAROTS (C11-SM 1980)

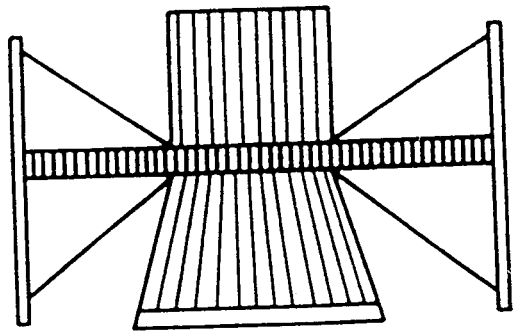

Figure 11.25.2 - Marots Service Module

The vehicles were subjected to a similar excitation field, so the extrapolation was only based on the mass per unit area ratio. The assumptions made for evaluating this ratio are given in Table 11.25.2. The prediction for the honeycomb platform to the new platform and from this platform to the side panels was acceptable for practical use; see Figures 11.25.3 and 11.25.4. The predictions for a corrugated cylinder and cone, based on data from a stiffened cylinder, were not so good; see Figures 11.25.5 and 11.25.6. It is expected that extrapolation using a corrugated cylindrical reference structure would yield a better comparison.

New Prediction	Reference Data	Mass per unit case, M	
MAROTS Component	EX1 Component	Mass Used	Area Used
Corrugated Cylinder		Corrugated shell + lightweight circular frames	Expanded area of corrugated shell
	Plain, stiffened cylinder	Shell + stiffeners (no frame)	Cylinder area
Corrugated Cone		Corrugated shell + lightweight frames + heavy machined ring*	Expanded area of corrugated shell
	Plain, stiffened cylinder (as above)	Shell + stiffeners (no frame)	Cylinder area
Honeycomb Platform		Mass including inserts (many)	Plan area
	Honeycomb platform	Mass including inserts (few)	Plan area
Honeycomb Panel		Mass including inserts (many)	Plan area
	Honeycomb platform (as above)	Mass including inserts (few)	Plan area

Note: * The heavy machined ring attached to MAROTS cone was included. The mass of the cone structure without ring would give a large overestimate of response.

Table 11.25.2 - Evaluation of the Mass per Unit Area Ratio

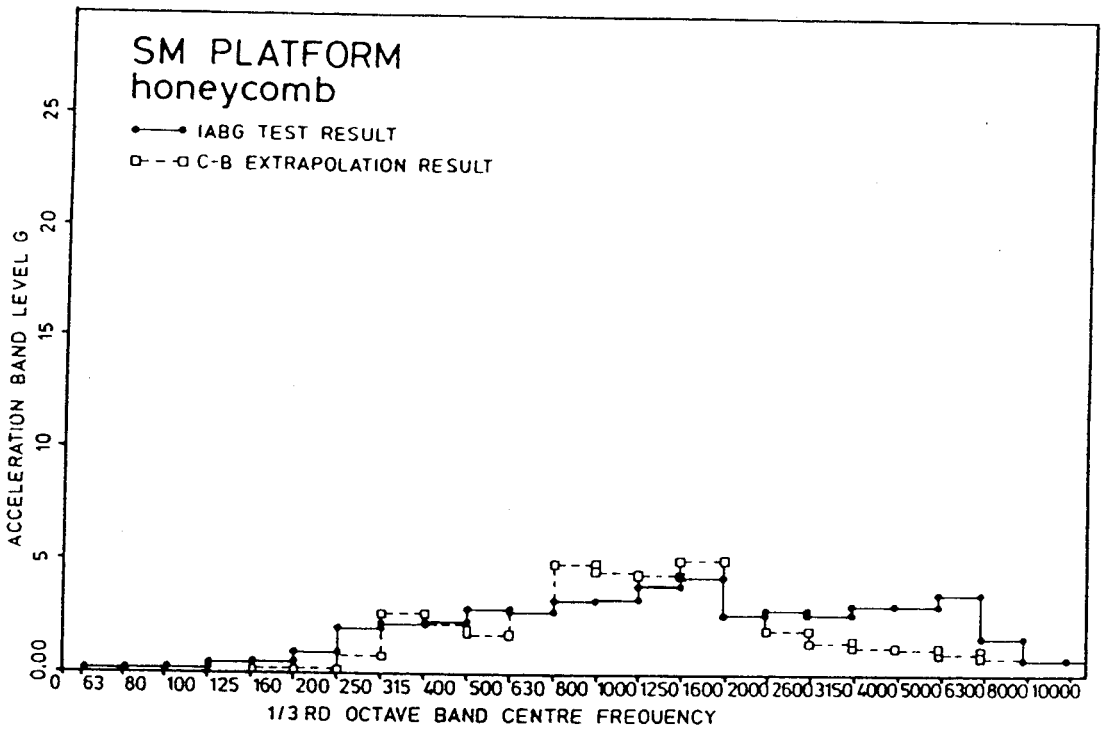

Figure 11.25.3 - Extrapolation & Test Acceleration Response Levels for Configuration 11 Marots SM Platform

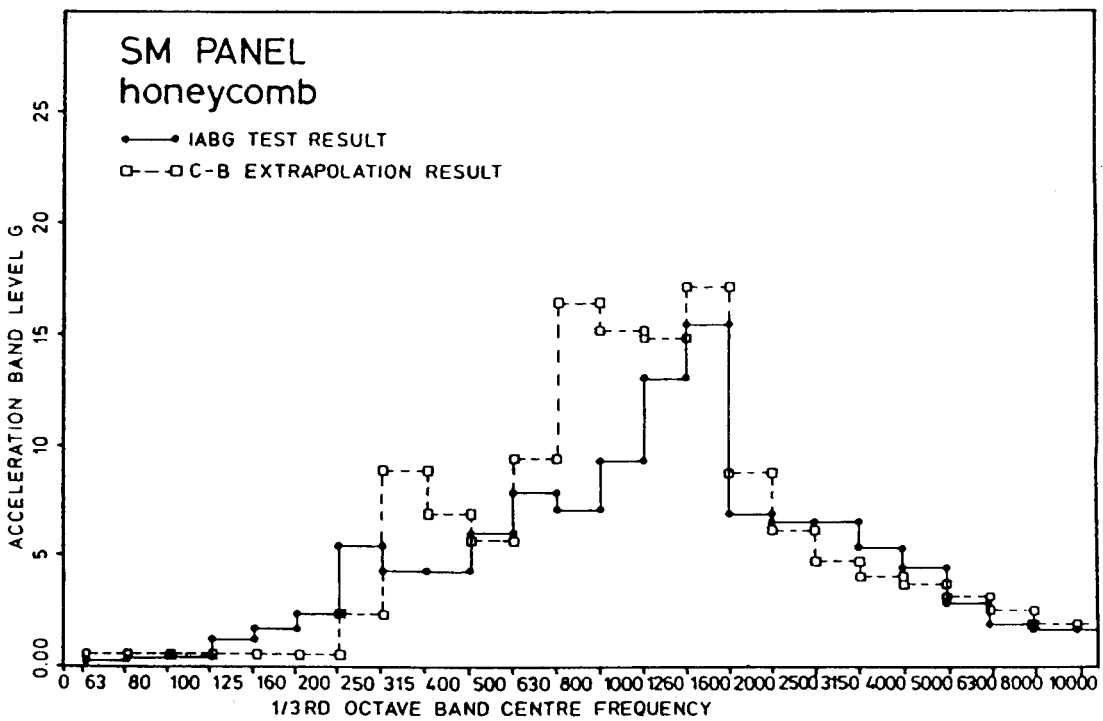

Figure 11.25.4 - Extrapolation & Test Acceleration Response Levels for Configuration 11 Marots SM Panel

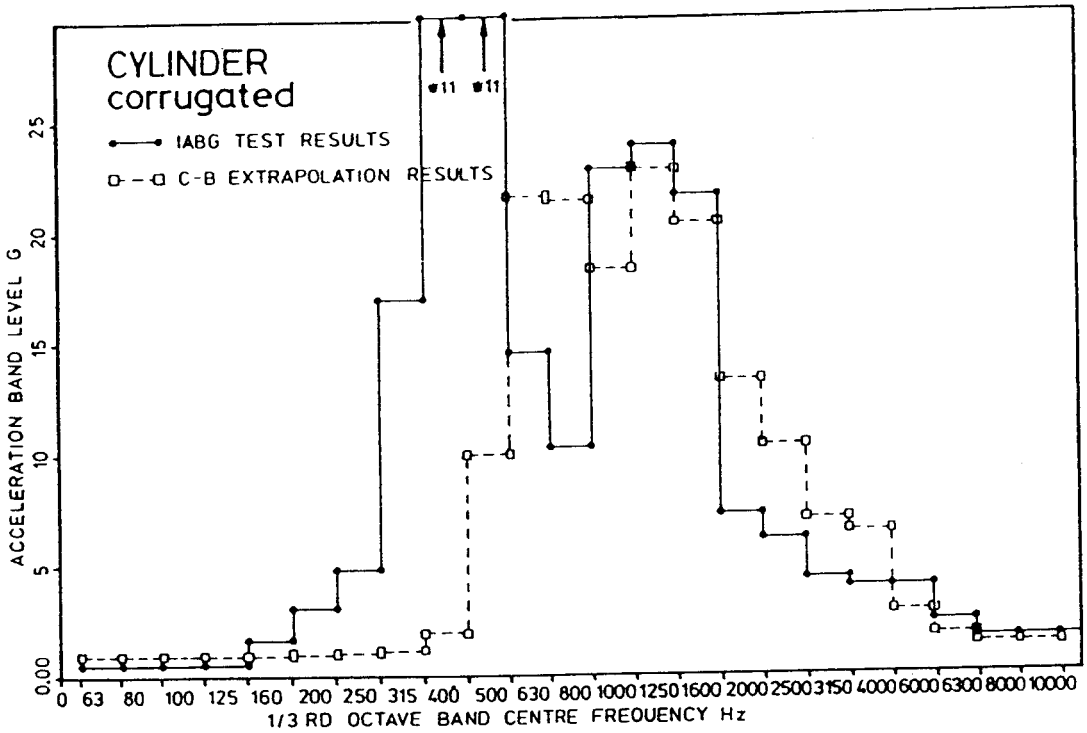

Figure 11.25.5 - Extrapolation & Test Acceleration Response Levels for Configuration 11 Marots SM Cylinder (*11 (400Hz)=31.1, *11 (500Hz)=30.5)

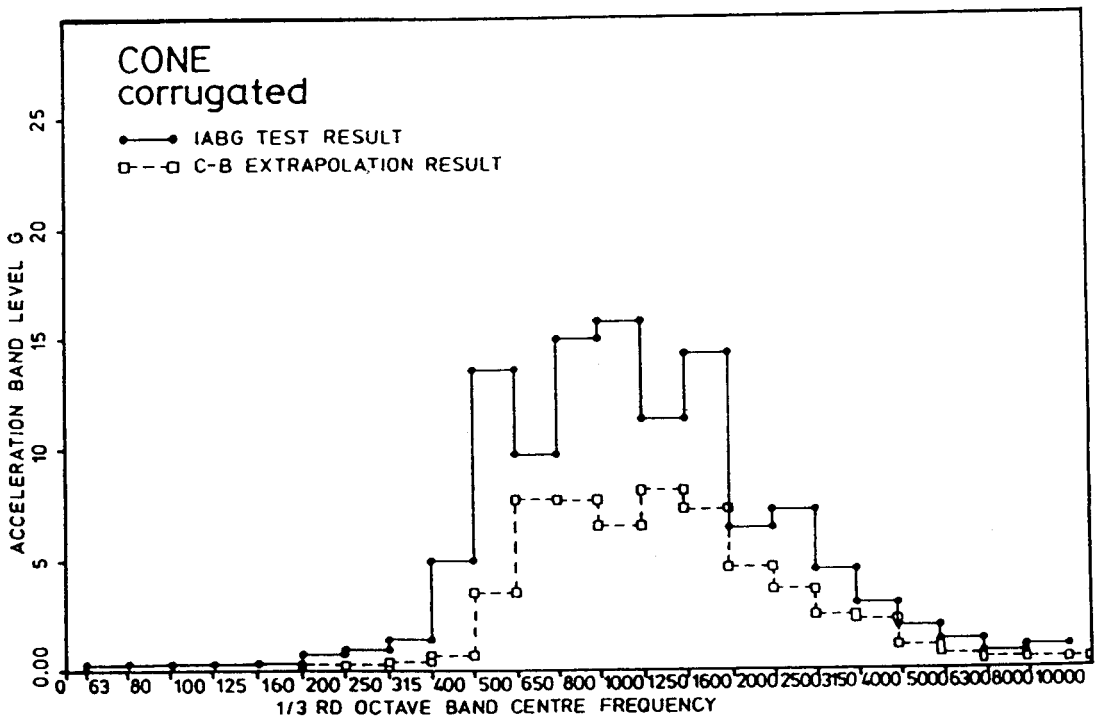

Figure 11.25.6 - Extrapolation & Test Acceleration Response Levels for Configuration 11 Marots SM Cone

11.26 SCALING PROCEDURES INCORPORATING SEA PARAMETERS

Two methods are reviewed which contain one or more SEA parameters in the scaling relation:

- On and Hendricks, [See: Topic 11.27]
- Scaling based on SEA power balance, [See: Topic 11.28].

In terms of the data used for scaling they would be closer to the specific extrapolation procedures, requiring relatively accurate prediction of the SEA parameters obtained from selected similar vehicles or construction.

11.27 ON & HENDRICKS METHOD

Ref. [23] describes a database management and prediction system called VAPEPS (Vibroacoustic Payload Environment Prediction System). The prediction procedure that has been incorporated in VAPEPS is designed to establish the random vibration and acoustic environments of new payload components using data obtained from similar designs that have been previously flown or ground tested. At high frequencies a SEA prediction is normally used (similar to GENSTEP3, but more limited); at low frequencies the following scaling procedure is adopted:

$$S_{NEW}(f) = S_{REF}(f) \times C_m \times C_{me} \times C_d \times C_e(f)$$

where:

$S_{NEW}(f)$ = Response spectrum of new structure,

$S_{REF}(f)$ = Response spectrum of reference structure,

$$C_m = \text{Surface mass density correction} = \left(\frac{\rho t_{REF}}{\rho t_{NEW}}\right)^2,$$

$$C_{me} = \text{Mass loading correction} = \left(\frac{\rho hA}{\rho hA + M_E}\right)_{NEW} \times \left(\frac{\rho hA + M_E}{\rho hA}\right)_{REF},$$

M_E = Nonstructural mass,

$$C_d = \text{Damping correction} = \left(\frac{\eta_{REF}}{\eta_{NEW}}\right),$$

$$C_e(f) = \text{Excitation correction} = \frac{[EXCITATION(f)]_{NEW}}{[EXCITATION(f)]_{OLD}}.$$

The frequencies are also corrected:

$$f_{NEW} = \left(\frac{AP_{REF}}{AP_{NEW}}\right)^{\frac{1}{2}} \times f_{REF}$$

where:

AP is the total surface area.

The corrected data are reorganised into standard 1/3 - octave bands based on the new frequency values. The VAPEPS database, from which reference vehicle data are taken, is based on 1/3 octave bandwidth data.

The symbols used above have been extracted from Ref. [24]. There may be a difference in the symbols used for thickness depending on the structure; t represents skin thickness used to calculate mass and h represents the equivalent thickness based on flexural stiffness. No derivation is given in Ref. [24].

It is assumed that the excitation correction is based on the power spectral density of the excitation sound-pressure level.

ASSUMPTIONS

- Vibration magnitude in terms of PSD is directly proportional to acoustic excitation level and inversely proportional to the surface weight density of the structure.
- Reference vehicle data are available for similar mission and structural design.

INFORMATION REQUIRED

- Vibration measurements for the reference vehicle.
- Acoustic excitation levels for the reference and new vehicles.
- Structural loss factors for the reference and new vehicles.
- Average surface weight density of reference and new vehicles.

ADVANTAGES

- Procedure is easy to use especially in its designed form with an information database (VAPEPS).
- Procedure can be applied to most structures, vehicle types and mission conditions, provided that appropriate reference measurements are available.

LIMITATIONS

- Depends on the availability of reference data for a similar vehicle or structure.
- Structural loss factors required for both reference and new vehicles.
- When incorporated in the original system (VAPEPS), all data and predictions are based on 1/3 - octave bandwidth analyses.

11.28 SCALING BASED ON SEA POWER BALANCE

Using the standard formulae for SEA as given in Appendix A, Topic A.29, Ref. [25] derives a scaling relationship based on a structural subsystem and acoustic excitation field. If it is assumed that the power radiated by the structure is small compared with the other power terms and that the new and reference excitation fields have the same (c/ρ) value, the scaling relation expressed in terms of $g.\text{Hz}^{-1/2}$ and referred to here as linear spectral density is as follows:

$$\langle acc\rangle_{NEW} = \langle acc\rangle_{REF}\left(\frac{S_p(f)_{NEW}}{S_p(f)_{REF}}\right)^{\frac{1}{2}} \cdot \frac{(\rho t)_{REF}}{(\rho t)_{NEW}} \times$$

$$\left[\frac{\Delta f \cdot f_{REF}}{\Delta f \cdot f_{NEW}} \cdot \frac{n_{NEW}}{n_{REF}} \cdot \frac{\eta_{REF}}{\eta_{NEW}} \cdot \frac{R_{RAD\,NEW}}{R_{RAD\,REF}} \cdot \frac{A^2_{REF}}{A^2_{NEW}}\right]^{\frac{1}{2}}$$

where:

<acc> = the acceleration level, linear spectral density ($g.\text{Hz}^{-1/2}$),

$Sp(f)$ = sound-pressure level, power spectral density ($\text{Pa}^2.\text{Hz}^{-1}$),

(ρt) = average structural mass per unit of exposed area,

A = exposed area,

f = frequency (centre frequency of bandwidth, Hz),

Δf = bandwidth (Hz),

n = modal density,

η = structural loss factor,

R_{RAD} = radiation resistance of structure.

It can be seen that the first part of the above equation relates to the Condos and Butler method; the extrapolation procedure recommended for general use in Topic 11.19, and the part contained in the square brackets includes the SEA parameters.

These latter terms require to be evaluated or, alternatively, scaled by their main dimensions. Both modal density (n) and radiation resistance (R_{RAD}) can vary with frequency, although modal density may also be independent of frequency depending on the type of structure (e.g. modal density for a flat plate has no frequency term). Both types of expression may also vary in different frequency regimes separated or marked, as in the case of cylinders, by the ring and coincidence frequencies. Expressions currently available for radiation resistance are based on the flat plate and cylinder results which are adapted for use on other configurations. It may be possible to scale modal density and radiation resistance on the basis of area (A), thickness (t) and density (ρ) for simpler structures, although the radiation relationships are complicated.

The structural loss factors (η) are usually evaluated experimentally and although some variation with frequency is found they can, in some cases, be approximated as constant with frequency. The analysis bandwidth (Δf) can be taken as the same for NEW and REF predictions with the use of constant bandwidth analysis. However, if there is a frequency shift due to scaling, causing the band centre frequency (f) to change, then the use of a constant percentage bandwidth analysis will probably require a frequency correction. The area (A), which appears as a separate term, will also be included in the modal density and radiation resistance terms.

ASSUMPTIONS

- Power flow from SEA subsystems to acoustic field ignored in system power balance.
- Similar ambient field conditions between reference and new excitations (i.e. c/ρ is similar).

INFORMATION REQUIRED

- Vibration measurements for reference vehicle.
- Acoustic pressure levels for reference and new vehicles.
- Average surface weight density for reference and new vehicles.
- Modal density, structural loss factor and radiation resistance of reference and new vehicles.

ADVANTAGES

- Could be used for prediction in a limited frequency range (probably low frequency), with assumptions incorporated in the SEA terms applicable to a particular structure type.
- The Condos and Butler expression would be used if SEA parameter data were not available.

LIMITATIONS

- Requires values for SEA parameters and therefore may not be more convenient to use than the GENSTEP3 program.
- With the SEA parameters dimensionally scaled, the resulting expression will only be applicable to the appropriate type of structure.

11.29 REFERENCES

[1] R.S. Langley
'A Dynamic Stiffness Technique for the Vibrational Analysis of Stiffened Shell Structures'
J. Sound Vib., 1992, 156(3), 521-540

[2] R.G. White & J.G. Walker (Eds)
'Noise and Vibration', Chapter 15 (M. Petyt)
Ellis Horwood Ltd, 1982, ISBN 0-85312-502-3

[3] A.G.R. Thompson & R.F. Lambert
'The Estimation of r.m.s. stresses in stiffened skin panels subjected to random acoustic loading'
Advisory Group for Aerospace Research and Development
NATO-AGARD-AG-162, Nov. 1972, Section 5

[4] R.D. Blevins
'An Approximate Method for Sonic Fatigue Analysis of Plates and Shells'
J. Sound Vib. (1989), 129(1), 51-71

[5] Blevins on TK Software
ESDU International Ltd, London W1R 7AD

[6] D.J. Bozich & R.W. White
'A Study of the Vibration Responses of Shells and Plates to Fluctuating Pressure Environments'
NASA Contractor Report CR-1515, March 1970

[7] R.W. White
'Acoustic and Blast Loads on Buildings'
Report WR 66-2

[8] D.C.G. Eaton
'Some Considerations of Current and Future Launcher Acoustic Environments: Implications in Terms of Design and Test Requirements'
Proc. of Int.. Symposium on Environmental Testing for Space Programmes, Test Facilities and Methods
ESTEC Noordwijk, Netherlands, 26-29 June 1990
(ESA SP-304, Sept. 1990), pp. 279-286

[9] N.W.M. Bishop & F. Sherratt
'Fatigue Life Prediction from power spectral data'
Environmental Engineering 1989
Part 1: Traditional Approaches, (March), pp. 11-14 & 29
Part 2: Recent Developments, (June), pp. 11-15 & 19

[10] R.W. White
'Theoretical Study of Acoustic Simulation of In-Flight Environments'
Sound & Vib. Bulletin, No. 37, Pt. 5, 1968, pp. 55-75

[11] Mathematica (Proprietary Software)
Macsyma Inc., Massachusetts, USA

[12] M.J. Crocker & R.W. White
'Some Integration Formulae which Simplify the Evaluation of Certain Integrals in Common Use by Engineers'
Wyle Laboratories, Report WR 66-24, 1966

[13] R.D. Blevins
'Formulas for natural frequencies and mode shape'
Van Nostrand Reinhold, ISBN 0-442-20710-7, New York

[14] R.W. White
'Predicted Variation Responses of Apollo Structure and Effects of Pressure Correlation Lengths on Response'
Wyle Laboratories, Report WR 67-4, March 1968 Revision

[15] R.J. Cummins
'Sound transmission into closed cylinder'
MSc Dissertation, University of Southampton (1970)

[16] F.J. Fahy
Sound and Structural Vibration, Ch. 6
Academic Press, London, 1985. ISBN 0-12-247670-0

[17] B.L. Clarkson, R.J. Pope & M.F. Ranky
'Experimental work to evaluate parameters required in the SEA prediction method'
ESA Contract No. 4100/79/NL/PP Rider 1 (1981)

[18] Sysnoise (proprietary software)
Numerical Integration Technologies NV
B-3001, Leuven, Belgium

[19] R.L. Barnoski et al.
'Summary of random vibration prediction procedures'
NASA CR-1302, April (1969)

[20] J.J. Wijker
'Dynamic responses of structures due to acoustic excitation'
Fokker Report No. RV80-111, October (1980)

[21] P.T. Mahaffey & K.W. Smith
'A method for predicting environmental vibration levels in jet-powered vehicles'
Shock & Vibration Bulletin, 28(4, August), 1 (1960)

[22] R.J. Cummins & I.R. Farrow
'Study of the evolution of structural acoustic design guides'
ESA CR(P)-1609 (1981)

[23] F.J. On & W. Hendricks
'Development of a vibroacoustic database management and prediction system for payloads'
Shock & Vibration Bulletin, 52, Part 2, May (1982)

[24] F.J. On & W. Hendricks
'Development of a vibroacoustic database management and prediction system for payloads'
Shock & Vibration Bulletin, 52, Pt. 2, May (1982)

[25] R.J. Cummins
'Development of structural acoustic design guides'
Final report. ESA CR(P)-1916, (1981)

[26] ESA PSS-02-301: ESA Standard on Environment Requirements Specification for Space Equipment. Unit Level Test Verification

[27] A. Powell
'On the Fatigue Failure of Structures due to Vibration Excited by Random Pressure Fields'
J. Acoustic. Soc. Am., 30, p.1130, 1958

[28] M.P. Norton
'Fundamentals of Noise and Vibration Analysis for Engineers'
Ch. 6.10, Cambridge University Press 1989

(Intentionally Left Blank)

Structural Acoustics Design Manual

Chapter 12
TEST SPECIFICATIONS

CONTENTS

12.01 GENERAL

One objective of this Design Manual is the prediction of test spectra for equipment and satellite vibration and acoustic testing. At present, work is still proceeding towards this aim. It is intended that information on how to derive test specifications will be included at a later date.

Information has recently become available concerning the possible sources of discrepancy during broad-band acoustic tests in reverberation chambers. It is worth considering these points when specifying tests and comparing test data. It is expected that further investigations will be performed on the accuracy and repeatability of this type of testing.

12.02 BROAD-BAND ACOUSTIC TESTS

In Ref. [1], comparisons have been made between measurements from broad-band noise response tests made on the same structural components at two facilities. Further investigations showed variations between tests performed on the same structure at the same facility, but separated by a year or longer. These tests were performed in a reverberation chamber in accordance with standard test practice and with the use of a typical launcher excitation spectral shape. It is hoped that the 'expected variation' between repeated tests can be quantified in future work. It was found that the variations mentioned here were greater than those detected during a single test series when repeatability was examined, [See: Topic 2.06 - 1980 Study Programme].

Consequently, when such measurements are used as a means of assessing the effects of component changes, equipment masses etc., it is important that the comparison be limited where possible to tests within the same series.

ALLOWANCES FOR TEST VARIATIONS

If comparisons have to be based on measurements from different sites or test series, then additional allowances should be made for test variations, some reasons for which are:

- The normal measurement limits for laboratory tests are ±2 dB on sound-pressure band levels and also on overall SPL. The noise field SPL is usually measured in one-third octave bands and spectral variation across a bandwidth is possible for the higher bandwidths. The ± 2 dB limits also apply to the measurement of the response.
- The sirens that produce the noise fields in the reverberation chambers are of different types. Although spectrum shaping is used to tailor the noise fields to within the ±2 dB limits, the excitation efficiency of these noise fields may differ.
- The method of mounting and/or suspending the specimens in the noise field can vary.
- Differences may be caused when structures and equipment packages are broken down and re-assembled between tests.
- The location of measurement transducers for comparable measurements is important. For example, one needs to know how many transducers are required and how the locations should be 'organised' to provide (in SEA terms) the spatial average response.

12.03 REFERENCES

[1] R.J. Cummins
'Development of structural acoustic design guides'
Final report. ESA CR(P)-1916, (1981)

Structural Acoustics Design Manual

Chapter 13
DAMPING OF STRUCTURES

CONTENTS

13.01 INTRODUCTION

It is intended to give here a brief overview of the basic aspects of damping, its specification and its influence on structural response. A number of texts are available which expand on this, e.g. Ref. [1, 2, 3], which were consulted for this Chapter.

Damping, along with mass and stiffness, is a parameter fundamental to the response of a structure in many cases. Specifically, only motions controlled by a balance of energy are affected by damping, whereas vibrational motions which depend on a balance of forces are little influenced by damping. In a single-degree-of-freedom system, the response well below the natural frequency is controlled mostly by the balance between applied force and spring force, whilst well above the natural frequency, response is controlled by the balance between applied force and the system's mass inertia. Only when excited near the resonance frequency, when the spring and inertia effects cancel each other, does the system primarily respond by admitting energy until a balance is reached between the energy input per cycle and the energy dissipated each cycle, the dissipation being due to damping, usually by conversion to heat.

Amplitudes near resonance frequencies, excited by periodic or random excitation, are therefore reduced by increasing dissipation by damping. When subjected to a broadband excitation, the mean square response of a single-degree-of-freedom system is inversely proportional to damping level, so increasing damping will typically reduce the overall r.m.s. level. Other benefits of damping are:

- reduced rate of response build-up near resonances and increased rate of decay of response to transients
- faster decay of freely propagating structural waves, with finite structures showing less reverberant behaviour
- reduced response to excitation by sound fields above the critical frequency.

Whilst increased damping is therefore generally desirable, the other effects of any modifications or added treatment in the form of resulting mass or stiffness changes must also be accounted for, as discussed further below. Before adopting added damping, the possibility of detuning structural filtering effects should be considered, as it may be possible to do this without introducing either extra mass or additional manufacturing. On moving components, the additional mass due to damping treatment may need additional compensating mass to restore balance.

13.02 PARAMETERS

Several measures of damping are available, primarily:

- **Dissipation loss factor (DLF)** η: average energy dissipated per radian/ maximum energy stored in the system during one cycle.
- **Damping capacity** ψ: as η, except per cycle instead of per radian (specific damping capacity designates the value for unit volume of a damping material).
- **Damping ratio (or factor)** ζ: viscous damping coefficient/critical damping coefficient.
- **Logarithmic decrement** δ: $\frac{1}{N} ln \left(\frac{X_i}{X_{i+N}} \right)$, when N is a number of cycles of motion over which the peak level reduces from value X_i to value X_{i+N}, at a natural frequency (usually N is taken as unity).
- **Quality (or magnification) factor,** Q: amplitude at resonance/notional static amplitude,

  where: notional static amplitude = $\frac{\text{Excitation force amplitude}}{\text{Static stiffness}}$
- **Half-power relative bandwidth,** b: $\Delta\omega/\omega_n$, = frequency range where response amplitude is at least:

  $\frac{1}{\sqrt{2}}$ $\frac{\text{of amplitude at resonance frequency}}{\text{resonant (natural) frequency}}$
- **Half-power bandwidth,** $\Delta\omega$: difference between the two frequencies at which the amplitude is $\frac{1}{\sqrt{2}}$ times the maximum amplitude.

These parameters are related directly in the case of viscous damping, which occurs when the motion of a single-degree-of-freedom system can be expressed as:

$$m\frac{d^2q}{dt^2} + c\frac{dq}{dt} + kq = P_0 e^{i\omega t}$$

in which: m = mass,

c = viscous damping coefficient (constant),

k = stiffness,

q = displacement,

t = time,

P_o = amplitude of applied forcing level,

ω = frequency.

For small values of c, the resulting motion when P_o is suddenly reduced to zero is a decaying sine wave of frequency $\omega_n = \sqrt{\frac{k}{m}}$ with the decay rate increasing with c, until there is no remaining evidence of ω_n in the decay time history, which becomes simply an exponential function. The value of c in this case is the critical damping coefficient c_{crit}. The notional static displacement is given by P_o/k.

The relationship between the damping parameters for viscous damping is:

$$\eta = \frac{\psi}{2\pi} = 2\zeta = \frac{\delta}{\pi} = \frac{1}{Q} = b$$

The relationship $\eta = 2\zeta$ is strictly valid for harmonic excitation only.

For SEA applications, two types of loss factor are relevant. Dissipation loss factor (DLF) is the value of loss factor for a whole subsystem, which may include structural joints and supported items. Coupling loss factor (CLF) is the proportion of a subsystem's vibrational energy which is transferred to adjacent mechanically coupled systems. Only DLF is considered in this section.

The measurement techniques recommended to obtain DLF values are described in Topic 10.03.

13.03 MODELS OF DAMPING: VISCOUS, POWER LAW, HYSTERETIC

Viscous damping is defined above, where the damping coefficient is of constant value. The velocity response of the excited mass is proportional to the applied force and in the opposite direction (anti-phase). The energy dissipated per cycle is proportional to the product of the frequency and the square of the displacement amplitude. Besides being analytically convenient, this model is often adequate for small-amplitude vibrations, especially in fluid.

Alternatively, the damping effect can be represented by other models, retaining the characteristic of a force opposing the system motion which is velocity dependent. In dry-friction (Coulomb) damping, the force magnitude is constant and only the phase changes to maintain opposition to the motion, but in other alternatives such as power law damping the force magnitude changes as a power of velocity (e.g. square-law damping).

A further alternative representation is hysteretic (or viscoelastic) damping which is commonly used for representing structural material losses. A damping force opposes velocity, but the magnitude is proportional to displacement. In this model, the energy dissipated per cycle is often independent of frequency but proportional to the square of the displacement amplitude. This representation can be included readily in complex-notation analysis. Stiffness is represented as a complex term, the real part representing strain energy storage and the imaginary part energy dissipation:

$$K(complex) = K(1 + j\eta)$$

In fact, the loss factor η can be modelled as frequency dependent.

If the amplitude of the motion rather than the spatial detail of the response is of concern, energy based models are suitable and the representation of damping selected should be that which gives the best estimate of energy dissipation in each cycle of response. 'Equivalent viscous damping', which results in the same energy dissipation as actually occurs without representing the system motion especially well, can therefore be used, simple analysis being retained, although strictly this is only correct for harmonic excitation.

13.04 STRUCTURAL DAMPING

The main origins of damping acting on a structure are:

- **structural hysteresis**, mostly from joints within composite elements (e.g. sandwich constructions) or between elements (e.g. panels linked as a built-up structure). Material damping is typically of only secondary order.
- **acoustic radiation damping** into fluid environments, [See: Topic 13.05].
- **attachments**, either as:
  - items supported by the structure (equipment, cabling, protection), [See: Topic 13.06], or
  - as added damping systems, [See: Topics 13.07 and 13.08].

Structural damping values are mostly known in air which can influence damping level due to mechanisms such as squeeze-film gas pumping between contacting surfaces Ref. [4]. This is not relevant to in-space conditions, where friction will remain a contributing mechanism. In-space damping remains an area of uncertainty and still the subject of investigation to determine data.

It has been found that flat aluminium honeycomb structural elements show very low damping, owing to their adhesive bonding, so structures using these elements in air experience most of their damping at joints between elements. Optimisation of damping in composite fibre face-plates is being investigated, but standard composites show very low damping: See: Chapter 9 and Ref. [3].

Ref. [5] provides a means of estimating damping levels in a rectangular multilayered panel vibrating in one of its lower-frequency natural modes, for simply supported or clamped edges.

13.05 ACOUSTIC RADIATION DAMPING

This is treated in SEA by the inclusion of a coupling loss factor between the structural subsystem and the fluid environment, for which expressions are given in Appendix A, Topic A.16 for homogeneous and sandwich panels.

The total damping of a structure of low internal DLF value immersed in a fluid is likely to be dominated by the acoustic radiation component above the coincidence frequency f_c. For example a honeycomb panel with aluminium faceplates 0.28 mm thick and core 29 mm thick has a coincidence frequency f_c of 421 Hz; See: Ref. [6].

13.06 ATTACHMENTS

SUPPORTED EQUIPMENT

Damping values in built-up conditions are poorly known and under investigation. Some indications are given in Topics 9.03 and 9.04.

13.07 ADDED DAMPING-LAYER SYSTEMS

APPLICATION PRINCIPLES

The most widely used added damping is viscoelastic material (VEM) applied as a constrained layer. Comparison with other approaches is shown in Table 13.07.1. The properties and applications of VEM are described in Ref. [2, 3]. Ref. [7] includes data for proprietary materials. The total mechanical properties of mass, stiffness and damping are required to assess the overall effect of added damping treatment. A typical aim would be to increase structural damping from 0.5 percent to 5 percent with the purpose of:

- reducing structural resonant response
- increasing acoustic transmission loss above f_c

	VEM	Viscous	Magnetic	Active Systems
Advantages	Many Different Applications	High Loss	Temperature Invariant	Adaptive in (pseudo) real-time
Disadvantages	Temperature Sensitive, Space Environment Sensitive	Fluid	Low Damping Force	Under Development, Special System for Application
Comments	Low Stiffness, High Loss	Loss Depends on Static Load-Carrying Ability	TMD is Best Application	Suits Large Components
Types of Treatments	Local, Usually Constrained Layer	Discrete, TMD	TMD	Discrete Sensors & Actuators
Temperature Sensitivity	High	Moderate	Low	Low
Thermal Control	Heaters	Heaters	None	None
Loss Factor	High	High	Moderate	High
Frequency Range	Wide	Moderate	Moderate	Potentially Wide
Mass	Low	Moderate	Moderate	Moderate to Low

Table 13.07.1 - Types of Added Damping (TMD = Tuned Mass Damper), After Ref. [12]

In order to transfer high energy into the damping material, shear distortion of the VEM induced when both surfaces of a thin layer are constrained is required rather than the extensional deformation available in a free-layer configuration; [See: Figure 13.07.1]. Constrained-layer damping provides additional damping for much less extra mass than free-layer treatment.

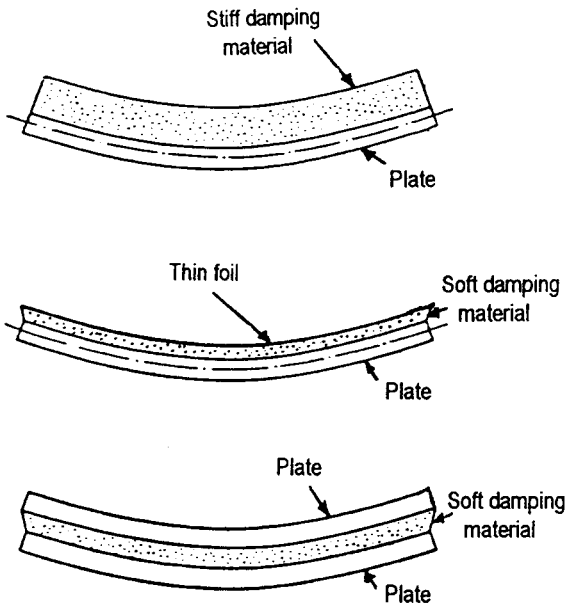

Figure 13.07.1 - Common VEM Configurations

This is usually achieved by using a foil-faced VEM which creates a local 'sandwich' for minimum additional mass. For cost- and mass-effective use, the VEM should be placed in regions of high flexure of the substrate structure, and thus finite-element or modal analysis, to determine the shape of modes dominating the response in the frequency region of concern, is often necessary for successful application. Good design practices are described in Ref. [3].

The objective in design for application of VEM for a particular modal response is to optimise the partition of structural and VEM modal strain energy so that the latter is maximised. Since (modal strain energy x loss factor) = modal damping, the high VEM loss factor will cause the VEM influence to dominate so that modal damping ≈ (VEM modal strain energy) x (VEM loss factor). Hence with an analysis available to give modal strain energy distribution in the structure, the preferred locations for treatment by VEM can be identified.

The highly damped structure will show modified natural frequencies, mainly due to stiffness changes, an effect which will influence the response of attached equipment by retuning the system, irrespective of the change in damping level. This may be of second order of importance if the source is broadband in nature.

VISCOELASTIC MATERIAL (VEM) PROPERTIES

A significant disadvantage of normal VEM for application to spacecraft structure in space is the sensitivity of its performance to temperature, as illustrated in Figure 13.07.2. In particular at low temperature, the VEM completely changes character and becomes a high-modulus, low-loss-factor material. This is the 'glassy' region, and the 'rubbery' temperature region is separated from it at higher temperatures by a transition region. During the critical initial period of launch, however, the change in temperature is not a problem compared with the wide temperature range experienced in space.

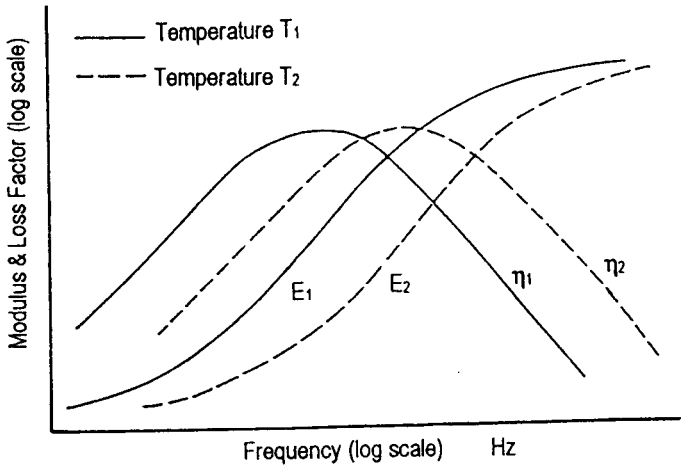

Figure 13.07.2 - Variation of Damping Parameters over an Extended Frequency Range

Best constrained layer performance can occur when the VEM is in its transition region. The material is too stiff in the glassy region, but in the rubbery region the shear modulus may be low enough to cause low damping in spite of high shear deformation.

Since VEM loss factor and complex modulus are both frequency dependent, it is desirable to characterise the VEM material properties, e.g. by complex stiffness tests over frequency and temperature ranges. The dependence of these properties is usually much less with respect to strain amplitude and pre-load than with respect to frequency and temperature. The sensitivity to temperature is typically much greater than the sensitivity to frequency. Values may be either based on measurements of tensile modulus, with the assumptions that shear modulus is very close to 1/3 of the tensile modulus value and that the loss factors for both moduli are about equal, or based on the shear modulus measured directly.

Standards DIN 53 440 and ASTM E756-83 specify a relative test method based on decay rate measurement of sample beams, but no ISO standard for absolute values of damping related parameters exists currently. Although these are simple tests to perform, the values obtained are inherently prone to error and must be regarded as being within a probability range; See: Ref. [7]. Values also vary between batches. When estimating the effect of added damping, this must be taken into account rather than assume nominal mean values.

The conventional method of property data presentation is by means of reduced-temperature nomograms. For a given operating frequency and temperature, the tensile modulus and loss factor can be found. This is illustrated in Figure 13.07.3.

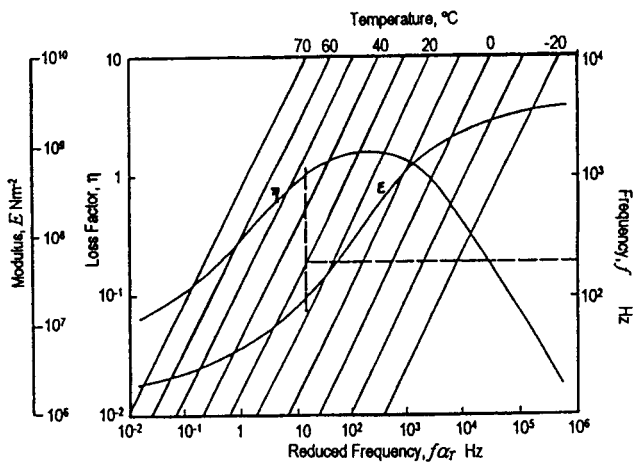

Figure 13.07.3 - Reduced Temperature Nomogram: Gives E and η for given Frequency and Temperature

ANALYSIS OF LAYERED DAMPING TREATMENTS

Structural loss factors and resonance frequency for a given mode of vibration and damping treatment can be estimated by the application of Ref. [8], which can cover multi-layer constrained-layer treatments. Full-area coverage by the treatment is assumed, together with simply supported boundaries but approximations for other edge conditions can be obtained.

For a given constraining layer, there are diminishing returns to be gained from increasing the VEM layer, or from increasing the constraining layer thickness for a given VEM layer thickness. Typical proportions which could give a good performance on a simple base panel might be about one third of the base panel thickness for both VEM and constraining layers, but each case requires individual analysis. A constrained layer system will contribute modally dependent damping since the flexural rigidity which determines the level of shear in the VEM depends on the structural mode. Typical values of damping ratio are given in Table 13.07.2 for a 1 mm thick aluminium plate.

Foil thickness (mm)	Damping layer thickness (mm)	Frequency (Hz)	$\zeta = \frac{\eta}{2}$
0.14	0.064	100 1000	0.0125 0.03
0.2	0.13	100 1000	0.032 0.055
0.3	0.13	100 1000	0.047 0.07

Table 13.07.2 - Values of the Damping Ratio of an Aluminium Plate (1mm thick) with Damping Tape on One Side

From Ref. [9], a thin-tape constrained layer gives 'stiffness ratio', s, and flexural loss factor, η_f:

$$s = \frac{\text{stiffness of damped element}}{\text{stiffness of plate and constraint}} = (EI)_{total} \Big/ \left(E_1 I_1' + E_3 I_3'\right)$$

$$= 1 + \frac{g\,Y\left(1 + g\left(1+\beta^2\right)\right)}{1 + 2g + g^2\left(I + \beta^2\right)}$$

$$\eta_f = \beta g\,Y \Big/ \left[1 + g(2+Y) + g^2(1+Y)\left(1+\beta^2\right)\right]$$

where g = shear parameter

$$= \frac{G'b}{h_2 K_B^2}\left[\frac{1}{E_1 A_1} + \frac{1}{E_3 A_3}\right]$$

and Y = geometric parameter

$$= \frac{(E_1 A_1)(E_3 A_3)\,d^2}{(E_1 A_1 + E_3 A_3)(E_1 I' + E_3 I_3')}$$

G' = shear modulus of VEM,

β = loss factor in shear of VEM,

$G'(1+i\beta)$ = complex shear modulus,

h_2, b = thickness, width of damping layer,

K_B = flexural wave number, $K_B^4 = \omega^2\mu/(EI_{total})$,

μ = mass per unit area,

E_1, E_3 = tensile module of base plate, constraining layer,

d = separation of base plate and constraint centroids,

A_1, A_3 = cross-section area of base plate, constraining layer,

I'_1, I'_3 = 2nd moment of area of base plate, constraint (about own neutral axis).

For harmonic excitation, the criterion for selecting a treatment to minimise response is to maximise the value of the product of s and η_f:

$$s\,\eta_f = \beta g Y \Big/ \left[1 + 2g + g^2\left(1+\beta^2\right)\right]$$

The influence of stiffness as well as damping must be taken into account since the influence on response of a high loss factor would be offset by a simultaneous reduction in stiffness ratio.

For random excitation, it is shown in Ref. [2] that the criterion is to maximise the term $g^{-1/4} s^{3/4} \eta_f^{1/2}$.

Both s and η_f are functions of g, typically as shown in Figure 13.07.4.

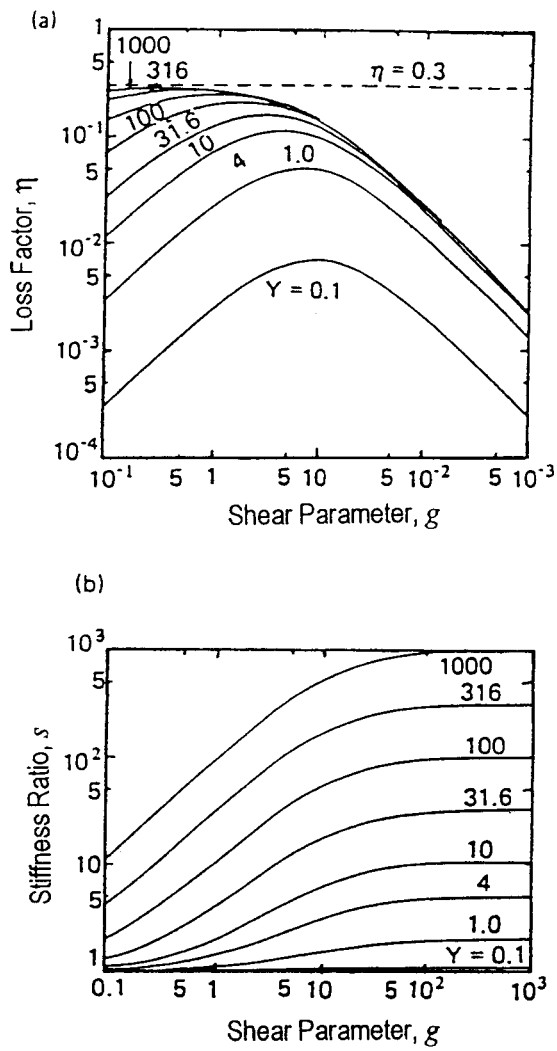

Figure 13.07.4 - η_f and s for Simply-supported Beams (β = 0.3)

For a very thin (foil) constraining layer, $s \approx 1$. For another common case, when constraining layers and base plates are of equal thickness and the damping layer is thin (a sandwich plate), $Y \approx 3$.

In this case:

$$\eta_f \approx 3\beta g \Big/ \left[1 + 5g + 4g^2\left(1+\beta^2\right)\right]$$

and: $s \approx 1$ for low g value

$s \approx 4$ for high g value.

The loss factor shows a peak value for given β when plotted against g. The value of g, to give max η_f, for a given geometry (Y value) is given by:

$$g_{opt} = 1 \Big/ \left[(1+Y)\left(1+\beta^2\right)\right]^{1/2}$$

$$\text{and } \eta_{f\,\max} = \beta Y \Big/ \left[(2+Y) + 2(1+y)^{1/2}\left(1+\beta^2\right)^{1/2}\right]$$

For a thin foil tape of $E_3 = E_1$, $Y \approx 3\, h_3 / h_1$

$$\text{then } \eta_{f\,\max} = \beta \frac{3}{2} \cdot \frac{h_3}{h_1} \Big/ \left[1 + \left(1+\beta^2\right)^{1/2}\right]$$

Examples of $\eta_{f\,max}$, given in Ref. [9], are shown in Table 13.07.3

Treatment	h_3 mm	h_1 mm	β	$\eta_{f\,max}$
Foil tape	0.125	0.9	1	0.083
Sandwich, $h_2 \le h_1$	=	=	1	0.28
Sandwich, $h_2 = h_1$	=	=	1	0.5

Table 13.07.3 - Layered Damping: Example Values of $\eta_{f\,max}$

VEM can be installed at joints, with maximum damping at an optimum thickness given by:

$$t_{opt} = \frac{2\ell b G \left(1+\beta^2\right)^{1/2}}{k_f}$$

where: 2ℓ = total overlapping length of joint plate,

b = fixture pitch,

k_f = shear stiffness of one fixing.

This is valid for longitudinal loading and a single line of fixings. The values of modal damping ratios are dependent on detail, but they are likely to be lower than those given by layered treatments.

Some aerospace applications of VEM are described in Ref. [10], and an example is shown in Figure 13.07.5. The incorporation of damping into composite components is described in Ref. [11].

13.08 ADDED TUNED DAMPERS

Tuned dampers are often fabricated with constrained-layer damping material, e.g. in the form of a beam to be located at a point of high amplitude response. They are inherently limited in their effective frequency range. Their characteristic result is to produce a pair of enhanced response frequencies equispaced about the resonance frequency at which they are designed to reduce the response, so these side-effects should be taken into consideration.

When there are adjacent resonance frequencies, suppression of the resonances will only be equitable if the vibration modes of the structure have similar strain energies. Otherwise the mode with the higher strain energy will be less damped.

Some configurations including shear-damped beams together with characteristics of tuned-mass dampers are given in Ref. [3].

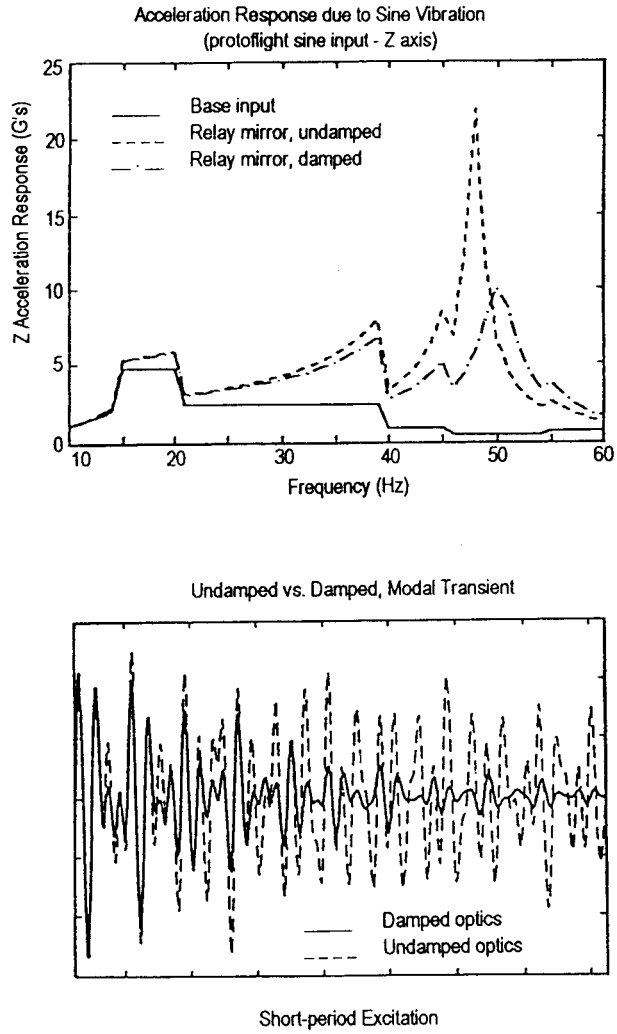

Figure 13.07.5 - Reduction of Optical Jitter by Added Damping (Constrained Layer), Ref. [12]

13.09 REFERENCES

[1] L.L. Beranek & I.L. Ver, (Eds)
'Noise and Vibration Control Engineering Principles and Applications'
Ch. 12: Structural Damping (E.E. Ungar)
J. Wiley & Sons Inc., 1992. ISBN 0-471-61751-2

[2] E.J. Richards & D.J. Mead
'Noise and Acoustic Fatigue in Aeronautics', Ch. 18
J. Wiley & Sons Ltd, 1968. ISBN 471-719447

[3] ESDU Item No. 91012: Methods for Improving Damping
Part 1: An Introduction and Guide to Practical Methods of Increasing Structural Damping
Aug. 1991, ESDU International plc, London. ISBN 0-85679-774-X

[4] L.C. Chow & R.J. Pinnington
'Practical Industrial Method of Increasing Structural Damping in Machinery, 1: Squeeze-film damping with air'
J. Sound Vib., 118 (1), 1987, 123-139

[5] ESDU Item No. 85012: Estimation of Damping in Laminated and Fibre-reinforced Plates
(also software ESDU pac A8512)
June 1985, ESDU International plc, London. ISBN 0-85679-518-6

[6] N.S. Ferguson
'A Note on the Critical Frequency of Sandwich Panels'
Letter to Ed., J. Sound Vib. 106(1), 171-172 (1986)

[7] ESDU Item No. 92001: Methods for Improving Damping
Part 3: Damping Material Data
Dec. 1992, ESDU International plc, London. ISBN-0-85679-851-7

[8] ESDU Item No. 91013: Methods for Improving Damping
Part 2: Layered Damping Treatment for Structures: Analysis and Examples
(also software A9113B)
Dec. 1991, ESDU International plc, London. ISBN 0-85679-775-8

[9] R.G. White & J.G. Walker, (Eds)
'Noise and Vibration', Ch. 25
Ellis Horwood, 1992. ISBN 0-85312-502-3

[10] L.C. Rogers
Proc. of Conf. on Aerospace Polymeric Visco-Elastic Damping Technology for the 1980's
USAF AFFDL-TM-78-78-FBA (1978)

[11] D.J. Barrett & C.A. Rotz
'Damped Advanced Composite Parts'
Proc. 2nd Intl. Congress on Recent Developments in Air- and Structure-borne Sound & Vibration
March 4-6, 1992, Auburn, USA, pp. 257-263

[12] E.M. Austin & C.D. Johnson
'Design and Application of Passive Damping Systems'
Seminar, 3M (UK) plc, 15 Sept. 1992, Bracknell, England

(Intentionally Left Blank)

Structural Acoustics Design Manual

Appendix A
GENSTEP3: GENERAL THEORY

CONTENTS

A.01 INTRODUCTION

The theoretical approach of the GENSTEP3 program is based on the concepts of Statistical Energy Analysis (SEA). This Appendix presents a summary of the theoretical expressions in the program subroutines used to evaluate the relevant SEA parameters, input powers, sound transmissions, subsystem energies and response.

Note: The basic SEA theory is dealt with in Ref. [1], while typical applications are reviewed in Ref. [2, 3].

A.02 EVALUATION OF MODAL DENSITY

For most structural configurations, the modal density can be determined theoretically. The following formulations, given in this Appendix, are included in the GENSTEP3 program:

- Flat unstiffened panels .....[See: Topic A.03]
- Beams, stringer or stiffener.....[See: Topic A.04]
- Hoop or frame .....[See: Topic A.05]
- Unstiffened cylinder.....[See: Topic A.06]
- Stiffened cylinder.....[See: Topic A.07]
- Stiffened panel .....[See: Topic A.08]
- Flat honeycomb panel (with isotropic core) ...[See: Topic A.09]
- Curved sandwich shells.....[See: Topic A.10]
  - Cylindrical.....[See: Topic A.11]
  - Double-curved .....[See: Topic A.12]
- Grid structure .....[See: Topic A.13]
- Acoustic cavities .....[See: Topic A.03]

A.03 MODAL DENSITY: FLAT UNSTIFFENED PANELS

RECTANGULAR

The modal density of a flat rectangular panel with no stiffening is, from Ref. [4]:

$$n(f) = \frac{A\sqrt{3}}{t \cdot C_L}$$

where:

$n(f)$ = modal density (modes Hz^{-1}),

A = panel area,

t = panel thickness,

C_L = longitudinal wave speed;

$$= \left(\frac{E}{\rho(1-\mu^2)}\right)^{1/2}$$

E = modulus of elasticity,

ρ = material density,

μ = Poisson's ratio.

CIRCULAR

The model density of a circular unstiffened panel is:

$$n(f)_{circular} = n(f)_{rectangular} \times \frac{8}{\pi^2} \quad \text{from Ref. [5]}$$

Very often the modal densities of circular and rectangular plates of the same area are taken to be the same.

IRREGULAR

The modal density of an irregularly shaped plate is taken to be the same as that of a rectangular plate of the same area and material properties.

A.04 MODAL DENSITY: BEAM, STRINGER OR STIFFENER

TRANSVERSE VIBRATIONS

In the case of a beam (or a stringer or stiffener), the modal density of vibrations in a transverse direction is, from Ref. [1]:

$$n(f) = \frac{1}{C_L} \cdot \left(\frac{C_L}{k \cdot 2\pi f}\right)^{1/2}$$

where:

l = length of beam,

C_L = longitudinal wave speed;

$$= \left(\frac{E}{\rho}\right)^{1/2}$$

k = radius of gyration of section about neutral axis;

$$= \left(\frac{I_{NA}}{a}\right)^{1/2}$$

where:

I_{NA} = second moment of area of section about NA,

a = beam cross-sectional area,

f = centre frequency of band.

TORSIONAL VIBRATIONS

The modal density of torsional vibrations for a beam (or a stringer, or stiffener) is, from Ref. [4]:

$$n(f) = \frac{2l}{C_s} \cdot k_p \left(\frac{a}{J}\right)^{1/2}$$

where:

l = length of beam,

C_s = shear wave speed;

$$= \left(\frac{G}{\rho}\right)^{1/2}$$

G = shear modulus,

ρ = material density,

K_p = radius of gyration about centre of gravity of section,

a = beam cross-sectional area,

J = torsional stiffness constant.

A.05 MODAL DENSITY: HOOP OR FRAME

The modal density of a hoop or frame type stiffener is, from Ref. [6]:

$$n(f)=\left(\frac{a\cdot R^2}{I}\right)^{1/4}\cdot\frac{R}{C_L}\cdot\left(\frac{f}{f_R}\right)^{-1/2}\cdot 2\pi$$

where:

a = cross-sectional area,

R = radius of hoop,

I = second moment of area of cross section about axis perpendicular to plane of bending, i.e. about neutral axis of section,

C_L = longitudinal wave speed of hoop material $=\left(\frac{E}{\rho}\right)^{1/2}$

f = band centre frequency,

f_R = ring frequency $=\frac{C_L}{2\pi R}$

A.06 MODAL DENSITY: UNSTIFFENED CYLINDER

The expressions for the modal density of an unstiffened cylinder are derived from Ref. [7]. A more detailed discussion of the expressions for the modal density of a cylinder is presented in Ref. [8], Appendix 1. The expressions used in GENSTEP3 depend on the fact that the frequency of the bandwidth is considered with respect to the ring frequency: f/f_R :

For $f/f_R \le 0.48$:

$$n(f)=\frac{5}{\pi}\cdot\left(\frac{f}{f_R}\right)^{1/2}\cdot\frac{A}{t\cdot C_L}$$

For $0.48 < f/f_R < 0.83$:

$$n(f)=\frac{7.2}{\pi}\cdot\frac{f}{f_R}\cdot\frac{A}{t\cdot C_L}$$

For $f/f_R \ge 0.83$:

$$n(f)=\frac{2A}{\pi\cdot t\cdot C_L}\left\{2+\frac{0.569}{F-(1/F)}\left[F\cdot\cos\left(\frac{1.745}{F^2}\left(\frac{f_R}{f}\right)^2\right)-\frac{1}{F}\cdot\cos\left(1.745F^2\left(\frac{f_R}{f}\right)^2\right)\right]\right\}$$

where:

f = centre frequency of band,

f_R = ring frequency $=\frac{C_L}{2\pi R}$

R = cylinder radius,

C_L = longitudinal wave speed $=\left(\frac{E}{\rho(1-\mu^2)}\right)^{1/2}$

E = modulus of elasticity,

ρ = material mass density,

A = cylinder surface area;
$= 2\pi R\,.\,l$

l = cylinder length,

t = skin thickness,

F = bandwidth factor $=\left(\frac{\text{lower limit band }(k+1)}{\text{lower limit band }(k)}\right)^{1/2}$

A.07 MODAL DENSITY: STIFFENED CYLINDER

The modal density of a stiffened cylinder is assumed to be the sum of the modal densities of the constituent parts in each bandwidth. For a cylinder stiffened by stringers and frames the modal density is:

$$n(f)_{\substack{\text{stiffened}\\\text{cylinder}}}=n(f)_{\substack{\text{unstiffened}\\\text{cylinder}}}+n(f)_{\substack{\text{stringer}\\\text{(transverse vibration)}}}+n(f)_{\text{frame}}$$

A.08 MODAL DENSITY: STIFFENED PANEL

Like the modal density of a stiffened cylinder (Topic A.07), that of a stiffened panel is:

$$n(f)_{\substack{\text{stiffened}\\\text{panel}}}=n(f)_{\substack{\text{unstiffened}\\\text{panel}}}+n(f)_{\substack{\text{stringer}\\\text{(transverse vibration)}}}$$

A.09 MODAL DENSITY: FLAT HONEYCOMB PANEL (WITH ORTHOTROPIC CORE)

This expression is incorporated in the program MODALEN. This expression for the theoretical determination of the modal density of this type of panel was developed by Aboutorabian and is summarised in Ref. [9]. The principal assumptions made in the development of the theory are:

- faceplate thickness is very much less than core thickness and, as a result,
- faceplate bending stiffness can be neglected.

If these assumptions are taken into account, modal density is given by:

$$n(f)=\frac{\pi abm}{gB}f\left(1+\frac{\left[m\omega^2+2g^2B(1-\mu^2)\right]}{\left[m^2\omega^4+4m\omega^2g^2B(1-\mu^2)\right]^{1/2}}\right)$$

where:

a, b = panel dimensions

B = faceplate longitudinal stiffness, given by:

$$d^2\left(\frac{E_{FT}\,t_{FT}\,E_{FB}\,t_{FB}}{E_{FT}\,t_{FT}+E_{FB}\,t_{FB}}\right)$$

d = section effective depth, given by: $t_c+\frac{t_{FT}}{2}+\frac{t_{FB}}{2}$

E_{FT}, E_{FB} = top and bottom faceplate Young's moduli,

f = frequency (Hz),

g = core stiffness, given by:

$$\frac{\sqrt{G_xG_y}}{t_c}\left(\frac{1}{E_{FT}t_{FT}}+\frac{1}{E_{FB}t_{FB}}\right)$$

m = total mass per unit area of panel,

t_c = core thickness,

t_{FT}, t_{FB} = top and bottom faceplate thickness,

μ = Poisson's ratio,

ω = radian frequency (rad.s^{-1}).

A.10 MODAL DENSITY: CURVED SANDWICH SHELLS

Ref. [10] gives modal density relationships for several types of curved sandwich shells, as summarised below.

- Cylindrical sandwich shells, [See: Topic A.11]
- Double-curved sandwich shells, [See: Topic A.12].

A.11 MODAL DENSITY: CYLINDRICAL SANDWICH SHELLS

The following expression for modal density has been derived when shear and rotary inertia effects are neglected, for identical faceplates:

$$n(f) \approx \frac{ab(\rho_F t_F + \rho_c t_c)f}{G t_c}\left\{\theta_2 + \int_0^{\theta_2} \frac{\left[f_1 + 2(1-\mu^2)\ S^2\right]d\theta}{\left[f_1^2 + 4(1-\mu^2)S^2 f_1\right]^{1/2}}\right\}$$

where $\theta_2 = \sin^{-1}\left(\frac{R \cdot 2\pi f}{A^{1/2}}\right)$ if $f < \frac{A^{1/2}}{2\pi R}$

and $\theta_2 = \pi/2$ if $f \geq \frac{A^{1/2}}{2\pi R}$

$$A = E_{Zc}/(\rho_F t_F + \rho_c t_c)$$

$$f_1 = \frac{4\pi^2}{A}\ t_F^2 f^2 - \frac{t_F^2 \sin^4\theta}{R^2}$$

The integral must be evaluated numerically, being hyperelliptic. A singularity occurs for $n(f)$ at the ring frequency but an estimate can be made by evaluating the function in narrow bands close to the ring frequency and then averaging over the bandwidth being used. At higher frequencies, $n(f)$ becomes asymptotic to the flat sandwich plate values which increase almost linearly with frequency.

A.12 MODAL DENSITY: DOUBLE-CURVED SANDWICH SHELLS

The general case from which the cylindrical shell relationship is derived is given in Ref. [10]. This again requires numerical integration and gives singularities at the upper and lower ring frequencies given at:

$$\Omega = t_F/R_2 \text{ and } \Omega = t_F/R_1$$

where: R_1, R_2 = radii of curvature

$$\Omega = 2\pi t_F f\left(\frac{\rho_F t_F + \rho_c t_c}{E_F t_c}\right)^{1/2}$$

Below the lower ring frequency, the modal density is zero. Above the upper ring frequency (at which the modal density peaks due to a singularity), the modal density becomes asymptotic to the value for a flat plate of equal area.

For $R_1 = R_2$ (spherical cap):

$$n(f) \approx \frac{ab}{4\pi S\, t_F^2} \cdot \frac{\Omega^2}{f}\left\{1 + \frac{f_2 + 2(1-\mu^2)S^2}{\left[f_2^2 + 4(1-\mu^2)S^2 f_2\right]^{1/2}}\right\}$$

where: $f_2 = \Omega^2 - t_F^2/R_1^2$

The behaviour of paraboloidal sandwich shells differs from the spherical cap at low frequencies where the effect of the non-constant radius of curvature causes finite modal density with no singularity evident in available test data. Tests show higher values than for a flat sandwich panel, with a stronger frequency dependence. There is no analytical expression at present for paraboloidal shells.

For future types of construction it may become important to include the effect of very high faceplate bending stiffness. However, the more exact result for the modal density cannot be expressed in explicit terms, see Ref. [10].

A.13 MODAL DENSITY: GRID STRUCTURE

The modal density of a grid composed of identical cross-section and material properties is obtained by using the total length of all the beams in the grid in the beam equation for transverse vibrations, (see subsection 2.2.3.1 of Ref. [8]).

A.14 MODAL DENSITY: ACOUSTIC CAVITIES

ONE-DIMENSIONAL CAVITY

The modal density for a space in which one-dimension is significantly greater than the other two is, from Ref. [11]:

$$n(f) = \frac{2l}{C_0} \text{ which is valid for } \lambda_0 > 2l_c$$

where:

- l = length of cavity,
- l_c = greatest cross-sectional dimension,
- λ_0 = acoustic wavelength,
- C_0 = speed of sound in air.

TWO-DIMENSIONAL CAVITY

The modal density for a space in which one dimension is significantly less than the other two (e.g. a thin flat space) is, from Ref. [1]:

$$n(f) = \frac{2\pi f a}{C_0^2} + \frac{p}{C_0} \text{ which is valid for } \lambda_0 > 2l_0$$

where:

- f = centre frequency of band,
- a = area (cross-section) of cavity,
- p = perimeter of cavity,
- l_0 = depth of cavity,
- C_0 = speed of sound in air.

THREE-DIMENSIONAL CAVITY

The modal behaviour for the general case of a cavity which is not restricted in any comparative dimension is assumed to be that of a rectangular walled cavity of the same value. The modal density is, from Ref. [1]:

$$n(f) = \frac{4\pi f^2 V}{C_0^3} + \frac{\pi f A}{2C_0^2} + \frac{l_e}{8C_0}$$

where:

- V = volume of cavity,
- A = surface area of cavity,
- l_e = total edge length,
- C_0 = speed of sound in air,
- f = centre frequency of band.

A.15 EVALUATION OF DISSIPATION LOSS FACTORS (DLF)

Currently, the only DLF evaluation available in GENSTEP3 is for a flat unstiffened panel. For all other structure types the user is referred to advice given in the relevant zone section and Chapter 9: 'Compendium of Loss Factors'. Values decided upon should then be input to GENSTEP3.

FLAT UNSTIFFENED PANEL

$$f < 80\text{ Hz} \quad \text{DLF} = 0.04$$

$$80\text{ Hz} \le f < 2500\text{ Hz} \quad \text{DLF} = \frac{2 \times 0.9065}{f^{0.87034}}$$

$$f \ge 2500\text{ Hz} \quad \text{DLF} = 0.002$$

OTHER TYPES OF STRUCTURE

No theory available.

A.16 EVALUATION OF COUPLING LOSS FACTORS (CLF)

The evaluation of CLFs for structure-to-structure coupling has been entirely experimental. and values must be input to GENSTEP3. The evaluation of CLF for coupling between an acoustic space and a structure, however, can be achieved theoretically. The various options available in the GENSTEP3 program for structure to acoustic space are described:

- General relationship for structure/acoustic-cavity coupling, [See: Topic A.17].
- Flat unstiffened panel, [See: Topic A.18].
- Flat stiffened panel, [See: Topic A.19].
- Unstiffened cylinder, [See: Topic A.20].
- Stiffened cylinder, [See: Topic A.21].
- Honeycomb panel with identical thin faceplates, [See: Topic A.22].
- Acoustic cavity (3-D) coupled to another acoustic cavity (3-D), [See: Topic A .23].

A.17 CLF: GENERAL RELATIONSHIP FOR STRUCTURE/ACOUSTIC-CAVITY COUPLING

If it is assumed that the acoustic space and the structure are subsystems 1 and 2 respectively, then the CLF, η_{21}, is given by:

$$\eta_{21} = \frac{R_{RAD}}{M \cdot A \cdot 2\pi f}$$

It should be noted that this expression gives the coupling loss in a specific direction: structure to acoustic cavity. The complementary CLF, cavity to structure, is found from the reciprocal relationship, viz:

$$\eta_{12} = \eta_{21} \cdot \frac{N_2}{N_1}$$

where:

η_{21} = CLF for structure to acoustic space,

η_{12} = CLF for acoustic space to structure,

N_1, N_2 = mode counts for acoustic space and structure, respectively,

n_1, n_2 = modal density for acoustic space and structure, respectively (for a bandwidth Δf, $N = n \cdot \Delta f$),

R_{RAD} = radiation resistance of structure,

m = mass per unit area of structure,

A = (radiating) surface area of structure,

f = centre frequency of band.

It can be seen that the theoretical problem is to establish R_{RAD} for the structural configurations under consideration. The following Topics give formulae for the structures currently available in the GENSTEP3 program.

Also considered is the case of coupling between two acoustic spaces which, of course, must be separated by a structural member.

A.18 CLF: FLAT UNSTIFFENED PANEL COUPLED TO AN ACOUSTIC CAVITY

These expressions were originally derived for simply supported flat rectangular panels by Maidanik, Ref. [12], with some later corrections by Price and Crocker, Ref. [13]. They are assumed to be applicable to other boundary conditions and plate geometries, The expressions are dependent on the frequency region governed by the critical coincidence frequency, f_c.

For $f < f_c$: $R_{RAD} = 2A\rho_0 C_0 \left[\left(\frac{\lambda_c \cdot \lambda_a}{A} \right) \cdot 2 \left(\frac{f}{f_c} \right) g_1 + \left(\frac{P\lambda_c}{A} \right) g_2 \right]$

For $f = f_c$: R_{RAD} becomes very large, Ref. [3] suggests an approximate value of $\left(\frac{P}{2\lambda_c} \right)^{1/2}$.

For $f > f_c$: $R_{RAD} = A\rho_0 C_0 \left(1 - \frac{f_c}{f} \right)^{-1/2}$

where:

R_{RAD} = radiation resistance,

A = panel surface area,

ρ_0 = air density,

C_0 = speed of sound in air,

λ_a = acoustic wavelength,

λ_c = wavelength corresponding to critical frequency $= \left(\frac{C_0}{f_c} \right)$

f = centre frequency of band,

f_c = critical coincidence frequency $= \frac{C_0^2 \sqrt{3}}{\pi t \cdot C_L}$

t = panel thickness,

C_L = longitudinal wave speed $= \left(\frac{E}{\rho(1-\mu^2)} \right)^{1/2}$

E = modulus of elasticity,

ρ = material density,

A = Poisson's ratio,

P = panel perimeter,

$$g_1 = \left(\frac{4}{\pi^4} \right) \cdot \left(\frac{1 - 2\Psi^2}{\Psi(1-\Psi^2)^{1/2}} \right) \quad for \frac{f}{f_c} < \frac{1}{2}$$

$$= 0 \quad for \frac{f}{f_c} \ge \frac{1}{2}$$

$$g_2 = \frac{1}{4\pi^2} \left[(1-\Psi^2) \log_e \left(\frac{1+\Psi}{1-\Psi} \right) + 2\Psi \right] \cdot \frac{1}{(1-\Psi^2)^{3/2}}$$

$$\Psi = \left(\frac{f}{f_c} \right)^{1/2}$$

At $f = f_c$ the radiation resistance becomes very large and there is no available theoretical expression. However, as this effect is over a narrow bandwidth, it does not greatly alter the practical average results.

The GENSTEP3 program is written to compute values from the expression for $f > f_c$. If f is equal to f_c, then the ratio f/f_c must be set to 1.01.

A.19 CLF: FLAT STIFFENED PANEL COUPLED TO AN ACOUSTIC CAVITY

The presence of stiffeners will affect the radiation characteristics at frequencies less than the critical frequency, f_c.

For $f < f_c$:

Allowance is made in the expression for the unstiffened flat panel by replacing the perimeter, P, by an effective perimeter, P_{eff}, given by:

$$P_{eff} = P + 2l_s$$

where:

P = unstiffened panel perimeter,

l_s = total length of stiffening.

For $f = f_c$:

There is no expression for R_{RAD} at the critical frequency. The GENSTEP3 program sets f/f_c at a value slightly greater than 1.0.

For $f > f_c$:

The equation for the unstiffened panel at this condition is used.

A.20 CLF: UNSTIFFENED CYLINDER COUPLED TO AN ACOUSTIC CAVITY

The expressions used are derived in Ref. [7] and are dependent on frequency regions defined by the ring frequency, f_R, and the critical coincidence frequency, f_c. The ring frequency, f_R, depends on the cylinder radius, while f_c depends on the cylinder shell thickness, which means that for possibly all aerospace structures f_R will be less than f_c.

For $f \le \frac{f_R}{F}$:

$$R_{RAD} = A\rho_0 C_0 \cdot \frac{\left(\frac{f}{f_R}\right)^{3/2} \cdot \left(\frac{f_R}{f_c}\right)}{2B\left(F - \frac{1}{F}\right)} \left(1 - \frac{f}{f_R}\left(1-\Psi^2\right)^{1/2}\right) \cdot C \cdot \left[12\left(1-\mu^2\right)\right]^{1/2}$$

where:

$$C = \frac{1}{\left(\frac{1}{F} - \frac{f}{f_R}\right)^{1/2}} - \frac{1}{\left(F - \frac{f}{f_R}\right)^{1/2}}$$

$$B = 2.5\left(\frac{f}{f_R}\right)^{1/2} \quad \text{for } \frac{f}{f_R} \le 0.48$$

$$= 3.6\left(\frac{f}{f_R}\right) \quad \text{for } 0.48 < \frac{f}{f_R} \le \frac{1}{F}$$

A = cylinder surface area,

ρ_0 = air density,

C_0 = speed of sound in air,

f = centre frequency of band,

f_R = ring frequency $= \frac{C_L}{2\pi R}$

C_L = longitudinal wave speed $= \left(\frac{E}{\rho\left(1-\mu^2\right)}\right)^{1/2}$

E = modulus of elasticity

ρ = material density

μ = Poisson's ratio

R = cylinder radius

$$\Psi = \left(\frac{f}{f_c}\right)^{1/2}$$

f_c = critical coincidence frequency $= \frac{C_0^2 \cdot \sqrt{3}}{\pi \cdot t \cdot C_L}$

t = skin thickness

F = bandwidth factor $= \left(\frac{\text{lower limit band}\left(K+1\right)}{\text{lower limit band}\left(K\right)}\right)^{1/2}$

For $\frac{f_R}{F} < f \le f_R$:

There are no expressions available for this region; the sound radiated can be high, i.e. R_{RAD} large. The GENSTEP3 program uses the expression for $f < f_R/F$, with the ratio, f/f_R set to:

$$\left(\frac{1}{F} - 0.001\right)$$

For $f_R < f < f_c$:

$$R_{RAD} = A\rho_0 C_0 \frac{\left(\frac{t \cdot R}{l^2}\right)^{1/2}\left[\log_e\left(\frac{1+\Psi}{1-\Psi}\right) \cdot \left(1-\Psi^2\right) + 2\Psi\right]}{\left\{12\left(1-\mu^2\right)\left[\left(\frac{f}{f_R}\right)^2 - 1\right]\right\}^{1/4} \cdot \pi\left(1-\Psi^2\right)^{3/2}}$$

where the symbols are as stated for $f \le 0.83 f_r$ with the addition of l cylinder length.

For $f = f_c$:

No theoretical expression is available; R_{RAD} is large. GENSTEP3 program uses a value for the ratio f/f_c set to 1.01 in the formula for region $f > f_c$.

For $f > f_c$:

The flat plate expression from Ref. [14] is used. This is as given in Topic A.18.

$$R_{RAD} = A\rho_0 C_0 \left[1 - \left(\frac{f_c}{f}\right)\right]^{-1/2}$$

The nomenclature is as given in Topic A.18.

A.21 CLF: STIFFENED CYLINDER COUPLED WITH AN ACOUSTIC CAVITY

The theoretical expressions are, in most cases, the same as those for the unstiffened cylinder coupled with an acoustic cavity. The region $f_R < f < f_c$ makes use of the flat plate behaviour.

For $f \leq \frac{f_R}{F}$:

The addition of stiffeners has no effect in this region, the appropriate equation in Topic A.20 is used.

For $\frac{f_R}{F} < f < f_R$:

No expression available; the GENSTEP3 program makes the same assumption as in Topic A.20.

For $f_R < f < f_c$:

Allowance is made for stiffening in the appropriate expression from Topic A.18 for $f < f_c$. This is because the behaviour of a cylinder is similar to that of a flat plate in this frequency region:

$$R_{RAD} = 2A\rho_0 C_0 \left[\left(\frac{\lambda_c \cdot \lambda_a}{A} \right) \cdot 2 \left(\frac{f}{f_c} \right) g_1 + \left(\frac{P\lambda_c}{A} \right) g_2 \right]$$

where the nomenclature is similar to that used in Topic A.18, except for the effective perimeter, $P_{eff} = 2\,(l_s + 2\pi R\,(1 + n))$, where:

- R = radius of cylinders,
- l_s = length of stiffening,
- n = the number of frames stiffening the cylinder, excluding the end frames.

For $f = f_c$:

No expression available; the GENSTEP3 program sets f/f_c to 1.01 and uses the formula for $f > f_c$.

For $f > f_c$:

The addition of stiffeners has no effect in this region and the flat plate expression is used from Ref. [14]. This is as given in Topic A.18, and as used for an unstiffened cylinder in Topic A.20:

$$R_{RAD} = A\rho_0 C_0 \left[1 - \left(\frac{f_c}{f} \right) \right]^{-1/2}$$

A.22 CLF: FLAT HONEYCOMB PANEL (METALLIC) COUPLED WITH AN ACOUSTIC CAVITY

For a honeycomb panel with identical thin faceplates, the acoustic critical frequency is given by, Ref. [15]:

$$f_c = \frac{C_0}{2\pi} \left(\frac{M_g \left(1 - \mu^2\right)}{\left(gB / C_0^2 \right) - M} \right)^{1/2}$$

$$\text{where} \quad g = \frac{\left(G_x G_y\right)^{1/2}}{E_F t_c} \cdot \frac{2}{t_F}$$

where: f denotes faceplate, c denotes core,

$B = d^2 E_F t_F / 2$, $d = t_F + t_c$

(other symbols in accordance with nomenclature).

For future types of construction it may become important to include the effect of very high faceplate bending stiffness. However, the more exact result for the modal density cannot be expressed in explicit terms, see Ref. [10].

RADIATION RESISTANCE

The radiation resistance is given by the following expressions:

For $f < f_c$:

$$R_{RAD} = 2A\rho_0 C_0 \left[\left(\frac{\lambda_c \cdot \lambda_a}{A} \right) \cdot 2 \left(\frac{f}{f_c} \right) g_1 + \left(\frac{P\lambda_c}{A} \right) g_2 \right]$$

For $f = f_c$:

At the critical frequency, there is no general expression for R_{RAD}. The program sets to 1.01 and uses the expression for $f > f_c$.

For $f > f_c$:

$$R_{RAD} = A\rho_0 C_0 \left[1 - \left(\frac{f_c}{f} \right) \right]^{-1/2}$$

where:

- A = panel surface area,
- ρ_0 = air density,
- λ_a = acoustic wavelength,
- f = centre frequency of band,
- ρ = material density,
- λ_c = acoustic wavelength corresponding to critical frequency,
- P = panel perimeter,

$$g_1 = \left(\frac{4}{\Pi^2} \right) \left(\frac{1 - 2\Psi^2}{\left(1 - \Psi^2\right)^{1/2}} \right) \quad \text{for } \frac{f}{f_c} < 0.5$$

$$= 0 \quad \text{for } \frac{f}{f_c} > 0.5$$

$$g_2 = \frac{1}{4\Pi^2} \left[\left(1 - \Psi^2\right) \log_e \left(\frac{1 + \Psi}{1 - \Psi} \right) + 2\Psi \right] \cdot \frac{1}{\left(1 - \Psi^2\right)^{3/2}}$$

$$\Psi = \left(\frac{f}{f_c} \right)^{1/2}$$

and the remaining nomenclature is given elsewhere in this section.

A.23 CLF: ACOUSTIC CAVITY (3-D) COUPLED TO ANOTHER ACOUSTIC CAVITY (3-D)

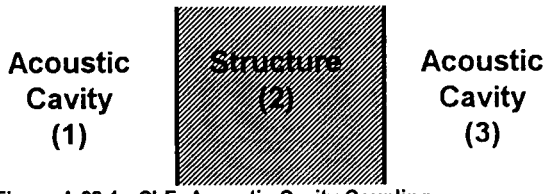

Figure A.23.1 - CLF: Acoustic Cavity Coupling

The coupling is dependent on the limp panel mass law transmission loss of the intervening structure in the case of flat panels. For cylinders, below their ring frequency, see Ref. [16].

The derivation makes use of standard sound transmission formulae, available in Ref. [1, 17] for example:

$$\log_{10}\eta_{13} = \frac{TL_{RI}}{10} + \log_{10}\left(\frac{C_0 A}{8\pi f V_1}\right)$$

where:

C_0 = speed of sound in air,

A = surface area of structure,

f = centre frequency of band,

V_1 = volume of cavity 1,

TL_{RI} = the random incidence mass law transmission loss, which is given by:

$$TL_{RI} = TL_{NI} - 10\log_{10}[0.23(TL_{NI})]$$

TL_{NI} = the normal incidence mass law transmission loss, which is given by:

$$TL_{NI} = 10\log_{10}\left[1 + \left(\frac{\pi f M}{\rho_0 C_0}\right)^2\right]$$

where:

M = mass/unit area of panel,

ρ_0 = air density,

and the remaining nomenclature is given elsewhere in this section.

A.24 INPUT POWER (FROM AN ACOUSTIC SOURCE)

The following Topics covers the cases of an acoustic excitation source providing a power flow into:

- a structural subsystem, [See: Topic A.25], and
- an acoustic cavity, [See: Topic A.26].

A.25 DIRECT POWER INPUT TO A STRUCTURE FROM AN ACOUSTIC FIELD

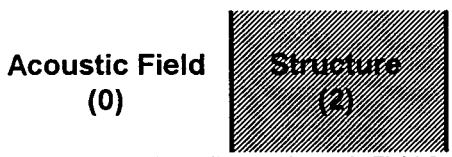

Figure A.25.1 - Input Power: Acoustic Field Coupling

The power input to the structure is given by:

$$\Pi_{02} = 2\pi f \,.\, E_0 \,.\, \eta_{02}$$

where:

Π_{02} = power received directly by structure 2 from acoustic field,

f = centre frequency of band,

E_0 = energy of acoustic field,

η_{02} = coupling loss factor (CLF) between acoustic field and structure.

The energy of the acoustic field is:

$$E_0 \frac{\langle P_0^2 \rangle V_0}{\rho_0 C_0^2}$$

where:

$\langle P_0^2 \rangle$ = spatial average mean square pressure of the acoustic field,

V_0 = volume of the 'source room',

ρ_0 = air density,

C_0 = speed of sound in air.

The method for evaluation of the required CLF's, η_{02} and η_{20}, is described in Ref. [18], section 2.3. η_{20} can be calculated from the relation:

$$\eta_{20} = \frac{R_{RAD}}{M \cdot A \cdot 2\pi f}$$

and R_{RAD} is found from the appropriate formulae in subsection 2.3.2 of Ref. [18]. The complementary CLF, η_{02}, is found with the help of the reciprocal relation:

$$\eta_{02} = \eta_{20} \cdot \frac{n_2}{n_0}$$

where the modal densities of the acoustic space and the structure, n_0 and n_2 respectively, are found from the appropriate formulae in subsection 2.3.1 of Ref. [18].

It can be seen that this theoretical approach is associated with a source acoustic space of known volume in modal density. It is applicable to the conditions obtained in a test chamber where a structure is being excited by a reverberant sound field.

The GENSTEP3 program also includes an option allowing the user to input values for the acoustic field power, so that an individual evaluation of different 'free-field' conditions can be used.

A.26 DIRECT POWER INPUT TO AN ACOUSTIC CAVITY

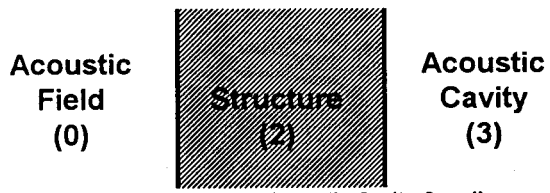

Figure A.26.1 - Input Power: Acoustic Cavity Coupling

The power input directly to the acoustic cavity is given by:

$$\Pi_{03} = 2\pi f \,.\, E_0 \,.\, \eta_{03}$$

where the symbols have the same meanings as in section 2.3.3 of Ref.[8], except that η_{03} = CLF between acoustic spaces.

The coupling loss factor η_{03} is dependent on the mass law sound transmissions of the structure 2 and is based on the relation:

$$\log_{10}\eta_{03} = \frac{-TL_{RI}}{10} + \log_{10}\left(\frac{C \cdot A}{8\pi f \cdot V_0}\right)$$

The solution to this expression, including formulae for the normal and random incidence mass law transmission, is given in section 2.3.2 of Ref. [8]. Again, as in section 2.3.3 of Ref. [8], the acoustic field is associated with a containing volume.

A.27 INPUT POWER (FROM A MECHANICAL SOURCE)

GENSTEP3 includes the scope to enter values of point force so that mechanical power input can be calculated, using the spacecraft's receiving structure impedance, (see Section 7, Power Card, of GENSTEP3 Manual).

A.28 SOUND TRANSMISSION

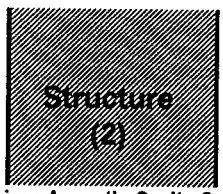

Figure A.28.1 - Sound Transmission: Acoustic Cavity Coupling

The most readily assessed practical measure of sound transmission is the noise reduction, NR, which is defined as the difference in sound pressure levels between the source space and the receiving space. In SEA terms, the noise reduction is given by:

$$NR = 10\log_{10}\left(\frac{E_1}{E_3}\right) + 10\log_{10}\left(\frac{V_3}{V_1} \cdot \frac{\rho_1 C_1^2}{\rho_3 C_3^2}\right)$$

where:

E_1 = energy in source acoustic space,

E_2 = energy in receiving space,

V_1 = volume of source space,

V_2 = volume of receiving space,

ρ_1, ρ_3 = air densities of respective spaces,

C_1, C_3 = speed of sound in respective space.

For most conditions the ρC^2 terms will cancel. If one requires to find a value of transmission loss, TL, for the intervening structure, (2), from the value of NR, then it is necessary to consider the acoustical properties of the source and receiving spaces. This correction tends to be controlled by the average sound absorption coefficient, α, for the surfaces of the receiving space, which is related to the dissipation loss factor for this space.

The average absorption coefficient is given by:

$$\alpha = 1 - \text{antilog}_{10}\left(-\frac{10.94\eta_3 \cdot f \cdot V_3}{C_0 \cdot A_3}\right)$$

where:

η_3 = dissipation loss factor of receiving acoustic cavity,

f = band centre frequency,

V_3 = volume of receiving acoustic cavity,

C_0 = speed of sound in air,

A_3 = wall surface area of receiving acoustic cavity.

The value for transmission loss can then be found from:

For $\alpha \leq 0.2$:

$$TL = NR + 10\log_{10}\left(\frac{A_3}{A_2 \cdot \alpha}\right)$$

For $0.2 < \alpha < 0.8$:

$$TL = NR + 10\log_{10}\left(\frac{1}{4} + \frac{A_3(1-\alpha)}{A_2 \cdot \alpha}\right)$$

For $\alpha > 0.8$:

$$TL = NR - 6$$

where:

A_2 = area of transmitting structure, and the remaining nomenclature as for α.

The values for NR and TL are expressed in dB.

A.29 EVALUATION OF THE SUBSYSTEM ENERGIES

The fundamental relation used is that of the conservation of energy for each subsystem, i.e. the balance between power entering and leaving the subsystem.

The power dissipated by the ith subsystem is:

$$\Pi_{i,DISS} = \omega \,.\, \eta_i \,.\, E_{i,TOT} \qquad (1)$$

and the power transferred from subsystem i to subsystem j is:

$$\Pi_{ij} = \omega \,.\, \eta_{ij} \,.\, E_{i,TOT} - \omega \,.\, \eta_{ji} \,.\, E_{j,TOT} \qquad (2)$$

where:

ω = the angular frequency,

η_i = the dissipation loss factor,

$E_{i,TOT}$, $E_{j,TOT}$ = the sum of potential and kinetic subsystem energies,

η_{ij}, η_{ji} = the coupling loss factors for the two subsystems, related by:

$$N_i\eta_{ij} = N_j\eta_{ji}$$

where:

N_i, N_j are the number of modes in the two subsystems in bandwidth Δf.

The power balance for each subsystem is then:

$$\Pi_{i,IN} = \Pi_{i,DISS} + \Sigma\Pi_{ij} \qquad (3)$$

where:

$\Sigma\Pi_{ij}$ is the sum of the power flow between the ith subsystem and the subsystem to which it is coupled, as in Eqn.(2).

The balance for the whole system results in a set of equations, which may be represented in matrix form as:

$$\{E\} = [N]^{-1}\,\{\Pi_{IN}\} / \omega$$

where:

$\{E\}$ = the subsystem energy matrix,

$[N]$ = the system matrix,

$\{\Pi_{IN}\}$ = the system power matrix,

ω = the centre frequency (rads.s^{-1}) of the analysis bandwidth.

The GENSTEP3 program solves the system equation for the subsystem energies. The system matrix [N] contains the coupling loss factors and total loss factors as shown below.

$$\begin{pmatrix} \eta_{1,TOT} & -\eta_{21} & -\eta_{31} & \cdot & \cdot & \cdot & -\eta_{N1} \\ -\eta_{12} & \eta_{2,TOT} & -\eta_{32} & \cdot & \cdot & \cdot & -\eta_{N2} \\ -\eta_{13} & -\eta_{23} & \eta_{3,TOT} & \cdot & \cdot & \cdot & -\eta_{N3} \\ \cdot & \cdot & \cdot & \cdot & \cdot & \cdot & \cdot \\ \cdot & \cdot & \cdot & \cdot & \cdot & \cdot & \cdot \\ \cdot & \cdot & \cdot & \cdot & \cdot & \cdot & \cdot \\ -\eta_{1N} & -\eta_{2N} & -\eta_{3N} & \cdot & \cdot & \cdot & \eta_{N,TOT} \end{pmatrix}$$

A.30 CONVERSION OF SUBSYSTEM ENERGIES INTO RESPONSE

The following expressions are used in GENSTEP3 to convert the subsystem energy into the requested form of response. They are given in terms of power spectral density (PSD).

APPLICABLE TO STRUCTURAL SUBSYSTEMS

Displacement

$$\frac{\langle d^2 \rangle}{\text{Hz}} = \frac{E_n}{M} \cdot \frac{1}{4\pi^2 f^2 \cdot \Delta f}$$

Velocity

$$\frac{\langle v^2 \rangle}{\text{Hz}} = \frac{E_n}{M} \cdot \frac{1}{\Delta f}$$

Acceleration

$$\frac{\langle acc^2 \rangle}{\text{Hz}} = \frac{E_n}{M} \cdot \frac{4\pi^2 f^2}{\Delta f}$$

Strain

$$\frac{\langle \xi^2 \rangle}{\text{Hz}} = \frac{K \cdot \langle v^2 \rangle}{C_L^2} = \frac{K \cdot E_n}{C_L^2 \cdot M \cdot \Delta f}$$

Stress

$$\frac{\langle \sigma^2 \rangle}{\text{Hz}} = Y_0^2 \cdot \frac{K \cdot E_n}{C_L^2 \cdot M \cdot \Delta f}$$

APPLICABLE TO ACOUSTIC-CAVITY SUBSYSTEMS

Pressure

$$\frac{\langle p^2 \rangle}{\text{Hz}} = \frac{E_n \cdot \rho_0 \cdot C_0^2}{V \cdot \Delta f}$$

Spectrum level

$$\text{Sound pressure level, } SPL\ (\text{dB}) = 10 \log_{10} \left(\frac{E_n \cdot \rho_0 \cdot C_0^2}{V \cdot \Delta f \cdot P_{ref}^2} \right)$$

NOMENCLATURE

The nomenclature for these expressions is:

$< acc^2 >$ = mean square acceleration $(m.s^{-2})^2$ which is also converted to 'g' when required in GENSTEP3,

$< d^2 >$ = mean square displacement (m^2),

$< v^2 >$ = mean square velocity $(m\ s^{-1})^2$,

$< \xi^2 >$ = mean square strain,

$< \sigma^2 >$ = mean square stress $(M\ m^2)^2$,

E_n = energy of subsystem n (Joule),

f = bandwidth centre frequency (Hz),

Δf = bandwidth (Hz),

M = subsystem mass (kg),

K = constant depending on type of vibration and system geometry, usually assumed to be 1.0,

$< p^2 >$ = mean square pressure $(N\ m^{-2})^2$,

P_{ref} = reference pressure (20×10^{-6} N m^{-2}),

V = volume of acoustic cavity,

Y_0 = modulus of elasticity (usually E) (N m^{-2}),

C_L = longitudinal wave speed (m s^{-1}),

C_0 = speed of sound in air (m s^{-1}),

ρ = material density (kg m^{-3}),

ρ_0 = air density (kg m^{-3}),

μ = Poisson's ratio.

The terms are expressed in S.I. units, which is the form required for input into the GENSTEP3 program. Output may be specified in other units or forms; refer to 'Response' cards, in GENSTEP3 Users' Manual, Ref. [4].

A.31 REFERENCES

[1] R.H. Lyon
'Statistical energy analysis of dynamical systems: theory and applications'
MIT Press (1975)

[2] F.J. Fahy
'Statistical energy analysis - a critical review'
Paper presented at a Colloquium of the Commission Acoustique S51 du Conseil International du Bâtiment, Liverpool (1973)

[3] J.J. Pocha
'Study of the acoustic excitation of structure, theory'
Final Report Vol, 1 (ESA Contract Study)

[4] P.J. Williams
'GENSTEP2 Users' Manual', Version 1.0
BAe Document No. GEN/B45/42592 (1986)
Revised 1994 to GENSTEP3 Users' Manual
ISVR Consultancy Services, Document Ref. R05 4274

[5] F.D. Hart & K.C Shah
'Compendium of modal densities'
NASA CR-1773 (1971)

[6] F.D. Hart & K.C. Shah
'Compendium of modal densities'
NASA CR-1773 (1971)

[7] E. Szechenyi
'Modal densities and radiation efficiencies of unstiffened cylinders using statistical methods'
J. Sound Vib., 19(1), 65 (1971)

[8] R.J. Cummins & W. Cooper
'Spacecraft structural acoustics'
Final report. ESA CR(P) - 1264

[9] B.L. Clarkson & M.F. Ranky
'Modal densities of honeycomb plates'
Journal of Sound and Vibration, 91(1), 103 (1983)

[10] N.S. Ferguson & B.L. Clarkson
'The Modal Density of Honeycomb Shells'
Jnl of Vibration, Acoustics, Stress and Reliability in Design (ASME), Oct 1986, Vol. 108, pp. 399-404

[11] R. H. Lyon
'Statistical energy analysis of dynamical systems: theory and applications'
MIT Press (1975)

[12] G. Maidanik
'Response of ribbed panels to reverberant acoustic fields'
JASA 34, 809 (1962)

[13] A.J. Price & M.J. Crocker
'Sound transmission through double panels using statistical energy analysis'
JASA 47, 683 (1970)

[14] G. Maidanik
'Response of ribbed panels to reverberant acoustic fields'
JASA. 34, 809 (1962)

[15] N.S. Ferguson
'A Note on the Critical Frequency of Sandwich Panels'
Letter to Ed., J. Sound Vib. 106(1), 171-172 (1986)

[16] E. Szechenyi
'Sound transmission through cylinder walls using statistical considerations'
J. Sound Vib. 19(1), 83-94 (1971)

[17] L.L. Beranek & I.L. Ver
'Noise and Vibration Control'
J. Wiley & Sons Inc., 1992. ISBN 0-471-61751-2

[18] R.J. Cummins & W. Cooper
'Spacecraft structural acoustic studies'
Final report - ESA CR(P)-1264

(Intentionally Left Blank)

Structural Acoustics Design Manual

Figures & Tables

Item	Caption	Chapter-Page

FIGURES

TABLES.

Structural Acoustics Design Manual

INDEX

The entries given in this Index are in Chapter-Page format.